CLIMATE CHANGE AND WATERSHED PLANNING

Understanding the Related Impacts and Risks

Arthur Hrast Essenfelder

A thesis presented for the degree of
Doctor of Philosophy

PhD Programme in Science and Management of Climate Change
Department of Economics
Università Ca'Foscari Venezia
Italy
2017

Università
Ca'Foscari
Venezia

Corso di Dottorato di ricerca in
Scienza e Gestione dei Cambiamenti Climatici
Ciclo 29°
Anno di discussione 2017

Tesi di Ricerca

Climate Change and Watershed Planning

Understanding the Related Impacts and Risks

SSD: AGR/02; FIS/02; SPS/10

Cordinatore del Dottorato
Prof. Carlo Barbante

Supervisore del Dottorando
Prof. Carlo Giupponi

Co-supervisore del Dottorando
Prof. Silvio Giove

Tesi di dottorato di
Arthur Hrast Essenfelder
Matricola: 956145

In memory of my loving mother and father

Acknowledgements

Three years of Ph.D. have offered me an incredible opportunity for learning new concepts, discussing and expanding ideas, gathering new knowledge, and meeting new people (while also learning how to say goodbye to loved ones). In essence, this journey has led me to an unprecedented professional and personal growth, following a path that was not always linear nor trivial. Professionally, I was given the chance to explore new areas of research that bear little relation with my original background as a environmental engineer. Particularly, I do believe that this is one of the best exercises for helping mind development, and the idea of facing these new challenges motivated me throughout what I classify as a gratifying Ph.D. journey. Personally, I have grown spiritually by facing life-changing experiences and learning the importance of having yours loved ones close to you, even if miles away apart. This section is dedicated as a memo to all the people who, directly or indirectly, have made this long journey possible.

The first person I would to thank and to whom I dedicate a special gratitude is my wife, Hellen. The incredible support she gave me throughout this three years period is unmeasurable and cannot be thank enough, being only felt by her tireless will to be by my side whenever, even during the most stressful moments or during sunny weekends and holidays that had to be replaced by dissertation-working-hours. I am deeply and sincerely thankful for her support, without which would have not rendered this dissertation feasible.

I thank all my family in Brazil for the fact that, besides the long distance between Italy and Brazil, they have never stopped supporting me throughout my Ph.D. journey. I reserve a special thank to my sister, Thais, my grandmother, Cely, and my godmother, Nereide, who have been major inspirations for the continuity of this dissertation.

Although a Ph.D. is mostly a lonely academic journey, I must say that the support, discussions, and ideas exchanged with my Ph.D. colleagues was a major contribution to the development of this dissertation. A special thank is then reserved to Fabio Cian, Francesca Grossi, Malcolm Mistry, and Michele Gaspari for making these three years of Ph.D. a less solitary academic experience.

I would also like to thank the administrative staff of the Ph.D. programme, in special Federica Varosio, for her always prompt and precise support in administrative issues.

Part of the work presented in this dissertation was only made possible due to an exchange period at the Institute of Soil Science and Site Ecology, University of Technology of Dresden, in Germany. A special thank, then, is reserved to Dr. Stefan Julich, Filipa Tavares Wahren, and Daniel Hawtree, specially for providing technical and practical knowledge regarding the usage and set-up of the SWAT model.

I take this opportunity also to sincerely thank Prof. Dr. Ricardo Carvalho de Almeida, from the Federal University of Parana, in Brazil, for providing interesting and useful insights and guidances regarding the applicability and modelling of neural networks models.

Also, the work presented in this dissertation was only possible due to the support from the Brazilian Government through the scholarship programme "Science Without Borders". Thereby, I express my most sincere thanks to this initiative, in particular to the CAPES Foundation, Ministry of Education of Brazil, for providing the scholarship.

Reaching to a conclusion, I cannot thank enough the support offered by my tutor, Prof. Carlo Giupponi, and my co-tutor, Prof. Silvio Giove. Their guidance, advices, and general support was a major contribution and inspiration to the work presented in this dissertation. I hereby state my deepest gratitude to both Professors.

And, at the very last, I would like to thank my parents, to whom I dedicate this dissertation and whom I cannot thank enough for being a major influence and inspiration in my life.

Summary

We are currently living in the era of the *Anthropocene*. Human actions no longer have consequences constrained to local or regional levels, but instead can affect the whole planet. Biogeochemical cycles are impacted by human activities, biogeophysical processes are linked with socio-economic processes, and humans are contributing to the currently observed global climate change. The hydrologic cycle is an example of such interaction, being no longer a process deriving only from the natural circulation of water around the globe, but a process resulting from interconnections and interdependencies between biological, geophysical, and human systems, which, combined, conceive the notion of water resources system and global water system. The management of water resources, then, is not feasible without taking into account the linkages between the hydrologic cycle and human actions. Currently, exists a lack of representation of how human adaptation actions and related feedbacks affect the climatic and hydrologic systems.

This dissertation proposes the study of the possible effects of climate change in the management of watersheds and how water resources management at a watershed-level might be affected by these changes. Specifically, this dissertation explores the possibility of using a Artificial Neural Networks – ANN models coupled with the physically-based hydrological model Soil and Water Assessment Tool – SWAT as a method for improving the description of the regional hydrologic cycle in a watershed by considering the relationships among geophysical and human systems when stressed by both climatic and anthropogenic factors and under long-term time periods.

The main objective of this dissertation is to contribute to the understanding of the relationships between the impacts of climate change and consequences of human actions in the management of watersheds. As watershed management is a

broad theme involving the consideration of several interconnected systems, such as biogeophysical and socio-economic systems, the dissertation first reviews basic concepts regarding the management of watersheds, the utilisation of hydrological models as tool in supporting the development of integrated watershed management plans, and the presentation of two case studies: The first one, named the Venice Lagoon Watershed – VLW, in Italy, and; The second case study, named the Itajaí River Watershed – IRW, in Brazil. In terms of structure the thesis is divided into five chapters, as follows:

The first chapter reviews fundamentals of watershed management, while introducing hydrologic modelling concepts and proposing innovative modelling techniques to be used throughout the dissertation, such as the consideration of the carbon dioxide fertilisation effect due to an increase concentration of carbon dioxide in the atmosphere and the contemplation of ANN as a technique capable of capturing and quantifying adaptive humans actions in a context of watershed management.

The second chapter presents the applicability of the developed ANN model when applied to the simulation of the stream stage of hydrologic systems, while also evaluating the main intrinsic uncertainties of this technology.

The third chapter describes the proposed SWAT-ANN model, while exploring a methodological framework tailored to target the simulation of specific hydraulic management actions under different hydro-meteorological conditions in the VLW, a watershed characterised for being highly modified by anthropogenic factors that, ultimately, affect the watershed's overall natural water flow pathways.

The fourth chapter presents the Italian case study under a context of climate change. This chapter relies on the use of the proposed SWAT-ANN model as a tool capable of translating the possible effects of climate change in the management of the VLW and in its regional hydrologic cycle.

Lastly, the fifth chapter presents the Brazilian case study, covering the topic of climate change effects on the rainfall-runoff process of the IRW as the first step required for the assessment of river flood risks in the watershed's area. Similarly to the Italian case study, this chapter utilises the SWAT-ANN model and future climate predictions as means of determining possible trajectories capable of affecting the management of the IRW and its regional hydrologic cycle.

Table of Contents

List of Figures

List of Tables

Nomenclature

Acronyms

ABM	Agent Based Model
AEM	Adaptive Environmental Management
ANA	Brazilian National Water Agency
ANN	Artificial Neural Network
$APEX$	Agricultural Policy/Environmental eXtender
AR	Assessment Report
ARS	Agricultural Research Service
BIA	Bureau of Indian Affairs
BMP	Best Management Practice
$CEOPS$	Alert System Operations Centre
$CMIP5$	Coupled Model Intercomparison Project
$CORDEX$	Coordinated Regional Climate Downscaling Experiment
CUP	Calibration and Uncertainty Programs
$DCP30$	Downscaled Climate Projections
DEM	Digital Elevation Model

$DNOS$	Brazilian National Department of Sanitation Works
$EARBD$	Eastern Alps River Basin District
EEA	European Environment Agency
$ENSO$	El Niño Southern Oscillation
EPA	United States Environmental Protection Agency
FMP	Forestry Management Plan
GCM	General Circulation Model
GHG	Greenshouse Gas
GIS	Geographical Information System
HEC	Hydrological Engineering Center
HMS	Hydrologic Modeling System
HRU	Hydrological Response Unit
ICA	Independent Component Analysis
IGF	Interbasin Groundwater Flow
$INMET$	Brazilian National Institute of Meteorology
$I-O$	Input-Output
$I-O.d$	Delayed Input-Output
$IPCC$	Intergovernmental Panel on Climate Change
IRW	Itajaí River Watershed
ISM	Indian Summer Monsoon
IWM	Integrated Watershed Management
$IWMP$	Integrated Watershed Management Plan

$KULTURisk$ Knowledge-based Approach to develop a Culture of Risk Prevention

LAD Leaf Area Duration

LAI Leaf Area Index

$LCLUC$ Land-Cover and Land-Use Changes

MLO Mauna Loa Observatory

MLP Multilayer Perceptron

MLR Multiple Linear Regression

MSE Mean of Squared Errors

NAR Non-Linear Autoregressive

$NARX$ Non-Linear Autoregressive with Exogenous Inputs

$NASA$ United States National Aeronautics and Space Administration

$NCCS$ NASA Center for Climate Simulation

NEX NASA Earth Exchange

$NOAA$ Untied States National Oceanic and Atmospheric Administration

$NRCS$ Natural Resources Conservation Service

NSE Nash-Sutcliffe model efficiency coefficient

$PBIAS$ Percent Bias

PCA Principal Component Analysis

PDF Probability Distribution Function

$R2$ Coefficient of Determination

RAS River Analysis System

$RBMP$	River Basin Management Plan
RCP	Representative Concentration Pathway
RDP	Rural Development Programme
$RFWR$	Renewable Freshwater Resource
RRA	Regional Risk Assessment
RUE	Radiation-Use Efficiency
$SCSCF$	Sistema per Calcolo Scientifico di Ca' Foscari
$SCSCN$	SCS Curve Number
$SREX$	Special Report on Managing the Risks of Extreme Events
SSE	Sum of Squared Errors
$SUFI2$	Sequential Uncertainty Fitting Algorithm
$SWAT$	Soil & Water Assessment Tool
TF	Transfer Function
$USDA$	United States Department of Agriculture
VLW	Venice Lagoon Watershed
WFD	Water Framework Directive
WG	Working Group
WMP	Watershed Management Plan
$WRCP$	World Climate Research Program
WRM	Water Resources Management
WRS	Water Resource System
WUE	Water-Use Efficiency

Neural Networks Model

$f(.)$	Activation function
α	Learning constant
b_j	Bias signal of neuron j
$E(\mathbf{x}, \mathbf{w})$	Sum of squared errors (output layer)
$e_{k,j}$	Absolute error of neuron j for for an input-output pattern k
$\mathbf{e_t}$	Error vector
$F(y_{k,j})'_{m_j,j}$	Derivative of non-linear relationship between neurons j and m_j
g	Gradient vector of steepest descent algorithm
$\mathbf{H}$	Hessian matrix
$\mathbf{I}$	Identity matrix
$\mathbf{J}$	Jacobian matrix
μ	Combination coefficient
$s_{k,j}$	Activ. function's slope of neuron j for input-output pattern k
$t_{k,j}$	Target value of neuron j for input-output pattern k
$u_{k,j}$	Linear output of neuron j for an input-output pattern k
$v_{k,j}$	Activation potential of neuron j for input-output pattern k
$\mathbf{w}$	Weight vector
wb_j	Bias weight connection with neuron j
$w_{i,j}$	Weight connection between neurons i and j
$\mathbf{x}$	Input vector
$x_{k,i}$	Input signal of neuron i for input-output pattern k

$y_{k,j}$	Real output of neuron j for input-output pattern k

SWAT Model

bio	Total plant biomass
CN_i	Curve number on day i
CO_2	Atmospheric concentration of carbon dioxide in atmosphere
$c_{p,i}$	Specific heat of air at constant pressure on day i
Δ_i	Slope of saturation vapour pressure-temperature curve on day i
Δbio_i	Potential increase in total plant biomass on day i
$E_{a,i}$	Actual evapotranspiration amount on day i
$E_{ch,i}$	Evaporation in reach on day i
$e_{z,i}$	Water vapour pressure of air at height z on day i
$e^o_{z,i}$	Saturation vapour pressure of air at height z on day i
G_i	Ground heat flux density on day i
γ	Psychrometric constant
g_ℓ	Effective leaf conductance
$g_{\ell,CO2}$	Modified leaf conductance
$H_{net,i}$	Net radiation on day i
$H_{phosyn,i}$	Active radiation intercepted photosynthetically on day i
$I_{a,i}$	Initial abstractions of SCS CN procedure on day i
LAI	Leaf area index
λ_v	Latent heat of vaporisation
$Q_{gw,i}$	Return flow amount on day i

$Q_{surf,i}$	Surface runoff amount on day i
$R_{day,i}$	Precipitation amount on day i that reaches soil surface
r_1	Radiation-use efficiency shape coefficient 1
r_2	Radiation-use efficiency shape coefficient 2
$r_{a,i}$	Aerodynamic resistance on day i
$r_{c,i}$	Plant canopy resistance on day i
$\rho_{air,i}$	Air density on day i
r_ℓ	Effective stomatal resistance of a single leaf
RUE	Radiation-use efficiency
S_i	Retention parameter of SCS CN procedure on day i
SW_0	Initial soil water content
SW_t	Soil water content on day t
$t_{loss,i}$	Transmission losses in reach on day i
$V_{bnk,i}$	Return flow to reach from bank storage on day i
$V_{div,i}$	Volume of water diverted to or from the reach on day i
$V_{in,i}$	Inflow volume of water stored in reach on day i
V_0	Initial volume of water stored in reach
$V_{out,i}$	Outflow volume of water stored in reach on day i
V_t	Volume of water stored in reach on day t
$w_{seep,i}$	Percolation leaving bottom of soil profile on day i

Introduction

Water is a fundamental resource not only for biogeophysical processes but also for socio-economic systems [45, 3]. For instance, due to its elevated specific latent heat, water is used in both natural and non-natural processes as a substance capable of regulating the temperature of a system. When we sweat, water evaporates from the surface of our skin, a process that absorbs energy in order to happen. This same process is fundamental to control the Earth's climate [18, 7]. As water evaporates from oceans and land areas, it is accumulated in the atmosphere as water vapour and stores energy as latent heat [6]. Due to the great mobility of water vapour in the air, water circulates throughout the whole planet, being one of the main agents in redistributing energy throughout the globe. Water vapour remains in the atmosphere until eventually reaching a condensation state and falling as precipitation.

Besides the global redistribution of energy, the concentration and spatial location of water vapour in the air is one of the main factors affecting the formation of clouds. This process, in turn, affects the total amount of solar radiation that actually reaches the planet's surface, and the distribution and intensity of precipitation events around the globe [6]. Moreover, water vapour is a Greenhouse Gas – GHG, meaning that it is capable of absorbing infrared radiation emitted from the Earth's surface. Although water vapour is not a strong GHG, it makes up for that weakness by being abundantly present in the atmosphere [19]. In fact, it is estimated that water vapour is the dominant contributor to the greenhouse effect[1], being responsible for absorbing roughly 50% of the total absorbed energy [33].

[1]Despite the fact that water vapour is a major contributor of the greenhouse effect, its

Indeed, water resources are extremely important and useful. One specific type of water resource stands out, though, as the most useful yet scarce variant: the Renewable Freshwater Resources – RFWRs. Approximately, only 3% of the totality of the planet's water is freshwater. Out of this total, 69% is trapped in glaciers, deep ice and snow, while 30% is groundwater and soil moisture. The remaining approximate value of just 1% is the RFWRs promptly available in ground ice, rivers, lakes, ponds and streams [23, 28, 42]. Even though the amount of RFWRs is low if compared to the total amount of water present in the planet Earth, or even if compared to the total amount of freshwater, current human demand for that resource represents only 10% of RFWRs availability at a global scale [28]. Even so, due to the fact that RFWRs are variable both in space and time, human demand for this resource is not always met and pressures worldwide tend to increase as population and economy grow [13, 44].

Spatially, some regions around the globe have limited access to RFWRs, such as Northern Africa and Middle East. In contrast, other regions have abundant access to this resource, such as the Amazon region, mostly of south-eastern area of South America, and South-Eastern Asia. Similarly, RFWRs' availability is also variable in time, being governed by the climate system and the hydrologic cycle. Such variability in time poses new threats to regions where water is known to be scarce. On the other hand, fluctuating seasonal weather patterns (e.g. Indian Summer Monsoon – ISM) and climatic cycles (e.g. El Niño Southern Oscillation – ENSO, etc.) are also know to be capable of affecting the distribution and availability of RFWRs during different instants in space and time, possibly leading to an excess of precipitation in some regions of the world and, ultimately, contributing to river flood episodes [21, 34]. Neither to much nor to little access to RFWRs is good, and optimal availability of this type of resource must be met, both spatially and temporally thus requiring management.

Even if the climate system is the main driver regulating the distribution and

importance to climate change falls short if compared to other gases GHGs (e.g. carbon dioxide) due to the fact that water vapour has a very low residence time and great mobility in the atmosphere, resulting in low concentrations if averaged globally [40]. However, as water vapour concentration in the atmosphere is dependent on temperature, water vapour concentrations in the atmosphere can be boosted due to increases in the average global temperature as a consequence of global warming, resulting in a positive feedback capable of amplifying the changes in the climate system [32, 43].

availability of RFWRs [16], other factors also do play a large role in regulating these processes at a regional scale, such as physical and environmental characteristics of a watershed. For instance, in mountainous regions precipitation patterns can be influenced by the orographic effect, resulting in highly non-uniform precipitation events, both in space and time [5, 36]. Moreover, specific soil and land-use conditions can also affect the circulation of water in a watershed by altering the infiltration and runoff processes which, in turn, can lead to a modification in soil erosion and river bed degradation rates [27, 22, 25]. Consequently, RFWRs require appropriate management, meaning that the understanding of the relationships among the regional climate, geophysical, and environmental characteristics of a watershed must be well know during the development of management plans. Hence, an appropriate understanding of the movement and distribution of water resources in a watershed is needed. The area of knowledge responsible for the study of these processes is hydrology.

Hydrology can be defined as the science responsible for the study of the origin, circulation, distribution and properties of water resources around the Earth [4]. Other sciences also study the movement of water resources around the globe, such as meteorology, however under different perspectives. Hydrology is a physical science specifically concerned with the continental water pathways and the global water balance. Even if hydrology is a physical science, the realisation that biological systems are very much capable of affecting the fluxes of water in the hydrologic cycle is well settled among hydrologists to the point that one of the main water fluxes in the water cycle is the evapotranspiration process, a combination of the physical evaporation and the biological transpiration processes.

Being a physical science, the practical scope of hydrology is the determination of the amount and/or flow rate of water that will be found at a specific location and at a specific time under natural conditions, without direct human control or intervention [6]. However, the water cycle is not affected only by climate, geophysical or even biological factors; humans are also capable of affecting the hydrologic cycle. By modifying natural environments and processes, humans can alter the water pathways of a watershed by direct actions, such as by changing the land-cover of a certain area or by altering the superficial water pathways of a stream by installing and managing control hydraulic devices, or indirect actions,

such as by emitting carbon dioxide and other GHGs capable of influencing in the global energy balance, ultimately affecting regional climate systems [40]. Thereby, the study of the hydrologic cycle as a solely physical process is somewhat limiting [28].

Indeed, in the era of the *Anthropocene* [9, 39], where humans are known to be capable of affecting natural processes and the circulation of natural resources, the realisation by the scientific community that the hydrologic cycle is a process resulting from not only a combination of interconnections and interdependencies between biological and geophysical systems, but also linked to human systems has leveraged the development of the concept of *Water Resource Systems* – WRSs and *global water system* [44, 45, 1, 3]. Similarly, the acknowledgement that the understanding of the water cycle dynamics over long periods of time is not possible without taking into account the linkages between the hydrologic cycle and socio-economic systems has led to the emergence of a new science known as *socio-hydrology* [37, 10].

Water Resources Management – WRM, then, requires the *integration* of knowledges from several areas [14, 46], which leads to the concept of Integrated Watershed Management – IWM. However, not only the integration of different knowledges is required, but also the definition and consideration of proper spatial and time dimensions for which the RFWRs are to be managed. At a watershed-level scale, an effective tool capable of offering not only such integration of knowledges but also dynamic enough to be capable of accommodating different time dimensions of interest is the Integrated Watershed Management Plan – IWMP.

IWMP can be understood as the process of organising and guiding land, water, and other natural resources used in a watershed to provide goods and services to people without adversely affecting the natural environment [4, 46]. The main objective of an IWMP is the continuous and sustainable use of RFWRs. The dilemma in watershed management is that Land-Cover and Land-Use Changes – LCLUC and natural resources allocation needed to promote the sustained progress of society in the long-term can be at conflict of interests with what is essential to the promote the development of individuals in the short-term [20, 30]. Hence, the main goal of an IWMP is to achieve sustainable management and use of natural

resources in a watershed. One should note that, by considering the just mentioned goal, an IWMP deals not only with the sustainable management of RFWRs but also with the capability and suitability of land, vegetative, and other natural resources to be managed for the sustainable development of socio-economic, human-institutional, and biogeophysical systems within a watershed.

As IWMP is a dynamic tool that requires the integration of multi-disciplinary knowledge [12], mathematical models present themselves as useful instruments capable of supporting the understanding of the processes involved with the management of and decision-making in watershed systems [24]. One of these models is the Soil & Water Assessment Tool – SWAT [2]. This dissertation relies on the use of the SWAT model as a mechanistic tool capable of reflecting the understanding of human pressures on water systems by the evaluation of LCLUC and respective management conditions in watershed systems.

Still, as the effects of climate change become clearer in the hydrologic cycle, IWMPs should also acknowledge the possible regional consequences arising from these changes when developing long-term watersheds plans. Indeed, climatic changes pose new threats to the management of watersheds, yet the 5th Assessment Report – AR by the Intergovernmental Panel on Climate Change – IPCC, Working Group – WG2, points out that the combined effects of climate change and human pressures has the potential to increase water-related risks, thereby potentially disrupting the management of watersheds, reservoirs, irrigation networks, and drainage system for infrastructural works [15]. Even if hydro-meteorological variables and related processes are highly uncertain in the future [35], General Circulation Models – GCMs present themselves as the best tools currently available for the study, understanding, and simulation of changes that might occur in the global climate system [26].

In general, GCMs are capable of simulating physical and biophysical processes in different systems, such as atmosphere, ocean, cryosphere, and land surface, while, at the same time, capturing their interconnections and interdependencies. These models, however, lack the ability to consider human adaptation and the related feedbacks on the climate system [29]. This dissertation, then, explores the possibility of coupling a mechanistic regional hydrological model with intensive data-driven machine-learning models in order to better describe some of the

linkages among the several systems that drive the hydrologic cycle at a watershed-level scale and affect the development of IWMPs, such as the management of reservoirs and flood-control hydraulic devices.

Motivation

The motivation behind this dissertation comes from the understanding that watershed management plans are dynamic tools, meaning they need to be flexible enough to accommodate not-foreseen problems and to adapt to new situations. This is exactly the case of climate change and related human adaptation: exists the need to better understand the possible consequences of climate and socio-economic changes on the planning and management of watersheds while, at the same time, exists the need to better understand the possible human adaptation actions in the long-term.

In order to evaluate the proposed methodology, this work brings two contrasting watersheds as case studies. The first is the Venice Lagoon Watershed – VLW, in Northeastern Italy, while the second case study is the Itajaí River Watershed – IRW, in Southern Brazil. The overall methodology is heavily based on the use of a modified SWAT model as the mechanistic component for the simulation of hydrologic related processes, and on the use of an Artificial Neural Network – ANN model as the empirical counter-part. Under this framework, it is assumed that the ANN model is capable of learning from observations and projecting results into the future, under controlled circumstances and for specific processes.

Objectives

The main objective of this study is to contribute to the understanding of the relationships between the impacts of climate change and specific hydraulic management solutions in the development of IWMP by proposing an innovative methodology capable of supporting the long-term scenario analysis in hydrologic systems. To check whether the proposed methodological framework is valid, two

case studies are evaluated covering site-specific concerns: i. The Italian case study aims at the evaluation of the impacts of climate change on water availability for irrigation purposes in the VLW, and; ii. The Brazilian case study seeks the evaluation of the consequences of climate change on the rainfall-runoff process in the IRW.

Driven by the investigation of the above described main objective, this study is organised in such a way that enables the examination of the following research questions and sub-objectives:

Objective 1: Develop an innovative methodology based on the use of a mechanistic focused eco-hydrological model (i.e. SWAT) and a machine learning focused technology (i.e. ANN) to assist the development of watershed management plans.

Specific Research Questions

- *What are the current limitations of the SWAT model when used in a context of long-term scenario analysis (e.g. climate change)?*
- *Can the coupling of mechanistic and empirical modelling techniques improve the understanding and description of the regional hydrologic cycle at watershed-level scales?*
- *Can technologies deriving from artificial intelligence and machine learning, such as ANN models, be useful in a context of watershed planning and management?*

Objective 2: Verify the applicability of ANN models and identify the main uncertainties coming from the application of this technology in hydrologic systems.

Specific Research Questions

- *Can ANN models be applied to the short term forecasting of a river's stream stage?*
- *What are the main intrinsic uncertainties of ANN models?*
- *What are the main uncertainties coming from hydro-meteorological variables and processes in a context of rainfall-runoff modelling that can affect the performance of ANN models?*

Objective 3: Explore the possible impacts of climatic and land management

changes in the regional hydrologic cycle and on the water availability to the agricultural sector of the VLW.

Specific Research Questions

- *Will the possible consequences in the hydrologic cycle deriving from climate change be able to affect the availability of water for irrigation in the VLW in the mid-to-long term?*
- *What kind of adaptation actions can be taken into consideration in a context of IWM?*

Objective 4: Assess the potential consequences of climate change in the rainfall-runoff process of the IRW, aiming at characterisation of river flood episodes under different climate change scenarios.

Specific Research Questions

- *How climate change impacts will affect the rainfall-runoff process in the IRW?*
- *How river basin managers may operate flood-control structures if an alteration of the rainfall-runoff process is verifies in the IRW?*
- *What are the possible direct consequences of these changes to river flooding?*

Thesis Outline

This dissertation covers the topic of watershed management under possible influences coming from impacts of regional climate change and land/water management on the regional hydrologic cycle. As the management of watersheds is a broad theme contemplating several areas of knowledge and the interactions among different systems, this dissertation focus in the study of specific hydraulic management solutions that are particular to the considered case studies (i.e. water pumping and flow partitioning stations in the VLW and flood control reservoirs in the IRW). The work presented in this dissertation is heavily based on the utilisation of an innovative watershed-scale model, resulting from the combination of a mechanistic eco-hydrological model (i.e. SWAT) and an empirical machine

learning model (i.e. ANN). The overall proposed methodological framework consists in representing the physical, biophysical and land management conditions through the use of the mechanistic module, while the empirical module is responsible for the estimation of the dynamics of specific hydraulic management conditions under future hydro-meteorological conditions.

As per structure, this dissertation is divided into five main chapters, each covering a specific topic or case study of interest, and two auxiliary sections, namely Introduction and Conclusions. Moreover, this dissertation also brings four appendices: i. Appendix 1 brings the Fortran code modifications made in the source SWAT model code in order to accommodate the proposed methodological framework; ii. Appendix 2 theoretically describes the developed ANN model; iii. Appendix 3 presents the source code of the developed ANN model, written in R language [31], and; iv. Appendix 4 presents results pertaining to the numerical analysis performed in Chapter 3. The overall structure of this dissertation together with its logical progress pathway are depicted in Figure I.1.

Chapter 1, entitled *"Watershed Management: Concepts, tools, and case studies"*, consists of three main distinct sections. The first main section presents a review of general concepts and state-of-the-art knowledges related IWM under an eco-hydrological perspective. A discussion on how climate change effects might influence the management of watersheds is also covered in this section. Subsequently, in the second section, hydrologic modelling is presented as an instrument capable of supporting the understanding and the decision-making process in the management of complex systems, such as the management of eco-hydrological systems. Focus is given to the introduction of the SWAT model as tool capable of delivering such results, together with a discussion regarding three identified model limitations, namely: i. The lacking ability to dynamically simulate the effects of increased CO_2 atmospheric concentration on the regional hydrologic cycle; ii. The inadequate representation of irrigation efficiency on the water balance of hydrologic units, and; iii. The absence of a module capable of dynamically accounting for human-driven actions on the management of specific hydraulic features. The second sections, then, moves to the introduction of new modelling capabilities by presenting proposed modifications in the original SWAT model source code to tackle the previously identified limitations. Finally, the third

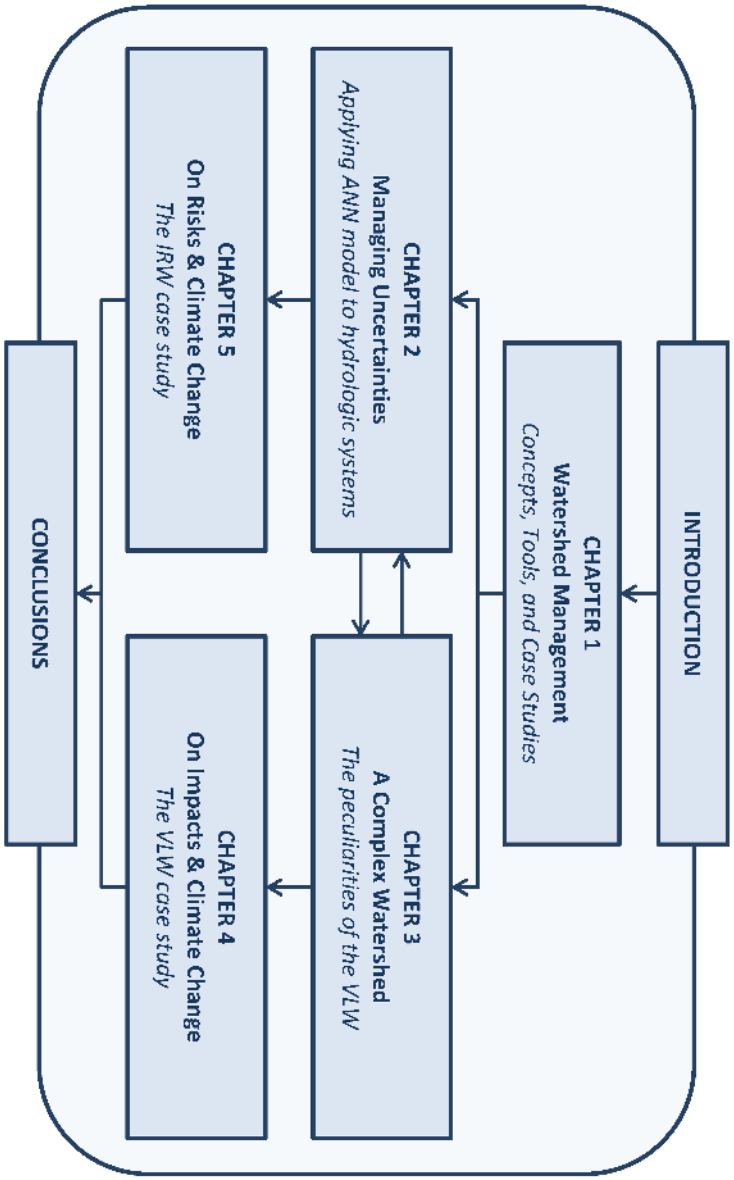

Figure 1.1: Flowchart depicting the structure of the dissertation.

section introduces the most relevant physical, social, and economic features of the two case study areas (i.e. the VLW and the IRW), prioritising a discussion about the specific hydraulic management solutions that are particular to each case study watershed. The case studies are described in this chapter so to avoid repetition throughout the dissertation's content, as both case studies are explored individually in different chapters and under different perspectives.

Chapter 2, entitled *"The ANN Model: Exploring its Applicability and Uncertainties"*, moves to the introduction of the developed ANN model, on the assessment of its applicability as a valid tool for the simulation of the short-term stream stage of the IRW, and on the study of uncertainties arising from the employment of ANNs models in a context of hydrologic modelling. Particular focus is given to the verification of the performance of the developed ANN when applied to the short-term forecasting of the stream stage of the IRW by assessing the most efficient model configuration and by comparing the results obtained by the ANN against reference modelling techniques, namely multiple linear regression and transfer functions models. This chapter also explores the main sources of uncertainty that are intrinsic to an ANN model while, at the same time, presents a discussion about possible sources of uncertainty that may arise from the stochastic nature of hydro-meteorological processes.

Chapter 3, entitled *"The SWAT-ANN Model: Making Use of its New Capabilities"*, explores a methodological framework targeting the simulation of specific hydraulic management actions under different hydro-meteorological conditions in the VLW, a watershed characterised for being highly modified by anthropogenic factors that, ultimately, affect the watershed's overall natural water flow pathways. This chapter is divided in two separate yet related parts: i. The first part relies on the use of Principal Component Analysis – PCA as a technique for the identification of the most relevant spatial and temporal hydro-meteorological variables capable of affecting the total external hydraulic influences to the Dese-Zero watershed, a sub-basin of the VLW, while exploring the use of two contrasting empirical models, namely a Multiple Linear Regression – MLR model and an ANN model, as modelling techniques able to quantitatively estimate the total external hydraulic loadings to the studied watershed, and; ii. The second part, instead, proposes a framework to simulate the complex water dynamics of the VLW by contemplating

a coupled mechanistic-empirical modelling approach, named SWAT-ANN model.

Chapter 4, entitled *"On Impacts & Climate Change: The VLW case study"*, presents the first case study contemplating the possible effects of climate change on IWM by relying on the use of the developed SWAT-ANN model. Specifically, this chapter covers the study and understanding of how climate change may impact the availability of water for irrigation purposes in the VLW. Relying in the understanding that future climatic and land management changes are certain during the future simulation period (i.e. 2015 - 2050), this chapter utilises predictions of future climate trajectories coming from a selection of GCMs as a way of capturing the possible effects of climate change in the regional hydrologic cycle of the VLW. The Representative Concentration Pathway – RCP 4.5 [8, 38, 47, 11] is selected as the representative future simulated climate scenario, while simulated climate data from six different GCMs is considered. At the same time, possible pathways of LCLUC and irrigation efficiency are evaluated as human induced factors capable of affecting the hydrology of the studied watershed. Finally, this chapter is based upon the use of the proposed modified SWAT model (see Chapter 1 for reference) coupled with the developed ANN model as a tool capable of translating both climate change effects (e.g. CO_2 fertilization effect) and specific artificial hydraulic management actions (e.g. irrigation water sources) under future hydro-meteorological conditions.

The last chapter, Chapter 5, entitled *"On Risks & Climate Change: The IRW case study"*, presents a discussion based upon the application of the developed developed SWAT-ANN model in a context of river flooding under the consideration of climate change scenarios. Specifically, this chapter covers the evaluation of the possible consequences of climate change in the rainfall-runoff process of the IRW, in Brazil, as the first step required for the assessment of river flood risks in the study area. Future simulated climate data is gathered from both the the United States National Aeronautics and Space Administration – NASA Earth Exchange Downscaled Climate Projections – NEX-DCP30 [41] and the COordinated Regional climate Downscaling Experiment – CORDEX [17] datasets, for a total of four GCMs and one RCP (i.e. 4.5 [8, 38, 47]). Similarly to the case study explored in Chapter 4, the methodological framework of the Brazilian case study consists in the use of the same modified SWAT model (see Chapter 1 for

reference) coupled with the developed ANN model as a tool capable of capturing human responses in the long-term management of the flood-control dams in the IRW.

References

[1] Alcamo, J., Vörösmarty, C. J., Naiman, R. J., Lettenmaier, D. P., Pahl-Wostl, C., 2008. A grand challenge for freshwater research: understanding the global water system. Environmental Research Letters 3 (1), 010202.

[2] Arnold, J. G., Srinivasan, R., Muttiah, R. S., Williams, J. R., 1998. Large Area Hydrologic Modeling and Assessment Part I: Model Development. Journal of the American Water Resources Association 34 (1), 73–89.

[3] Bogardi, J. J., Dudgeon, D., Lawford, R., Flinkerbusch, E., Meyn, A., Pahl-Wostl, C., Vielhauer, K., Vörösmarty, C. J., 2012. Water security for a planet under pressure: Interconnected challenges of a changing world call for sustainable solutions. Current Opinion in Environmental Sustainability 4 (1), 35–43.

[4] Brooks, K. N., Ffolliott, P. F., Magner, J. A., 2013. Hydrology and the Management of Watersheds, 4th Edition. John Wiley & Sons, Inc., Iowa, USA.

[5] Browning, K. A. and Hill, F. F. and Pardoe, C. W., 1974. Structure and mechanism of precipitation and the effect of orography in a wintertime warm sector. Quarterly Journal of the Royal Meteorological Society 100 (425), 309–330.

[6] Brutsaert, W., 2013. Hydrology: An Introduction, 8th Edition. Cambridge University Press, Cambridge, United Kingdom.

[7] Chahine, M. T., 1992. The hydrological cycle and its influence on climate. Nature 359 (6394), 373–380.

[8] Clarke, L. E., Jacoby, H., Pitcher, H., Reilly, J., Richels, R., 2007. Scenarios of Greenhouse Gas Emissions and Atmospheric Concentrations. Sub-report 2.1A of Synthesis and Assessment Product 2.1 by the U.S. Climate Change Science Program and the Subcommittee on Global Change Research. Tech. Rep. July, Department of Energy, Office of Biological & Environmental Research, Washington, DC, USA.

[9] Crutzen, P. J., 2002. Geology of mankind. Nature 415 (January), 23.

[10] Di Baldassarre, G., Viglione, A., Carr, G., Kuil, L., Salinas, J. L., Blöschl, G., 2013. Socio-hydrology: Conceptualising human-flood interactions. Hydrology and Earth System Sciences 17 (8), 3295–3303.

[11] Edenhofer, O., Pichs-Madruga, R., Sokona, Y., Kadner, S., Minx, J., Brunner, S., Agrawala, S., Baiocchi, G., Bashmakov, I., Blanco, G., Broome, J., Bruckner, T., Bustamante, M., Clarke, L., Conte Grand, M., Creutzig, F., Cruz-Núñez, X., Dhakal, S., Dubash, N., Eickemeier, P., Farahani, E., Fischedick, M., Fleurbaey, M., Gerlagh, R., Gómez-Echeverri, L., Gupta, S., Harnisch, J., Jiang, K., Jotzo, F., Kartha, S., Klasen, S., Kolstad, C., Krey, V., Kunreuther, H., Lucon, O., Masera, O., Mulugetta, Y., Norgaard, R., Patt, A., Ravindranath, N., Riahi, L., Roy, J., Sagar, A., Schaeffer, R., Schlömer, S., Seto, K., Seyboth, K., Sims, R., Smith, P., Somanathan, E., Stavins, R., von Stechow, C., Sterner, T., Sugiyama, T., Suh, S., Ürge-Vorsatz, D., Urama, K., Venables, A., Victor, D. G., Weber, E., Zhou, D., Zou, J., Zwickel, T., 2014. Technical Summary. In: Edenhofer, O., Pichs-Madruga, R., Sokona, Y., Farahani, E., Kadner, S., Seyboth, K., Adler, A., Baum, I., Brunner, S., Eickemeier, P., Kriemann, B., Savolainen, J., Schlömer, S., von Stechow, C., Zwickel, T., Minx, J. C. (Eds.), Climate Change 2014: Mitigation of climate change. Contribution of Working Group III to the Fifth Assessment Report of the Intergovernmental Panel on Climate Change. Cambridge University Press, Cambridge, United Kingdom and New York, NY, USA., Ch. Tec. Summ., pp. 33–107.

[12] EPA, 2013. Principles of Watershed Management. Tech. rep., U.S. Environmental Protection Agency, Chicago, IL, USA.

[13] Falkenmark, M., Widstrand, C., 1992. Population and water resources: a delicate balance. Population bulletin 47 (3), 1–36.

[14] Ffolliott, P. F., Baker, M. B., Edminster, C. B., Dillon, M. C., Mora, K. L., 2002. Land Stewardship through Watershed Management: Perspectives for the 21st Century. Springer Science & Business Media, New York, NY, USA.

[15] Field, C., Barros, V., Mach, K., Mastrandrea, M., van Aalst, M., Adger, W., Arent, D., Barnett, J., Betts, R., Bilir, T., Birkmann, J., Carmin, J., Chadee, D., Challinor, A., Chatterjee, M., Cramer, W., Davidson, D., Estrada, Y., Gattuso, J.-P., Hijioka, Y., Hoegh-Guldberg, O., Huang, H., Insarov, G., Jones, R., Kovats, R., Romero-Lankao, P., Larsen, J., Losada, I., Marengo, J., McLean, R., Mearns, L., Mechler, R., Morton, J., Niang, I., Oki, T., Olwoch, J., Opondo, M., Poloczanska, E., Pörtner, H.-O., Redsteer, M., Reisinger, A., Revi, A., Schmidt, D., Shaw, M., Solecki, W., Stone, D., Stone, J., Strzepek, K., Suarez, A., Tschakert, P., Valentini, R., Vicuña, S., Villamizar, A., Vincent, K., Warren, R., White, L., Wilbanks, T., Wong, P., Yohe, G., 2014. Technical Summary. In: Field, C., Barros, V., Dokken, D., Mach, K., Mastrandrea, M., Bilir, T., Chatterjee, M., Ebi, K., Estrada, Y., Genova, R., Girma, B., Kissel, E., Levy, A., MacCracken, S., Mastrandrea, P., White, L. (Eds.), Climate Change 2014: Impacts, Adaptation, and Vulnerability. Part A: Global and Sectoral Aspects. Contribution of Working Group II to the Fifth Assessment Report of the Intergovernmental Panel on Climate Change. Cambridge University Press, Cambridge, United Kingdom and New York, NY, USA., Ch. Tec. Summ., pp. 35–94.

[16] Gain, A. K., 2013. Climate change impact and vulnerability assessment of water resources systems: the case of Lower Brahmaputra River Basin. Dottorato di ricerca in scienza e gestione dei cambiamenti climatici, ciclo 25, Ca' Foscari University of Venice.

[17] Giorgi, F., Jones, C., Asrar, G. R., 2009. Addressing climate information needs at the regional level: The CORDEX framework. World Meteorological Organization Bulletin 58 (3), 175–183.

[18] Gleick, P. H., 1989. Climate change, hydrology, and water resources. Reviews of Geophysics 27 (3), 329.

[19] Henson, R., 2014. The Thinking Person's Guide to Climate Change. American Meteorological Society, Boston, US.

[20] Jacobs, K., Lebel, L., Buizer, J., Addams, L., Matson, P., McCullough, E., Garden, P., Saliba, G., Finan, T., 2010. Linking knowledge with action in the pursuit of sustainable water-resources management. Proceedings of the National Academy of Sciences 113 (17), 1–6.

[21] Jakobsen, F., Hoque, A. Z., Paudyal, G. N., Bhuiyan, M. S., 2005. Evaluation of the Short-Term Processes Forcing the Monsoon River Floods in Bangladesh. Water International 30 (3), 389–399.

[22] Kosmas, C., Danalatos, N., Cammeraat, L. H., Chabart, M., Diamantopoulos, J., Farand, R., Gutierrez, L., Jacob, A., Marques, H., Martinez-Fernandez, J., Mizara, A., Moustakas, N., Nicolau, J. M., Oliveros, C., Pinna, G., Puddu, R., Puigdefabregas, J., Roxo, M., Simao, A., Stamou, G., Tomasi, N., Usai, D., Vacca, A., 1997. The effect of land use on runoff and soil erosion rates under Mediterranean conditions. Catena 29 (1), 45–59.

[23] Lvovitch, M. I., 1970. World water balance: General report. Symposium on World Water Balance II (93), 401–415.

[24] Mirchi, A., Watkins, J. D., Madani, K., 2011. Modeling for Watershed Planning, Management, and Decision Making. In: Vaughn, J. C. (Ed.), Watersheds: Management, Restoration and Environmental Impact. Nova Science Publishers, Inc., New York, NY, USA, Ch. 6, pp. 1–25.

[25] Morgan, J. A., 2013. Bed Degradation of the Lower Missouri River. Msc. thesis, University of Missouri-Kansas City.

[26] Murphy, J. M., Sexton, D. M. H., Barnett, D. N., Jones, G. S., Webb, M. J., Collins, M., Stainforth, D. A., 2004. Quantification of modelling uncertainties in a large ensemble of climate change simulations. Nature 430 (August 2004), 768–771.

[27] Nicolau, J. M., Solé-Benet, A., Puigdefabregas, J., Gutierrez, L., 1996. Effects of soil and vegetation on runoff along a catena in semi-arid Spain. Geomorphology 14 (4 SPEC. ISS.), 297–309.

[28] Oki, T., Kanae, S., 2006. Global Hydrological Cycles and World Water Resources. Science 313 (5790), 1068–1072.

[29] Palmer, P. I., Smith, M. J., 2014. Model human adaptation to climate change. Nature 512 (August), 365–366.

[30] Perman, R., Ma, Y., Common, M., Maddison, D., McGilvray, J., 2011. Natural Resource and Environmental Economics, 4th Edition. Pearson Education Limited, Essex, England.

[31] R, C. T., 2016. R: A Language and Environment for Statistical Computing. URL https://www.r-project.org/

[32] Rind, D., Chiou, E.-W., Chu, W., Larsen, J., Oltmans, S., Lerner, J., McCormick, M. P., McMaster, L., 1991. Positive water vapour feedback in climate models confirmed by satellite data. Nature 349 (February), 500–503.

[33] Schmidt, G. A., Ruedy, R. A., Miller, R. L., Lacis, A. A., 2010. Attribution of the present-day total greenhouse effect. Journal of Geophysical Research Atmospheres 115 (20), 1–6.

[34] Schöngart, J., Junk, W. J., 2007. Forecasting the flood-pulse in Central Amazonia by ENSO-indices. Journal of Hydrology 335 (1-2), 124–132.

[35] Shackley, S., Young, P., Parkinson, S., Wynne, B., 1998. Uncertainty, Complexity and Concepts of Good Science in Climate Change Modelling: Are GCMs the Best Tools? CIlimatic Change 38 (2), 159–205.

[36] Singh, P., Kumar, N., 1997. Effect of orography on precipitation in the western Himalayan region. Journal of Hydrology 199 (1-2), 183–206.

[37] Sivapalan, M., Savenije, H. H. G., Blöschl, G., 2012. Socio-hydrology: A new science of people and water. Hydrological Processes 26 (8), 1270–1276.

[38] Smith, S. J., Wigley, T., 2006. Multi-Gas Forcing Stabilization with Minicam. The Energy Journal 27, 373–391.

[39] Steffen, W., Grinevald, J., Crutzen, P., McNeill, J., 2011. The Anthropocene: conceptual and historical perspectives. Philosophical transactions of the Royal Society. Series A, Mathematical, physical, and engineering sciences 369 (1938), 842–67.

[40] Stocker, T. F., Dahe, Q., Plattner, G.-K., Alexander, L. V., Allen, S. K., Bindoff, N. L., Bréon, F.-M., Church, J. A., Cubash, U., Emori, S., Forster, P., Friedlingstein, P., Talley, L. D., Vaughan, D. G., Xie, S.-P., 2013. Technical Summary. In: Stocker, T., Qin, D., Plattner, G.-K., Tignor, M., Allen, S., Boschung, J., Nauels, A., Y. Xia, V. B., Midgley, P. (Eds.), Climate Change 2013: The Physical Science Basis. Contribution of Working Group I to the Fifth Assessment Report of the Intergovernmental Panel on Climate Change. Cambridge University Press, Cambridge, United Kingdom and New York, NY, USA., Ch. Tec. Summ., pp. 33–115.

[41] Trasher, B., Xiong, J., Wang, W., Melton, F., Michaelis, A., Nemani, R., 2013. New downscaled climate projections suitable for resource management in the U.S. NEX-DCP30: Downscaled 30 Arc-Second CMIP5 Climate Projections for Studies of Climate Change Impacts in the United States 1 . Intent of This Document and POC.

[42] Trenberth, K. E., Fasullo, J., Smith, L., Qian, T., Dai, A., 2006. Estimates of the Global Water Budget and Its Annual Cycle Using Observational and Model Data. Journal of Hydrometeorology 8, 758–769.

[43] Voigt, A., Shaw, T. A., 2015. Circulation response towarming shaped by radiative changes of clouds andwater vapour. Nature Geoscience 8 (January), 102–106.

[44] Vörösmarty, C. J., Green, P., Salisbury, J., Lammers, R. B., 2000. Global Water Resources: Vulnerability from Climate Change and Population Growth. Science 289 (July), 284–288.

[45] Vörösmarty, C. J., Lettenmaier, D., Leveque, C., Meybeck, M., Pahl-Wostl, C., Alcamo, J., Cosgrove, W., Grassi, H., Hoff, H., Kabat, P., Lansigan, F., Lawford, R., Naiman, R. J., 2004. Humans Transforming the Global Water System. EoS, Transactions, American Geophysical Union 85 (48), 509–520.

[46] Wang, G., Mang, S., Cai, H., Liu, S., Zhang, Z., Wang, L., Innes, J. L., 2016. Integrated watershed management: evolution, development and emerging trends. Journal of Forestry Research 27 (5), 967–994.

[47] Wise, M., Calvin, K., Thomson, A., Clarke, L., Bond-Lamberty, B., Sands, R., Smith, S. J., Janetos, A., Edmonds, J., 2009. Implications of Limiting CO2 Concentrations for Land Use and Energy. Science 324 (May), 1183–1186.

Chapter 1

Watershed Management

Concepts, Tools, and Case Studies

Abstract

The management of water resources is a very broad subject requiring the integration of several areas of knowledge. Hence, it is necessary the definition of some basic concepts. This chapter presents a brief review of the history behind the notion of watershed management and some basic concepts related to WRM. The discussion, then, is directed to the presentation of hydrologic models as useful tools for providing quantitative information regarding the dynamics of a watershed and for supporting the development of watershed management plans. Still discussing about hydrologic models, the chapter introduces the SWAT model as a successful example of a support tool for the development of IWMPs. A deeper explanation of the main hydrologic processes as considered by the SWAT model is presented, as well as some of its limitations and some proposed improvements. Finally, the chapter is concluded after the presentation of the most relevant physical, environmental, and socio-economic aspects of the VLW and the IRW, as well as some aspects of their current management plans.

1.1 Introduction

Why do we need to manage a watershed?

Although simple, this question brings a lot of meaning behind it. Everyone lives inside a watershed, even if the majority of the world's population might not be aware of it. A watershed is not only the area where humans can exploit water resources, it is the area that provides most of the resources and services required by socio-ecosystems. In not managed, the overexploitation of these resources and services can lead to impacts on the soil, ecosystems, and water resources, especially RFWR, among others. These actions have the potential of ultimately damaging socio-economic systems [95]. In short, a healthy water system is essential for a robust economy and a good quality of life. Hence the need of managing a watershed.

But, what is a watershed?

A watershed can be understood as the land area that drains water to a specific point in space by a stream network system. Hence, a watershed is an area resulting from natural hydrology, representing the most logical unit for the management of continental water resources [39]. The origins of the modern concept of watershed management can traced back to the 1930's when, in southern Ontario, Canada, an effort for a coordinated management of Ontario's watersheds arose as a response to growing problems related to water supply and sewage disposal as a consequence of uncontrolled land, water and forestry resources exploitation [52, 28]. In fact, the origins of watershed management are closely related to the unrestricted exploitation of the environment [46].

By the 1960s, the unrestricted use of forest resources has led to significant changes in the hydrological regime of rivers in Europe and North America, leading to an acceleration of erosion processes and the increase in the occurrence of water related hazards in downstream areas. During the same period, between the 1950s and 1970s, big irrigation schemes and the installation of huge hydropower dams in Asia, Africa, and Latin America has often led to unaccounted negative impacts on the environment and local communities [47]. These issues helped to increase the awareness of policy-makers and stakeholders to the importance of

managing watersheds as an integrated system, where not only economic factors where accounted for, but also their implications on the environment and the social systems. The realisation that an integrated approach was required in order to manage such a complex environment that is a watershed has eventually become the concept nowadays known as IWM. From this concept, an instrument capable of synthesising the knowledge required to manage watersheds was born, known as Watershed Management Plan – WMP [111].

A WMP is a dynamic and interactive tool that involves the understanding and translation of the interrelationships and interactions among the biogeophysical and socio-economic systems. If on the one hand it is well known that the hydrologic cycle and energy relationships are a fundamental knowledge for the study of hydrology, and, consequently, for WRM [22], on the other hand the realisation that the relationships between environmental costs and socio-economic impacts are also capable of affecting the management of water resources has led to the understanding that these spheres of knowledge must also be taken into account during the development of watershed management approaches [31]. If successfully implemented, WMPs can be powerful and useful tools for attaining and/or maintaining water quality standards in a watershed, consequently promoting the protection of the environment, the restoration of ecosystems [39, 40], and supporting the long-term development of local communities [22].

The successfulness of a WMP depends on how well the general needs of a watershed are captured by the management plan and on how effective the proposed management actions can be. As a watershed is an ensemble of unique biogeophysical and socio-economic features, it becomes necessary the characterisation and understanding of each of these components for the development of a successful WMP. Moreover, besides the individual characterisation of each component of a watershed, the comprehension of the interaction among these elements is also fundamental for the development of a successful WMP as each component may be the result of unique and sometimes intricate interactions among themselves. Knowing and managing a watershed means coming to understand not only the natural processes working within the watershed boundaries, but also human influences and the possible outcomes of this interaction. The keyword here is *integration*.

A WMP should contemplate, whenever possible and needed, other specific sectoral programs, practices, or plans, such as Forestry Management Plans – FMP or Rural Development Programmes – RDP. This integration of knowledge leads to the concept of IWMP[1].

The holistic approach necessary for the successful development and maintenance of a WMP offers the possibility of identifying and addressing issues that previously could not be tackled in traditional watershed management approaches. Moreover, through a continuous and cyclical process involved in the preparation of a WMP, and taking into account considerations from stakeholders [124], actions addressing the identification of issues and concerns can then be implemented, monitored, reported on, and updated as required in order to adapt to changes and new stressors, or for the implementation of better management practices [88].

Indeed, a WMP must be an instrument capable of adaptation. Similarly to the way living organisms adapt to their surrounding environment and to changes, WMPs must be well inserted in a watershed's environment by identifying and proposing sustainable solutions to the issues pertaining the management of a watershed, while, at the same time, be flexible enough in order to enable quick adaptive actions to be taken into consideration under new situations. Just like a law that becomes inefficient when is excessively complex, a WMP that is excessively complex lacks the ability of adaptation, being doomed to failure due to the inability in delivering lasting benefits [3]. The capability to adapt to new situations is one of the key principles of a successful WMP and is known as Adaptive Environmental Management – AEM [77, 27, 28].

The notion of AEM applied to WRM comes in handy in the era of the Anthropocene [29, 107]. Climate change is nowadays widely accepted as a fact by the scientific community, and the implications of a changing climate on the global hydrologic cycle and global water system have the potential to impact the regional and local management of watersheds at different scales [108]. As humans continue to influence the climate system, the global water system will likely continue to be influenced by changes in the climate system. Hence, adaptive

[1] Acknowledging the fact the integration is fundamental for the management of watersheds, this study considers the terms WMP and IWMP to be interchangeable, unless explicitly mentioned.

actions must be taken into account when developing a WMP in order to achieve the sustainable use of water resources.

In summary, a WMP should propose actions prioritising the integrated management of natural and water resources under a holistic perspective, aiming at the achievement of a sustainable watershed management and development. Consequently, the main goal of a WMP can be understood as the study and identification of the relevant aspects of a watershed aiming at the sustainable use, management and distribution of its resources by means of creating and implementing plans, programs, and projects to sustain and enhance watershed functions and services within the watershed's boundary [86].

1.2 Hydrologic Modelling

Hydrologic modelling is a very useful instrument for supporting the development of WMPs. Commonly, hydrologic modelling consist in the use of mathematical hydrologic models to simulate the hydrologic cycle. When applied at a watershed-level scale, these models are referred to as regional hydrologic models. Mathematical models of watershed hydrology can be employed to address a wide range of environmental and water resources issues. Depending on the complexity and level of detail of the model, it is possible to simulate not only the hydrologic cycle, but also hydrologic-related processes such as the transportation of sediments and nutrients throughout a watershed, vegetation and crop growth, and the provision of ecosystem services. Hence, the use of hydrological models as a support tool during the decision making process in a context of watershed management is an efficient and effective way of providing quantitative information about the dynamics of watershed.

As models are the representation of a system, hydrologic models are very useful to describe and explain phenomena that are of interest to the management of water resources and of watersheds in general. Not only, models in general allow the quantitatively exploration of situations that may be of interest to the system. For instance, hydrologic models can be used to assess the consequences of alternative management scenarios or Best Management Practices – BMPs, or

to assess the impacts of climate change in the management of a watershed by considering plausible future climate scenarios.

The science that studies the cycling of water in the natural environment (i.e. hydrologic cycle) is hydrology. In general, there seems to be a consensus that hydrology is a physical science, concerned mainly with the understanding of the water cycle of continental areas [23]. Being a natural phenomenon itself, the hydrologic cycle is governed by the principles of conservation of mass, momentum, and energy, which can be expressed by a number of equations that provide a mathematical description of the process [23]. Hence, at the global scale, a fundamental concept of the hydrologic cycle is that water is neither lost nor gained from Earth over time. However, the quantities of water in the atmosphere, surface water, soils, groundwater, and any other storage component of the hydrologic cycle are constantly changing because of its dynamic nature [22]. Therefore, based on the understanding the the hydrologic cycle follows the principle of the conservation of mass, the hydrologic balance of a watershed can be expressed as represented as follows:

$$\Delta S = P + GW_i - Q - ET - GW_o \tag{C1.1}$$

where P is the precipitation; GW_i is the groundwater flow entering the watershed; Q is the streamflow leaving the watershed; ET is the actual evapotranspiration; GW_o is the groundwater flow leaving the watershed, and; ΔS is the change in the amount of water stored in the watershed.

The water balance equation shown in Eq. C1.1 may appear simple, however, as the representation of a natural system is usually limited by the number of available or known conservation equations and the scale in which the problem is being mathematically represented, additional relationships must be introduced in order to account for these issues, a process known as parametrisation[2] [23].

Even though the hydrologic cycle can be seen as a natural process, hydrology may well be affected by human actions. The ability that humans have to change

[2]Parametrisation can be understood as a mathematical means of describing the relationships of phenomena occurring at different resolution scales than of the problem's resolvable scale variables. Parameters are usually based on experimentation and observation, and are one of the sources of uncertainty when using hydrologic models.

the landscape, for instance, is one of the many ways in which humans can affect the hydrologic cycle. Climate change, as already discussed, is another way in which humans are affecting the Earth's water circulation. Thereby, the prediction of the water cycle dynamics over long time-scales is not feasible without including the interactions and feedbacks with human systems [105]. One of the tools that allows the quantification of human impacts in the regional hydrologic cycle, be them from land-use or climatic changes, is the SWAT model, briefly introduced in the following Sub-Sections.

1.2.1 The SWAT Model

SWAT is a public domain eco-hydrological model jointly developed by the United States Department of Agriculture – USDA Agricultural Research Service – ARS and Texas A&M AgriLife Research, part of The Texas A&M University system [10]. The model has been systematically improved throughout the past decades by receiving contributions from users, universities and several other federal agencies from the United States, the most relevant being: the United States Environmental Protection Agency – EPA; the Natural Resources Conservation Service – NRCS; the Untied States National Oceanic and Atmospheric Administration – NOAA, and; the Bureau of Indian Affairs – BIA [83].

The SWAT model is written in Fortran language in a modular fashion [113]. Due to this feature, the model can run in any system configured with the required libraries to interpret Fortan language, even though some of developed user-interfaces requires the use of specific third-party software and operating system (e.g. [127], [33, 34], [1], and [43]). Some of the key-features of the SWAT model are that the model is physically based, it uses mostly readily available inputs, it is computationally efficient, and it enables the study of long-term impacts in the management of watersheds [83]. Currently, the model code is being reviewed, updated and expanded in order to better harmonise the data exchanges between the Agricultural Policy/Environmental eXtender – APEX and SWAT databases, and to enable parallel processing [115].

Regarding its applicability, SWAT is an eco-hydrological watershed-scale model which offers the capability of assessing the impacts of different watershed-related

management processes and operations, such as different crop rotation schedules, application of water for irrigation, and many other agriculture-related practices [83, 69]. The model is a very versatile tool and has been applied in an extensive array of studies, including land-use and climate change scenarios, alternative BMPs, and the simulation of the transport and movement of sediments, nutrients and pesticides throughout a watershed [21, 117, 2, 131, 73, 13]. Indeed, due to its versatility, the model has been widely used as a support tool for WRM not only in academic research but also by many governmental agencies, private companies and research institutes around the globe [92, 41, 63, 125].

For modelling purposes, the SWAT model considers a watershed as an area composed of a mosaic of smaller units, defined as sub-basins. Each sub-basin is host to a stream channel which is, in turn, connected to a downstream sub-basin's stream channel in such a way that the movement of water, nutrients, and other hydrologic-related processes is possible throughout the watershed's river network system, until eventually reaching the watershed's outlet. Each sub-basin is further spatially subdivided into smaller units known as Hydrological Response Units – HRUs [83, 127]. An HRU can be understood as a lumped land areas within a sub-basin that is comprised of unique combination of land cover, soil, slope, and management, which, altogether, consist the main inputs to the SWAT model [9]. Such subdivision enables the model to reflect differences in the hydrologic cycle for various crops and soils, both temporally and spatially.

The HRU is the basic computing unit of the SWAT model. In order to simulate the hydrologic cycle in a watershed, SWAT calculates first the hydrologic balance for each HRU, a process known as the *land phase*. Sequentially, the movement of water and other hydrologic-related processes (e.g. nutrients, sediments, etc.) is computed throughout the channel network of the watershed, in a process known as the *routing phase* [83]. The hydrologic balance of both process are briefly reviewed in the following sections in order to build the basis of the proposed SWAT model modifications, latter covered in the Sub-Section 1.2.2.

1.2.1.1 Land Phase

The SWAT model assumes water to be the main driver of energy circulating in a watershed, which, in turn, is the main driver for the movement of pesticides, sediments and nutrients in a river basin. In order to accurately simulate these processes, then, the simulated hydrologic cycle must conform to the actual water movement in the watershed [83]. The main equation describing the water balance as considered by the SWAT model is shown in Eq.C1.2, while Figure C1.1 depicts the available water pathways as considered by the SWAT model.

$$SW_t = SW_0 + \sum_{i=1}^{t} (R_{day,i} - Q_{surf,i} - E_{a,i} - w_{seep,i} - Q_{gw,i}) \tag{C1.2}$$

where i is the index for days; t is the current day of the simulation; SW_t is the soil water content on day t [mmH_2O]; SW_0 is the initial soil water content [mmH_2O]; $R_{day,i}$ is the amount of precipitation on day i that reaches the soil surface [mmH_2O]; $Q_{surf,i}$ is the amount of surface runoff on day i [mmH_2O]; $E_{a,i}$ is the amount of actual evapotranspiration on day i [mmH_2O]; $w_{seep,i}$ is the amount of water entering the vadose zone from the bottom of soil profile on day i [mmH_2O], and; $Q_{gw,i}$ is the amount of return flow on day i [mmH_2O].

When simulating the regional hydrologic cycle of a watershed, the SWAT model considers precipitation as the main mechanism of water transfer from the atmospheric phase to the land phase of the hydrologic cycle, as shown in Figure C1.1 and captured in Eq.C1.2. Indeed, precipitation in its different types affects the temporal and spatial distributions, and the quantity and quality of water stored in a watershed [22]. Hence, a correct representation of precipitation is fundamental for the study of hydrology, and consequently to hydrological modelling and IWM. Although capable of simulating precipitation events, it is recommended the use of measured precipitation data when using the SWAT model to simulate the water balance of a watershed.

Not all the amount of water that precipitates from the atmosphere reaches the ground. The SWAT model considers that canopy interception reduces the total amount of rainfall by trapping a portion of this total [83]. The model

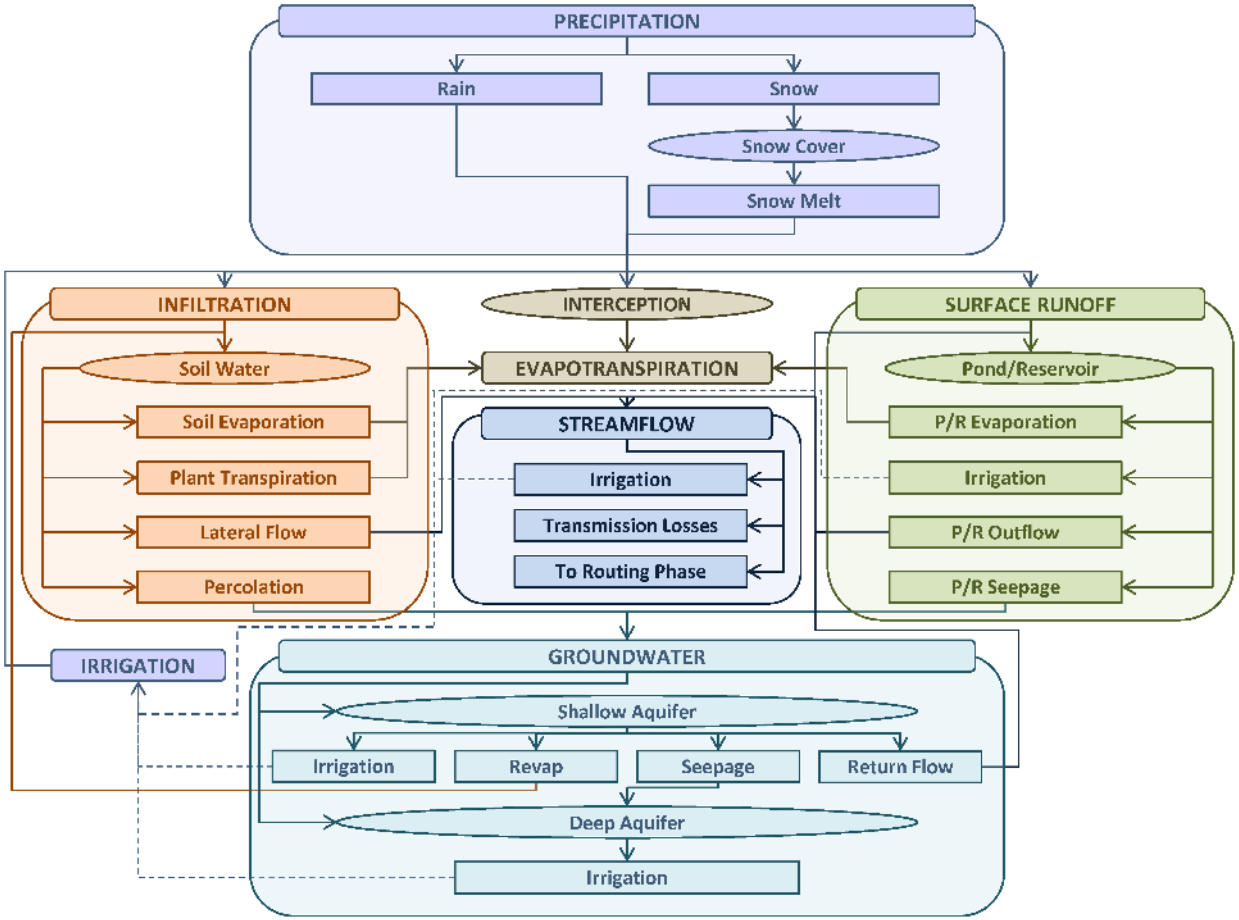

Adapted from: Neitsch et al. [83]

Figure C1.1: Flowchart depicting the land phase processes as considered by the SWAT model.

considers the amount of intercepted water to be stored in a "reservoir" defined as canopy storage. The maximum size of the canopy storage reservoir in an HRU is a function of the density and type of vegetation cover, which is variable throughout the simulation period. The SWAT model assumes that the amount of water stored during the interception process will never reach the ground, being only consumed during the evapotranspiration process. Consequently, $R_{day,i}$ is a function of the total precipitation amount and the size of the canopy storage reservoir [83].

Other less relevant inputs to the hydrologic cycle are also contemplated by the SWAT model, namely point source discharges and irrigation. As considered by the model, point source discharges do not cycle directly within the land phase of the hydrologic cycle, being added as a direct input to the routing phase (see Figure C1.1). Water coming from irrigation applications, instead, is applied directly to the soil surface and will circulate within the regional hydrologic cycle. Although not explicitly depicted in the schematic representation shown in Figure C1.1, irrigation water can be either an input to Eq.C1.2 if the water source is an unlimited source outside the watershed, or a recirculation mechanism if the water source is internal to the watershed [9].

After accounting for the main inputs to the water balance equation, the SWAT model computes the outputs of the equation, namely surface runoff $Q_{surf,i}$, evapotranspiration $E_{a,i}$, percolation $w_{seep,i}$, and return flow $Q_{gw,i}$. The SWAT model provides two methods for the estimation of the surface runoff, namely the SCS Curve Number – SCS CN procedure[3] [104], and the Green & Ampt Infiltration method [55]. The SCS CN procedure is calculated as follows:

$$Q_{surf,i} = \frac{(R_{day,i} - I_{a,i})^2}{(R_{day,i} - I_{a,i} + S_i)} \tag{C1.3}$$

and:

$$S_i = 25.4 \cdot \left(\frac{1000}{CN_i} - 10\right) \tag{C1.4}$$

where $I_{a,i}$ is the initial abstractions (e.g. canopy storage) on day i [mmH_2O];

[3] All the case studies covering the utilisation of the SWAT model in this dissertation rely on the use of the SCS CN procedure for the estimation of surface runoff.

S_i is the retention parameter on day i [mmH_2O], and; CN_i is the curve number[4] on day i.

If the HRU being simulated by the SWAT model is a superficial water body (e.g. reservoir), then water may accumulate in the HRU. In that case, water may also evaporate, returning to the atmospheric phase of the hydrologic cycle. Similarly, in HRUs covered by land water may evaporate from the top soil layers or be transpirated by the vegetation covering the HRU. The summation of evaporation and transpiration is defined as evapotranspiration, and can be estimated in a number of ways. The SWAT model incorporates three methods for the estimation of the potential evapotranspiration [83], namely: i. The Penman-Monteith method [81, 6]; ii. The Priestley-Taylor method[5] [97], and; iii. The Hargreaves method [57]. The Penman-Monteith method is mathematically described as:

$$E_{a,i} = \frac{\Delta_i \cdot (H_{net,i} - G_i) + \rho_{air,i} \cdot c_{p,i} \cdot \left(\frac{e^o_{z,i} - e_{z,i}}{r_{a,i}} \right)}{\left[\Delta_i + \gamma \cdot \left(1 + \frac{r_{c,i}}{r_{a,i}} \right) \right] \cdot \lambda_v} \tag{C1.5}$$

where $E_{a,i}$ is the evapotranspiration on day i [mmH_2O]; Δ_i is the slope of the saturation vapour pressure-temperature curve on day i [kPa °C^{-1}]; $H_{net,i}$ is the net radiation on day i [MJ m^{-2}]; G_i is the heat flux density to the ground on day i [MJ m^{-2}]; $\rho_{air,i}$ is the air density on day i [kg m^{-3}]; $c_{p,i}$ is the specific heat of air at constant pressure on day i [MJ kg^{-1} °C^{-1}]; $e^o_{z,i}$ is the saturation vapour pressure of air at height z on day i [kPa]; $e_{z,i}$ is the water vapour pressure of air at height z on day i [kPa]; γ is the psychrometric constant [kPa °C^{-1}]; $r_{c,i}$ is the plant canopy resistance on day i [s m^{-1}]; $r_{a,i}$ is the aerodynamic resistance on day i [s m^{-1}], and; λ_v is the latent heat of vaporisation [MJ kg^{-1}].

The water that does not runoff or is lost to evapotranspiration can remain in the soil profile, flow laterally and add to the streamflow, or percolate past the bottom of the soil profile. The water that leaves the soil profile through percolation is added to the aquifer system of the watershed. The SWAT model

[4] The CN_i is a function of the soil's properties, land-use, terrain slope, and antecedent soil water conditions.

[5] All the case studies covering the utilisation of the SWAT model in this dissertation rely on the use of the Penman-Monteith method for the estimation of evapotranspiration.

the aquifer system of a sub-basin as a composition of two distinct yet connected groundwater systems: a shallow aquifer and a deep aquifer [9, 83].

The shallow aquifer is an unconfined aquifer system and is basically interpreted as an underground reservoir of water by the SWAT model. Water may leave this groundwater system in a number of ways. Naturally, water from the shallow aquifer may contribute to the streamflow of the main channel of the sub-basinin in which this groundwater system is located. Alternatively, water from the shallow aquifer may further percolate, recharging the deep aquifer system. Still, water may move from the shallow aquifer to the overlying unsaturated zone through capillarity, a process known as *revap* in the SWAT methodological framework, as shown in Figure C1.1. Finally, water may be pumped from the shallow aquifer for irrigation purposes.

Differently from the shallow aquifer, that is well integrated in the hydrologic balance of a watershed, the deep aquifer is considered to be a confined aquifer system, meaning that this aquifer system does not directly contribute to the streamflow of the simulated watershed, contributing only to flows somewhere outside of the watershed [8]. The only way to recirculate the water stored in the deep aquifer is through irrigation, as shown in Figure C1.1.

In general terms, the water balance equation considered by the SWAT model (i.e. Eq.C1.2) is very similar in structure to Eq. C1.1, the main difference being that Eq. C1.1 considers not only precipitation as a main hydrological input to the water balance of a watershed, but also groundwater flow that may be entering the watershed from external sources. This input may be relevant in cases where the hydrologic balance of a watershed is highly influenced by groundwater systems covering an area that differs from the area covered by the watershed of interested, a process known as Interbasin Groundwater Flow – IGF [128, 51, 50]. A case study exploring a similar situation is discussed in the Chapter 3 of this dissertation.

1.2.1.2 Routing Phase

Routing can be understood as the process of estimating the flow hydrograph of a channel at a certain section by making use of known flow hydrographs at one or more upstream sections. In order to perform the routing calculations, the

SWAT model first connects each sub-basin's main channel in such a way that each sub-basin has only one outlet and ensuring that water flows from the higher to the lower areas until reaching the watershed's outlet. After the channel network is defined, the SWAT model routes water throughout the channel network by using either the variable storage routing method[6] or the Muskingum river routing method [83].

Similarly to the land-phase, the SWAT model utilises a water balance equation to compute the changes in the amount of water stored in a channel during the simulation procedure. The channel water balance equation used by the SWAT model is shown in Eq.C1.6, while Figure C1.2 depicts a schematic representation of this equation.

$$V_t = V_0 + \sum_{i=1}^{t} (V_{in,i} - V_{out,i} - t_{loss,i} - E_{ch,i} + V_{div,i} + V_{bnk,i}) \qquad \text{(C1.6)}$$

where i is the index for days; t is the current day of the simulation; V_t is the volume of water stored in the reach on day t [m^3 H_2O]; V_0 is the initial volume of water stored in the reach [m^3 H_2O]; $V_{in,i}$ is the volume of water flowing into the reach on day i [m^3 H_2O]; $V_{out,i}$ is the volume of water flowing out of the reach on day i [m^3 H_2O]; $t_{loss,i}$ is the volume of water lost from the reach via transmission through the channel bed on day i [m^3 H_2O]; $E_{ch,i}$ is the evaporation from the reach on day i [m^3 H_2O]; $V_{div,i}$ is the volume of water added to or removed from the reach on day i [m^3 H_2O], and; $V_{bnk,i}$ is the volume of water added to the reach via bank storage return flow on day i [m^3 H_2O];

The volume of water entering a reach $V_{in,i}$ is a function of the streamflow contributions coming from the water balance calculations for each HRU in the sub-basin as performed in the land phase (see Figure C1.1), and the volumes of water coming from upstream channels as calculated in the routing phase. The volume of water leaving the channel water storage $V_{out,i}$ depends on the routing method employed during the simulations. If the variable storage routing method

[6] All the case studies covering the utilisation of the SWAT model in this dissertation rely on the use of the variable storage routing method for the routing of water throughout the watershed's channel network.

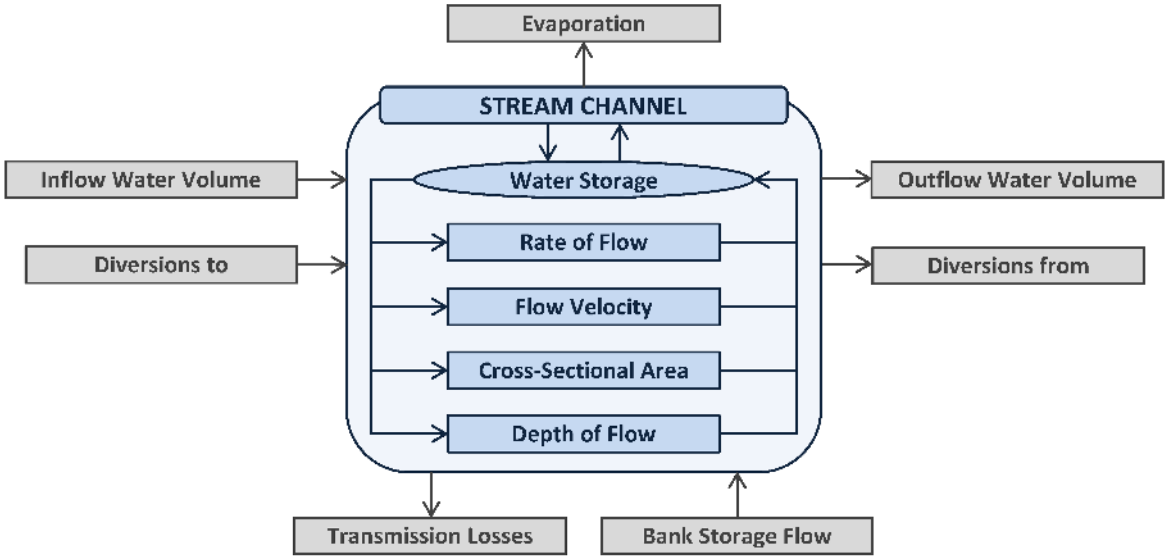

Adapted from: Neitsch et al. [83]

Figure C1.2: Channel water balance during the routing phase as considered by the SWAT model.

is chosen, then $V_{out,i}$ is a function of $V_{in,i}$ and the initial volume of water stored in the channel V_0.

Transmission losses $t_{loss,i}$ can be understood as the water that leaves a stream channel due to infiltration into the bed, the banks, and the flood plain [85]. These losses occur during dry periods when a stream does not receive groundwater flow contributions [83]. The SWAT model assumes that transmission losses will either recharge the deep aquifer or enter bank storage. The water that is stored in the bank storage, in turn, may return to the main channel as the return flow to reach from bank storage $V_{bnk,i}$ or move to an adjacent unsaturated zone.

Water stored in a channel may also be removed due to evaporation $E_{ch,i}$. The SWAT model estimates that the amount of water removed due to evaporation is a function of the potential evaporation for the day in the channel and the channel characteristics, such as length and width [83].

Finally, water may also enter or leave a reach due to diversions. The volume of water that is diverted to or from a reach on a given day $V_{div,i}$ is a function of a number of other processes simulated by the SWAT model. Examples of these processes include irrigation diversion, point source discharges, and water withdrawals for human consumption.

1.2.2 Modifications in the SWAT Model

The SWAT model is a very useful yet complex eco-hydrological model. Even if the model is capable of covering a variety of processes, ranging from the simulation of how hydro-meteorological variables can affect the rainfall-runoff process to the consideration of how different land management processes can affect the hydrologic cycle, some improvements can be made in order to better account for the direct or indirect anthropogenic effects on the hydrologic cycle, such as the removal of water for irrigation and the effects of a higher concentration of carbon dioxide in the atmosphere. This section, then, presents the proposed modifications in the SWAT model source code.

1.2.2.1 The CO_2 Fertilization Effect

As already discussed in the previous sections, climate change has the potential to affect the hydrologic cycle by unbalancing the Earth's energy budget, mainly due to the intensification of the greenhouse effect by an increased concentration of GHGs, such as carbon dioxide. The increased concentration of CO_2 in the atmosphere, however, does not influence only the climate. Being an essential component of photosynthesis, the higher concentration of CO_2 in the atmosphere has led the scientific community during the past few decades to study the possible effects of this change in plant growth and development (e.g. [65], [61], [5], [68], [79] and [75]). Under ideal conditions, it is estimated that plant growth and yield can typically increase to more than 30% with a doubling of CO_2 atmospheric concentration (i.e. from 280 p.p.m.v. to 560 p.p.m.v.) [67]. Moreover, elevated atmospheric CO_2 concentrations can lead to a remarkable increase in Leaf Area Index – LAI and Leaf Area Duration – LAD of plants, possibly increasing the carbon gain during the growth stage of crops and ultimately resulting in higher yields and biomass production [72, 70].

Interestingly, a higher concentration of CO_2 in the atmosphere can also affect the evapotranspiration process. Higher concentration levels of CO_2 in the atmosphere allows plants to generally open less their leaf stomatal pores than they do at lower CO_2 concentrations [76]. This change allows plants to reduce their water loss by transpiration while, at the same time, increase the amount of carbon plants can gain per unit of water consumed, a concept known as Water-Use Efficiency – WUE. It is estimated a consistent decrease in actual evapotranspiration ranging from 5% to 20% at elevated CO_2 concentration levels [66, 70]. Furthermore, the effect of decreased evapotranspiration at elevated CO_2 concentration levels can also lead to an increase in soil moisture [70], as less water is consumed from the soil profile. If true, this process can result in plants being less susceptible to negative effects of dry spells during the growing season.

The SWAT model acknowledges that a higher concentration of CO_2 in the atmosphere can affect the growth process of plants by incorporating two equations: i. The first equation (Eq. C1.7), proposed by Easterling et al. [36], accounts for the impact different CO_2 atmospheric concentration levels on leaf conductance,

and; ii. The second equation (Eq. C1.8), proposed by Stockle et al. [109], accounts for the impact of different CO_2 atmospheric concentration levels on Radiation-Use Efficiency – RUE of plants. Both equations are shown below.

$$g_{\ell,CO2} = g_{\ell} \cdot \left[1.4 - 0.4 \cdot \left(\frac{CO_2}{330}\right)\right] \tag{C1.7}$$

where $g_{\ell,CO2}$ is the leaf conductance modified to reflect the effects of higher concentration levels of CO_2 in the atmosphere [m s^{-1}]; g_{ℓ} is the effective leaf conductance [m s^{-1}], and; CO_2 is the atmospheric concentration of carbon dioxide in the atmosphere [p.p.m.v.].

$$RUE = \frac{100 \cdot CO_2}{CO_2 + e^{(r_1 - r_2 \cdot CO_2)}} \tag{C1.8}$$

where RUE is the radiation-use efficiency of the plant [kg ha^{-1} $(MJ/m^2)^{-1}$], and; r_1 and r_2 are shape coefficients.

Both Eq. C1.7 and Eq. C1.8 were developed for a CO_2 ranging between 330-660 p.p.m.v., being not recommended their use outside this range. In fact, as shown in Eq. C1.7, the SWAT model assumes a value of 330 p.p.m.v. to be the minimum possible value for CO_2. In case a value lower than 330 p.p.m.v. is read by the model, no adjustment is done.

By the expression presented in Eq. C1.7, an increase in the concentration of CO_2 in the atmosphere will lead to a decrease in the leaf conductance of a plant $g_{\ell,CO2}$. The $g_{\ell,CO2}$ is the inverse of the effective stomatal resistance of a single leaf r_{ℓ}, which, in turn, is a variable used for the calculation of the plant canopy resistance r_c, as follows:

$$g_{\ell} = \frac{1}{r_{\ell}} \tag{C1.9}$$

$$r_c = \frac{r_{\ell}}{0.5 \cdot LAI} \tag{C1.10}$$

where r_{ℓ} is the effective stomatal resistance of a single leaf [s m^{-1}]; r_c is the plant canopy resistance [s m^{-1}], and; LAI is the leaf area index of the canopy.

Consequently, an increase in the concentration of CO_2 in the atmosphere will lead to an increase in the plant canopy resistance r_c, ultimately leading to a

decrease in the evapotranspiration amount $E_{a,i}$, according to Eq. C1.5.

Regarding the RUE, Eq. C1.8 indicates that an increase in the atmospheric concentration of CO_2 leads to an increase in the RUE, which, in turn, affects the potential increase in total plant biomass Δbio and total plant biomass bio, as follows:

$$\Delta bio_i = RUE \cdot H_{phosyn,i} \tag{C1.11}$$

$$bio = \sum_{i=1}^{t} \Delta bio_i \tag{C1.12}$$

where i is the index for days; t is the current day of the simulation; RUE is the radiation-use efficiency of the plant [kg ha^{-1} (MJ/m^2)$^{-1}$]; $H_{phosyn,i}$ is the amount of intercepted photosynthetically active radiation on day i [MJ m^{-2}]; Δbio_i is the potential increase in total plant biomass on day i [kg ha^{-1}], and; bio is the total plant biomass on day t [kg ha^{-1}].

Consequently, an increase in the concentration of CO_2 in the atmosphere will lead to an increase in the radiation-use efficiency of the plant RUE, ultimately leading to an increase in the total plant biomass bio.

Interestingly, the SWAT model assumes that the concentration of CO_2 in the atmosphere is variable in space but not in time. Based on the concept that the concentration of CO_2 in the atmosphere is relatively homogeneous throughout the globe due to the fact that a typical molecule of CO_2 stays in the atmosphere for more than a century [59], this dissertation proposes a modification in the SWAT model source code to account for changes in the concentration of CO_2 in time, while keeping it spatially constant. The proposed change assumes that the concentration of CO_2 is updated at the beginning of each year during the simulation process, remaining constant throughout the year, even if in reality the concentration of carbon dioxide in the atmosphere is known the sightly vary according to the seasons [64, 116]. The observed values used as reference for the CO_2 concentration in the atmosphere were obtained as measured by the Mauna Loa Observatory – MLO [114], while the carbon dioxide concentration values for the considered RCPs (i.e. 4.5 [25, 106, 130] and 8.5 [98]) were obtained from

the Coupled Model Intercomparison Project – CMIP5 RCP Database [26]. The proposed code modifications can be seen at Appendix 1 – The CO_2 Fertilization Effect.

1.2.2.2 Irrigation

As depicted in Figure C1.1, irrigation is the only anthropogenic process fully incorporated into the available water pathways during the estimation of the hydrologic balance as considered by the SWAT model. Moreover, irrigation operations are capable of interacting with all major process of the hydrologic cycle on land, such as surface runoff, while being the only process capable of recirculating water from the deep aquifer into the watershed [83]. In fact, of such importance can be the irrigation process that the water budget in watersheds where irrigation is used as an extensive agricultural practice can be drastically affected [56, 112, 71].

The SWAT model allows farmers to apply irrigation water to their crops in two different ways: i. The first one, defined as *manual irrigation*, by following a schedule of specific dates, and; ii. The second one, defined as *auto-irrigation*, that is triggered depending on the water stress of crops or soil water deficit. The irrigation water may come from 5 distinct sources, as follows: a reach, a reservoir, a shallow aquifer, a deep aquifer, or a source outside the watershed [83].

If the source or irrigation water is a reach, a shallow aquifer, or a deep aquifer, the water is taken from the source located in the sub-basin from which the HRU demanding irrigation water belongs. If the source is a reservoir, the reservoir from which water is taken must be specified. Still, if the irrigation water source is a reach, the model allows the user to define some parameters that allows the setting of a minimum in-stream flow before, a maximum irrigation water removal amount per day, and a percentage of the total flow in the reach that is available for removal on any given day. These parameters prevent the over-exploitation of water from a reach. Finally, the model also takes into consideration the efficiency of irrigation water applications, which is seen as a function of the conveyance efficiency and the field application efficiency[7].

[7] Conveyance efficiency represents the efficiency of transportation of irrigation water from

By reviewing the SWAT model source code, three issues can be identified with the simulation of irrigation operations:

1. Currently, the model consider that irrigation water losses can be converted only to surface runoff;

2. When auto-irrigation takes place and the source is a reach, a shallow aquifer, or a deep aquifer, the amount of water removed from the source can be different from the amount of water that is taken for the irrigation operation, and;

3. The irrigation procedure is not computed as a single operation, meaning that different configurations of irrigation (e.g. manual or auto-irrigation, water sources, etc.) are calculated by different sub-routines.

The first issue with the irrigation procedure as considered by the SWAT model is a limitation of the model, that assumes that water losses coming from irrigation operations can be converted only to surface runoff, the difference (if any) being removed from the system. The second issue is somehow worrisome as it basically violates the law of conservation of energy and mass. Note that this item is different from the concept of water losses due to the efficiency of irrigation applications, where losses to evapotranspiration and infiltration are computed. This issue basically occurs because the SWAT model computes first the amount of water applied to the field (taking into account the irrigation efficiency), and later computes the amount of water removed from the source. Finally, the third issue is nothing more than a topic pertaining to good programming practices. Considering that and irrigation operation (i.e. application of water to land) is the same independently of which water source or type of schedule is used (i.e. manual or automated operation), it makes sense to write a single function to compute this procedure.

Taking into account the discussed model limitations, it is proposed an update to the sub-routine responsible for simulating irrigation applications by the SWAT model. The proposed updated irrigation sub-routine tackles the identified issues

the source to the field. Field efficiency represents the efficiency of the application of irrigation water in the field.

by: i. Integrating the irrigation application into a single sub-routine, called *irrigation.f*; ii. Proposing a new sub-routine, called *irr_source.f*, that is responsible for processing all the specific tasks of the different water sources; iii. Incorporating two new variables, the first called *tird* responsible for storing the total amount of water removed from the source, and the second called *lird* responsible for storing the amount of water lost due to lack of efficiency in the irrigation system that is not converted to surface runoff, and; iv. reordering the irrigation process to better reflect how irrigation is actually performed in the field (i.e. first the removal of water from source is computed, then the water that is available for irrigation is computed).

The proposed modifications in the simulation of irrigation processes assumes that the water losses due to lack of efficiency will recharge the shallow aquifer, being, then, incorporated into the land phase of the hydrologic cycle as shown in Figure C1.1. The proposed modifications can be seen in Figure C1.3, which depicts a comparison of the irrigation process when the source is a reach for the original irrigation procedure, on top, and the proposed updated irrigation procedure, on bottom. The proposed code modifications, instead, are shown in Appendix 1 – The Irrigation Process.

A description of the variables shown in Appendix 1 – The Irrigation Process is presented as follows: $Flow$ is the current streamflow [m^3 s^{-1}]; $Flow_{min}$ is the minimum streamflow allowed for the reach [m^3 s^{-1}]; wtr_{avail} is the amount of water available to be used from the source for irrigation [m^3 d^{-1}]; div_{max} is the maximum amount of water that can be diverted from the source for irrigation [m^3 d^{-1}]; vmm is amount of water actually diverted from the source for irrigation [m^3 d^{-1} or mmH_2O]; $aird$ is the amount of irrigation water that is added to the soil profile and that can actually be used by crops [mmH_2O]; $qird$ is the amount of irrigation water that is lost to surface runoff [mmH_2O]; $lird$ is the amount of irrigation water that is lost due to lack of irrigation efficiency, being added to the shallow aquifer [mmH_2O]; $tird$ is the total amount of irrigation water that is diverted from the source [mmH_2O]; sq_{rto} is the fraction of irrigation water that is converted to surface runoff, and; irr_{eff} is the irrigation efficiency.

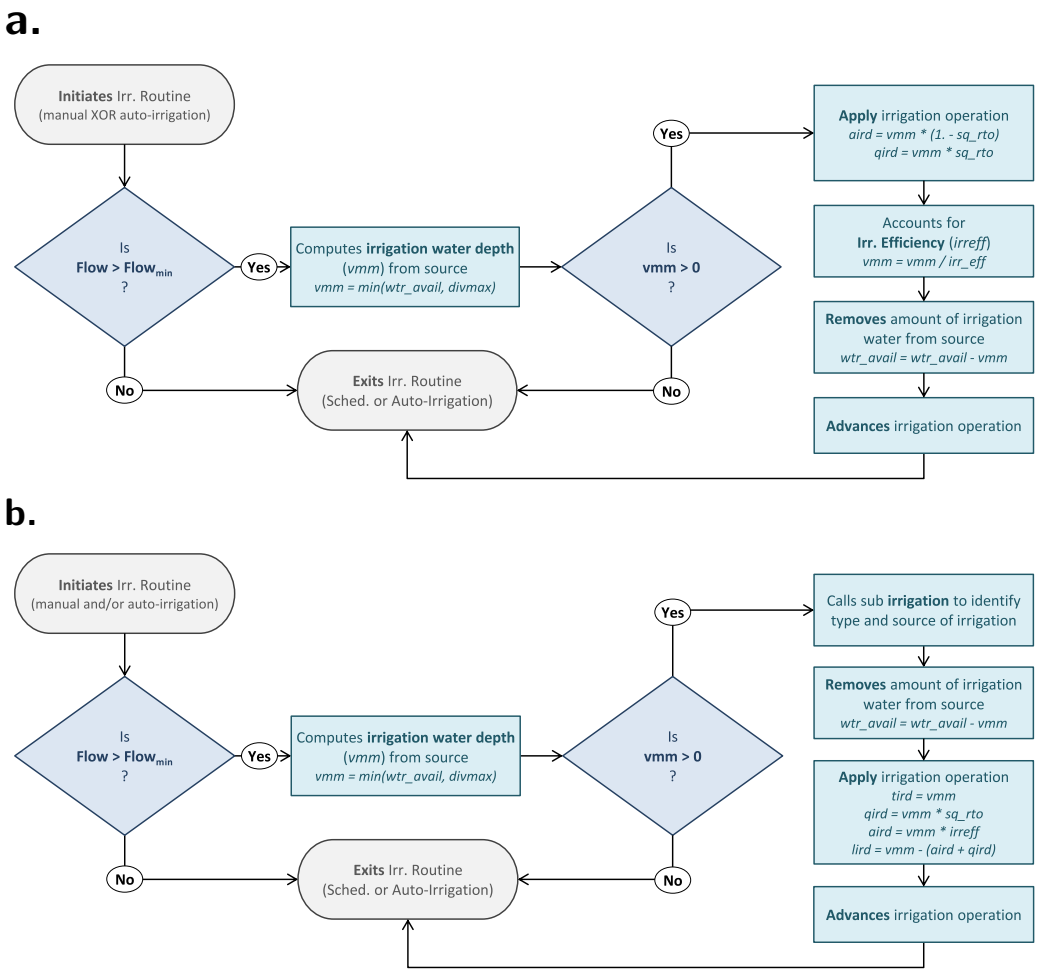

Figure C1.3: Comparison between how the irrigation process is considered by the SWAT model, on top, and the proposed updated version, on bottom.

1.2.2.3 Neural Networks

The ability to adapt to the surrounding environment is a key factor determining human evolution [129, 123]. However, not only do humans adapt to their surrounding environment, but they also have the capability of modifying the environment in order to better fit their needs [53, 74]. Leveraged by the increased understanding of human consequences on the global climate, the idea that humans are an important part of the environment in which they are inserted into and not only simply consumers of goods and services provided by it [95], has led the scientific during the past few decades to develop new concepts and sciences to better comprehend this complex interconnected system, such as the concept of *global water system* [121, 122, 4, 20] and the *socio-hydrology* science [105, 32]. Indeed, in a context o hydrologic modelling the idea of not considering possible consequences of human actions on the hydrologic cycle is infeasible, translating in the idea of *"stationary is dead"* [80].

As in any new research area that requires the development of concepts and the consolidation of theories in order to better cement the knowledge that builds the foundation of a new science, the realisation of how the relationships between human and biogeophysical systems is not yet completely understood and some issues still persist. One these issues is the inquiry whether it is possible, and if so, how to model human adaptation to climate change and how to capture the feedbacks between human actions and the climate system [91]. Two main challenges can be identified as hindrances that limit the current capability of modelling human adaptation to climate change. The first refers to the problem of capturing human decisions, a process that depends on human choices and behaviours which is per se uncertain [103]. The second challenge refers to the capability of identifying and describing the relationships between biogeophysical and socio-economic systems [91], and how changes in one system affect the other.

Different research areas have attempted to emulate human behaviour with vary degree of success by using different mathematical modelling techniques. For instance, when trying to capture individual's behaviour under climate change conditions, Agent Based Models – ABMs (e.g. [93], [102], and [15]) and integrated models (e.g. [62] and [45]) are popular choices. From the computational science,

attempts to simulate human decisions involve the use of fuzzy logic (e.g. [94]) and machine learning algorithms (e.g. [87], [90], [82], and [110]), such as ANNs.

ANNs are an interesting choice. This family of models is a technology born from the human attempt to translate the knowledge on how the human brain works into a quantitative model [58]. In fact, the understanding of how the human brain and nervous system work is quite challenging and is constantly evolving. The same is valid for ANNs models. Inspired by the operation of the natural nervous system, ANNs are capable of acquiring and storing knowledge from the surrounding environment, ultimately being capable of learning from this interaction. Indeed, the capability of learning is one of the most important and fascinating features of ANN models [126]. Together with the notion of learning comes the idea of adaptability. Similarly to the human brain, ANN models have the capability of adapting their synaptic weights according to their perception of the surrounding environment, a process know as training. From the notion of training, comes the concept of generalisation. A well trained ANN model must be able to generalise the problem to which they are applied, meaning that the model must be capable of producing reasonable outputs for input patterns which were not present during the learning phase of the model [60]. To some extent, this is a concept similar to certain human adaptation actions under an unknown future climate scenario.

The coupling of the SWAT and the ANN models, then, is proposed as a methodology capable of adding variability to specific anthropogenic processes that are likely to be altered in future socio-economic and climatic scenarios. By considering this approach, the notion of *"stationary is dead"* as proposed by Milly et al. [80] is taken into account, and variables that otherwise would be fixed in time or be input directly by the user can now be computed and altered accordingly to the outputs of an ANN model capable of adapting under new situations. Chapter 3 explores the feasibility of coupling both models, while Chapters 4 and 5, besides exploring some site-specific issues, makes use of this notion of adaptability.

A theoretical description of the developed ANN model is presented in Appendix 2. The source code of the model is available for consultation in Appendix 3. The modifications proposed in the SWAT model source code in order to accommodate

the coupling with the developed ANN model are shown in Appendix 1 – Coupling with ANN Model.

1.3 The VLW

The VLW is a drainage basin located in the Italian Region of Veneto, covering an area of approximately 1,850 km^2. This watershed represents the area where the surface water network flows into the Lagoon of Venice. The VLW is composed of 8 major sub-basins (covering around 90% of its total area) and 6 minor sub-basins [118]. Figure C1.4 shows the VLW and its sub-basins. The major sub-basins, from north to south, are: Vela; Dese-Zero; Marzenego; Naviglio-Brenta; Lusore; Fiumazzo; Montalbano, and; Trezze. The Avenale, Brenton del Maglio and Cambroso sub-basins, represented by the diagonal-lined polygons, contribute only partially to the overall water balance of the VLW. The dark grey area corresponds to the smaller sub-basins of the VLW. Figure C1.4 considers the overall operation of the VLW during ordinary flow conditions.

In its most northern/north-western region, the VLW is characterised by the influence of significant amounts of spring waters coming mainly from outside the watershed's land area. This mostly external contribution comes from an open aquifer originating in the Venetian high plains, playing an important role in the overall water budget and nutrient balance of the watershed [118, 100, 99, 13]. Being a diffuse source and coming from below the ground level, the quantification of the total spring water influx is a challenging task. Moreover, this contribution is also highly variable throughout a year, being dependent on the amount of water available on the aquifer, which, in turn, depends on past meteorological conditions and upstream withdrawals, among other factors [12, 44]. This complex and difficult to quantify water influx affects the management of the VLW and is one of the reasons why this watershed is characterised by a complex and intricate stream network system.

Nevertheless, due to the fact that the VLW is mainly a plain area and some of its area is actually bellow the sea level, land reclamation has played and still plays a central role in the configuration of the watershed, resulting in a complex

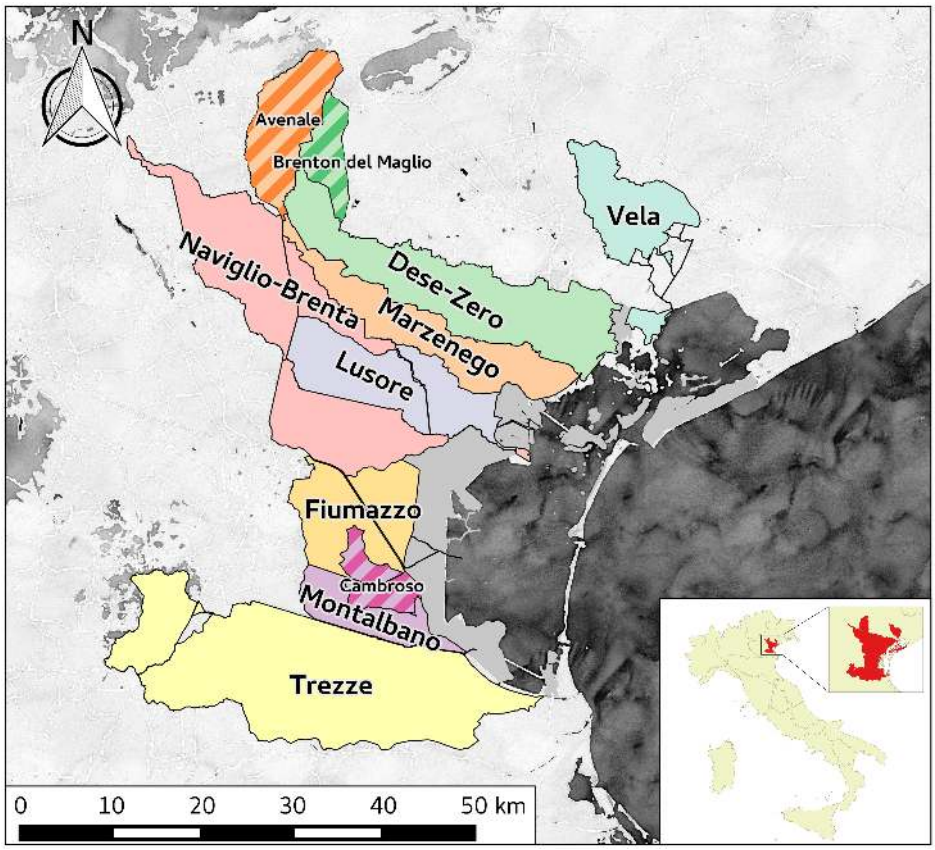

Data source: Veneto [119]

Figure C1.4: The VLW and its sub-basins.

environment that has been remarkably modified throughout the centuries. This intricate environment is the result of an incredible implementation of hydraulic engineering works that sums up to a length of approximately 20,000 km of canals, 400 draining pumps for water lifting, and thousands of hydraulic control devices, ultimately resulting in a complex yet fascinating system [16]. Besides land reclamation, irrigation has historically and consistently played a crucial role in promoting the economic development and, consequently, in the configuration of the VLW, allowing for greater income security in a complex physical environment [18].

Several of the implemented hydraulic works, such as modifications in the superficial water pathways and the implementation of hydraulic devices, are spread around the watershed in order to either limit or assist the flow of water in channels. This is specially true in the areas closer to the Lagoon of Venice, as these areas are characterised by depressions on the surface terrain (some of which are below the mean sea level), modest slopes, and thin soil. Combined, these characteristics make the natural drainage of surface water a very difficult task [89]. This is one of the reasons why the VLW is managed by a complex hydraulic system, requiring the operation of specific hydraulic devices in areas that are often subject to mechanical drainage. As a matter of fact, the mechanical lifting of water is an indispensable instrument for the management of flood safety in the VLW. It is estimated that about 44% of the VLW's hydraulic devices are located in areas below the sea level, while more than 63% of the mechanical lifting devices are located in areas not higher tahn just 2.5 m.a.s.l. [16].

Figure C1.5 depicts the Digital Elevation Model – DEM of the VLW, indicating how plain the terrain is and how extensive the areas subject to mechanical drainage can be.

Indeed, the VLW is a very complex environment well worthy of complex management solutions. In general terms, the general hydraulic management of the VLW can be divided in two distinct phases: one during low-flow conditions and another during high-flow conditions. The low-flow phase is understood as streamflow under ordinary conditions VLW [16]. The contrast between the two hydraulic management phases of the VLW is such to the point that, during the high-flow phase, the totality of some sub-basins' open channel flow is diverted to

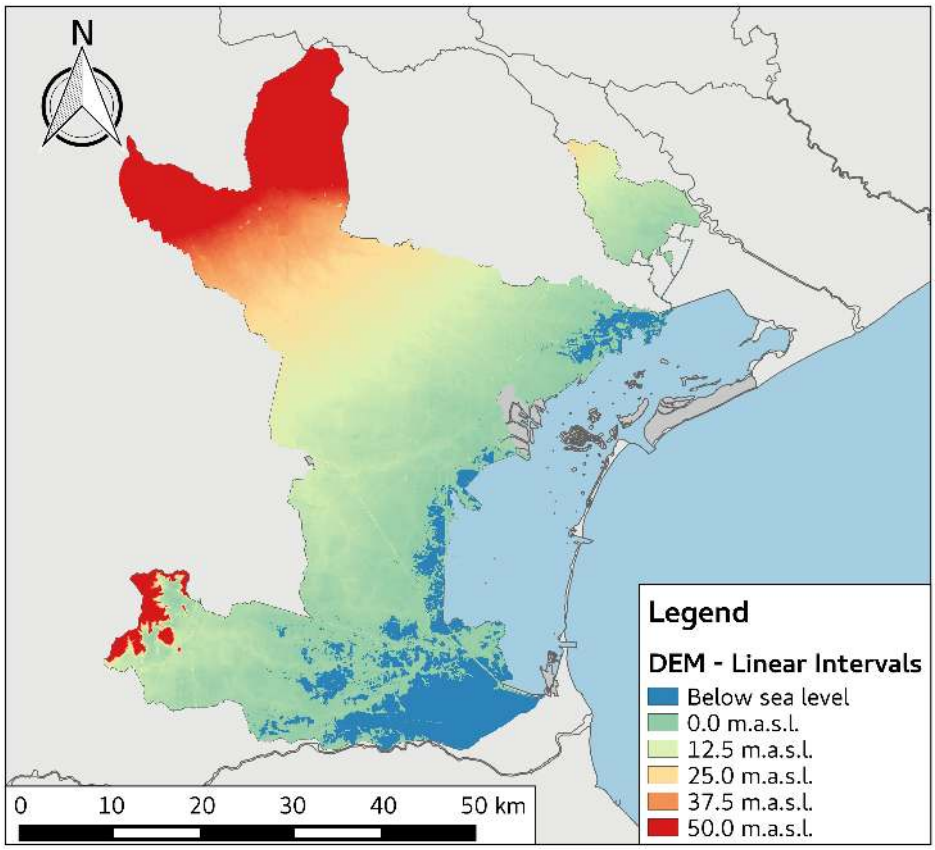

Data source: Veneto [119]

Figure C1.5: Elevation map of the VLW.

neighbour river basins which do not discharge in the Lagoon of Venice [17]. This artificially-driven water pathway is responsible for the dynamic behaviour of the VLW, creating a dynamic watershed that has a maximum contribution area of 2,006.5 km^2 during ordinary flow conditions, and a minimum area of 1,853.4 km^2 during the high-flow phase [17].

Two are the elements that mainly affect the hydraulic management of the VLW, namely: i. The streamflow levels of the rivers belonging to the VLW, and; ii. The total amount of water entering the watershed from external sources [12]. The external sources, in turn, can be segregated into two major groups, namely: i. Incoming groundwater sources, and; ii. Artificially controlled streamflow coming from the surrounding watersheds. Figure C1.6 shows the location where most of the groundwater contribution takes place in the VLW, as well as the approximate location of some of the most relevant hydraulic devices. The hydrography represented by the blue lines in Figure C1.6 depicts the streams of interest to the Directive 2000/60/EC, while the hydrography represented by the red-dashed lines indicates the rivers which do not belong to the VLW [16]. The groundwater recharge area is represented by the blue dotted-polygon to the north of the watershed while the spring belt is the area between the two thick blue lines, to the south of the groundwater recharge area [120].

In average values, the majority of the external water volume entering the VLW from external sources comes from the aquifer system depicted in Figure C1.6. This aquifer is characterised for being an open and deep aquifer system, located mainly to the north/north-west of the VLW in the Venetian high plains. The depth of this aquifer may go down to a hundred metres, especially in its most northern section [12]. Southwards, closer to the VLW's borders, the depth of this aquifer system consistently decreases until reaching a transitional region between the Venetian high plains and the Venetian lowlands (the so-called *'media pianura Veneta'*). At this point, the aquifer's water table intersects the surface topography, originating the spring area as show in Figure C1.6 [12]. The spring belt area is characterised by the presence of several river sources. Due to its nature, rivers originating in this area are referred to as resurgence rivers.

In general terms, the groundwater recharge process of this aquifer is characterised by a bimodal system, composed of two low groundwater level phases and

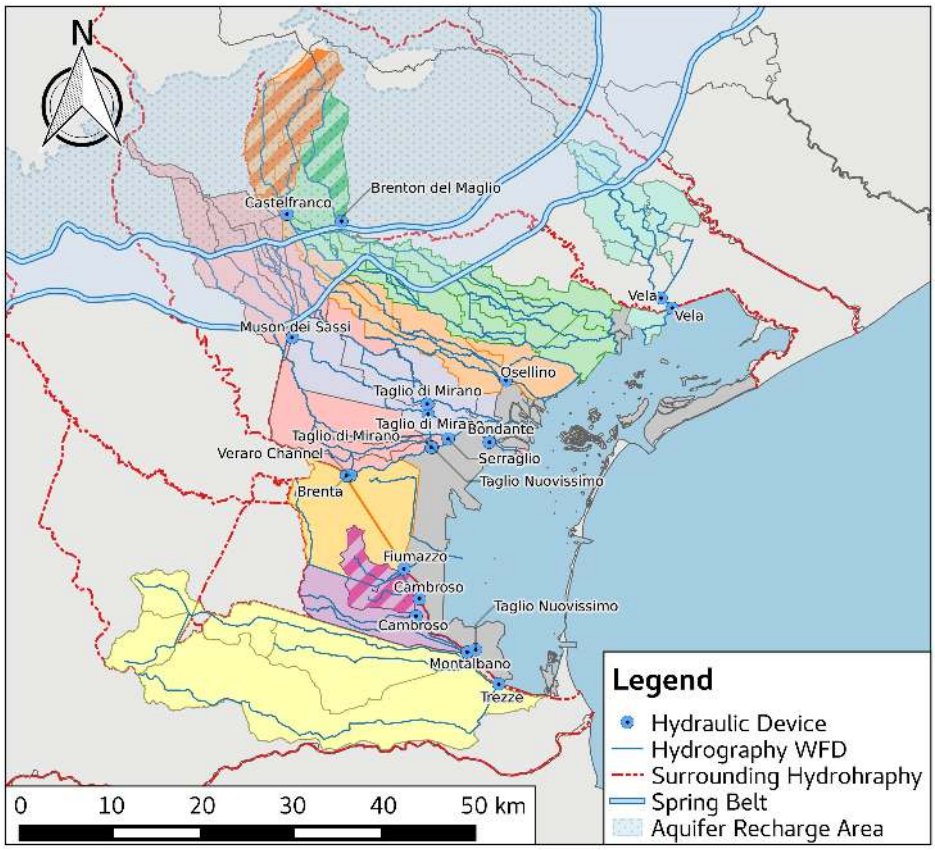

Data source: Veneto [119]

Figure C1.6: Main hydrologic features of the VLW.

two peak groundwater level phases. The first peak groundwater level phase can be identified during the late-spring and is linked with the snow-melting process taking place in the Dolomites. The second peak groundwater level phase, instead, is usually less pronounced and commonly identified around autumn, when precipitation amounts are usually more pronounced over the North-Eastern Italy [12]. In average terms, the annual precipitation amount in the VLW varies from about 700 mm in its most meridional part to 1,000 mm in its most septentrional part [11, 89]. Usually, the period around November is known to be the wetter in the VLW area. The average monthly temperature, instead, varies from a minimum average of approximate 3.0 °C in January to a maximum of 24.0 °C in July [11].

The second major external water source to the VLW is the artificially controlled superficial flow deviated either from bordering watersheds or watersheds that contribute only partially to the water budget of the VLW. Figure C1.4 shows the three watersheds that contribute only partially to the VLW. The artificial management of these sub-basins affect mainly the Dese-Zero, the Marzenego, and the Montalbano watersheds. The main artificial external water sources to the Dese and Marzenego rivers come from deviations of the Avenale watershed, which covers an area of approximately 100 km^2. Similarly, the Brenton del Maglio watershed, which covers an area of approximately 45 km^2, can be controlled to discharge its waters in either the Zero river or the Sile drainage network. Finally, the main artificial external water source to the Montalbano watershed comes from the Cambroso sub-basin. The Avenale and Brenton del Maglio watersheds contribute only partially to the VLW, as part of its hydraulic contribution is directed to channels which do not discharge in the Venice Lagoon. Similarly, roughly half of the superficial water flow coming from the Cambroso sub-basin is deviated to the Brenta-Bacchiglione system, the rest being directed to the VLW. Table C1.1 shows an estimate of the streamflow partitioning of those watersheds during the two distinct flow conditions of the VLW.

During dry periods, the return flow coming from the aquifer system shown in Figure C1.6 might not be enough to grant an optimal supply of water for the needs of some of the VLW's sub-basins. Consequently, the artificially controlled superficial flow in the VLW exert a fundamental role in maintaining a satisfactory streamflow level for the whole watershed [118]. Usually, dry periods in the VLW

Table C1.1: Flow partition estimates in the VLW.

Sub-basin	Low-Flow			High-Flow		
	VLW	Brenta-Bacchiglione	Sile	VLW	Brenta-Bacchiglione	Sile
Avenale	25%	75%	0%	12%	88%	0%
Brenton del Maglio	33%	0%	67%	33%	0%	67%
Cambroso	50%	50%	0%	0%	100%	0%
Muson Vecchio	100%	0%	0%	83%	17%	0%
Tergola	100%	0%	0%	0%	100%	0%
Trezze	100%	0%	0%	75%	25%	0%

Adapted from: Bixio et al. [17]

are verified during the spring and summer seasons, when the amount of water withdrawals increase not only because of the higher rate of evapotranspiration, but also because of the increased water intake due to irrigation use for agricultural practices [17]. In order to deal with this particular issue, an irrigation schedule based on rotational turns currently takes place in the VLW, considering specific factors, such as water needs of the crops, soil characteristics, and the availability of water [18, 96]. Interestingly, this same intricate hydraulic control system enables the administration of the VLW streams system when the availability of water is high, raising concerns related to floods. Under these situations, the controlled hydraulic devices can work as a flood control system by not allowing water intake from bordering watersheds and by transposing water volumes from one drainage network system to another when streamflow levels are dangerously high.

Due to its complexity, the VLW is managed by a number of watershed districts, even though it is formally part of a larger watershed district known as the Eastern Alps River Basin District – EARBD. The most relevant watersheds districts are [89]:

1. Dese-Sile, covering most of the Dese-Zero and Marzenego watersheds, and parts of the Vela watershed;

2. Adige-Bacchiglione, covering the Trezze watershed, and;

3. Sinistra-Medio Brenta, covering parts of the Dese-Zero, Marzenego, Naviglio-Brenta, Lusore, and Fiumazzo watersheds.

Other river basin districs also cover parts of the VLW, even if in smaller amounts than the three watershed districts listed above. These minor watershed districts are: Bacchiglione-Brenta; Destra Piave; Basso Piave; Pedemontano Brentella di Pederobba, and; Pedemontano Brenta [89]. The following sub-sections describe in deeper details each of the major sub-basins of the VLW.

1.3.1 Vela Sub-basin

The Vela watershed is mostly managed by the Destra Piave watershed district. This sub-basin covers an area of approximately 110 km^2 and is characterised for being an "appendix" sub-basin to the VLW, located in its most northern section [89]. Most of this sub-basin is composed of natural flowing channels, the most important being the rivers Vallio and Meolo [17], which drain their waters to an artificial channel named Vela, hence the name of the sub-basin. Once reaching the Vela channel, no other hydraulic contribution is received by the channel, which ultimately discharges into the Lagoon of Venice after passing under the Sile river, a few kilometres after receiving the contributions from its tributaries [17, 89]. The average streamflow discharge of the Vela watershed is about 3 $m^3\ s^{-1}$ [89].

Both Vallio and Meolo rivers are originated from return flow coming from the big aquifer system located to the north/north-west of the VLW (see Figure C1.6 for reference), being classified as resurgent rivers. The Vallio river originates near the city of San Biagio di Callalta, draining waters from parts of the territories of Roncade, Biancade, and also San Biagio di Callalta. Near the city of Meolo, the rivers Vallio and Meolo merge, ultimately draining their water to the Vela channel. The Meolo river originates near the city of Breda di Piave, draining water from areas covered by the cities of San Biagio di Callalta, Monastier, and Breda di Piave [17].

1.3.2 Dese-Zero Sub-basin

The Dese-Zero is the third largest major sub-basin of the VLW, covering an area of, approximately, 250 km^2 and representing approximately 14% of the total VLW area. The Dese-Zero watershed consists of two major rivers, namely Dese and

Zero, and several small streams distributed among the watershed. The main river is the Dese river, meeting its main tributary, the Zero river, at just about 100m before discharging into the Lagoon of Venice. Both rivers are classified as resurgence rivers, as they receive significant amounts of spring waters from a groundwater system near the city of Castelfranco Veneto. The average streamflow discharge of the watershed varies from ca. 1 m^3 s^{-1} to 8 m^3 s^{-1} [89].

Although the Dese-Zero watershed is one of the most natural sub-catchments of the VLW [118], its drainage network is still rather complex. The watershed is rather plain, while the area closer to the Venice Lagoon is characterised by the presence of depressions in the terrain, some of which are below the sea level. Consequently, water flow in this area is subject to mechanical drainage [89]. As a matter of fact, approximately 10% of the Dese-Zero watershed's area is below sea level, while approximately 82% is below 25 m.a.s.l, indicating how plain the watershed is.

A number of hydraulic works take place on the upper-basin of the Dese-Zero watershed, the most important one being the hydraulic junction of Castelfranco Veneto [89], which diverts water from the Avenale river system to the Dese river, near the city of Castelfranco Veneto. Similarly, the Zero river receives hydraulic contributions from the Brenton del Maglio watershed, as managed by a hydraulic node located near the city of Albaredo di Vedelago [17, 120].

1.3.3 Marzenego Sub-basin

Smaller than the Dese-Zero watershed, the Marzenego sub-basin covers an area of, approximately, 140 km^2. The main river names the watershed, being renamed to Osellino channel in its final stretch, ranging from the city of Mestre to the river's mouth, at the Lagoon of Venice. Similarly to the Dese and Zero rivers, the Marzenego river receives significant amounts of spring waters around the area Castelfranco Veneto, being classified as a resurgence river. The average discharge of the Marzenego watershed varies between 2 and 7 m^3 s^{-1} [89]. Similarly to the Dese-Zero watershed, the Marzengo sub-basin is characterised for being a very plain watershed to the point that almost 93% of its total area is below 25 m.a.s.l.. Due to this fact, around 30% of its watershed area is subject to

mechanical drainage, while the remaining is subject to gravity or alternate drainage [17, 120]. Similarly to the Dese river, the Marzenego watershed receives hydraulic contributions from the Avenale sub-basin, as managed by the upstream hydraulic junction of Castelfranco Veneto [89].

1.3.4 Naviglio-Brenta Sub-basin

The Naviglio-Brenta is the second largest sub-basin of the VLW, covering an area of approximately 310 km^2. This sub-basin is characterised for being a highly modified watershed, specially in its area closer to the Lagoon of Venice [89]. In its most northern section, rivers like Tergola and Muson Vecchio, two of the most important reaches in this area, are originated from the return flow coming from the aquifer system depicted in Figure C1.6. Both rivers eventually discharge their waters into the Naviglio-Brenta river, the river that names the watershed. The Tergola river discharges into the Naviglio-Brenta channel at two distinct points after being split in two distinct channels: the first near the city of Strà, by a channel named Veraro, and; the second and most important near the city of Mira, by a channel named Serraglio, which is actually the natural course of the Tergola river. Near the city of Mira, the Muson Vecchio river also merges with the Navigation-Brenta by a channel named Taglio di Mirano [17, 89]. The Taglio di Mirano channel is the water course that crosses the Lusore sub-basin, spliting it into two sections. Both the Tergola and the Muson Vecchio streamflows can be partially deviated to the Brenta river system during exceptional flow conditions [17].

The Naviglio-Brenta is, in fact, the original course of the Brenta river which has been systematically modified throughout the centuries and nowadays discharges most of its waters directly into the Adriatic Sea. Some of the streamflow originating from the Brenta watershed, however, still discharges into the Lagoon of Venice as part of its total flow is deviated by an hydraulic device located near the city of Strà to its old original course, originating the Naviglio-Brenta [17, 89]. The Naviglio-Brenta system is, hence, an artificially controlled watershed [118]. The Naviglio-Brenta is also a navigable channel, flowing for about 27 km until eventually discharging into the Lagoon of Venice [17]. This process is not

linear, though. Just after receiving the contributions from the Taglio di Mirano channel, the Naviglio-Brenta is split in two: the first branch follows the natural course of the Naviglio-Brenta channel, and; the second branch originates the Taglio Nuovissimo channel, an artificial channel the flows to the south of the VLW eventually merging with the Montalbano channel and discharging into the Lagoon of Venice [17, 18]. About 5 km before reaching the Lagoon of Venice, the Navilgio-Brenta branch is split once again. A first branch follows its original course, while a second branch creates the Bondante channel, that eventually discharges in the Lagoon of Venice after flowing for a stretch of about 3 km [17].

The average streamflow discharge of the Naviglio-Brenta channel varies from ca. 6 $m^3 s^{-1}$ to 10 $m^3 s^{-1}$ [89], a modest value if compared to the amount of water that is receives from its tributaries throughout its course [17]. During low-flow conditions, the main source of water to the Naviglio-Brenta is the Brenta river, as managed by an hydraulic device located near the city of Strà. This deviation is done mainly by gravity and the flow magnitude that can be deviated depends on the flow levels in the Brenta river [89].

1.3.5 Lusore Sub-basin

The Lusore sub-basin's stream network system is composed of two major channels, named Lusore and Veternigo-Menegon, which are fed by waters originating mainly in the spring belt area, more precisely between the cities of Cittadella and Castelfranco [118]. Since this area is located outside of the area covered by the Lusore watershed, the water that actually flows in this watershed is deviated from the surrounding channels. Precisely, the Lusore channel is fed by water deviated from the Muson dei Sassi channel, while the Veternigo-Menegon channel receives water from a deviation of the Muson Vecchio [118, 89]. The watershed covers an area of approximately 155 km^2 that is basically split in half due to the fact that it is crossed by the Taglio di Mirano channel [17]. The average streamflow discharge of the Lusore watershed is around 3 $m^3 s^{-1}$ [89].

1.3.6 Fiumazzo Sub-basin

The Fiumazzo watershed is the land area that covers the superficial drainage network that discharges in the Fiumazzo channel. The watershed area is about 125 km^2. Two are the main channels that cover this area, namely Fiumicello and Cornio. Both channels merge near the location of Corte, fraction of the city Piove di Sacco, forming the Fiumazzo channel. This channel ultimately discharges into the Lagoon of Venice after after passing under the Brenta river and the Taglio Nuovissimo channel [89]. The average streamflow discharge of the Vela watershed is around 1.5 $m^3\ s^{-1}$ [89]. Most of the area covered by the Fiumazzo watershed is subject to either mechanical or alternate drainage due to terrain characteristics, such as the presence of depressions in the terrain surface [89].

1.3.7 Montalbano Sub-basin

Moving to the meridional part of the VLW, it is possible to locate the Montalbano watershed. Without taking into consideration the sub-basins draining only partially to the VLW, the Montalbano watershed is the smallest in area coverage. This sub-basin covers an area of, approximately, 60 km^2, corresponding to just 3.5% of the total VLW area. The main stream is named Montalbano channel and names the watershed. Similarly to the Dese, Zero, and Marzenego rivers, the Montalbano channel is a natural stream [89], although somewhat modified throughout the past centuries due to human interventions [17].

Differently from most of the major sub-basins of the VLW, the Montalbano watershed does not discharge directly into the Lagoon of Venice. Instead, it merges its waters with the Taglio Nuovissimo channel, which ultimately discharge in the Lagoon of Venice near the city of Chioggia [17]. The average outflow of the Montalbano watershed is the lowest among all major sub-basins of the VLW, corresponding to a mean value of just 0.35 $m^3\ s^{-1}$ as measured by streamflow station between the years of 2005 and 2007 [89]. Depending on specific hydraulic management conditions, the Montalbano watershed may or may not receive hydraulic loadings from an area covered by the Cambroso watershed. The area covered by the Cambroso watershed is, in fact, the drainage area covered by a

hydraulic pump located in the city of Codevigo, stretching for about 45 km^2. This hydraulic device was installed with the purpose of serving as a flood-control device, being capable of pumping a maximum water flow of 16 m^3 s^{-1} during high-flow events and with respect to specific hydraulic management circumstances [14].

1.3.8 Trezze Sub-basin

The Trezze watershed is the largest sub-basin of the VLW, covering an area of approximately 470 km^2, representing roughly 26% of the total area of the VLW. Most of the watershed's area is the result of land reclamation, resulting in a the terrain profile that is characterised for being mostly plain and a soil profile that characterised for being generally very thin [17]. Moreover, most of its area is characterised by the presence of depressions on the surface terrain, many of which is below the sea level (see Figure C1.5 for reference). As a matter of fact, it is estimated that about 210 km^2 are below sea level, a value that represents approximately 43.5% of the watershed's total area. Consequently, most of the area covered by the Trezze watershed is subject to either mechanical or alternate drainage [89].

The Trezze watershed is composed of two main drainage channels, namely Altopiano and Cuori [118]. Both channels merge near the location of Ca' Bianca di Chioggia to form the Morto channel [89]. From there, under ordinary flow conditions, its superficial waters are driven to the Lagoon of Venice after passing under both the Bacchiglione and Brenta rivers by means of a hydraulic device named Trezze, which names the watershed. Under high flow conditions, though, part of the total watershed's flow can be deviated to the Bacchiglione river [17]. In average values, the streamflow discharge of the watershed varies from ca. 1 m^3 s^{-1} to 3 m^3 s^{-1} [89].

1.4 The IRW

The IRW is located to the north-east of the Brazilian Federal State of Santa Catarina, in Southern Brazil. More precisely, the latitudinal extremes of the basin are 26°27'S; 49°54'W to the north and 27°52'S; 49°14'W to the south while its longitudinal extremes are 27°07'S; 50°21'W to the west and 26°55'S; 48°38'W to the east [49]. The total area covered by the watershed is approximately 15,000 km^2. According to the Brazilian Ministry of the Interior – National Department of Sanitation Works – DNOS, the IRW is composed of seven sub-basins, namely: Itajaí-Mirim; Itajaí do Sul; Itajaí do Oeste; Itajaí do Norte; Benedito; Luiz Alves, and; Itajaí-Açú. Figure C1.7 depicts the location of the IRW and its sub-basins. Table C1.2, instead, shows some details regarding the sub-basins of the IRW.

Table C1.2: The sub-basins of the IRW.

Sub-basin	Main River's Length [km]	Area Covered [km^2]	Mean Flow Discharge [m^3 s^{-1}]
Itajaí-Mirim	170.0	1,677.2	71.4
Itajaí do Sul	101.0	2,027.6	32.7
Itajaí do Oeste	132.0	3,013.7	41.2
Itajaí do Norte	185.0	3,354.2	39.2
Benedito	83.0	1,500.1	41.5
Luis Alves	59.6	587.7	17.4
Itajaí-Açú	188.0	2,780.0	504.6

Adapted from: do Itajaí and FAAVI [35]

In general terms, the overall hydrography of the Santa Catarina Federal State can be divided into two larger drainage systems, namely: ii. The Atlantic drainage system, to the east, and; ii. The Continental drainage system, to the west. The Continental drainage system consists of two larger river basins: the Paraná river's basin and the Uruguay river's basin. Both rivers eventually meet farther downstream, between Argentina and Uruguay, where they form the La Plata estuary, eventually draining its waters into the Atlantic Ocean. The Atlantic drainage system, instead, is part of a larger drainage basin known as South Atlantic basin. Differently from the Continental drainage system, the Atlantic drainage system drains its waters directly to the Atlantic Ocean. As a consequence, all the river basins which belongs to this drainage system are much smaller if compared to the large river basins belonging to the Continental drainage system (e.g. the

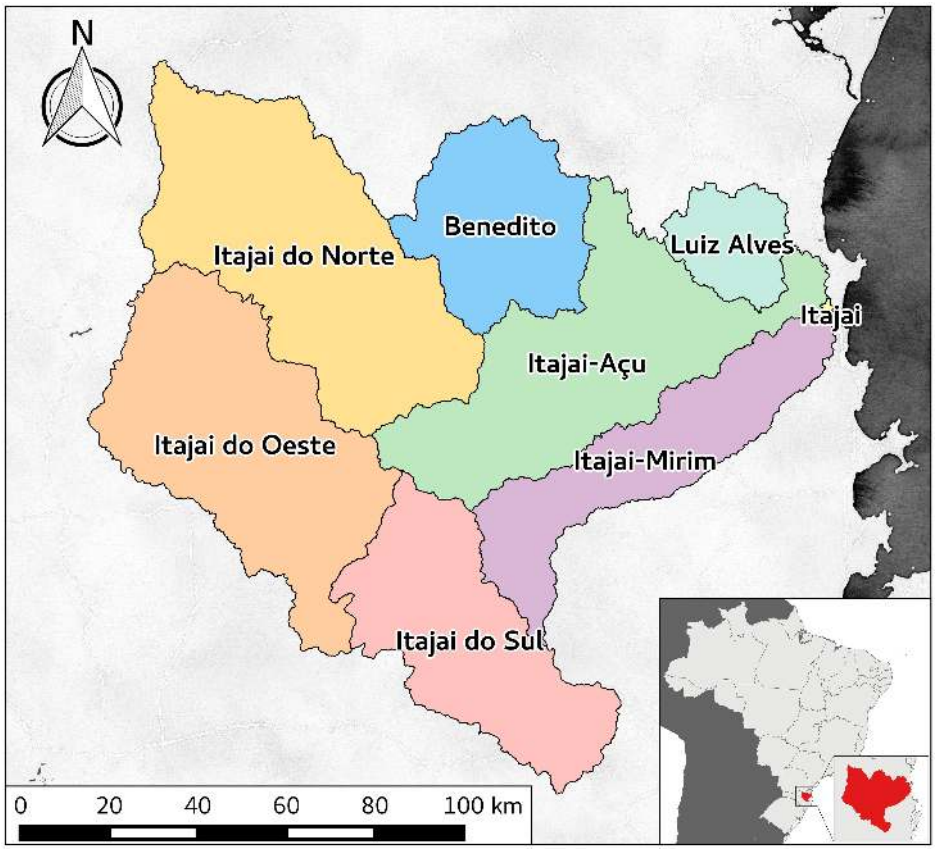

Data source: ANA [7]

Figure C1.7: The IRW and its sub-basins.

Paraná and the Uruguay river basins). Among the several water basin which compose the South Atlantic basin, the IRW stands out as the second largest watershed [7].

The IRW is also one of the most important areas of the Federal State of Santa Catarina, both under the hydrological and the socio-economic points of view. The IRW is the largest watershed in the Santa Catarina Federal State, hosting around 20% of its total population and covering an area of approximately 16.5% of its total area [35]. In economic terms, the most important productive sectors are the textile, metal-mechanic, and glass, concentrated around the cities of Blumenau, belonging to the Itajai-Açú sub-basin, and Brusque, belonging to the Itajaí-Mirim sub-basin. Interestingly, the merging of these two sub-basins, at just about 5 km before reaching the Atlantic Ocean, is responsible for the formation of the Itajaí river, which, in turn, hosts the city of Itajaí and one of the most important Brazilian port complexes [54].

Besides its economic importance, the IRW is also well known for its propensity to river flooding. In fact, river flood episodes have been (and are still being) registered since the beginning of the colonisation process in the region, back to the 19^{th} century. As a matter of fact, the first recorded flood event taking place in the city of Blumenau was recorded in 1852, registering a flood peak of 16,3 m for the Itajaí-Açú river [19]. Flood episodes are still a recurrent issue in the region and in recent decades the most devastating floods occurred in 1983, when a flood peak of 15.34 m and 49 deaths were registered, and in 2008, when a flood peak of 11.72 m and 135 deaths were registered. Both episodes were also characterised by severe environmental and socio-economic consequences [19, 84].

In the 1950s, after a series of four large flood episodes in the IRW, a Presidential Decree was issued determining the formation of a study group to tackle the issue [48]. The study group was responsible for the identification and proposal of measures and actions to manage river flooding in the IRW, while also for the investigation of the economic situation in the watershed, aiming at the economic development of the region. The final report of this study indicated that the economic benefits of investing in works for multiple use of the basin's rivers would be economically beneficial, suggesting the construction of five dams in the upper Itajaí valley along with several other earthworks such as stream rectifications,

construction of dikes, and irrigation channels [35]. From the original number of suggested dams, only three were actually built, commonly know as South, North and West dams. Figure C1.8 depicts their spatial location inside the IRW while Table C1.3 summarises their main characteristics [35, 30].

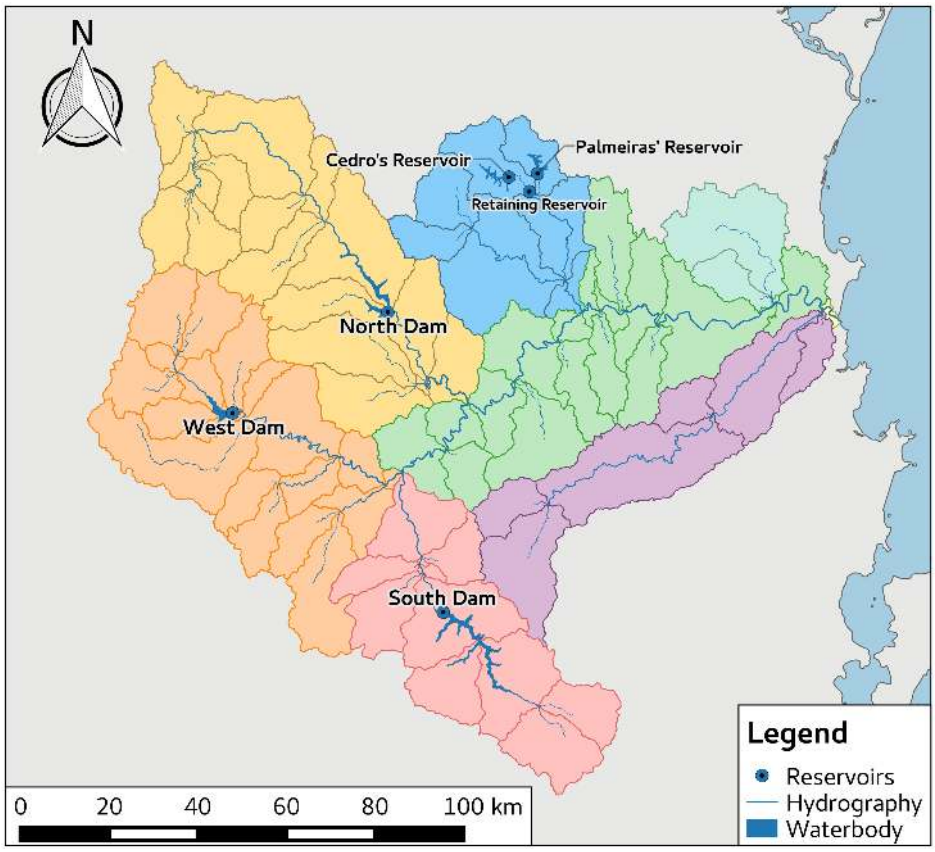

Data source: ANA [7]

Figure C1.8: Main hydrologic features of the IRW.

Due to a combination of factors ranging from meteorological inputs to terrain characteristics, the IRW is subject to an extremely variable streamflow regime throughout a year cycle. As a matter of fact, the maximum registered daily flow measured by the Brazilian National Water Agency – ANA at the stream gauge station *"83800002 - Blumenau (PCD)"* is 6,988 $m^3\ s^{-1}$ while the minimum registered value is just 4 $m^3\ s^{-1}$ [7]. In general, however, the mean streamflow as measured by the same stream gauge is approximately 400 $m^3\ s^{-1}$, for a standard

Table C1.3: Main features of the IRW's dams.

Item	South Dam	North Dam	West Dam
Municipality	Ituporanga	José Boiteux	Taió
Sub-Basin	Itajaí do Sul	Itajaí do Norte	Itajaí do Oeste
Purpose	Flood control	Flood control, Irrigation	Flood control, Irrigation
Built in	1976	1992	1973
Construction Type	Rock-fill, embankment	Rock-fill, embankment	Concrete, gravity
Height [m]	43.50	58.50	20.00
Catchment Area (km^2)	1,273.0	2,318.0	1,042.0
Reservoir Area (km^2)	8.4	14.0	8.6
Spillway Capacity (m^3)	93,500,000.00	357,000,000.00	83,000,000.00

Adapted from: do Itajaí and FAAVI [35]

deviation of approximately 350 $m^3\ s^{-1}$. It is interesting to notice the high standard deviation value with regards to the mean streamflow, illustrating how variable the river's streamflow regime really is.

The IRW's terrain is quite heterogeneous and is characterised by great geological diversity and complexity. Along the coastal area, the terrain is characterised by predominantly flat or gently rolling relief, while hilly and mountainous landscapes, commonly reaching altitudes of more than 800 m.a.s.l., are observed to the western and south-western areas of the watershed. Figure C1.9 show the DEM for the IRW's area.

The current landscape of the upper IRW is the result of past geological and climatic processes which contributed to the formation of *"V"* shaped valleys and rugged surface terrain, often characterised by the presence of steep and bent slopes. The floodplains around the streams and rivers of these valleys are often small and narrow. Moreover, the soil profile in these valleys is usually very thin, showing poor drainage of excess water. When combined, these factors contribute to the occurrence of flash flood episodes in these areas [35]. However, not only flash flooding is verified in the IRW, as the general shape and terrain characteristics of the upper IRW are determinant for the occurrence of flood events also in the lower valley [35].

In the upper and middle Itajaí valleys, the slope is rather steep varying from 1.6 m/km to 6.0 m/km, while in the lower Itajaí valley the terrain is almost plain (e.g. 0.013 m/km in the section between the cities of Blumenau and Itajaí). Consequently, the upper and middle Itajaí valleys are characterised by the presence of rapids and waterfalls, while the lower valley is characterised by the presence of

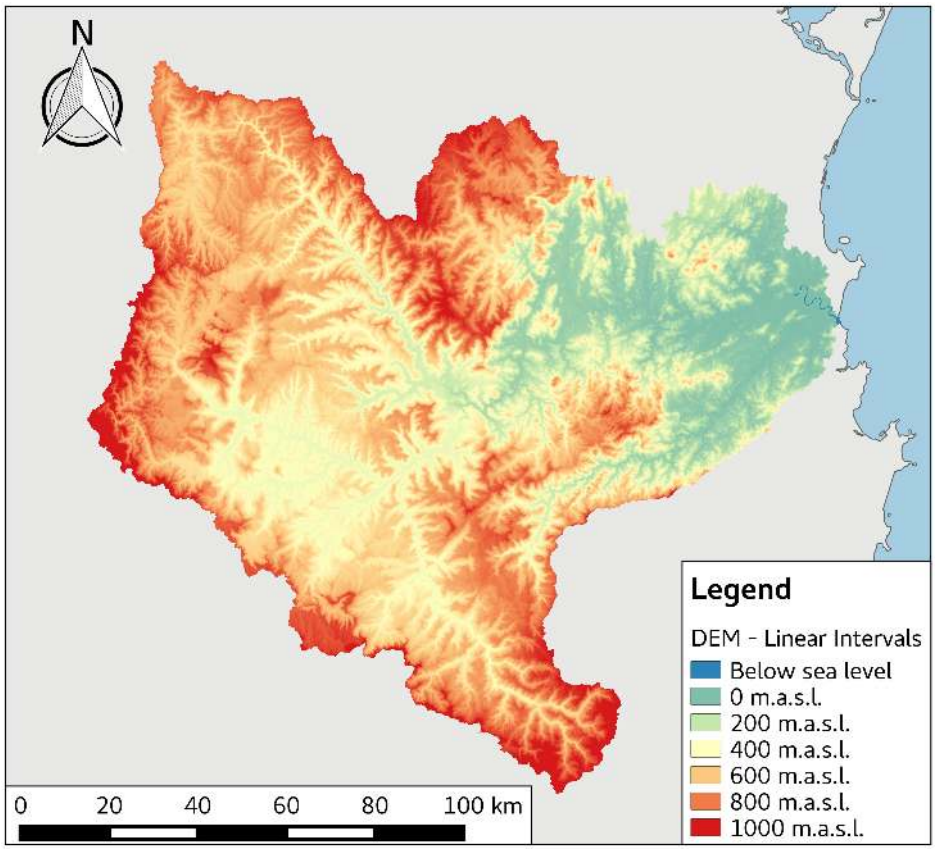

Data source: METI et al. [78]

Figure C1.9: DEM of the IRW.

large flood plains and generally slower flowing waters. The lower plains located in the lower Itajaí valley also hosts the mouth of the Itajaí river, which is a saline wedge estuary under a micro-tidal regime and characterised by a dramatically varying streamflow level throughout the year [101, 35]. The estuary of the Itajaí's river is very long, beginning near the city of Blumenau and stretching in length for about 70 km and covering an area of, approximately, 14 km^2. All these features, when combined, contribute to the occurrence of large flood events in the lower Itajaí valley, especially in the lowland section downstream of the city of Blumenau, where the Itajaí's estuary is located.

Notwithstanding the contribution of the IRW's relief to the occurrence of flood episodes, the basin's soil type and distribution is another determinant factor affecting the river flooding process. In the upper and middle Itajaí valleys, the soil's thickness is variable, being very shallow in some points while very deep in others [37, 38, 42]. In areas where the soil is thick and has a good hydraulic conductivity, water can easily infiltrate and be stored into the soil profile, thereby diminishing the intensity of river flooding in the downstream areas. On the other hand, however, in areas where the soil is thin and with low permeability, the soil can easily become saturated, consequently creating a lubricated zone in those areas, a process that ultimately favours land-slides and river flooding processes throughout the watershed. The soil distribution of the IRW is shown in Figure C1.10. Table C1.4, instead, shows some information regarding the major soil group types present in the IRW

Table C1.4: The major soil group types of the IRW.

Soil Group Code[1]	Soil Group Description[1]	Area (km^2)	Total area %
PVA	Argissolo Vermelho-Amarelo	3,338.81	20.0%
CX	Cambissolo Háplico	6,595.26	39.5%
CH	Cambissolo Húmico	1,250.79	7.5%
E	Espodossolo Cárbico	25.67	0.2%
GX	Gleissolo Háplico	1,020.17	6.1%
GM	Gleissolo Melânico	39.52	0.2%
LB	Latossolo Bruno	69.54	0.4%
RY	Neossolo Flúvico	24.18	0.1%
RL	Neossolo Litólico	4,115.35	24.6%
RQ	Neossolo Quartzarênico	60.08	0.4%
NB	Nitossolo Bruno	170.30	1.0%

[1] According to the Brazilian soil classification system.
Data source: EPAGRI and CIRAM [42]

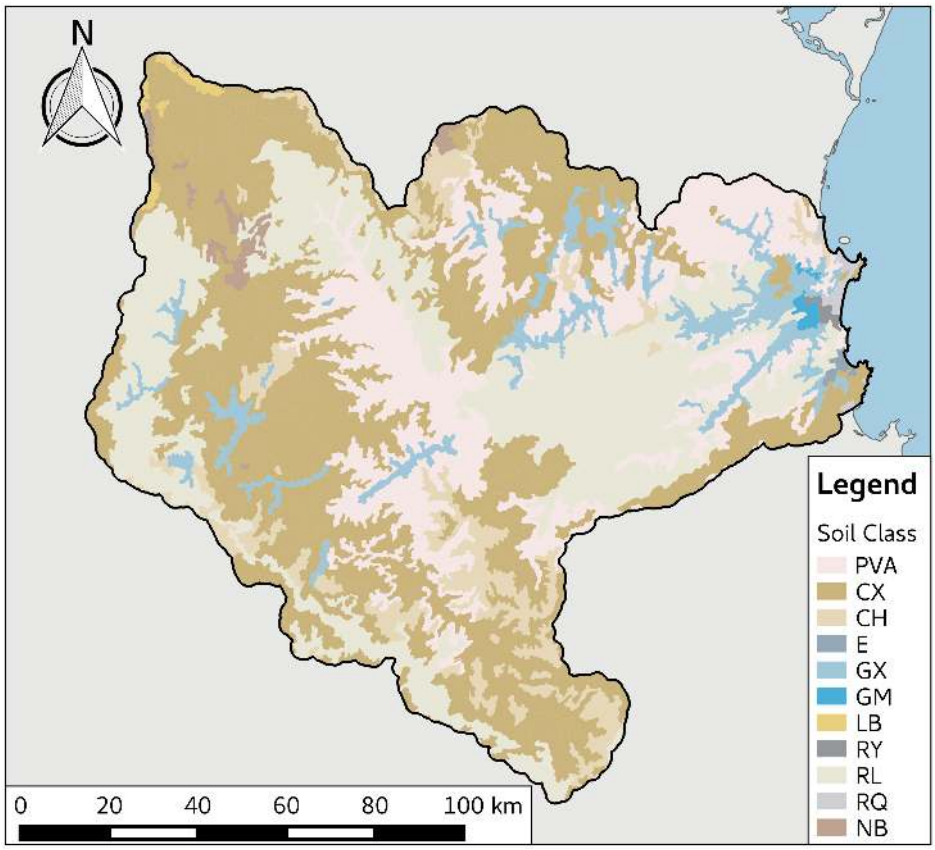

Data source: EPAGRI and CIRAM [42]

Figure C1.10: Soil distribution of the IRW.

As shown in Figure C1.10 and Table C1.4, the three major soil groups in the IRW are, respectively, Cambisols (i.e. *"Cambissolo"*), Fluvisols/Leptosols (i.e. *"Neossolo"*), and Acrisols (i.e. *"Argissolo"*) soil group classes [37, 38]. The understanding of these soil groups and their properties is fundamental for the characterisation of flood events in the IRW.

The Cambisols soil group is a B horizon soil which can be found in various relief types. This soil group fertility is variable according to the region where it is present and it is mainly used to grow corn, beans, potato, rice, banana, tobacco, soy and wheat, but also for pasture and reforestation. This soil type is characterised for being shallow and well-drained [37, 38].

The *"Neossolo"* soil group is characterised for being a recent soil formation and is usually very shallow, such as those formed by alluvial deposits (i.e. Fluvisols) or shallow soils found in mountainous areas (i.e. Leptosols). Generally, in those type of soils the source rock is usually found at a depth of no more than 50cm from the surface. The properties of this soil group type are entirely determined by the composition of its source rocks [38]. The predominant variant of *"Neossolo"* in the IRW is Leptosol. This type of soil is characterised for being very shallow, by a texture varying from medium loam to clay loam, and by a medium drainage capacity [37].

Finally, the soils belonging to the Acrisols soil group are characterised for being base-rich mineral soils. These soils are also non-hydromorphic, usually characterised by the presence of high amounts clay. This soil group can have variable drainage characteristics, varying from poor to good drainage soils [38]. In average, the variants of Acrisols found in the IRW's area are characterised for being clay predominant, with a depth ranging from 60cm to 150cm, and with a medium drainage capacity [37].

Currently, a flood warning system is in operation in the IRW, being managed by the Alert System Operations Centre – CEOPS. This flood warning system monitors the stream stage of the Itajaí-Açú river and performs hydrological forecasts by making use of specific equipment, such as data loggers, weather stations, wireless sensors, and water level loggers [24]. Depending on the amount of rainfall and its temporal and spatial distribution, the river level situation may evolve from a state of attention to a state of flood alert or emergency within

a fraction of a few hours. Under these situations, the collection of hydrologic and meteorological data by the telemetric stations can be performed at hourly intervals. Usually, this situation begins when the observed level of the river is above the level of attention and/or when the total last 24 hours precipitation is higher than 60 mm in the watershed's area. Currently, the stream stage of the Itajaí-Açú river is predicted only for the city of Blumenau, while studies are currently being held to expand the prediction alert system to other cities in the IRW [24].

The following sub-sections describe in deeper details the main characteristics that are particular to some of the major sub-basins of the IRW.

1.4.1 Itajaí-Mirim

The Itajaí-Mirim is the last major tributary of the Itajaí-Açú river, both meeting at the city of Itajaí at just, approximately, 5 km before discharging into the Atlantic Ocean. The Itajaí-Mirim river's source, instead, is located in the city of Vidal Ramos. The river flows for 177 km before meeting with the Itajaí-Açú river, covering a drainage area of, approximately, 1,700 km^2. Approximately 10% of the total flow of the IRW is attributed to the Itajaí-Mirim river, a value of approximately 71.4 $m^3\ s^{-1}$ [35].

The Itajaí-Mirim sub-basin was one of the IRW's sub-basins indicated to host a flood control dam by the technical report discussed in Section 1.4 [48]. This dam, however, was never built as the necessity of building it was supposed to be reviewed after the construction of a channel ratification in its lower section [35]. This channel ratification consists of an artificial channel built near the city of Itajaí that spans for, approximately, 8,100 m. A collateral effect of this hydraulic work is the loss of importance in terms of water flow, ultimately accumulating urban sewage discharges and currently constituting an environmental and public health issue [35]. The most important urban centres belonging to the Itajaí-Mirim sub-basin are Brusque, Gaspar, and Itajaí, the last two belonging only partially to the sub-basin's area.

1.4.2 Itajaí-Açú

The Itajaí-Açú river is formed by the merging of the Itajaí do Sul and Itajaí do Oeste rivers, in the exact location where the city Rio do Sul can be found. The river then flows for about 188 km until merging with the Itajaí-Mirim river to form the Itajaí river. During its course, the river Itajaí-Açú receives contributions from the Itajaí do Norte, Benedito, and Luiz Alves rivers, all on the left margin. The Itajaí-Açú is the largest river of the IRW and its total contribution area sums up to, approximately, 13,000 km^2.

Being the largest sub-basin complex of the IRW, the Itajaí-Açú sub-basin is responsible for most of the flow contribution to the IRW, accounting for approximately 90% of the total flow (the remaining 10% is attributed to Itajaí-Mirim river) [35]. The average streamflow of the Itajaí-Açú is about 504.6 $m^3 s^{-1}$. The most important urban centre located inside the Itajaí-Açú sub-basin is the city of Blumenau, with a population of approximately 300,000 inhabitants and accounting, alone, for 25% of the total IRW's population. Other major cities that are located fully or partially located inside the sub-basin's area are Rio do Sul, Indaial, Gaspar, and Itajaí [54].

References

[1] Abbaspour, K. C., 2014. SWAT-CUP 2012: SWAT Calibration and Uncertainty Programs - A User Manual. Tech. rep.

[2] Abbaspour, K. C., Yang, J., Maximov, I., Siber, R., Bogner, K., Mieleitner, J., Zobrist, J., Srinivasan, R., 2007. Modelling hydrology and water quality in the pre-alpine/alpine Thur watershed using SWAT. Journal of Hydrology 333 (2-4), 413–430.

[3] Achouri, M., Tennyson, L., Upadhyay, K., White, R., 2005. Preparing for the Next Generation of Watershed Management Programmes and Projects. Proceedings of the Asian Regional Workshop (September 2003), 163.

[4] Alcamo, J., Vörösmarty, C. J., Naiman, R. J., Lettenmaier, D. P., Pahl-Wostl, C., 2008. A grand challenge for freshwater research: understanding the global water system. Environmental Research Letters 3 (1), 010202.

[5] Allen, L. H., 1990. Plant Responses to Rising Carbon Dioxide and Potential Interactions with Air Pollutants. Journal of Environmental Quality 19 (1), 15–34.

[6] Allen, R. G., Jensen, M. E., Wright, J. L., Burman, R. D., 1989. Operational Estimates of Reference Evapotranspiration. Agronomy Journal 81 (4), 650–662.

[7] ANA, A. N. d. Á., 2014. HidroWeb - Sistema de Informações Hidrológicas. URL http://hidroweb.ana.gov.br/default.asp

[8] Arnold, J., Allen, P., Bernhardt, G., 1993. A comprehensive surface-groundwater flow model. Journal of Hydrology 142 (142), 47–69.

[9] Arnold, J. G., Kiniry, J. R., Srinivasan, R., Williams, J. R., Haney, E. B., Neitsch, S. L., 2012. Soil & Water Assessment Tool: Input/Output Documentation. Version 2012. Tech. rep., Texas A&M AgriLife, USDA Agricultural Rsearch Service, College Station, TX, USA.

[10] Arnold, J. G., Srinivasan, R., Muttiah, R. S., Williams, J. R., 1998. Large Area Hydrologic Modeling and Assessment Part I: Model Development. Journal of the American Water Resources Association 34 (1), 73–89.

[11] ARPAV, 2015. ARPAV - Dati Meteorologici. URL http://www.arpa.veneto.it/temi-ambientali/meteo/dati

[12] ARPAV, Veneto, R., 2008. Le acque sotterranee della pianura veneta: I risultati del Progetto SAMPAS. Tech. rep., Regione Veneto, ARPAV, Iniziativa cofinanziata dall'Unione Europea - FESR - DOCUP Ob. 2 anno 2000-2005 - Progetto SAMPAS, Padova, PD, Italy.

[13] Azzellino, A., Carpani, M., Cevirgen, S., Giupponi, C., Parati, P., Ragusa, F., Salvetti, R., 2013. Managing the nutrient loads of the Venice Lagoon

Watershed: are the loads external to the watershed relevant under the WFD River Basin District framework? Journal of Coastal Research (1, 65), 25–30.

[14] Bacchiglione, C. d. B., 2010. Piano Generale di Bonifica e di Tutela del Territorio. Tech. rep., Consorzio di Bonifica Bacchiglione, Padova, PD, Italy.

[15] Balbi, S., Bhandari, S., Gain, A. K., Giupponi, C., 2013. Multi-agent agro-economic simulation of irrigation water demand with climate services for climate change adaptation. Italian Journal of Agronomy 8 (e23), 175–185.

[16] Bixio, V., Celegon, E. A., Fanton, P., Fiume, A., Vazzoler, C., Zanetti, S., Bixio, A. C., Rech, F., 2009. Documento Propedeutico ai Piani Generali di Bonifica e Tutela del Territorio dei Consorzi di Bonifica del Veneto: Caratteri fisici e climatici dei comprensori di bonifica del Veneto. Tech. rep., Regione Veneto, Piazzola sul Brenta.

[17] Bixio, V., Celegon, E. A., Fanton, P., Fiume, A., Vazzoler, C., Zanetti, S., Bixio, A. C., Rech, F., 2009. Documento Propedeutico ai Piani Generali di Bonifica e Tutela del Territorio dei Consorzi di Bonifica del Veneto: La Bonifica idraulica nella Regione Veneto. Tech. rep., Regione Veneto, Piazzola sul Brenta.

[18] Bixio, V., Celegon, E. A., Fanton, P., Fiume, A., Vazzoler, C., Zanetti, S., Bixio, A. C., Rech, F., 2009. Documento Propedeutico ai Piani Generali di Bonifica e Tutela del Territorio dei Consorzi di Bonifica del Veneto: L'irrigazione nella Regione Veneto. Tech. rep., Regione Veneto, Piazzola sul Brenta.

[19] Blumenau, D. C. D. E., 2012. Cota-Enchente De Blumenau. Relatório Técnico Final - Parceria Técnico-Científica. Tech. Rep. Novembro, Centro de Operação do Sistema de Alerta da Bacia do Itajaí - CEOPS, Universidade Regional de Blumenau - FURB, Blumenau-SC, Brasil.

[20] Bogardi, J. J., Dudgeon, D., Lawford, R., Flinkerbusch, E., Meyn, A., Pahl-Wostl, C., Vielhauer, K., Vörösmarty, C. J., 2012. Water security for

a planet under pressure: Interconnected challenges of a changing world call for sustainable solutions. Current Opinion in Environmental Sustainability 4 (1), 35–43.

[21] Bressiani, D. d. A., Gassman, P. W., Fernandes, J. G., Garbossa, L. H. P., Srinivasan, R., Bonumá, N. B., Mendiondo, E. M., 2015. A review of soil and water assessment tool (SWAT) applications in Brazil: Challenges and prospects. International Journal of Agricultural and Biological Engineering 8 (3), 1–27.

[22] Brooks, K. N., Ffolliott, P. F., Magner, J. A., 2013. Hydrology and the Management of Watersheds, 4th Edition. John Wiley & Sons, Inc., Iowa, USA.

[23] Brutsaert, W., 2013. Hydrology: An Introduction, 8th Edition. Cambridge University Press, Cambridge, United Kingdom.

[24] CEOPS, C. d. O. d. S. d. A., 2017. CEOPS - Sistema de Alerta - Previsão de Nível.
URL http://ceops.furb.br/index.php/sistema-de-alerta/previsao-de-nivel

[25] Clarke, L. E., Jacoby, H., Pitcher, H., Reilly, J., Richels, R., 2007. Scenarios of Greenhouse Gas Emissions and Atmospheric Concentrations. Sub-report 2.1A of Synthesis and Assessment Product 2.1 by the U.S. Climate Change Science Program and the Subcommittee on Global Change Research. Tech. Rep. July, Department of Energy, Office of Biological & Environmental Research, Washington, DC, USA.

[26] CMIP5, 2016. RCP data comparison.
URL http://tntcat.iiasa.ac.at:8787/RcpDb/

[27] Conservation Ontario, 2010. Integrated Watershed Management: Navigating Ontario's Future. Tech. rep., Conservation Ontario, Newmarket, Canada.

[28] Conservation Ontario, 2016. Watershed Management in Ontario: Lessons Learned and Best Practices. Tech. rep.

[29] Crutzen, P. J., 2002. Geology of mankind. Nature 415 (January), 23.

[30] da Silva, L. A. C., Schult, E. H., Grunwald, P. A., Müller, O. R., Schult, S. M., Demarch, M. S., Mattos, M., 2013. As Barragens de Contenção de Cheias da Bacia Hidrográfica do Rio Itajaí-Açu. Tech. rep., Associação Comercial Industrial de Rio do Sul ACIRS, Associação dos Municípios do Alto Vale do Itajaí AMAVI, Fundação Educacional do Alto Vale do Itajaí FEDAVI, Rio do Sul-SC, Brasil.

[31] Darghouth, S., Ward, C., Gambarelli, G., Styger, E., Roux, J., 2008. Watershed Management Approaches, Policies, and Operations: Lessons for Scaling Up. Tech. Rep. 11.

[32] Di Baldassarre, G., Viglione, A., Carr, G., Kuil, L., Salinas, J. L., Blöschl, G., 2013. Socio-hydrology: Conceptualising human-flood interactions. Hydrology and Earth System Sciences 17 (8), 3295–3303.

[33] Dile, Y., Srinivasan, R., George, C., 2017. QGIS Interface for SWAT (QSWAT). Tech. Rep. v 1.4, Texas A&M AgriLife, USDA Agricultural Rsearch Service, College Station, TX, USA.

[34] Dile, Y. T., Daggupati, P., George, C., Srinivasan, R., Arnold, J., 2016. Introducing a new open source GIS user interface for the SWAT model. Environmental Modelling and Software 85, 129–138.

[35] do Itajaí, C., FAAVI, F. A. d. Á. d. V. d. I., 2010. Plano de Recursos Hídricos da Bacia Hidrográfica do Rio Itajaí. Tech. rep., Comitê do Itajaí, Realização: Fundação Agência de Água do Vale do Itajaí Apoio:Programa Petrobras Ambiental, por meio do Projeto Piava; Universidade Regional de Blumenau, por meio de projetos de pesquisa financiados pelo CT-Hidro e pela FAPESC, Secretaria, Itajaí-SC, Brasil.

[36] Easterling, W. E., Rosenberg, N. J., McKenney, M. S., Jones, C. A., Dyke, P. T., Williams, J., 1992. Preparing the erosion productivity impact

calculator (EPIC) model to simulate crop response to climate change and the direct effects of CO2. Agricultural and Forest Meteorology 59 (1), 17 – 34.

[37] EMBRAPA, 2004. Solos do Estado de Santa Catarina. Tech. rep., EMBRAPA, Rio de Janeiro, RJ.

[38] EMBRAPA, 2006. Sistema Brasileiro de Classificação de Solos. Tech. rep., Rio de Janeiro, RJ.

[39] EPA, 2013. Introduction to Watershed Planning. Tech. rep., U.S. Environmental Protection Agency, Chicago, IL, USA.

[40] EPA, 2013. Principles of Watershed Management. Tech. rep., U.S. Environmental Protection Agency, Chicago, IL, USA.

[41] EPA, 2015. Lake Champlain Basin SWAT Model Configuration, Calibration and Validation. Tech. Rep. April, U.S. Environmental Protection Agency, Chicago, IL, USA.

[42] EPAGRI, E. d. P. A. e. E. R. d. S. C., CIRAM, C. d. I. d. R. A. e. d. H. d. S. C., 2014. Projeto IFFSC - Projeto Inventário Florístico Florestal de Santa Catarina.

[43] Essenfelder, A. H., 2016. SWAT Weather Database: A Quick Guide. v 0.16.07. Tech. Rep. July, Centro Euro-Mediterraneo sui Cambiamenti Climatici - CMCC, Lecce, Italy.

[44] Essenfelder, A. H., Giove, S., Giupponi, C., 2016. Identifying the Factors Influencing the Total External Hydraulic Loads to the Dese-Zero Watershed. In: 8th International Congress on Environmental Modelling and Software. Vol. 3. Toulouse, France, pp. 731–738.

[45] Esteve, P., Varela-Ortega, C., Blanco-Gutiérrez, I., Downing, T. E., 2015. A hydro-economic model for the assessment of climate change impacts and adaptation in irrigated agriculture. Ecological Economics 120, 49–58.

[46] FAO, F., of the United Nations, A. O., 2016. Watershed Management. Tech. rep.

[47] FAO, F., of the United Nations, A. O., EOMF, E. O. o. M. F., ICIMOD, I. C. f. I. M. D., REDLACH, R. L. d. C. T. e. M. d. C. H., ICRAF, W. A. C., 2006. The new generation of watershed management programmes and projects. Tech. rep., Food and Agriculture Organization of the United Nations, Rome, Italy.

[48] Fraga, N. C., 2009. Enchentes Urbanas no Vale do Itajaí, Brasil. 25 Anos da Enchente Catástrofe de 1983 - Reflexos Sociambientais e Culturais no Século XXI. In: 12 Encuentro de Geógrafos de América Latina. 7-Proceses de la interacción sociedad-naturaleza. Montevideo, Uruguay, p. 15.

[49] Fraga, N. C., Köhler, V. B., 1999. As Enchentes no Vale do Itajaí-Açú: Das Obras de Contenção à Indústria da Enchente. Boletim de Geografia 17, 81–92.

[50] Frisbee, M. D., Tysor, E. H., Stewart-Maddox, N. S., Tsinnajinnie, L. M., Wilson, J. L., Granger, D. E., Newman, B. D., 2016. Is there a geomorphic expression of interbasin groundwater flow in watersheds? Interactions between interbasin groundwater flow, springs, streams, and geomorphology. Geophysical Research Letters 43 (3), 1158–1165.

[51] Genereux, D. P., Jordan, M., 2006. Interbasin groundwater flow and groundwater interaction with surface water in a lowland rainforest, Costa Rica: A review. Journal of Hydrology 320 (3-4), 385–399.

[52] Goldstein, J., Huber-Lee, A., 2004. Global Lesson for Watershed Management. Tech. rep., Water Environment Research Foundation, London, UK.

[53] Goudie, A. S., 2013. The human impact on the natural environment: past, present, and future, 7th Edition. John Wiley & Sons Ltd., Oxford, UK.

[54] Grando, T. V., 2011. Os Recursos Hídricos e os Planos Diretores Municipais na Bacia do Rio Itajaí-Açu. Msc thesis, Federal University of Santa Catarina - UFSC.

[55] Green, W. H., Ampt, G. A., 1911. Studies on Soil Physics. Part I. The Flow of Air and Water through Soils. Journal of Agricultural Research 4 (1), 1–24.

[56] Haddeland, I., Lettenmaier, D. P., Skaugen, T., 2006. Effects of irrigation on the water and energy balances of the Colorado and Mekong river basins. Journal of Hydrometeorology 324 (1), 210–223.

[57] Hargreaves, G. H., Samani, Z. A., 1985. Reference crop evapotranspiration from temperature. Applied Engineering In Agriculture 1 (2).

[58] Haykin, S., 2001. Neural Networks: A Comprehensive Foundation, 2nd Edition. Prentice Hall, Inc., Upper Saddle River, NJ, USA.

[59] Henson, R., 2014. The Thinking Person's Guide to Climate Change. American Meteorological Society, Boston, US.

[60] Hsieh, W. W., 2009. Machine Learning Methods in the Environmental Sciences: Neural Networks and Kernels. Cambridge University Press, New York, NY, USA.

[61] Idso, S. B., Kimball, B. A., Anderson, M., Mauney, J. R., 1987. Effects of atmospheric CO2 enrichment on plant growth: the interactive role of air temperature. Agriculture, Ecosystems & Environment 20 (1), 1–10.

[62] Ignaciuk, A., Mason-D'Croz, D., 2014. Modelling adaptation to climate change in agriculture. OECD Food, Agriculture and Fisheries Papers (70), 58.

[63] Inc., H. E., 2013. Buffalo River Watershed SWAT Modeling. Tech. rep., Buffalo - Red River Watershed District.

[64] Keeling, C. D., Bacastow, R. B., Bainbridge, A. E., Ekdahl Jr., C. . A., Guenther, P. R., Waterman, L. S., Chin, J. F. S., 1976. Atmospheric

carbon dioxide variations at Mauna Loa Observatory, Hawaii. Tellus 28 (6), 538–551.

[65] Kimball, B. A., 1983. Carbon Dioxide and Agricultural Yield: An Assemblage and Analysis of 430 Prior Observations. Tech. rep., Unites States Water Conservation Laboratory, Phoenix, Arizona.

[66] Kimball, B. A., Lamorte, R. L., Jr, P. J. P., Wall, G. W., Hunsaker, D. J., Adamsen, F. J., Leavitt, S. W., Thompson, T. L., Matthias, A. D., 1999. Free-air C02 enrichment and soil nitrogen effects on energy balance and evapotranspiration of wheat. Water Resources Research 35 (4), 1179–1190.

[67] Kimball, B. A., Mauney, J. R., Nakayama, F. S., Idso, S. B., 1993. Effects of increasing atmospheric CO2 on vegetation. Vegetatio 104-105 (1), 65–75.

[68] Körner, C., Miglietta, F., 1994. Long term effects of naturally elevated CO2 on mediterranean grassland and forest trees. Oecologia 99 (3-4), 343–351.

[69] Krysanova, V., Arnold, J. G., 2008. Advances in ecohydrological modelling with SWAT—a review. Hydrological Sciences Journal 53 (5), 939–947.

[70] Leakey, A. D. B., Ainsworth, E. A., Bernacchi, C. J., Rogers, A., Long, S. P., Ort, D. R., 2009. Elevated CO2 effects on plant carbon, nitrogen, and water relations: Six important lessons from FACE. Journal of Experimental Botany 60 (10), 2859–2876.

[71] Leng, G., Huang, M., Tang, Q., Gao, H., Leung, L. R., 2014. Modeling the Effects of Groundwater-Fed Irrigation on Terrestrial Hydrology over the Conterminous United States. Journal of Hydrometeorology 15 (3), 957–972.

[72] Li, W., Han, X., Zhang, Y., Li, Z., 2007. Effects of elevated CO2 concentration, irrigation and nitrogenous fertilizer application on the growth and yield of spring wheat in semi-arid areas. Agricultural Water Management 87 (1), 106–114.

[73] Li, Z., Liu, W.-z., Zhang, X.-c., Zheng, F.-l., 2009. Impacts of land use change and climate variability on hydrology in an agricultural catchment on the Loess Plateau of China. Journal of Hydrology 377 (1-2), 35–42.

[74] Londsale, K., Pringle, P., Turner, B., 2015. Transformational adaptation: what it is, why it matters and what is needed. Tech. rep., University of Oxford, Oxford, UK.

[75] Ma, H., Zhu, J., Xie, Z., Liu, G., Zeng, Q., Han, Y., 2007. Responses of rice and winter wheat to free-air CO2 enrichment (China FACE) at rice/wheat rotation system. Plant and Soil 294 (1-2), 137–146.

[76] Matsui, T., Namuco, O. S., Ziska, L. H., Horie, T., 1997. Effects of high temperature and CO2 concentration on spikelet sterility in indica rice. Field Crops Research 51 (3), 213–219.

[77] McLain, R., Lee, R., 1996. Adaptive Management: Promises and Pitfalls. Environmental Management 20 (4), 437–48.

[78] METI, M. o. E. T., Industry, NASA, U. S. N. A., Administration, S., 2014. ASTGTM2 - ASTER Global Digital Elevation Map.
URL https://asterweb.jpl.nasa.gov/gdem.asp

[79] Miglietta, F., Giuntoli, A., Bindi, M., 1996. The effect of free air carbon dioxide enrichment (FACE) and soil nitrogen availability on the photosynthetic capacity of wheat. Photosynthesis Research 47 (3), 281–290.

[80] Milly, P. C. D., Betancourt, J., Falkenmark, M., Hirsch, R. M., Kundzewicz, Z. W., Lettenmaier, D. P., Stouffer, R. J., 2008. Stationarity Is Dead: Whither Water Management? Science 319 (5863), 573–574.

[81] Monteith, J. L., 1965. Evaporation and the environment. In: The state and movement of water in living organisms. 19th Symposia of the Society for Experimental Biology. Vol. 19. Cambridge University Press, London, UK, pp. 205–234.

[82] Nazir, A., Liljenstrom, H., 2015. A biologically based neural network model for decision making. BMC Neuroscience 16 (Suppl 1), P146.

[83] Neitsch, S. L., Arnold, J. G., Kiniry, J. R., Williams, J. R., 2011. Soil & Water Assessment Tool Theoretical Documentation. Version 2009. Tech.

Rep. TR-406, Texas A&M AgriLife, USDA Agricultural Rsearch Service, College Station, TX, USA.

[84] Neto, A. B., EPAGRI, E. d. P. A. e. E. R. d. S. C., CIRAM, C. d. I. d. R. A. e. d. H. d. S. C., 2011. Histórico dos Desastres em Santa Catarina e Ações da Secretaria de Estado da Defesa Civil.

[85] NRCS, N. R. C. S., 2007. Transmission Losses. In: Moody, H. F. (Ed.), National Engineering Handbook. United States Department of Agriculture - National Resources Conservation Service, Washington, DC, USA, Ch. 19, pp. 1–8.

[86] of Conservation, C. D., 2014. 2008-2012 Watershed Coordinator Grants Report. Tech. rep., California Department of Conservation, Division of Land Resource Protection, Sacramento, CA, USA.

[87] Oliver, N. M., Rosario, B., Pentland, A. P., 2000. A Bayesian computer vision system for modeling human interactions. IEEE Transactions on Pattern Analysis and Machine Intelligence 22 (8), 831–843.

[88] Ontario, C., 2012. An Integrated Watershed Management Approach to Great Lakes Protection: Conservation Ontario Recommendations for a Great Lakes Protection Act. Tech. rep., Conservation Ontario, Newmarket, Canada.

[89] Orientali, A., 2010. Subunità Idrografica Bacino Scolante, Laguna di Venezia e Mare Antistante. Tech. rep., Venezia VE.

[90] Özkan, G., İnal, M., 2014. Comparison of neural network application for fuzzy and ANFIS approaches for multi-criteria decision making problems. Applied Soft Computing 24, 232–238.

[91] Palmer, P. I., Smith, M. J., 2014. Model human adaptation to climate change. Nature 512 (August), 365–366.

[92] Parati, P., 2009. Attivita' di Monitoraggio dei Corpi Idrici nel Bacino Scolante nella Laguna di Venezia.

[93] Patt, A., Siebenhüner, B., 2005. Agent Based Modeling and Adaptation to Climate Change. Vierteljahrshefte zur Wirtschaftsforschung 74 (2), 310–320.

[94] Peña-Reyes, C. A., 2004. Evolutionary Fuzzy Modeling Human Diagnostic Decisions. Annals of the New York Academy of Sciences 1020 (May), 190–211.

[95] Perman, R., Ma, Y., Common, M., Maddison, D., McGilvray, J., 2011. Natural Resource and Environmental Economics, 4th Edition. Pearson Education Limited, Essex, England.

[96] Piave, C. d. B., 2011. Regolamento per l'Utilizzazione delle Acque a Scopo Irriguo e per la Tutela delle Opere Irrigue. Tech. rep., Consorzio di Bonifica Piave, Montebelluna, Italy.

[97] Priestley, C. H. B., Taylor, R. J., 1972. On the assessment of surface heat flux and evaporation using large-scale parameters. Monthly Weather Review 100 (2), 81–92.

[98] Riahi, K., Grübler, A., Nakicenovic, N., 2007. Scenarios of long-term socio-economic and environmental development under climate stabilization. Technological Forecasting and Social Change 74 (7), 887–935.

[99] Salvetti, R., Acutis, M., Azzellino, A., Carpani, M., Giupponi, C., Parati, P., Vale, M., Vismara, R., 2008. Modelling the point and non-point nitrogen loads to the Venice Lagoon (Italy): the application of water quality models to the Dese-Zero basin. Desalination 226 (1-3), 81–88.

[100] Salvetti, R., Azzellino, A., Gardoni, D., Vismara, R., Carpani, M., Giupponi, C., Acutis, M., Vale, M., Parati, P., 2007. Application of SWAT Model on Three Watersheds within the Venice Lagoon Watershed (Italy): Source Apportionment and Scenario Analysis. In: Proceedings - 4th International SWAT Conference Application. pp. 408–417.

[101] Schettini, C. A. F., 2002. Caracterização Física do Estuário do Rio Itajaí-Açu , SC. Revista Brasileira de Recursos Hídricos 7 (1), 123–142.

[102] Schreinemachers, P., Berger, T., 2011. An agent-based simulation model of human-environment interactions in agricultural systems. Environmental Modelling and Software 26 (7), 845–859.

[103] Schumann, A. H., 2011. Flood risk assessment and management: How to specify hydrological loads, their consequences and uncertainties. Springer Science, Business Media, Bochum, Germany.

[104] SCS, S. C. S., 1972. Hydrology. In: National Engineering Handbook. Ch. Section 4.

[105] Sivapalan, M., Savenije, H. H. G., Blöschl, G., 2012. Socio-hydrology: A new science of people and water. Hydrological Processes 26 (8), 1270–1276.

[106] Smith, S. J., Wigley, T., 2006. Multi-Gas Forcing Stabilization with Minicam. The Energy Journal 27, 373–391.

[107] Steffen, W., Grinevald, J., Crutzen, P., McNeill, J., 2011. The Anthropocene: conceptual and historical perspectives. Philosophical transactions of the Royal Society. Series A, Mathematical, physical, and engineering sciences 369 (1938), 842–67.

[108] Stocker, T. F., Dahe, Q., Plattner, G.-K., Alexander, L. V., Allen, S. K., Bindoff, N. L., Bréon, F.-M., Church, J. A., Cubash, U., Emori, S., Forster, P., Friedlingstein, P., Talley, L. D., Vaughan, D. G., Xie, S.-P., 2013. Technical Summary. In: Stocker, T., Qin, D., Plattner, G.-K., Tignor, M., Allen, S., Boschung, J., Nauels, A., Y. Xia, V. B., Midgley, P. (Eds.), Climate Change 2013: The Physical Science Basis. Contribution of Working Group I to the Fifth Assessment Report of the Intergovernmental Panel on Climate Change. Cambridge University Press, Cambridge, United Kingdom and New York, NY, USA., Ch. Tec. Summ., pp. 33–115.

[109] Stockle, C. O., Dyke, P. T., Williams, J. R., Jones, C., Rosenberg, N. J., 1992. A method for estimating the direct and climatic effects of rising atmospheric carbon dioxide on growth and yield of crops: Part II—Sensitivity analysis at three sites in the Midwestern USA. Agricultural Systems 38 (3), 239 – 256.

[110] Strnad, D., Nerat, A., Kohek, S., 2015. Neural network models for group behavior prediction: a case of soccer match attendance. Neural Computing and Applications 28, 287–300.

[111] Strzepek, K., 2004. Global Lessons for Watershed Management in the United States. Tech. Rep. 00, Water Environment Research Foundation.

[112] Sun, H.-Y., Liu, C.-M., Zhang, X.-Y., Shen, Y.-J., Zhang, Y.-Q., 2006. Effects of irrigation on water balance, yield and WUE of winter wheat in the North China Plain. Agricultural Water Management 85 (1-2), 211–218.

[113] SWAT, 2016. SWAT Model Executables.
URL http://swat.tamu.edu/software/swat-executables/

[114] Tans, P. P., Ralph Keeling, 2017. Trends in Atmospheric Carbon Dioxide: Mauna Loa CO2 annual mean data.

[115] Taylor, R., Jeong, J., White, M. J., Arnold, J. G., 2014. The Future Evolution of APEX & SWAT.
URL http://swat.tamu.edu/media/77424/f32-taylor.pdf

[116] Thoning, K. W., Tans, P. P., Komhyr, W. D., 1989. Atmospheric carbon dioxide at Mauna Loa Observatory: 2. Analysis of the NOAA GMCC data, 1974–1985. Journal of Geophysical Research 94 (D6), 8549.

[117] Ullrich, A., Volk, M., 2009. Application of the Soil and Water Assessment Tool (SWAT) to predict the impact of alternative management practices on water quality and quantity. Agricultural Water Management 96, 1207–1217.

[118] Veneto, R., 2000. Piano Direttore 2000 - Piano per la prevenzione dell'inquinamento e il risanamento delle acque del Bacino Idrografico immediatamente sversante nella Laguna di Venezia. Tech. rep., Regione Veneto, Segreteria Regionale All'Ambiente, Direzione Tutela Dell'Ambiente, Venezia VE.

[119] Veneto, R., 2014. Infrastruttura dei Dati Territoriali del Veneto - Catalogo dei Dati.
URL http://idt.regione.veneto.it/app/metacatalog/

[120] Veneto, R., ARPAV, 2009. Bacino Scolante nella Laguna di Venezia: Rapporto sullo stato ambientale dei corpi idrici. Tech. rep.

[121] Vörösmarty, C. J., Green, P., Salisbury, J., Lammers, R. B., 2000. Global Water Resources: Vulnerability from Climate Change and Population Growth. Science 289 (July), 284–288.

[122] Vörösmarty, C. J., Lettenmaier, D., Leveque, C., Meybeck, M., Pahl-Wostl, C., Alcamo, J., Cosgrove, W., Grassi, H., Hoff, H., Kabat, P., Lansigan, F., Lawford, R., Naiman, R. J., 2004. Humans Transforming the Global Water System. EoS, Transactions, American Geophysical Union 85 (48), 509–520.

[123] Wagner, G. P., Altenberg, L., 1996. Perspective: Complex Adaptations and the Evolution of Evolvability. Evolution 50 (3), 967–976.

[124] Wani, S. P., Sreedevi, T. K., Singh, H. P., Rego, T. J., Pathak, P., Singh, P., 2003. A consortium approach for sustainable management of natural resources in watershed. In: Integrated Watershed Management for Land and Water Conservation and Sustainable Agricultural Production in Asia. Proceedings of the ADB-ICRISAT-IWMI Project Review and Planning Meeting. Hanoi, Vietnam, pp. 218–225.

[125] Wardynski, B., Nejadhashemi, P., 2009. Effects of Historic and Current Land Covers on Water Budget and Water Quality in Agricultural Regions of Michigan and Wisconsin. Tech. rep.

[126] Wilamowski, B. M., Irwin, J. D., 2011. The Industrial Electronics Handbook: Intelligent Systems, 2nd Edition. CRC Press, Inc., New York, NY, USA.

[127] Winchell, M., Srinivasan, R., Di Luzio, M., Arnold, J. G., 2013. ArcSWAT Interface For SWAT2012: User's Guide. Tech. rep., Texas A&M AgriLife, USDA Agricultural Rsearch Service, Temple, TX, USA.

[128] Winter, T. C., Rosenberry, D., LaBaugh, J. W., 2003. Where does the ground water in small catchment come from? Ground Water 41 (7), 989–1000.

[129] Winterhalder, B., 1980. Environmental Analysis in Human Evolution and Adaptation Research. Human Ecology 8 (2), 135–170.

[130] Wise, M., Calvin, K., Thomson, A., Clarke, L., Bond-Lamberty, B., Sands, R., Smith, S. J., Janetos, A., Edmonds, J., 2009. Implications of Limiting CO2 Concentrations for Land Use and Energy. Science 324 (May), 1183–1186.

[131] Zhang, X., Srinivasan, R., Hao, F., 2007. Predicting hydrologic response to climate change in the Luohe river Basin using the SWAT model. American Society of Agricultural and Biological Engineers 500 (3), 901–310.

Chapter 2

The ANN Model

Exploring its Applicability and Uncertainties

Abstract

ANNs have been successfully used in hydrological research since the late 90s. Due to its black-box nature, however, the uncertainties pertaining to the use of ANN models can be a limiting factor when applied to the simulation of physical processes. This chapter has two main objectives: i. To verify the applicability of the developed ANN to perform the short-term forecasting (i.e. periods from 1 to 4 days) of the stream stage of the IRW, and; ii. To explore uncertainties of ANN models (i.e. input data, model initialisation, model architecture, and model type) when applied to this particular hydrologic problem. The results suggest that the developed ANN model is very much capable of forecasting the short-term stream stage of the IRW, while much of the uncertain aspects of the model comes from the composition and quality of the sample data used during the training phase, the weight connections initialisation, and the model's type (i.e. delayed input-output and autoregressive). The results also suggest that, among all the input information, the ANN model is capable of delivering the best overall results when using both temperature and precipitation as exogenous input information, while being more sensitive to previous stream stage and precipitation input data.

2.1 Introduction

ANNs are a family of mathematical models based on the non-linear, complex, and parallel data processing operation of the human cerebral organ [17]. ANNs can be seen as empirical models, thereby consisting in receiving certain input information, its processing, and generation of a response by means of mathematical functions which, in general, bear no relation with the physical laws governing the simulated processes. Since the late 90s, ANN models have been applied with relatively success in several fields of research, such as remote sensing, image classification, cancer cell image classification, and human behaviour prediction [18, 12, 39, 34].

In hydrology and related areas of research, the application of ANN models has also been widely deployed since the late 90s and beginning of the 2000's. Hsieh and Tang [19] studied the implementation of four distinct modelling techniques in meteorology and oceanography: i. Linear regression and correlation; ii. PCA; iii. Canonical relations, and; iv. ANNs. The authors concluded that ANNs are a powerful technique capable of augmenting traditional linear statistical methods in data analysis and forecasting. Atiya *et al.* [6] proposed the comparison of different ANN modelling techniques in order to forecast the streamflow of the Nile river, in Egypt. The authors concluded that ANNs can produce fairly accurate results for the studied process. In Italy, Campolo *et al.* [10] proposed the use of ANNs as a flood forecasting model. The case study was the Arno river, located in Tuscany, Italy. The authors conclude that the considered model is able to accurately forecast short-term flood events in the study area, stating that the model is particularly suited for flood forecasting purposes. Several other studies were published making use of ANN models and reinforcing its applicability in streamflow forecasting (e.g. [11], [37], and [23]).

Despite the undeniable applicability of ANNs in a context of hydrologic research, there is still a large amount of uncertainty surrounding this technology, mainly due to the nature of ANN models. The so called *"black-box"* nature of ANNs is a serious drawback to a wider use of this technology among researchers [7], specially if it is considered the fact that well developed and calibrated hydrologic mathematical models can produce similar or better results than the results provided

by ANN model, with the advantage of physically describing the hydrology of the system, thereby reducing the overall uncertainty surrounding the model's nature.

But, what is uncertainty?

Before identifying and characterising uncertainty, it is useful to understand the definition of the term. Uncertainty in modelling is affected by several other factors, such as errors, model accuracy, and precision. In a context of hydrologic modelling, error is the absolute difference between a simulated value and the real value of a variable. Errors can generally be classified as two types: systematic and random. Systematic error are a type of error that can be post-corrected, such as a positive or negative bias in air temperature measurements. Random errors, instead, cannot be corrected and are randomly caused by unpredictable factors, such as noise in the measurement of air temperature due to changes in wind patterns. Accuracy is a term indicating how well a model is able to simulate the true value of a variable in absolute terms [22]. A good accuracy indicates low total error and is of fundamental importance for uncertainty reduction. Another concept that is essential for handling uncertainties is precision. Precision is a term indicating how consistent a simulation can be made under similar or near-identical starting conditions [21]. Since precision does not take into account the real value of the variable being simulated, it depends only on random errors. A good precision is also fundamental for uncertainty reduction. Uncertainty in modelling, then, can be understood as the a combination of factors which decrease the degree of confidence in a simulated result. Uncertainty sources may range from measurement errors to model assumptions, among other factors.

In a context of hydrologic modelling, the quantification of uncertainty is fundamental for the development of useful modelling tools. If uncertainties are not accounted for, then the illusion of model's perfectness in reproducing the system to which it is applied to arises [33]. This can be extremely dangerous in some situations, such as flood control. If uncertainties are neglected and the illusion of model's perfectness arises, a false sense of security from flooding may emerge, a process that may ultimately increase the exposure of humans to flood hazard, being the exact opposite of what is expected by a flood control measure [35]. Uncertainties must also not be overestimated. The adequate accounting of uncertainties in the construction of flood control structures, for instance, may

reduce its costs while at the same time increasing its effectiveness.

Unfortunately, not all sources and types of uncertainty can be accounted for. Unaccounted uncertainties are one of the reasons why, for instance, flood control measures never ensure total security against flooding. An useful way of better understanding uncertainties is through categorisation, such as the following [3, 29, 33]:

1. Epistemic uncertainty: Arising from the lack of knowledge of or in the ability to describe a process;

2. Aleatoric uncertainty: Related to the non-deterministic (i.e. stochastic) nature of a process, and;

3. Surprisal uncertainty: Originating from completely unforeseen and unexpected factors.

Epistemic uncertainties are usually the focus of scientific research, as this type of uncertainty can be reduced as more and better data is collected, and new research findings and technologies are discovered, helping in better characterising a problem. Aleatoric uncertainties, instead, cannot be reduced by further research as this type of uncertainty is intrinsic to the stochastic nature of a process, being possible only its characterisation and quantification (e.g. probability theory) [33]. Due to the nature of surprisal uncertainties, it is not possible to identify let alone quantify it. Hence, epistemic uncertainties can be seen either as ignored knows (e.g. sub-scale processes) or known unknowns (e.g. parametrisation of empirical models), aleatoric uncertainties can be seen as known unknowns (e.g. spatio-temporal variability of precipitation events), and surprisal uncertainties can be seen as unknown unknowns (no example as it is not possible its identification).

Similarly to other hydrologic modelling techniques, a significant part of the ANNs' uncertainties arises from the composition and quality of its input data. Nevertheless, the quality of the data series used in hydrologic studies influences not only the performance of ANN models, but also several other processes such as flood frequency analysis and the calibration of mathematical models [13]. Moreover, sources of uncertainty to mathematical hydrologic models, such as the watershed's characteristics, meteorological dynamics, and the spatio-temporal

resolutions [28] are also added the overall uncertainty of ANN models when applied to a context of hydrologic modelling.

An example is the consideration of precipitation data in the context of hydrologic modelling. As precipitation is the main driver of the hydrologic cycle in a watershed [9], this meteorological information is essential in any hydrologic modelling framework. However, several sources of uncertainty may be transferred from the simple consideration of this variable in a hydrologic model. Hydrologic studies of watersheds are often constrained by a scarce number of rainfall gauges, by imprecisions of measured rainfall data, or by the lack of long-enough precipitation records [8]. Instrumental and sampling errors[1], when not accounted for, add to the overall uncertainty of the model. Moreover, dynamic process such as changes in the surrounding landscape, lack of maintenance, or replacement of equipment may also affect the process of measuring rainfall amounts.

The study of the uncertainty when using ANN models has been explored by Alvisi and Franchini [1], who explored the utilisation of a grey neural networks for the forecasting of a river stage. The model utilised by the authors is set up using grey numbers, allowing the output of the model to be an interval instead of a fixed value, thereby enabling the quantification of uncertainty. The results obtained, according to the authors, reveal that the outputs intervals of the model generally have a slightly narrower width if compared to the uncertainty bands produced by a similar approach, namely the Bayesian neural network. Asefa [4], in turn, explored the idea of performing ensemble streamflow forecasting by means of a GLUE-based ANNs approach. The authors argues that a wide number of ANNs capable of providing similar results when applied to a same task can better expose the range of uncertainty in predicting this particular task (e.g. streamflow prediction). Moreover, the author states that the combination of these results in an ensemble fashion can provide better general performance than any of the single ensemble-ANN models. Several other studies explored the subject and specific topics, such as the utilisation of bootstrap analysis [15], Bayesian neural

[1] Instrumental errors are related to the accuracy with which a rain gauge can record the real rainfall amount, while sampling errors are associated with how well the rain gauge network of a watershed represents the real rainfall over the watershed's area.

networks [24], and the exploration of input variable selection techniques [27].

This chapter, then, seeks to explore the uncertainty sources coming from the application of ANN models in a context of hydrologic modelling. It is emphasised the study of the intrinsic uncertainties of ANN models, such as model structure and data processing, while also exploring the stochastic nature of hydrologic processes. In order to verify the validity of the considered ANN model, the results of the ANN are compared against other modelling techniques, namely: i. MLR, and; ii. Transfer Functions – TF.

2.2 Methodology

2.2.1 The ANN Model

The ANN model used in this study was developed by the authors in R language using the following libraries[2]: *R-core*; *parallel* [31]; *fBasics* [32], and; *ggplot2* [36]. The developed ANN model is theoretically explained in Appendix 2, while the source code of the model can be found in Appendix 3.

The developed ANN model consists of a Multilayer Perceptron – MLP neural network model, using back-propagation as the supervised training algorithm and either the Steepest-Descent or the Levenberg-Marquardt[3] as optimisation algorithms [14, 38]. Regarding the training process, the developed ANN model evaluates the evolution of the Sum of Squared Errors – SSE of the model outputs with regards to the targets as a way of assessing the generalisation property of the resulting model [26, 19]. Finally, the model is configured in such way to offer the possibility of selecting between two variants: an one-hidden layered or a two-hidden layered architecture, each consisting of a varying number of neurons per layer.

The input and target information is normalised by feature scaling (see Eq. A3.12) before being processed by the ANN model. The initial number

[2]The *parallel* library is imported to enable the use of multi-core processing. The *fBasics* library is used to calculate some array and matrix statistics. The *ggplot2* library is imported to create output graphical results.

[3]For the purposes of this study, only the Levenberg-Marquardt algorithm is utilised.

of hidden neurons per hidden layer is estimated as two-thirds of the summation of the number of neurons in the previous and next layers [16]. The output layer, instead, is constituted of only one neuron, meaning that each specific model configuration is optimised for a specific time-step of forecast. Regarding the activation functions, a hyperbolic-tangent function is used for the connections with neurons in the hidden layers, while the connection with neurons in the output layer is activated by a simple linear transfer function. This configuration is interesting as it does not limit the output range of the ANN model. Before being presented to model, the input information is randomly split between three distinct datasets, namely training, validation, and test[4], and in the following ratio, respectively: 70%; 20%, and; 10%. In order avoid any possible bias coming from the random split of the original dataset into training, validation, and test datasets, several training attempts are performed (i.e. 2048), each with a different initial weight initialisation and training dataset composition. The 32 models with the best overall results are stored for each calibration run. The final ANN model is, then, an ensemble of the 32 best ANNs retrieved after the calibration procedure.

2.2.1.1 The Uncertainty Analysis

Aiming at the identification of the uncertainties intrinsic to ANN models, it is proposed the study of the some different model configurations capable of affecting the overall performance of this type of models. To do so, a series of different set-ups of the ANN are run, each with an unique combination of features. The proposed variable features are[5]:

1. Input data variables (i.e. precipitation and temperature);

2. ANN model structure (i.e. number of hidden layers), and;

[4]The training set is used to calibrate the ANN model, meaning that the weight connections between neurons is updated with respect to the data available in this dataset. The validation set is utilised to avoid the overtraining or over-fitting of the ANN model. This dataset is not directly used for the training of the model, but it is used during the calibration process to signal when to stop the training procedure. The test set is not presented to the model during the calibration procedure, and is used only as a way of verifying the efficiency of a calibrated ANN when stressed by new data.

[5]The description of the different model types utilised throughout this chapter can be found in Appendix 2.

3. ANN model type (i.e. delayed input-output – I-O.d or autoregressive – NARX).

This analysis is performed for a fixed forecasting step of 1 day. The results obtained from this analysis are, then, used as an indication of the "best" ANN model configuration, which is then applied to the other considered forecasting scenarios, ranging from 1 to 4 days. Finally, performance of these ANN models can then be verified by means of inter-comparison among different modelling techniques.

2.2.1.2 The Comparison Models

To test the efficiency of the developed ANN model, the results obtained from this model are compared with the results obtained from similar modelling techniques, namely: i. a MLR model, and; ii. a TF model. Differently from the developed ANN model, the two comparison models are employed by using the MATLAB 2015b, version 8.6.0.267246, running under an Unix system. The MLR model is estimated by utilising the MATLAB's function *regress*. The TF model is employed by using the *System Identification Toolbox 9.2*. Besides those more complex modelling techniques, the Naïve and the Trend models are also selected to be used as comparison models because of their simplicity and their ability to clearly indicate poor model performance [5].

To compare the results between the different models, the split between training, validation, and test datasets is fixed, where the training and test datasets are used as calibration and validation datasets, respectively, for all the modelling techniques other than the ANN model. Two distinct efficiency evaluation techniques are considered for a quantitatively assessment of models' performance, namely: i. Nash-Sutcliffe model efficiency coefficient – NSE, and; the Percent Bias – PBIAS. Based on specialised literature on the topic, the assumed values for the NSE and PBIAS in order to judge the performance of a model as satisfactory are, respectively: $NSE > 0.50$ and $|PBIAS| \leq 0.25$ [25, 30]. These two different model evaluation techniques were chosen firstly because they are common ways of measuring a model's efficiency in hydrological researches, and secondly because NSE involves the calculation of the squared difference between the observed and

simulated values, what leads to an overestimation of these accuracy criteria if extreme values (e.g. flood event) are not-accurately simulated by a model. The NSE is calculated as shown in Eq. C2.1, while the calculation of the PBIAS is shown by Eq. C2.2.

$$NSE = 1 - \frac{\sum_{i=1}^{n} \left(X_{obs,i} - X_{sim,i}\right)^2}{\sum_{i=1}^{n} \left(X_{obs,i} - \overline{X}_{obs}\right)^2} \tag{C2.1}$$

$$PBIAS = \frac{\sum_{i=1}^{n} \left(X_{obs,i} - X_{sim,i}\right) \cdot 100}{\sum_{i=1}^{n} X_{obs,i}} \tag{C2.2}$$

where i is the index of observations; n is the total number of observations; $X_{obs,i}$ is the observed value at index i; $X_{sim,i}$ is the simulated value at index i, and; $\overline{X}_{obs}$ is the mean value of the observations.

2.2.2 The Case Study

The IRW is selected as a case study for the research topic explored in this chapter. A detailed explanation of this watershed and its sub-basins can be found in Chapter 1, Section 1.4. Regarding the data which is used, two are the main data sources: i. ANA-HidroWeb [2], and; the Brazilian National Institute of Meteorology – INMET [20]. All the rainfall and stream stage information was collected from the online hydrologic information system of the ANA, a website database called HidroWeb. The temperature information was collected from INMET.

The stream gauge chosen for this study is the station *"83800002 – BLUMENAU"*, located near the city of Blumenau and managed by the ANA. FigureC2.1 depicts the histogram of the selected stream stage station, in black, and the fitted generalised extreme value distribution, in red. The spatial location of the selected stream gauge is shown in FigureC2.2. The stream stage data is available as a daily information, which is taken as a simple mean between two daily observations. The measurement is available in centimetres.

The rain gauge stations chosen for this study were selected according to the

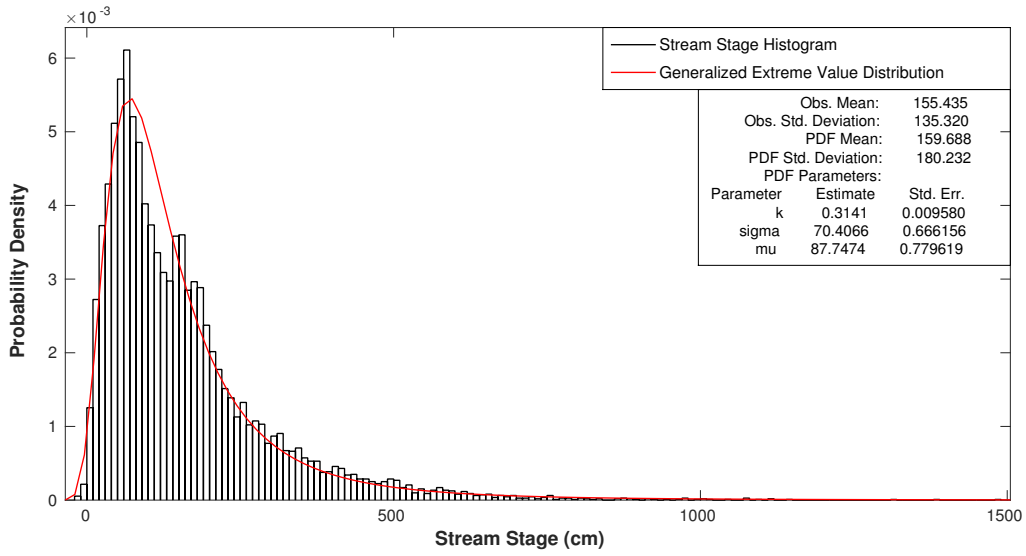

Data source: ANA [2]

Figure C2.1: Stream stage histogram of the station *"83800002 – BLUMENAU"*.

following criteria:

1. Upstream from the selected stream gauge station;
2. Downstream from the major dams;
3. Data series length and consistency, and;
4. The more spatially distributed as possible.

By considering these criteria, a total of six rain gauge stations were selected, namely: *"2649004 - TIMBO"*; *"2649005 - INDAIAL"*; *"2649007 - BLUMENAU"*; *"2749005 - NOVA BREMEN"*; *"2749017 - BARRAGEM SUL"*, and; *"2750014 - BARRAGEM OESTE"*. The spatial location of all precipitation stations can be seen in FigureC2.2. The rainfall information is available as the total daily amount of precipitation, in millimetres.

Regarding temperature, this study considers two automated stations, namely: *"83872 – INDAIAL"*, located near the city of Indaial and relatively close to the city

of Blumenau, and; *"83897 - FLORIANOPOLIS"*, located outside the IRW's area. The available temperature data is available in three formats: i. Daily maximum; ii. Daily minimum, and; iii. Daily average, all of them measured in degrees Celsius. FigureC2.2 shows the location and the codes of the selected temperature stations. Figure C2.3, instead, depicts the average monthly distribution of temperature and precipitation in the the IRW.

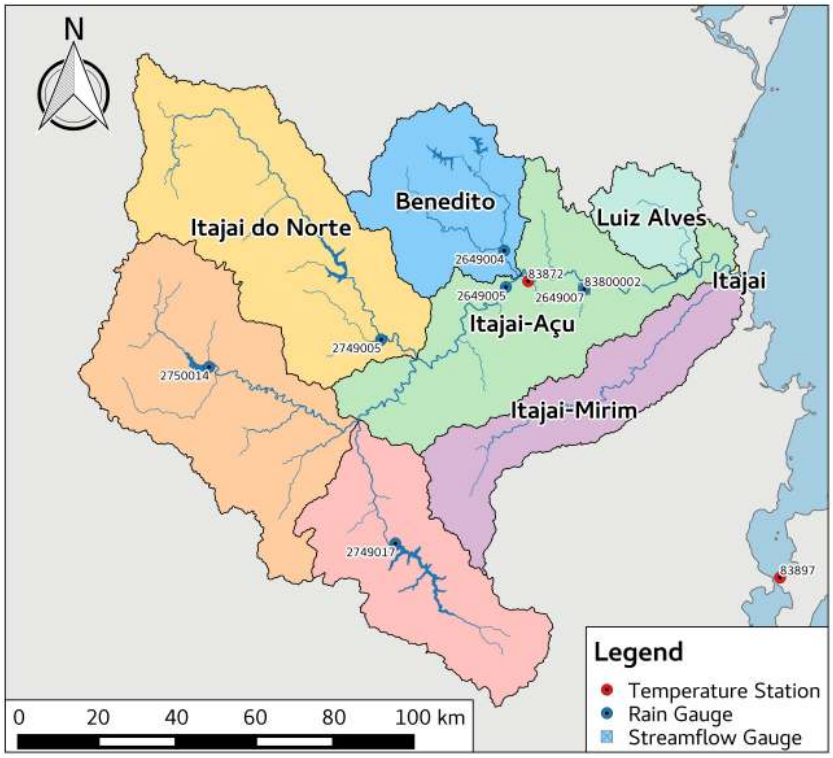

Data source: ANA [2], INMET [20]

Figure C2.2: Spatial location of selected hydro-meteorological stations.

Even though the available hydro-meteorological information covers the period from the late 1950's to the early 2000's, the data used in this study was selected only after January of 1977[6] due to two reasons, as follows: i. To remove the effects of the constructed dams over the stream stage time series, as the West Dam was finished in 1973 and the South Dam in 1973, and; ii. Because of the more consistent database after the 70s, with less missing information.

[6]Even if the North Dam was finished only in 1992 and its construction surely affects the

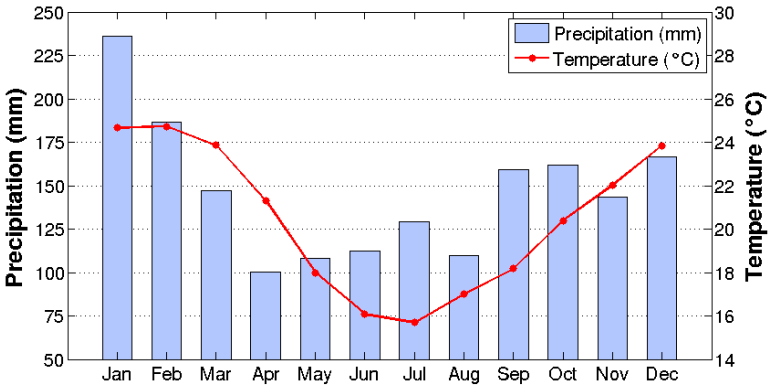

Data source: ANA [2], INMET [20]

Figure C2.3: Monthly averaged temperature and precipitation values for the IRW area.

2.3 Results and Discussions

This section presents the most important results of and a relevant discussion about the proposed uncertainty analysis in applying ANN models for the forecasting of the stream stage in the IRW. This section is divided in two sub-sections, following the discussion presented in the methodology section. The first sub-section, named *Sensitivity Analysis*, consists in presenting the results and discussing about some different model configurations capable of affecting the overall performance of ANN models. The second sub-section, named *Model Inter-Comparison*, instead, summarises the discussion regarding the applicability of ANN models for the forecasting of the stream stage in the IRW by comparing the results of several different modelling techniques when applied for the forecasting of the stream stage of the IRW and for different forecasting periods.

hydrology of the watershed, if data was to be selected only after that date it would drastically reduce the amount of available information to the calibration of the models.

2.3.1 Sensitivity Analysis

Following the methodology proposed in this chapter and described in Section 2.2, the results presented in this sub-section covers only the test dataset and are summarised as follows:

- Table C2.1 – SSE variation range of the ensemble of ANN models. The exogenous variables are precipitation and temperature, being referred to as the terms *Pcp.* and *Tmp.*, respectively.
- Figure C2.4 – Comparison of each scenario scatter plot. The elements of this plot are: The black dots represent the simulated (y-axis) versus observed (x-axis) values; The black dashed lines are the range of simulated values; The red solid line indicates a perfect of observed values, and; The shaded area represents the range of the linear regression between the simulated and the observed values.
- Figure C2.5 – Whisker diagram of the NSE results. The elements of this plot are: The bottom whisker mark indicates the minimum value, excluding outliers; The box spans from the 1st quartile, in the bottom, to the 3rd quartile, in the top. The median value is the tick black line inside the box. The top whisker mark indicated the maximum value, excluding outliers. The dots are outlier values.
- Figure C2.6 – Whisker diagram of the PBIAS results. The elements of this plot are the same as of Figure C2.5.

Table C2.1: ANN model results – SSE variation range.

		Input Variables					
		Pcp.		Tmp.		Pcp.&Tmp.	
Model Structure	**Model Type**	Min.	Max.	Min.	Max.	Min.	Max.
1 Hidden Layer	I-O.d	3.0557	4.1909	3.6231	5.2198	2.9621	3.8029
	NARX	0.2234	1.1062	0.5653	1.1965	0.2453	0.6686
2 Hidden Layer	I-O.d	3.0961	4.0990	3.8461	5.5257	2.9067	3.7826
	NARX	0.2334	0.6132	0.6291	1.3246	0.2256	0.6463

From the results shown in Table C2.1, it is possible to verify that the simulation of the rainfall-runoff process in the IRW is significantly better when the ANN model is configured as an open-loop NARX model type. When the model does not consider autoregressive information and is configured only as a simple I-O.d model type, its total error is approximately ten times greater, independently from which exogenous input information is presented to the ANN model. Figure C2.4 corroborates these findings.

The graphical results shown in Figure C2.4 indicate that, between the two exogenous input variables considered (i.e. precipitation and temperature), precipitation is fundamental for the simulation of the rainfall-runoff process in the IRW, while the incorporation of temperature as an exogenous input variable increases the overall prediction capability of the ANN model. In fact, the best results are obtained when the ANN model is configured as a NARX model type and using both temperature and precipitation as exogenous input information, both for the single or double hidden layered model architectures. Interestingly, the prediction capability of the ANN model is comparable among the single and double hidden layered model architectures, with the double layered ANN model version presenting slightly more accurate yet less precise results. Figures C2.6 and C2.6 confirms the results obtained from the analysis of Table C2.1 and Figure C2.4.

Another interesting finding obtained from the uncertainty and sensitivity analysis of the considered ANN model regards the training procedure of the model. During the training phase of an ANN model, it is expected a reduction of the training set's total error, as the backpropagation training algorithm adjusts the weight connections between the neurons in order to minimise the error between the predicted and observed values. However, as this process is non-linear and dependant on several factors such as the initialisation of the network's weights and on past training epochs, the minimisation of the training set's total error may not be an ideal solution for a particular problem. This issue leads to one of the uncertainties of ANN models: the training stop criteria. Figure C2.7 depicts a situation of two contrasting yet comparable training procedures for a same ANN model configuration.

In Figure C2.7, it is possible to verify that, although the training set's total error is reduced as the training procedures advances on both examples, the

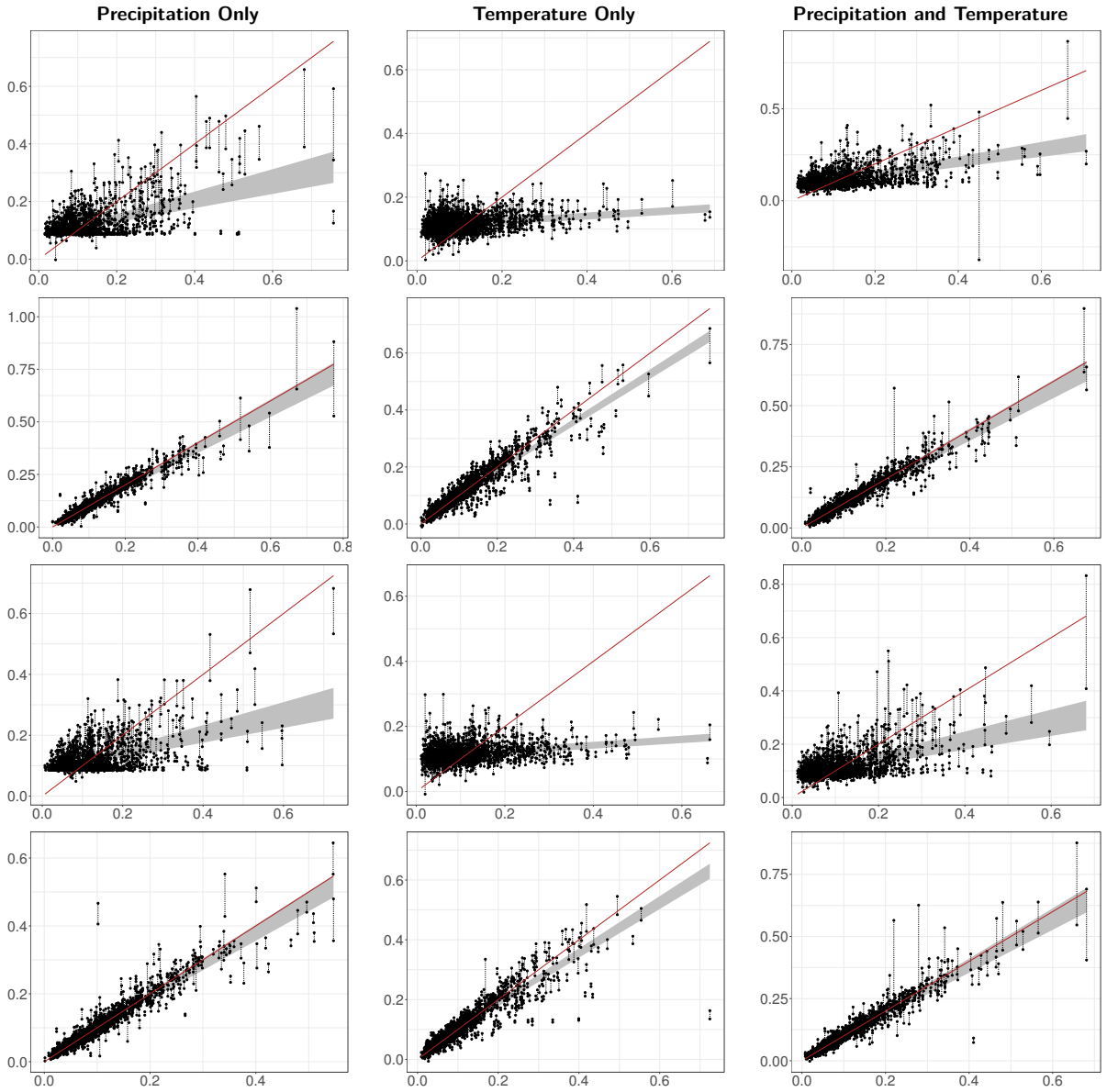

Figure C2.4: ANN model results – Scatter plots for each scenario. From left to right: 1st Column: Precipitation only; 2nd Column: Temperature only; 3rd Column: Precipitation and Temperature. From top to bottom: 1st Row: 1-Hidden-Layer, I.O.d model configuration; 2nd Row: 1-Hidden-Layer, NARX model configuration; 3rd Row: 2-Hidden-Layer, I.O.d model configuration; 4th Row: 2-Hidden-Layer, NARX model configuration.

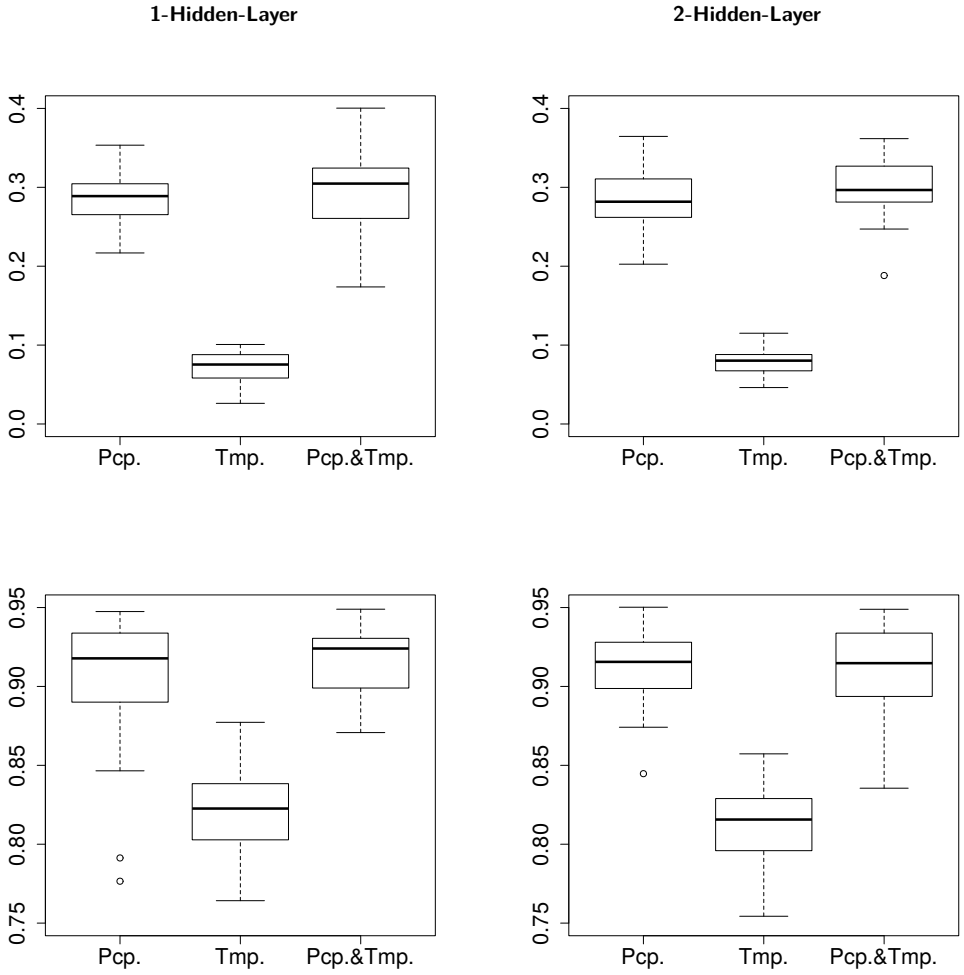

Figure C2.5: ANN model results – NSE box plots for each scenario. From left to right: 1st Column: 1-Hidden-Layer; 2nd Column: 2-Hidden-Layer. From top to bottom: 1st Row: I.O.d model type; 2nd Row: NARX model type.

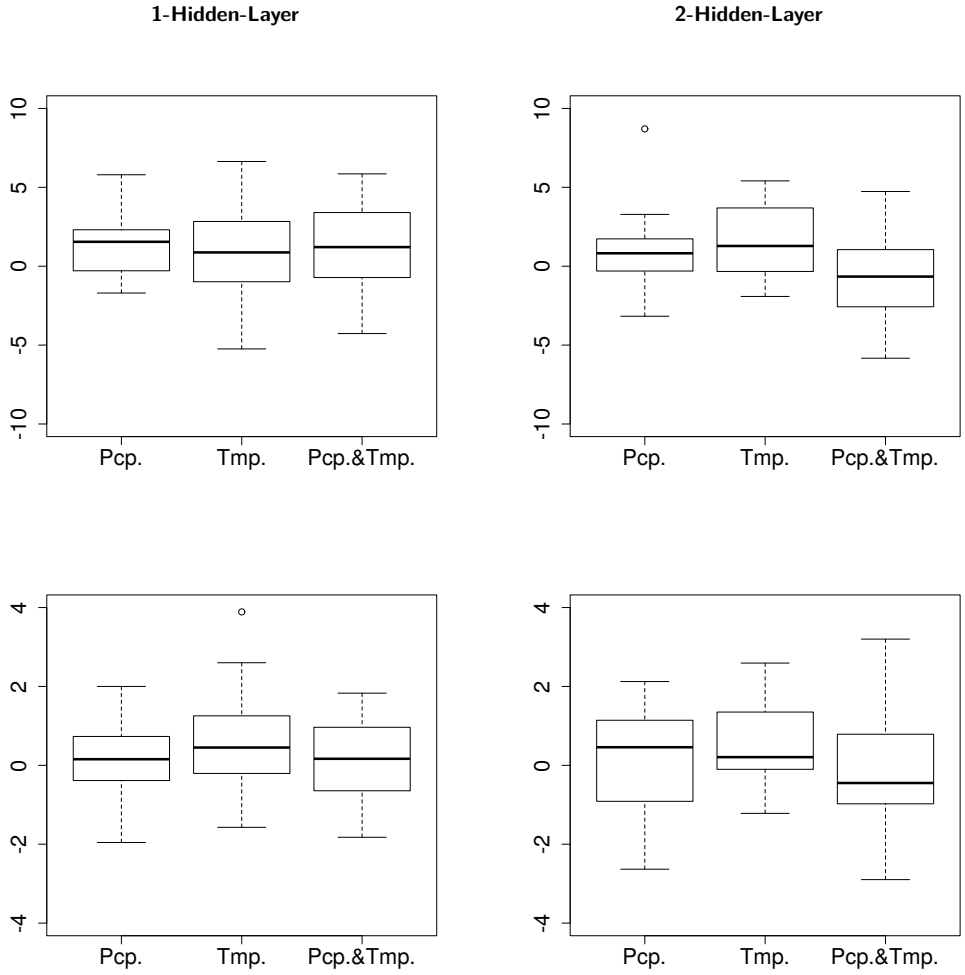

Figure C2.6: ANN model results – PBIAS box plots for each scenario. From left to right: 1st Column: 1-Hidden-Layer; 2nd Column: 2-Hidden-Layer. From top to bottom: 1st Row: I.O.d model type; 2nd Row: NARX model type.

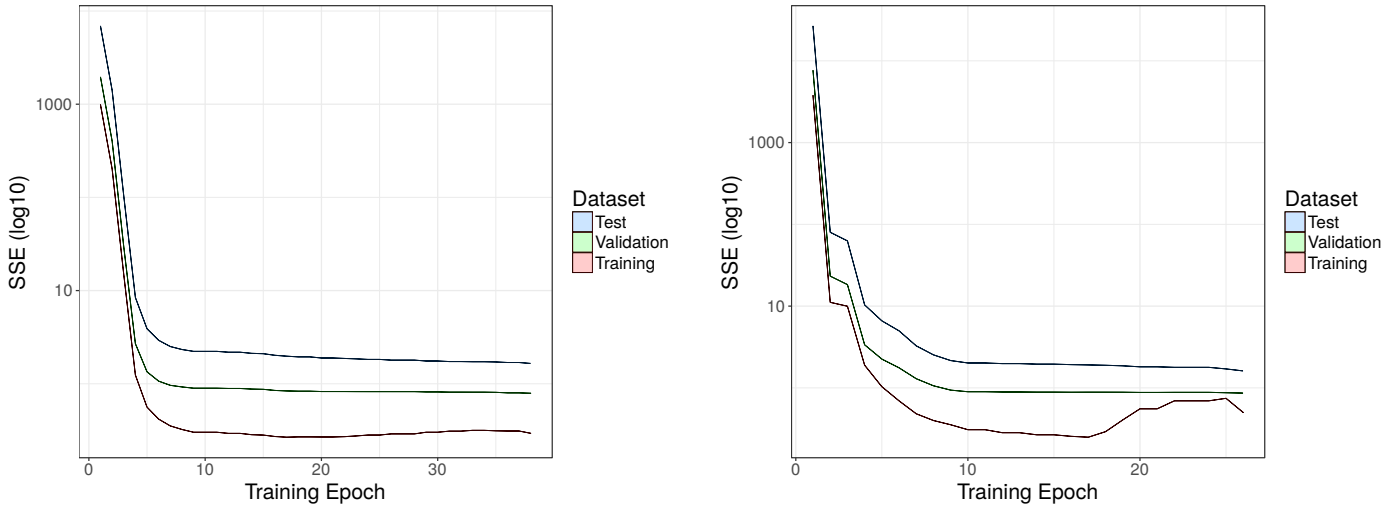

Figure C2.7: ANN model results – Example of the evolution of the SSE during the training procedure of an ANN model. Results shown here are for two autoregressive ANN models structured with two-hidden layers and utilising both temperature and precipitation as exogenous input information.

righten plot depicts a situation where the total error is not reduced as much as it potentially could, having a "step" around the second training epoch. Additionally, even if both the training and validation sets' total errors are always reduced, the same behaviour is not verified when analysing the test set's total error, as it increases during the final training epochs. Such behaviour indicates that, for this particular ANN model, the training stop criteria has failed to identify an ideal generalised solution to the problem and the model may be overfitted. This behaviour can occur due to several reasons, such as the initialisation of weight connections and the random composition of the training, validation, and test datasets.

2.3.2 Model Inter-Comparison

The model efficiency results of the models inter-comparison phase, for the forecasting period ranging from 1 to 4 days, are summarised in Tables C2.2 and C2.3.

Table C2.2: Model inter-comparison results for the test dataset – NSE.

Model		Forecasting Period (days)			
		1	2	3	4
ANN	Min.	0.7716	0.7483	0.7370	0.7484
	Mean	0.9112	0.8325	0.8065	0.8016
	Max.	0.9435	0.8871	0.8649	0.8537
Naive	-	0.8621	0.6569	0.5534	0.3666
Trend	-	0.7821	0.3872	0.3726	0.2066
MLR	-	0.9401	0.8260	0.7168	0.5810
TF	-	0.9485	0.8410	0.7321	0.6024

Table C2.3: Model inter-comparison results for the test dataset – PBIAS.

Model		Forecasting Period (days)			
		1	2	3	4
ANN	Min.	-3.2243	-1.9879	-1.5908	-3.0160
	Mean	0.2642	0.4546	0.6128	0.4733
	Max.	3.2008	3.6727	4.9117	4.3683
Naive	-	-0.0178	0.7545	-0.0595	-1.6581
Trend	-	0.0248	-0.7903	1.5686	1.5391
MLR	-	0.0862	0.2000	-0.0682	-0.3097
TF	-	-1.8638	2.3769	-3.0729	3.1385

From the results shown in Tables C2.2 and C2.3, it can be stated that, among all the studied modelling techniques and considering all forecasting periods, the

ANN model is the most efficient for the forecasting of the stream stage of the IRW. If the forecasting period are to be considered alone, for 1 day forecasting the TF model is slightly superior to both the ANN and MLR models, while the last two can be considered equivalents. For a forecasting period of 2 days, both the ANN and TF models are the best overall modelling techniques. For a forecasting period of 3 or 4 days, the ANN model is decisively the model with best results. These results highlights the potential applicability of ANN models in time-series prediction and modelling, such as the forecasting of the stream stage of rivers. Another interesting result is the fact that both the MLR and TF models are significantly more efficient in forecasting the stream stage of the IRW if compared to the Naïve and Trend models. This last result is consistent for all forecasting periods.

Aiming at the visualisation of how the overall efficiency decreases with an increase in the forecasting period, Figure C2.8 depicts a series of scatter plots, one for each forecasting period.

The results show in Figure C2.8 indicate that the ANN model generally loses accuracy and precision in predicting the stream stage of the IRW as the forecasting period increases. This finding is confirmed by the results shown in Tables C2.2 and C2.3 and is somehow expected, as the more distant in the future the prediction is, the less information is available to make the prediction, thus the less efficient the model is in forecasting the stream stage of the IRW. Such deficiency can also be partly attributed to the stochastic nature of the considered hydro-meteorological variables, such as precipitation, which contributes by adding aleatoric uncertainty to the overall uncertainty of ANN models.

Another interesting observation that can be noticed from the results shown in Figure C2.8 is the fact that most of the prediction accuracy of the ANN is lost at higher stream stage values, as graphically seen in Figure C2.8 and numerically assessed in Table C2.3. This behaviour can be mainly attributed to the fact that empirical models are, in general, heavily based on observations. Since most of the stream stage observation values are concentrated around its mean value and very few on extreme values (see Figure C2.1), the ANN model is less efficient in learning the behaviour of the system under extreme conditions due to the lack of training examples, thus resulting in lower model performance under these

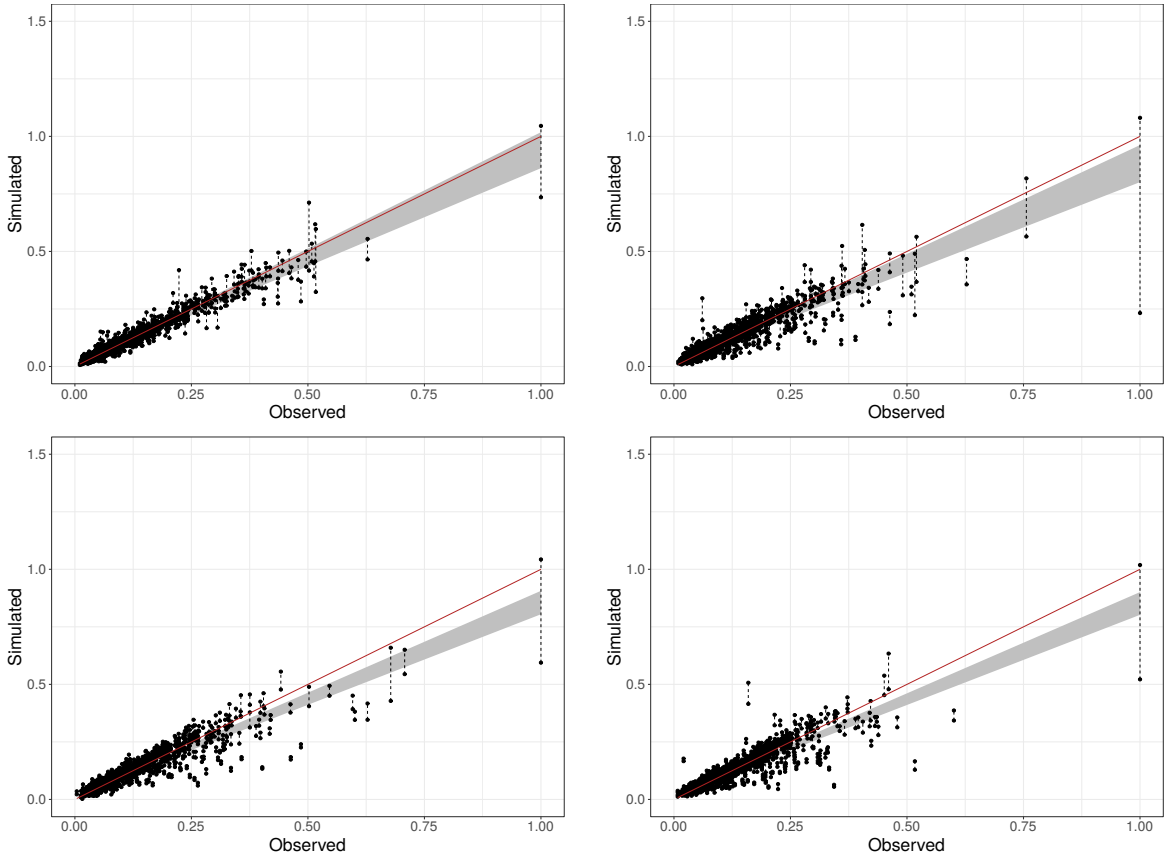

Figure C2.8: Stream stage forecasting periods when using an autoregressive, double hidden layered ANN model – Scatter plots. Top left: 1 day forecasting period; Top right: 2 days forecasting period; Bottom left: 3 days forecasting period; Bottom right: 4 days forecasting period.

circumstances. Even though the lower performance is visible when simulating extreme values, the ANN model is still capable of forecasting extreme values, as indicated by the uncertainty range of the simulated values, as graphically depicted in Figure C2.8.

In general, though, it can be stated that ANN models are a good modelling technique to be applied for the forecasting of rivers stream stage. Figure C2.9 depicts a graphical representation of how the ANN model performs in forecasting the stream stage of the IRW against observed values during the period from June to September of 1977.

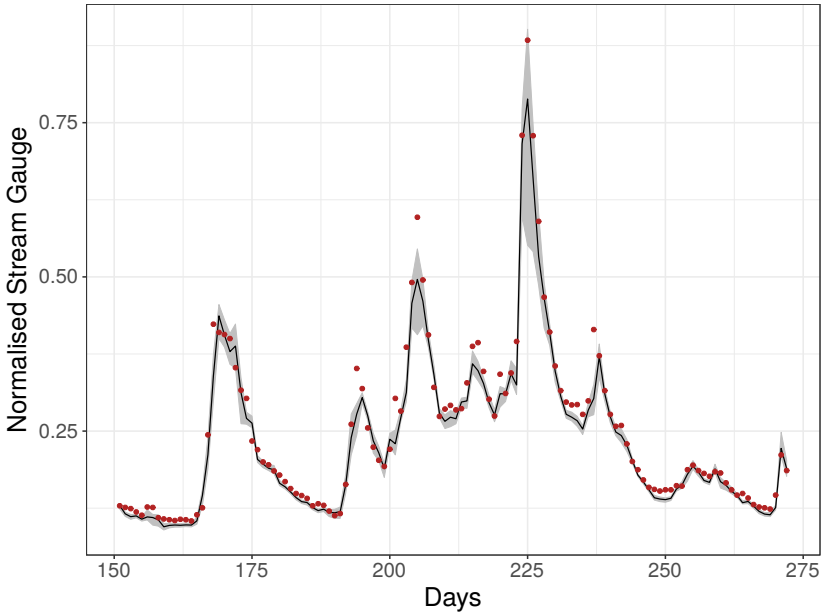

Figure C2.9: Ensemble ANN forecast of the stream stage of the IRW. The red dots represent the observations. The grey area represents the range of predictions made by the ensemble of ANN models. The black line represents the mean prediction value of the ensemble of ANN models. The time frame depicted here covers the period from June to September of 1977.

2.4 Conclusions

The intrinsic uncertainties of ANN models are a serious limitation for a wider usage of this technology. This chapter has explored some of the intrinsic uncertainties of ANN models by studying how different model configurations can affect the overall performance of these models, while, at the same time, evaluating the efficiency of the developed ANN model. A case study involving the forecasting of the stream stage of the IRW is proposed in order to identify the possible intrinsic sources of uncertainties to ANN models and to evaluate the models' performance. It is found that much of the uncertain aspects of ANN models come from three main factors, namely: i. The composition and quality of the input data; ii. The initialisation of the weight connections between the neurons, and; iii. The ANN model type. As the considered ANN model learns from observations, the availability and quality of observation records in certain value ranges can greatly influence the overall performance of the model.

Regarding the exogenous input information, it is found that the best results are obtained when both temperature and precipitation are utilised together as exogenous input information to the ANN model. For what concerns the ANN model structure and information flow, it is found that the NARX model type is much more suitable for the prediction of the stream stage of the IRW than the I-O.d model type. Finally, the difference in performance between the single and double hidden layered model architectures is minimal with respect to the previous discussed factors. The main difference between both architectures is that, generally, the double hidden layered variant is capable of producing more accurate yet less precise results in forecasting the stream stage of the IRW.

In order to deepen the understanding of how uncertainties can affect the performance of ANN models, some recommendations can be made. First, the study of how a varying composition of hidden layers can affect the overall performance of ANN models is recommended in similar future studies. Moreover, the consideration of other hydro-meteorological variables as exogenous input information is another interesting topic to be explored, such as the inclusion of solar radiation and/or relative humidity. Finally, a comparison between the results

obtained from the use of ANN models and physically-based hydrologic models, such as the SWAT model, can help in evaluating and understanding data and site-specific uncertainties capable of affecting the overall performance of both modelling techniques.

Acknowledgements

The work presented in this chapter was possible due to the possibility of performing some calculations on the *Sistema per Calcolo Scientifico di Ca' Foscari* – SCSCF computer cluster (www.dais.unive.it/scscf), a multiprocessor system owned by Ca' Foscari University of Venice and running under a GNU/Linux operating system.

References

[1] Alvisi, S., Franchini, M., 2012. Grey neural networks for river stage forecasting with uncertainty. Physics and Chemistry of the Earth 42-44, 108–118. URL http://dx.doi.org/10.1016/j.pce.2011.04.002

[2] ANA, A. N. d. Á., 2014. HidroWeb - Sistema de Informações Hidrológicas. URL http://hidroweb.ana.gov.br/default.asp

[3] Apel, H., Thieken, a. H., Merz, B., Blöschl, G., 2004. Flood risk assessment and associated uncertainty. Natural Hazards and Earth System Science 4 (2), 295–308.

[4] Asefa, T., 2009. Ensemble streamflow forecast: A glue-based neural network approach. Journal of the American Water Resources Association 45 (5), 1155–1163.

[5] Askew, A., 1989. Real-time intercomparison of hydrological models. In: New Directions for Surface Water Modeling - Proceedings of the Baltimore Symposium. No. 181. IAHS, pp. 125–132.

[6] Atiya, A. F., El-Shoura, S. M., Shaheen, S. I., El-Sherif, M. S., 1999. A Comparison Between Neural-Network Forecasting Techniques—Case Study: River Flow Forecasting. IEEE Transactions on Neural Networks and Learning Systems 10 (2), 402–409.

[7] Benitez, J. M., Castro, J. L., Requena, I., 1997. Are Artificial Neural Networks Black Boxes? IEEE Transactions on Neural Networks 8 (5), 1156–1164.

[8] Brooks, K. N., Ffolliott, P. F., Magner, J. A., 2013. Hydrology and the Management of Watersheds, 4th Edition. John Wiley & Sons, Inc., Iowa, USA.

[9] Brutsaert, W., 2013. Hydrology: An Introduction, 8th Edition. Cambridge University Press, Cambridge, United Kingdom.

[10] Campolo, M., Soldati, A., Andreussi, P., 2003. Artificial neural network approach to flood forecasting in the River Arno. Hydrological Sciences Journal 48 (June), 381–398.

[11] Elshorbagy, B. A., Simonovic, S. P., Panu, U. S., 2000. Performance Evaluation of Artificial Neural Networks for Runoff Prediction. Journal of Hydrologic Engineering 5 (October), 424–427.

[12] Giacinto, G., Roli, F., 2001. Design of effective neural network ensembles for image classification purposes. Image and Vision Computing 19 (9-10), 699–707.

[13] Haddad, K., Rahman, A., Weinmann, P. E., Kuczera, G., Ball, J., 2010. Streamflow data Preparation for Regional Flood Frequency Analysis: Lessons from Southeast Australia. Australasian Journal of Water Resources 14 (1), 17–32.

[14] Hagan, M. T., Menhaj, M. B., 1994. Training Feedforward Networks with the Marquardt Algorithm. IEEE Transactions on Neural Networks 5 (6), 989–993.

[15] Han, D., Kwong, T., Li, S., 2007. Uncertainties in real-time flood forecasting with neural networks. Hydrological Processes 21, 223—-228.

[16] Han, J., 2002. Application of Artificial Neural Networks for Flood Warning Systems. Phd thesis, North Carolina State University.

[17] Haykin, S., 2001. Neural Networks: A Comprehensive Foundation, 2nd Edition. Prentice Hall, Inc., Upper Saddle River, NJ, USA.

[18] Heermann, P. D., Khazenie, N., 1992. Classification of multispectral remote sensing data using a back-propagation neural network. IEEE Transactions on Geoscience and Remote Sensing 30 (1), 81–88.

[19] Hsieh, W. W., Tang, B., 1998. Applying Neural Network Models to Prediction and Data Analysis in Meteorology and Oceanography. Bulletin of the American Meteorological Society 79 (9), 1855–1870.

[20] INMET, I. N. d. M., 2014. Banco de Dados Meteorológicos para Ensino e Pesquisa - BDMEP.
URL http://www.inmet.gov.br/projetos/rede/pesquisa/

[21] ISO, 2011. Accuracy (trueness and precision) of measurement methods and results - Part 1: Introduction and basic principles. Tech. rep., International Organization for Standardization, Vernier, Geneva, Switzerland.

[22] JCGM, J. C. F. G. I. M., 2008. Evaluation of measurement data — Guide to the expression of uncertainty in measurement. Tech. Rep. September, Document produced by Working Group 1 of the Joint Committee for Guides in Metrology (JCGM/WG 1), Geneva.

[23] Kasiviswanathan, K., He, J., Sudheer, K., Tay, J.-H., 2016. Potential application of wavelet neural network ensemble to forecast streamflow for flood management. Journal of Hydrology 536, 161–173.
URL http://dx.doi.org/10.1016/j.jhydrol.2016.02.044http://www.scopus.com/inward/record.url?eid=2-s2.0-84960112960{&}partnerID=tZOtx3y1

[24] Khan, M. S., Coulibaly, P., 2006. Bayesian neural network for rainfall-runoff modeling. Water Resources Research 42 (7), 1–18.

[25] Krause, P., Boyle, D. P., 2005. Advances in Geosciences Comparison of different efficiency criteria for hydrological model assessment. Advances In Geosciences 5 (89), 89–97.

[26] Maier, H. R., Dandy, G. C., 2000. Neural networks for the prediction and forecasting of water resources variables: A review of modelling issues and applications. Environmental Modelling and Software 15 (1), 101–124.

[27] May, R. J., Maier, H. R., Dandy, G. C., Fernando, T. M. K. G., 2008. Non-linear variable selection for artificial neural networks using partial mutual information. Environmental Modelling and Software 23 (10-11), 1312–1326.

[28] Merwade, V., Olivera, F., Arabi, M., Edleman, S., 2008. Uncertainty in Flood Inundation Mapping: Current Issues and Future Directions. Journal of Hydrologic Engineering 13, 608–620.

[29] Merz, B., Thieken, A. H., 2005. Separating natural and epistemic uncertainty in flood frequency analysis. Journal of Hydrology 309 (1-4), 114–132.

[30] Moriasi, D. N., Arnold, J. G., Van Liew, M. W., Binger, R. L., Harmel, R. D., Veith, T. L., 2007. Model evaluation guidelines for systematic quantification of accuracy in watershed simulations. Transactions of the ASABE 50 (3), 885–900.

[31] R, C. T., 2016. R: A Language and Environment for Statistical Computing.
URL https://www.r-project.org/

[32] Rmetrics, C. T., Wuertz, D., Setz, T., Chalabi, Y., 2014. fBasics: Rmetrics - Markets and Basic Statistics.
URL https://cran.r-project.org/package=fBasics

[33] Schumann, A. H., 2011. Flood risk assessment and management: How to specify hydrological loads, their consequences and uncertainties. Springer Science, Business Media, Bochum, Germany.

[34] Strnad, D., Nerat, A., Kohek, S., 2015. Neural network models for group behavior prediction: a case of soccer match attendance. Neural Computing and Applications 28, 287–300.

[35] Tobin, G. a., 1995. The Levee Love Affair: A Stormy Relationship? Water Resources Bulletin. Journal of the American Water Resources Association 31 (3), 359–367.

[36] Wickham, H., 2009. ggplot2: Elegant Graphics for Data Analysis.

[37] Wu, C. L., Chau, K.-W., Li, Y. S., 2009. Methods to improve neural network performance in daily flows prediction. Journal of Hydrology 372, 80–93.

[38] Yu, H., Wilamowski, B. M., 2011. Levenberg-Marquardt Training.

[39] Zhou, Z.-H., Jiang, Y., Yang, Y.-B., Chen, S.-F., 2002. Lung cancer cell identification based on artificial neural network ensembles. Artificial Intelligence in Medicine 24 (1), 25–36.

Chapter 3

The SWAT-ANN Model

Making Use of its New Capabilities

Abstract

The accurate representation of a watershed and its water dynamics is the first step required in order to perform any kind of quantitative or qualitative analysis of hydrological-related processes. Some watersheds, however, are characterised by complex water dynamics which, in turn, require complex artificial hydraulic management mechanisms. An example is the VLW, a watershed heavily affected by anthropogenic factors located in North-East Italy. Hydrological modelling is particularly challenging under these circumstances, requiring not only accurate quantitative information, but also the fine-tuning and specialisation of already existing modelling frameworks. This chapter proposes a methodological framework based on the use of a coupled mechanistic-empirical model (i.e. SWAT-ANN) to simulate particularly complex hydrologic features of the VLW. Three sub-basins of the VLW (i.e. Dese-Zero, Marzenego and Montalbano) with particular hydraulic management operations are taken as case studies for the evaluation of the proposed methodological framework. It is found that the proposed coupled SWAT-ANN model is capable of accurately reproducing the overall water and nutrient balances of the studied watersheds.

3.1 Introduction

A watershed, in very simple words, can be understood as the land area which drains water to a specific point in space by means of a stream network system. Under this concept, a watershed can also be seen as a control system, where the overall water balance is the result of the interaction between inputs (e.g. precipitation, incoming groundwater, etc.) and outputs (e.g. surface runoff, evapotranspiration, outgoing groundwater, etc.). Even though a watershed is spatially defined according to its surface flow drainage network, its overall water movement is rather complex as other water pathways may contribute to the open channel flow of a drainage basin which, in turn, might be affected by factors external to the watershed area, such as the incoming groundwater. Consequently, a same watershed may have different surface and groundwater contribution regions, a process known as IGF. An example is the VLW[1], in Italy. Not only the VLW's water budget is heavily influenced by groundwater coming from outside its superficial coverage area, but also by human activities that, in turn, transforms the simple task of delineating its catchment into a large and complex effort.

Hydrologic modelling under these circumstances is particularly challenging. In general, hydrologic models require detailed quantified information about various hydrologic processes, such as infiltration, runoff and evapotranspiration. Still, other information may be required depending if/which non-hydrologic processes are considered, such as water quality dynamics, transportation of sediment, and vegetation growth. Moreover, human interferences in the hydrologic and non-hydrologic processes may substantially increase the difficulty in modelling a watershed's hydrologic response [34]. In summary, all these processes and interactions combined constitute a complex and dynamic system, requiring not only a complex model but also a significant amount of input information coming from field measurements and hydrological observations [23]. Unfortunately, such detailed information may not always be available or may be insufficient.

Currently, there is a lack of detailed quantified information for hydrologic simulation purposes regarding the complex hydraulic dynamics taking place in the

[1] A detailed description of this watershed can be found in Section 1.3.

VLW, not only in terms of the quantity and/or quality of groundwater entering the watershed but also regarding the amount and/or quality of superficial water deviated from/to bordering watersheds.

Past studies have assessed the external hydraulic and nutrient loadings entering the VLW by means of hydrological modelling: Salvetti et al. [30] employed the SWAT model to assess the total source apportionment of three sub-basins of the VLW into the Lagoon of Venice, noting that external hydraulic influences from groundwater sources contributes significantly to the total water discharge of these sub-basins into the Lagoon of Venice and estimating that around 35% of the yearly total phosphorus apportionment comes from external channel loads to the VLW; still, Salvetti et al. [29] studied the source apportionment of the Dese-Zero watershed into the Lagoon of Venice by employing two distinct models (i.e. QUAL2E and BASINS-SWAT), concluding that, under dry weather conditions, 80% of the total nitrogen load is attributed to groundwater/spring recharge and tributary/irrigation channels coming from bordering watersheds; Azzellino et al. [6], in turn, analysed the total apportionment of nutrient loads from the VLW discharged to the Lagoon of Venice while evaluating if the external loads to the VLW are relevant under the Water Framework Directive – WFD, concluding that there is significant contribution coming from outside sources of the VLW and suggesting that River Basin Management Plans – RBMPs in the area should not be limited to their watershed boundaries; finally, Essenfelder et al. [13][2] proposed a methodology to identify the factors contributing to the total external hydraulic loads to the Dese-Zero watershed by presenting a coupled mechanistic-empirical modelling technique to quantify these influences, concluding that hydro-meteorological information is essential in order to quantify this non-linear process.

Summing it all up, the current complexity of the VLW associated with the lack of specific information about the external load contributions to its sub-basins and the artificial hydraulic management make it very difficult to carry out any kind of reliable future hydrological scenario analysis over the VLW area at a watershed-level, such as the evaluation of impacts due to climate change. Indeed, due to the water management challenges of the VLW, a holistic perspective of

[2]The referred publication constitutes the first part of this chapter.

the issues is necessary, requiring, in turn, the integration of multiple modelling techniques [14]. In fact, still exists the lack of a consolidated framework capable of estimating and quantifying the total external influences to the VLW, not only by contemplating the total amount of water entering/leaving the watershed but also regarding the amount of nutrients carried by these processes.

Thus, this chapter evaluates a methodological framework to identify the factors influencing the complex water and nutrients exchanges among the VLW and its surrounding river basins, while, at the same time, proposing a methodology to estimate the overall water and nutrient balance of a watershed heavily influenced by artificial hydraulic management operations such as the VLW. The proposed modelling technique consists in a coupled mechanistic-empirical modelling approach and assumes that the physically-based hydrological model is capable of simulating the hydrological processes occurring inside the watershed while the empirical model is able to account for the complex hydraulic dynamics affecting the water balance of the VLW (in particular the exchanges of water from the surrounding watersheds). The models utilised in this study are: i. the SWAT model as the mechanistic part, and; ii. an ANN or MLR models as the possible empirical counterpart. The mechanistic and empirical models are combined into a single tool and are run simultaneously during the hydrological simulations.

Structure-wise, the work presented in this chapter can be sub-divided into two parts. The first part proposes the identification of the main factors contributing to the total external hydraulic influences to the Dese-Zero watershed, a sub-basin of the VLW, by means of PCA, while, at the same time, proposing the identification of the most accurate empirical modelling technique to be utilised for hydrologic modelling in the study area. The second part presents a case study considering three sub-basins of the VLW for the quantification of the estimated total external hydraulic loads, namely: i. the Dese-Zero; ii. the Marzenego, and; iii. the Montalbano sub-basins. The overall proposed methodological framework contemplates the use of a coupled mechanistic-empirical modelling approach. Under such configuration, the physically-based model takes the role of simulating the process occurring inside the watersheds (e.g. rainfall-runoff, infiltration, evapotranspiration, etc.) while the empirical model accounts for the above described external hydraulic influences to the VLW. The physically-based model

selected for this study is the SWAT model, which has already been applied to the same area in previous studies [30, 29, 6, 13], providing a solid starting point and good comparison basis. For the empirical counter-part, it is proposed the study of a linear MLR model and of a non-linear ANN[3] model [13, 22, 11].

3.2 Methodology

3.2.1 The Study Area

The sub-basins selected as case study for this chapter are the Dese-Zero, Marzenego, and Montalbano, all three being major sub-basins of the VLW[4], as shown in Figure C1.4. Figure C3.1, instead, shows the location where most of the groundwater contribution takes place for the study areas, as well as the approximate location of the most important hydraulic devices affecting the overall water budget of these sub-basins.

3.2.2 The Hypothesis

The general complexity of the VLW is a clear obstacle when simulating any hydrologic-related process by means of hydrologic modelling. Besides, the lack of data in the region regarding the amount of water that is actually deviated from/to the VLW sub-basins and the exact contribution of the external aquifer system is another big challenge to be taken into account when performing any kind of hydrologic study in the region. The combination of these factors poses a serious challenge for an accurate simulation of hydrologic-related processes in the VLW as a whole.

In a complex system, the integration of knowledge can be an useful approach to manage a situation or to solve a specific problem. In the case of the VLW, expert

[3] A theoretical description of the utilised ANN model can be found in Appendix 2, while the source code of the developed model can be found in Appendix 3.

[4] A detailed description of the whole VLW is covered in Chapter 1, Section 1.3, while more information regarding the Dese-Zero, Marzenego and Montalbano sub-basins can be found in Sub-Sections 1.3.2, 1.3.3, and 1.3.7, respectively.

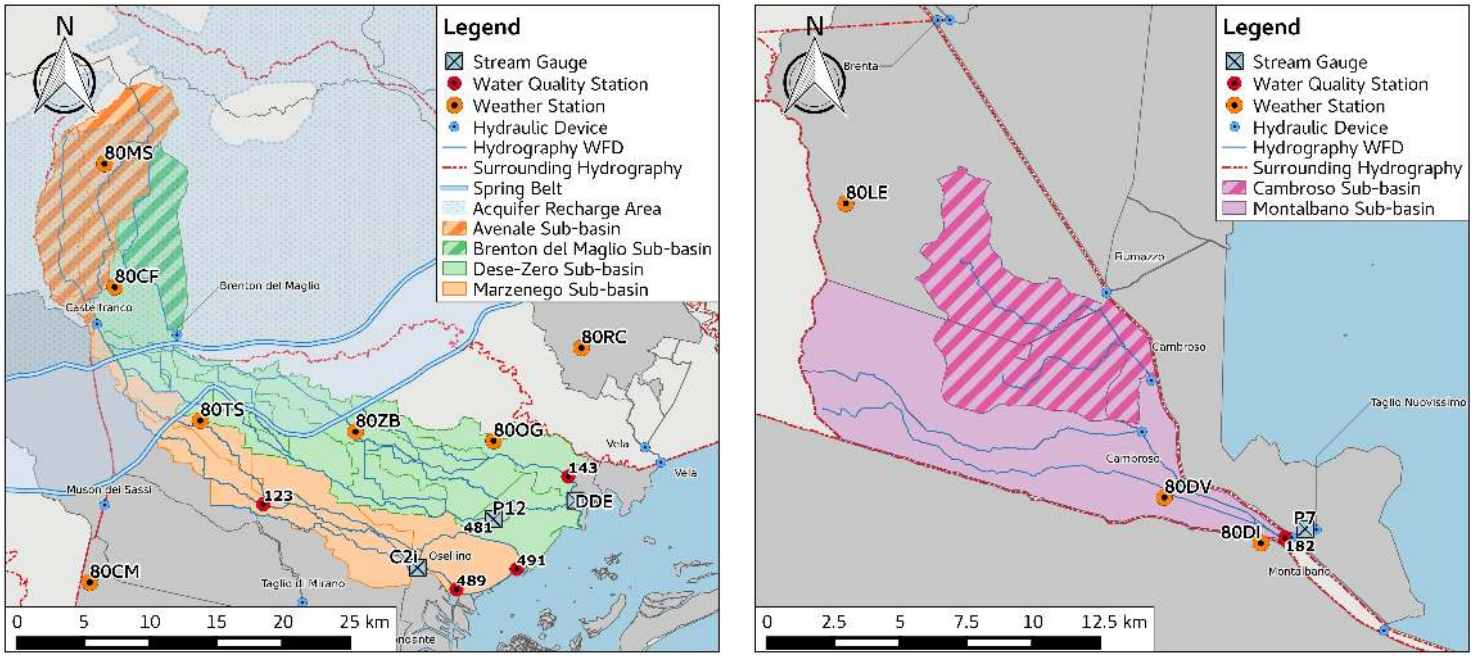

Data source: Veneto [32], ARPAV [4]

Figure C3.1: The study area, covering the Dese-Zero, Marzenego, and Montalbano watersheds.

local knowledge on irrigation, land reclamation, and hydraulic management of the watershed must be integrated with the understanding of hydro-meteorological parameters for the proper management of the VLW's sub-basins [10], as these play an important role not only in the operation of the hydraulic devices but also in the recharging process of the Venetian aquifers [5].

Recent studies have demonstrated that some hydrological models which have been applied to the VLW area have some limitations when simulating the influence of spring waters in the upper Dese-Zero and Marzenego sub-basin, as a large extent of the aquifer's recharge area is located outside the area covered by the VLW [29, 6, 13]. Hence, there is the need to accurately reproduce the overall water budget of these watersheds, particularly when dealing with future scenario studies, such as the evaluation of possible impacts of climate change or the valuation of best management practices.

Thus, based on what has been discussed so far, this research presents and is build upon the following hypothesis:

Hypothesis. *Exists a mathematical relation capable of efficiently and accurately simulating the complex water dynamics that is observed in the Venice Lagoon Watershed by considering a priori known hydro-meteorological information.*

3.2.3 The SWAT Model

The SWAT[5] model is a river basin scale model which allows a number of different physical processes to be simulated in a watershed while also enabling the evaluation of diverse land management practices on the runoff, water quality, sediment transport, and agricultural chemical yields processes. Nonetheless, the SWAT model offers the capability of assessing different weather scenarios, such as climate change scenarios, while also providing tools for the assessment of its impacts on hydrological-related processes [3, 21].

The very basic information needed by the SWAT model in order to set-up a project is the DEM, soil characteristics and spatial distribution, land-use characteristics and spatial distribution, relevant land-use management operations,

[5]A more deep description of the model can be found in Chapter 1, Sub-Section 1.2.1. A full explanation of the model can be found in either [2] or [21].

and weather information [2]. Table C3.1 shows the data source and reference year of the input data used for the set-up of theSWAT model. Besides this basic input information, measured streamflow and water quality data are used for calibration purposes. This data is also shown in Table C3.1. The spatial location of the weather stations, stream gauge, and water quality measurement points, instead, are shown in Figure C3.1.

Table C3.1: SWAT model input and related data.

ID	Data Provider	Description	Ref. Year
DEM	Regione Veneto	Digital elevaton model for the Veneto Region (5x5m cells)	2000
Weather Data	ARPAV	Meteorological data for the Veneto Region	-
Streamflow	ARPAV/Regione Veneto	Measured streamflow data	-
Water Quality	ARPAV/Regione Veneto	Measured water quality data (Nitrogen and Phosphorus)	-
Hydrography	ARPAV	Hydrography of interest to the Directive 2000/60/EC (scale 1:10.000)	2012
Sub-basins	ARPAV	Regional watersheds' limits (scale 1:10.000)	2015
Land-use	Regione Veneto	Land-use map and classes for the Veneto Region (scale 1:10.000)	2000
Soils	ARPAV	Soil map and classification for the VLW (scale 1:50.000)	2000

Data source: Veneto [32], ARPAV [4]

The original DEM was aggregated from an original resolution of 5x5m to a 20x20m resolution by using the resample bilinear method. In order to maintain spatial integrity, both soil and land-use vector maps were converted to raster format at a 20x20m resolution grid by using the resample majority method. Still, the original soil map, consisting of 101 different classes, was combined into 18 representative classes according to their textures [12]. In a similar approach, the original classes of the land-use map (i.e. 79 classes) were combined and converted to SWAT-compatible land-use classes according to their representativeness in terms of total covered area resulting in a final number of 13 land-use classes, ranging from the most relevant crop varieties (e.g. corn, sugar-beet and vineyard) to urban areas (e.g. high and low density).

Considering the information described in Table C3.1 and the input data pre-processing, the Dese-Zero watershed was sub-divided into 14 sub-basins, for a total of 476 HRUs, the Marzenego watershed was sub-divided into 9 sub-basins, for a total of 253 HRUs, and the Montalbano watershed was sub-divided into 3

sub-basins, for a total of 60 HRUs.

In order to account for the external influences of the Avenale, Brenton del Maglio, and Cambroso sub-basins to the studied watersheds, a SWAT project was set-up for each of these sub-basins. Hence, the Avenale sub-basin was sub-divided into 79 HRUs, the Brenton del Maglio sub-basin was partitioned into 16 HRUs, and the Cambroso sub-basin was split into 63 HRUs. The simulated streamflow and water quality loadings, as calculated by the SWAT model for each of these watersheds, is, then, imported to the studied sub-basins, according to the partition presented in Table C1.1.

The weather data available for this study covers the period from Jan/1993 to Dec/2014, on a daily basis, for the weather variables shown in Table C3.2. The spatial location of each meteorological station is shown in Figure C3.1.

Table C3.2: Weather variables information and ID codes.

Weather Variable	Unit	Weather Station ID
Relative Humidity	$-$	80CF, 80DI, 80DV, 80LE, 80MS, 80OG, 80TS, 80VV, 80ZB
Precipitation	mm	80CF, 80DI, 80DV, 80LE, 80MS, 80OG, 80TS, 80VV, 80ZB
Solar Irradiance	$MJ \cdot m^{-2}$	80CF, 80DI, 80DV, 80LE, 80OG, 80VV, 80ZB
Maximum Temperature	$^{\circ}C$	80CF, 80DI, 80DV, 80LE, 80MS, 80OG, 80TS, 80VV, 80ZB
Minimum Temperature	$^{\circ}C$	80CF, 80DI, 80DV, 80LE, 80MS, 80OG, 80TS, 80VV, 80ZB
Wind Speed	$m \cdot s^{-1}$	80DV, 80MS, 80TS

Data source: ARPAV [4]

Streamflow data was available as measured by four distinct stream gauges, two located in the Deze-Zero watershed, one in the Marzengo watershed and another in the Montalbano watershed. Observed water quality data, instead, was available as measured by four distinct water quality collecting points, two located in the Dese-Zero watershed, one in the Marzenego watershed and one in the Montalbano watershed. For calibration purposes of the SWAT model, the overall measured streamflow and water quality databases were arranged into the calibration and validation datasets aiming at a validation:calibration ratio of around 1:4. Table C3.3 shows more details on the data used for the calibration of the model, such as the the frequency in which the data is available and at which time period.

Table C3.3: Streamflow and water quality data summary.

Variable	Station ID	Unit	Frequency	Time Period
Streamflow	C2i	$m^3 \cdot s^{-1}$	Daily	2005-2012
	DDE	$m^3 \cdot s^{-1}$	Daily	1998-2000
	P7	$m^3 \cdot s^{-1}$	Daily	2004-2012
	P12	$m^3 \cdot s^{-1}$	Daily	1997-2005
Water Quality	143	$mg \cdot l^{-1}$	Monthly	2002-2011
	182	$mg \cdot l^{-1}$	Monthly	2005-2013
	481	$mg \cdot l^{-1}$	Monthly	2002-2011
	489	$mg \cdot l^{-1}$	Monthly	2004-2011

Data source: ARPAV [4]

3.2.4 The Empirical Models

Based on previous studies that proves the feasibility of integrating ANNs and the SWAT models [13, 22, 11], the empirical model developed for this study is a non-linear ANN model. The ANN[6] model used in this chapter was developed by the authors in R language, being able to be configured in a number of variations and to run on a multi-core cluster system. Following the work discussed in Chapter 2, a MLR is also introduced as a potential empirical model. The MLR is chosen as it is a statistical technique used to predict, under linear assumptions, the outcome of a certain variable according to one or more explanatory variables, being capable of producing satisfactory results while being a simple and computationally efficient modelling technique. The MLR model utilised in this chapter relies on the use of the R's function *lm* [28]. Although both the ANN and MLR models are empirical modelling techniques, it is interesting to compare the performance of both, as ANNs are non-linear models and MLR are linear models.

Regarding the coupling of the empirical models with the SWAT model, the empirical models receive on-line information from and are called iteratively by the SWAT model during the routing phase of the hydrologic simulations[7]. The results of the empirical models are, then, incorporated into the SWAT hydrologic simulations and passed to the subsequent routing phase calculation steps. The user can specify the sub-basin in which the empirical model is called by the mechanistic component, representing the location where the connection between

[6] A theoretical description of the utilised ANN model can be found in Appendix 2, while the source code of the developed model can be found in Appendix 3.

the two models takes place. This can be done by adding a boolean control check to the *route* command of the SWAT input file named *"fig.fig"* (i.e. addition of a new column, where the value '1' means proceed with the SWAT-ANN coupled model computation, and '0' means not calling the empirical component). Additionally, the user can create another control file that is read by the SWAT model after the empirical computational procedure is finalised and serving the only purpose of specifying the spatial location where the outputs of empirical models should be accounted for in the SWAT model. Further explanation regarding the coupling of the SWAT and the ANN models can be found in Chapter 1, Sub-Section 1.2.2, and in Appendix 1.

Recognising the statement made at the Hypothesis 3.2.2, the possible meteorological inputs to the empirical models are roughly the same as the meteorological data used as input information to the SWAT model (see Table C3.2), with the only difference being daily temperature, which is condensed into a daily average value by taking the average of the daily maximum and minimum temperatures. Other than weather data, the empirical models consider as possible input data some relevant hydrologic information passed by the SWAT model, such as streamflow and soil water content, while also considering some artificial water demand, such as irrigation water demand.

All this information is presented to the empirical models in order to transmit the knowledge of when the water availability and water demand of the studied watersheds might be under a critical situation, thereby requiring the operation of the artificial hydraulic control system as described in Chapter 1, Section 1.3. Nonetheless, temporal information is also passed as a boolean value from the mechanistic model to the empirical models, representing the season of the year when the combination of hydro-meteorological parameters is occurring [13]. A summary of the all input data to the empirical models is presented in Table C3.4[8].

[7] The proposed SWAT source code modifications pertaining to the coupling with the ANN model can be found in Appendix 1, while the source code of the developed ANN model can be found in Appendix 3. Both models communicate by exchanging information stored in *.csv* files.

[8] The Dese-Zero watershed is split into Dese and Zero river systems because of the two distinct inputs, one coming from the Avenale and the other from the Brenton del Maglio watersheds, following the discussion presented in Chapter 1, Section 1.3.

Table C3.4: Empirical models input variables.

		Value Range				
Variable	**Symbol**	**Dese**	**Zero**	**Marzenego**	**Montalbano**	**Unit**
Streamflow	FLOW	0.02 – 4.25	0.17 – 3.52	0.16 – 3.35	0.00 – 1.43	$m^3 \cdot s^{-1}$
Act. Evapotranspiration	EVAP	0.01 – 4.78	0.02 – 5.34	0.04 – 5.35	0.06 – 5.82	$mm\ H_2O/day$
Return Flow	GWQ	0.00 – 1.49	0.00 – 1.49	0.00 – 2.36	0.00 – 1.49	$mm\ H_2O/day$
Soil Water Content	SW	65.7 – 190.9	65.7 – 190.9	107.0 – 236.2	89.6 – 210.4	$mm\ H_2O/day$
Irrigation Water Demand	IRR	0.00 – 4.28	0.00 – 25.12	0.00 – 4.29	0.00 – 4.27	$mm\ H_2O/day$
Relative Humidity	HMD	0.59 – 0.93	0.61 – 0.96	0.56 – 0.93	0.59 – 0.94	$-$
Solar Irradiance	SLR	2.51 – 25.07	1.96 – 26.87	2.55 – 25.52	2.40 – 27.57	$MJ \cdot m^{-2}$
Avg. Temperature	TMP	0.15 – 24.75	-0.59 – 24.18	-0.29 – 25.12	1.51 – 25.16	$^{\circ}C$
Wind Speed	WND	0.34 – 1.26	0.42 – 1.80	0.40 – 1.67	0.50 – 2.92	$m \cdot s^{-1}$
Precipitation	PCP	0.00 – 9.63	0.00 – 9.23	0.00 – 8.83	0.00 – 7.80	$mm\ H_2O/day$
Spring	SPR	0 or 1	0 or 1	0 or 1	0 or 1	$-$
Summer	SUM	0 or 1	0 or 1	0 or 1	0 or 1	$-$
Autumn	AUT	0 or 1	0 or 1	0 or 1	0 or 1	$-$
Winter	WIN	0 or 1	0 or 1	0 or 1	0 or 1	$-$
Organic Nitrogen	ORGN	0.0 – 1417.9	0.0 – 1695.6	0.0 – 3486.8	0.0 – 1492.3	kgN/day
Ammonium	NH4	0.0 – 628.9	0.0 – 675.4	0.0 – 1436.8	0.0 – 346.5	kgN/day
Nitrite	NO2	0.0 – 177.7	0.0 – 193.5	0.0 – 565.3	0.0 – 84.8	kgN/day
Nitrate	NO3	0.0 – 2723.9	0.0 – 2905.7	0.0 – 3093.3	0.0 – 521.8	kgN/day
Organic Phosphorus	ORGP	0.0 – 300.0	0.0 – 356.6	0.0 – 130.8	0.0 – 241.3	kgP/day
Mineral Phosphorus	MINP	0.0 – 682.9	0.0 – 687.7	0.0 – 455.5	0.0 – 244.0	kgP/day

In order to reduce the influence of possible data noises coming from the hydro-meteorological input data (e.g. exceptional point discharges) and acknowledging the fact uncertainties might be transmitted from the SWAT model to the empirical models, the input information to the empirical models is presented only after taking the past 30-days moving average of each variable. Simulations made by the empirical model are updated for every simulated time-step made by the mechanistic model. The variables that are then fed-back to the mechanistic model (i.e. target variables) are either directly added as streamflow, in case the process being simulated is the estimation of the total external hydraulic loadings, or directly added as a total nutrient load (i.e. organic nitrogen, ammonium, nitrite, nitrate, organic phosphorus, and mineral phosphorus), in case the process being simulated is the nutrient balance. Similarly as performed for the input data variables, this information is condensed in a 30-days average in order to maintain temporal compatibility.

Aiming at the reduction of the uncertainties coming from extreme values and due to the fact that ANN models are know to be sensitive to the input data [26], values below the 5th percentile and above the 95th percentile (i.e. extreme values) of the resulting dataset are discarded. Such data pre-processing is performed to allow the empirical models to capture a signal, if any, of the input hydro-meteorological data to the studied watersheds throughout a year cycle at a monthly scale. Finally, due to the nature of ANNs, the identified inputs to the empirical models are also normalised by feature scaling (Eq. A3.12) with respect to the input value range for each watershed before being presented to the model. Table C3.4 shows the minimum and maximum values used during the feature scaling normalisation process.

For performance evaluation purposes, the input-response dataset is randomly split into calibration (70%), validation (20%) and test (10%) datasets. The validation dataset is used during the training phase of the ANN model in order to avoid the over-fitting of the model, not being used, however, for the calibration of the ANN model itself. The test dataset, instead, is used only after the completion of the ANN training to evaluate its performance, thereby not being presented to the model during the training phase.

3.2.5 The Methodological Framework

The proposed methodological framework adopted in this study is depicted in Figure C3.2.

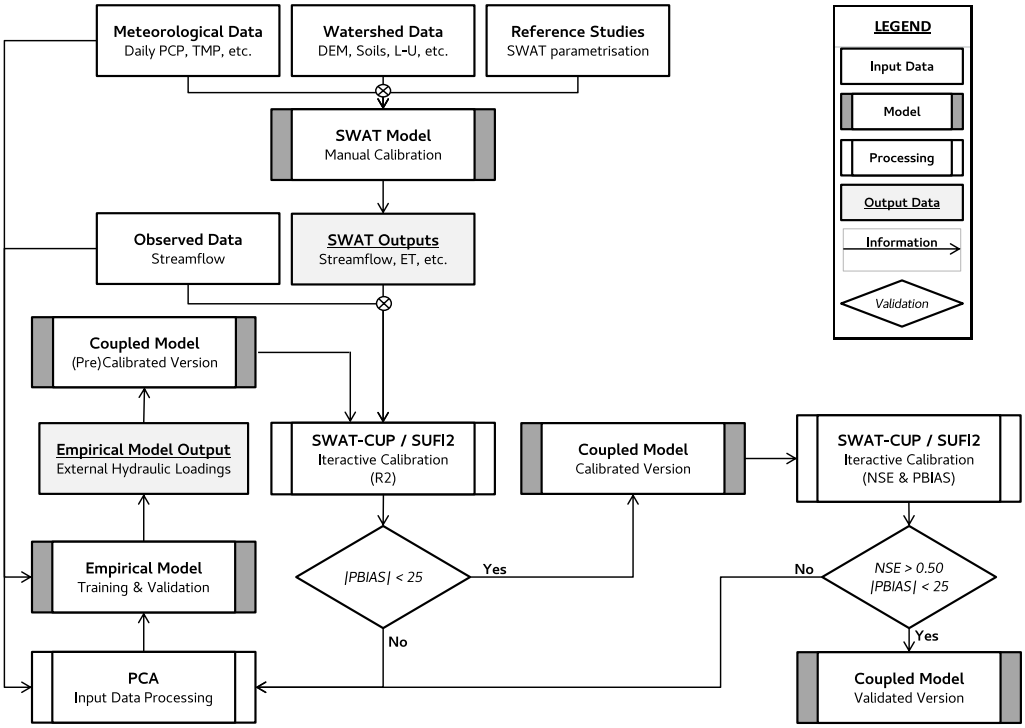

Figure C3.2: Flowchart depicting the proposed methodological framework.

The first step of the proposed methodological framework consists in the manual calibration of the SWAT model based on information and results already published on the literature for the study area [30, 29, 6, 13], as well as other related publications [8, 9, 10, 5, 31, 24].

Subsequently, based on the assumption that the SWAT manually calibrated model is capable of reproducing physically consistent results, the next step contemplates an iterative calibration procedure of the SWAT model by evaluating the Coefficient of Determination – R2 as the objective function. The software used in this step is the SWAT Calibration and Uncertainty Programs – SWAT-CUP, using the Sequential Uncertainty Fitting Algorithm – SUFI2 procedure [1]. The

number of iterations for each calibration cycle varies from 500 to 999, whereas the first calibration cycle always runs 999 iterations. As for the objective function, the R2 is selected as the efficiency criterion because this function is capable of indicating the level of collinearity between the observed and the simulated data [18, 17, 20]. Such consideration means that the analysis performed in this passage does not consider how accurate the actual outputs values are being simulated with respect to the observations, but only how its variation is being reproduced in time (e.g. the variation of the flow with respect to a precipitation event). Hence, this step can be considered as a refinement post-process operation of the previous manual calibration step and is, from now on, referred to as SWAT pre-calibrated model.

The pre-calibrated SWAT model results are, then, evaluated by means of PBIAS (Eq. C2.2). This steps aims at the identification of how accurately the model is able to reproduce the water and nutrient balances of the studied watersheds in absolute terms, as the PBIAS model efficiency criteria is capable of expressing the tendency of the simulated data to over-or-underestimate the reference observed data [20]. In case the results are not considered satisfactory, as it is expected for the VLW due to the significant amount of external hydraulic and nutrient loadings entering the watershed, it is possible to estimate the total external contributions as the difference between the observed and simulated values. The PBIAS efficiency criterion and the threshold value of 25 was adopted from the literature [20].

As the number of input variables to the empirical models may be considerably large due to the consideration of both spatial and temporal dimensions, the succeeding methodological step consists in pre-processing all the possible input data to the empirical models (see Table C3.4 aiming at the identification of the possible most relevant variables by means of PCA as a method for dimensionality reduction [27, 16, 13]. Acknowledging the fact that PCA is based on linear assumptions and, moreover, does not account for any information about the predictands [19], it is proposed the evaluation of two different scenarios, based on the principal components that explain the input data variance at, approximately: i. 80%, and; ii. 95% [13]. Moreover, two criteria are selected as basis for the determination of the most relevant input information, namely: i. The absolute

linear correlation values that are higher than 0.50 between the original input variables and the principal components, and; ii. The variables contributions that are higher than 70% to the principal components. The consideration of these criteria means that variables that are both strongly correlated with and have strong contribution to the factors explaining the input data variance at scenario i. 80% or ii. 95% are considered as interesting to be kept as input information. Moreover, variables with similar criteria values and with the same physical meaning are considered as redundant information, therefore being individually evaluated to be discarded (e.g. out of two temperature stations with similar PCA results, only the one with higher criteria results is kept).

The following methodological step aims at the calibration and identification of the most accurate empirical model by considering the input as pre-processed in the preceding stages. For the ANN model specifically, in order to ensure that the calibration of the models is efficient, the training process is run 1000+ times, each time randomly restarting the initial weight connection values, adjusting the ANN structure, and randomising the training, validation, and test datasets. The best model run is, then, stored by evaluating the SSE and the Mean of Squared Errors – MSE of the validation dataset. A stopped training criteria is implemented to avoid the over-fitting of the model by assessing the evolution of the SSE of the validation dataset [15], as well by evaluating how much the training has improved during the last few training epochs. The resulting calibrated empirical models are then coupled with the SWAT model.

In order to check whether a coupled SWAT-Empirical model is capable of reproducing the overall water and nutrient balance of the studied watersheds, the now re-calibrated SWAT-Empirical model is validated by evaluating the resulting PBIAS, as performed in a previous phase. In case of a positive validation check, the resulting coupled model is then iteratively re-calibrated by using the SWAT-CUP software. This time, however, two efficiency criteria are simultaneously evaluated, namely the NSE (Eq. C2.1), and, again, the PBIAS (Eq. C2.2). Differently from R2, NSE does a better job in identifying not only how well the simulated values of a model are being reproduced in time but also how accurate these results are with respect to the observations. This occurs mainly to the fact that the calculation of the NSE criterion involves the computation of the squared difference between

the observed and predicted values. Due to this property, however, the NSE model efficient coefficient falls short when dealing with the high extreme values of the analysed dataset [20, 17]. The PBIAS, instead, is re-evaluated in order to ensure that the resulting coupled model is not over or underestimating the observations. Finally, the coupled model is re-validated by confronting the model results with thresholds values obtained from the literature [20]. This final validation step is performed by using an independent observed dataset period, not yet used during previous calibration steps.

3.3 Results and Discussions

3.3.1 SWAT Model – Pre-Calibrated

Following the methodological framework described in Sub-Section 3.2.5 and summarised in Figure C3.2, the first attempt to calibrate the SWAT model is performed by manually adjusting the SWAT parameters based on consolidated knowledge regarding the hydrological modelling in the study area by means of specialised literature review, followed by a calibration step using the SWAT-CUP and the SUFI2 procedure to further refine the manual calibration procedure. Regarding the water balance calibration, this procedure consists in modifying a total of 23 distinct SWAT parameters, focusing on three main hydrological-related processes (i.e. surface runoff, baseflow, and soil hydraulic properties) and on parameters governing nutrients balance (i.e. nitrogen and phosphorus). The list of modified parameters and their final calibrated values for this step is shown in Table C3.5. In accordance with the proposed methodology, the performance of the pre-calibrated SWAT model is evaluated by means of the R2. The results regarding the performance evaluation of the pre-calibrated SWAT model are shown in Table C3.6.

The results shown in Table C3.6 indicate an acceptable behaviour if R2 is considered as the sole model efficiency criterion, both under the daily and monthly model configurations for streamflow and also under the monthly basis scenario for the nutrient loadings. Regarding the streamflow, the monthly basis

Table C3.5: SWAT-CUP/SUFI2 results of the pre-calibrated SWAT model.

		Calibrated Value (min–max)		
Parameter	**Description**	**Dese-Zero**	**Marzenego**	**Montalbano**
CN2	Initial SCS CN II value	80.1 (70.4–89.9)	82.0 (72.0–92.0)	77.4 (66.0–89.4)
ESCO	Soil evaporation compensation factor	0.90	0.74	0.97
EPCO	Plant uptake compensation factor	0.87	0.97	0.88
SURLAG	Surface runoff lag coefficient	4.45	4.98	5.86
OV_N	Manning's 'n' - overland flow	0.13 (0.01–0.29)	0.18 (0.01–0.41)	0.17 (0.01–0.37)
CH_N1	Manning's 'n' - tributary channels	0.08	0.09	0.15
CH_N2	Manning's 'n' - main channel	0.23	0.18	0.13
GW_DELAY	Groundwater delay time	22.95	17.00	17.04
ALPHA_BF	Baseflow alpha factor[1]	0.8785	0.8766	0.7430
GWQMN	Shallow aquifer water depth for return flow to occur	641.11	676.71	510.72
GW_REVAP	Groundwater "revap" coefficient	0.1685	0.0543	0.2000
RCHRG_DP	Deep aquifer percolation fraction	0.0473	0.0480	0.0492
ALPHA_BF_D	Deep aquifer alpha factor	0.0868	0.1033	0.0970
SOL_AWC()	Available water capacity of the soil layer	0.13 (0.03–0.18)	0.13 (0.03–0.16)	0.14 (0.06–0.19)
SOL_K()	Saturated hydraulic conductivity	15.29 (0.01–92.48)	11.45 (0.09–79.39)	11.32 (1.47–80.13)
NPERCO	Nitrate percolation coefficient	1.00	1.00	1.00
PPERCO	Phosphorus percolation coefficient	10.00	10.00	10.00
PHOSKD	Phosphorus soil partitioning coefficient	200	200	200
RS4	Organic N settling rate in reach at 20°C	0.6286	0.5258	0.4026
RS5	Organic P settling rate in reach at 20°C	0.6477	0.3270	0.2188
BC1	Biological oxidation rate (NH4 to NO2) in reach at 20°C	0.1805	0.2956	0.2449
BC2	Biological oxidation rate (NO2 to NO3) in reach at 20°C	0.2666	0.3048	0.3017
BC4	Mineralisation rate (OrgP to SolP) in reach at 20°C	0.0748	0.0830	0.0346

[1] Values are higher for sub-basins located upstream the aquifer recharge area.

Table C3.6: Pre-calibrated SWAT model results (calibration dataset).

Variable	**Sub-basin**	**Scenario**	**R2**	**NSE**	**PBIAS**
Streamflow	Dese-Zero	Daily basis	0.542	0.222	51.243
		Monthly basis	0.595	-0.134	51.263
	Marzenego	Daily basis	0.529	-0.485	65.883
		Monthly basis	0.828	-2.431	65.004
	Montalbano	Daily basis	0.749	0.018	-46.262
		Monthly basis	0.881	-0.136	-46.275
Total N	Dese-Zero	Monthly basis	0.714	-0.857	77.795
	Marzenego		0.801	-0.027	69.606
	Montalbano		0.693	0.477	-43.800
Total P	Dese-Zero	Monthly basis	0.664	0.454	41.012
	Marzenego		0.665	0.471	42.695
	Montalbano		0.804	-2.166	-182.172

configuration shows slightly better results than the daily basis scenario. However, the results for the NSE and PBIAS are both non-acceptable for all the three studied watersheds, clearly showing indications that its results are mispredicting the observed streamflow and total nutrient loadings. This behaviour is confirmed by a considerable large underestimation bias for streamflow, on the order of 51% for the Dese-Zero and 65% for the Marzenego, and a large overestimation bias for streamflow, on the order of 46%, for the Montalbano watershed.

Even if numerically the results seem to be not capable of reproducing the reality, they are theoretically consistent with the hydraulic operation of the watersheds, meaning that while the Dese-Zero and Marzenego watersheds are characterised for receiving significant amounts of external water coming from the big external aquifer located north-north-west of the VLW and by the artificial management of hydraulic nodes, the Montalbano watershed is characterised for being a small watershed and for having almost 25% of its total area below the sea level, thereby requiring the operation of hydraulic devices to artificially manage its superficial flow, especially during peak flow conditions, what can be verified by a large overestimation bias for the simulated streamflow. The poor modelling results of the pre-calibrated SWAT model are also verified when analysing the NSE.

In general, under the assumed configuration and due to the complexity of the studied watersheds, the SWAT model alone is not capable of reproducing the overall water and nutrient balances of neither of the studied watersheds. As already discussed in Sub-Section 3.2.1, this fact can be attributed to particular and complex characteristics of each sub-basins of the VLW. However, even if some components of the system are still missing, the proposed pre-calibrated SWAT model is capable of producing simulations somewhat linearly correlated to the observed data, as the coefficient of determination indicates. In fact, on a daily basis, the linear correlation between the observed streamflow and the simulated streamflow is 0.736 for the Dese-Zero sub-basin, 0.793 for the Marzenego sub-basin, and 0.865 for the Montalbano sub-basin.

In summary, the results for the pre-calibrated SWAT model suggest that, although the proposed model configuration is not capable of accurately simulating the hydrology of the studied watersheds, it is capable to linearly reproduce its behaviour in time, even if it systematically fails to accurately simulate the observed

values.

3.3.2 Principal Component Analysis

In compliance with the methodological framework described in the Sub-Section 3.2.5, PCA is applied as a technique for the identification of the most relevant input variables to be used during the estimation of the total hydraulic hydraulic loadings to the studied watersheds. The results of this computation are summarised in Figure C3.3. A set of tables presenting the completion of the linear correlation values between the PCA components and variables is presented in Appendix 4, for each studied sub-basin.

The results shown in Figure C3.3 and summarised in Appendix 4 suggest that some variables can be dropped while maintaining at least 95% of the variance of the original input data. As expected, some variables play a larger role in explaining the variance of the input data, such as precipitation and evapotranspiration, while other variables are less relevant, such as wind speed. Interestingly, irrigation water demand also results as a variable playing a minor role in describing the variance of the input data, which can be attributed to the fact that during the majority of the days in a year irrigation is not taking place. These results are graphically depicted by the second row of the Figure C3.3, depicting only the first two most important components.

In general, the PCA input data processing produces the following outcome when considering the PCA Scenario II only: i. For the Dese river, a reduction of 51.7% of variables (29 to 14); ii. For the Zero river, a reduction of 51.7% of variables (29 to 14); iii. For the Marzenego river, a reduction of 44.0% of variables (25 to 14), and; iv. For the Montalbano river, a reduction of 53.3% of variables (30 to 14). The complete listing of variables, the linear correlation between the variables and the PCA components, and the final listing of selected variables is shown in the Appendix 4.

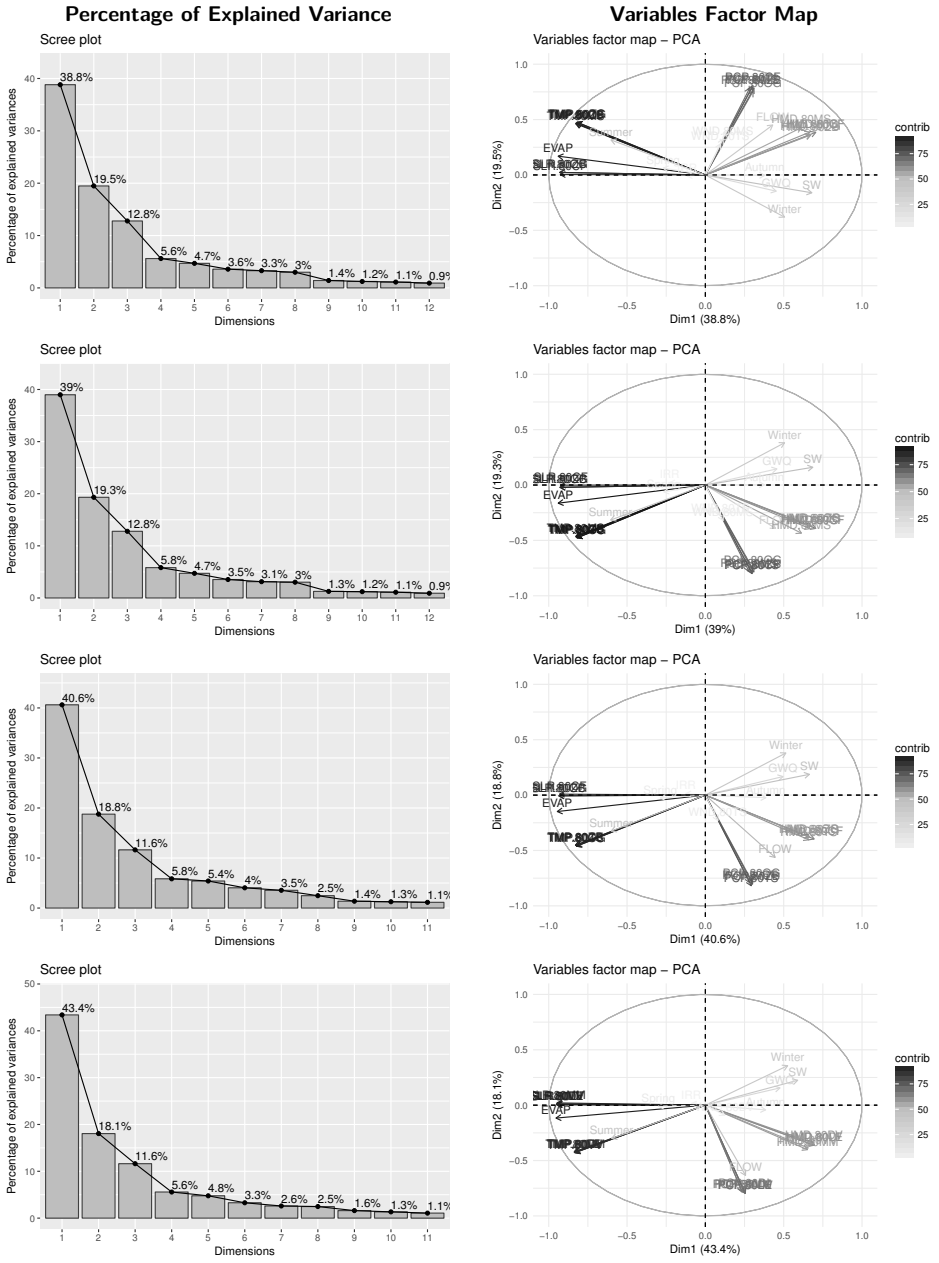

Figure C3.3: Summary of PCA data processing for the streamflow variable. From left to right: 1st Column: Percentage of explained variance by each PCA component; 2nd Column: Variables contribution map to the 1st and 2nd components. From top to bottom: 1st Row: Dese; 2nd Row: Zero; 3rd Row: Marzenego; 4th Row: Montalbano.

3.3.3 Empirical Models

Recognising the fact that some components of the hydrological system are still missing (see Figure C3.2), the next proposed methodological step consists in identifying the most adequate empirical modelling technique to estimate the total external hydraulic loads to the VLW. As described in the Sub-Section 3.2.4, two modelling techniques are evaluated for this purpose, namely: i. An ANN model developed by the authors, and; ii. A MLR model. For this analysis, the Dese-Zero sub-basin is taken as a case study. The results of this analysis are shown in Table C3.7.

Table C3.7: MLR and ANN model comparison results. Dese-Zero only.

		MLR			ANN		
PCA Scenario	**Dataset**	**R2**	**NSE**	**PBIAS**	**R2**	**NSE**	**PBIAS**
Scenario I	Training	0.208	0.207	0.001	0.533	0.532	0.794
	Validation	–	–	–	0.494	0.493	0.065
	Test	0.183	0.171	3.569	0.478	0.476	-1.861
Scenario II	Training	0.292	0.291	0.001	0.845	0.844	-0.798
	Validation	–	–	–	0.864	0.861	0.881
	Test	0.243	0.230	-4.842	0.799	0.798	-0.885

The results shown in Table C3.7 indicate that the total amount of external water entering the Dese-Zero watershed from external sources can be better simulated by a non-linear approach, such as the utilised ANN model. This result is consistent for both considered data input scenarios. The overall best results are obtained by the ANN model under PCA Scenario II. These results indicate that solar radiation, soil water content, groundwater flow, and irrigation water demand are relevant information for the description of the total external hydraulic loads to the studied watershed.

An interesting observation, though, is the fact that even though the MLR model fails to accurately simulate the total external loads of the Dese-Zero watershed, the linear model is capable of reproducing the mean estimated total amount of external water entering the studied watershed, as indicated by a consistent very low PBIAS result. The ANN model, on the other hand, is not only capable of reproducing the mean values, but also to replicate, to some extent, the variations of the total external hydraulic loads in time. In numerical terms, for

Scenario II, while 40.3% of the simulated values by the MLR model fall between the absolute error range of -0.25 – 0.25 m^3 s^{-1}, 70.9% of the simulated values by the ANN model falls in the same range, indicating a superior simulating capability of the non-linear approach.

Being identified the best empirical modelling technique, the next methodological step consists in estimating the total hydrologic influences resulting from the complex water movement of the studied watersheds. The results of this operation are summarised in Table C3.8, while Figure C3.4 depicts the information regarding the ANN training progress and model performance for each studied watershed. As discussed in Sub-Section 3.2.4, the Dese-Zero watershed is split into Dese and Zero river systems.

Table C3.8: ANN model results, for streamflow variable.

Sub-basin	Dataset	R2	NSE	PBIAS	MSE
Dese	Training	0.891	0.889	-0.849	0.114
	Validation	0.892	0.889	0.323	0.113
	Test	0.865	0.865	-0.668	0.129
Zero	Training	0.802	0.800	0.748	0.208
	Validation	0.837	0.834	1.438	0.160
	Test	0.735	0.731	1.015	0.247
Marzenego	Training	0.897	0.896	-0.253	0.103
	Validation	0.898	0.897	-0.266	0.114
	Test	0.863	0.863	0.109	0.145
Montalbano	Training	0.908	0.908	2.221	0.091
	Validation	0.897	0.897	-1.426	0.103
	Test	0.884	0.884	-0.386	0.121

The results shown in Table C3.8 and Figure C3.4 indicate that the considered ANN model is capable of satisfactory reproducing the estimated total hydraulic influences from external sources to the studied watershed. In fact, both the NSE and PBIAS results shown in Table C3.8 suggest a very good capability of the ANN model to reproduce the desired hydraulic influences at a monthly scale.

The ANN model shows the poorest results when attempting to simulate the estimated total hydraulic influences from external sources to the Zero watershed. Even so, however, the results are considered to be satisfactory, as the NSE is, approximately, 0.73 and the PBIAS, approximately, 1.0 for the test dataset, the latter suggesting a slightly tendency of the ANN model to an underestimation behaviour. The strong modelling capability of the ANN model is graphically

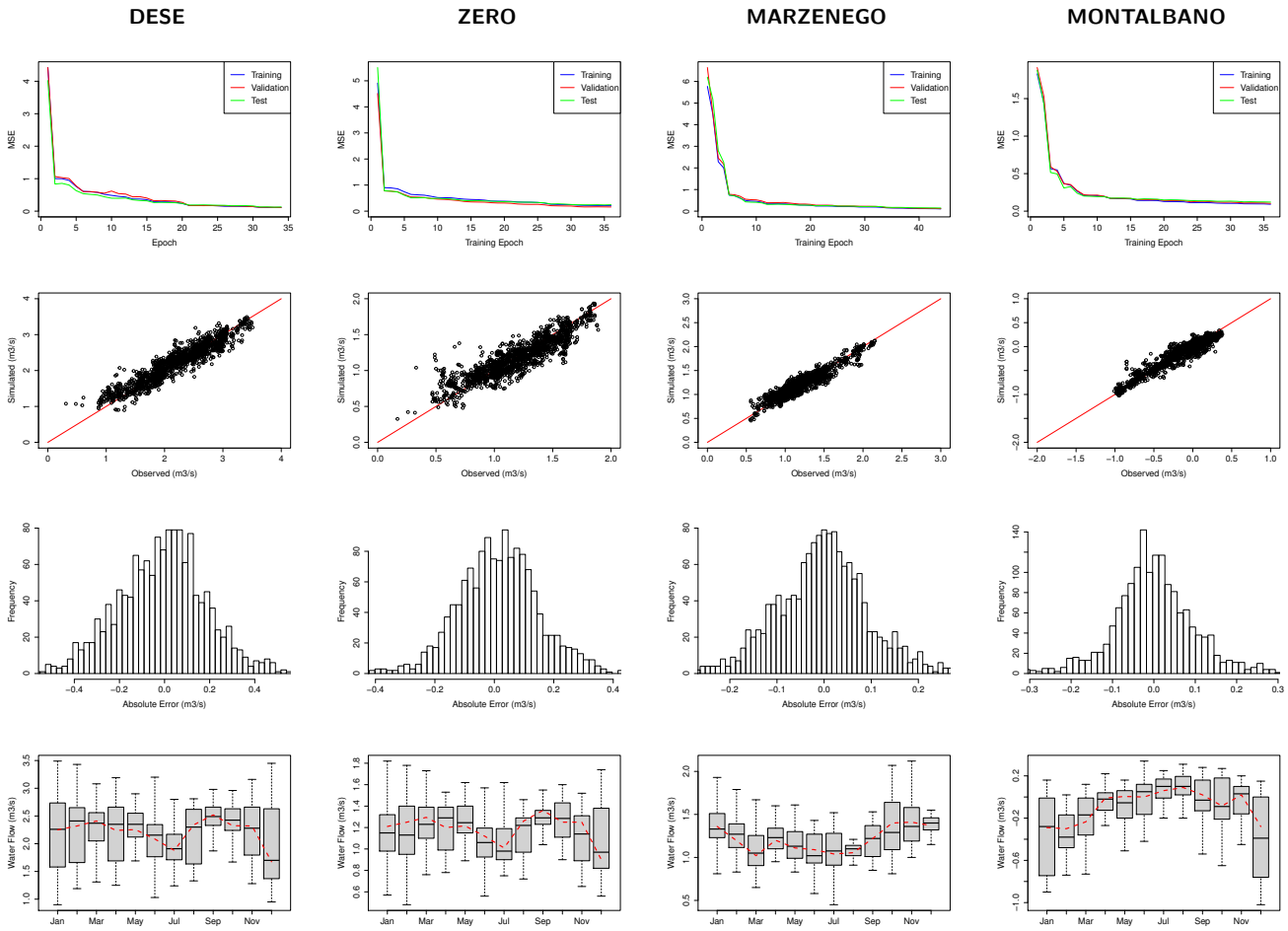

Figure C3.4: ANN model results summary, for streamflow variable. From left to right: 1st Column: Dese; 2nd Column: Zero; 3rd Column: Marzenego; 4th Column: Montalbano; From top to bottom: 1st Row: MSE evolution during training process; 2nd Row: Scatter Plot (Observed vs. Simulated values - a perfect fit is represented by the red diagonal line); 3rd Row: Error Histogram (absolute error values between the 1st and 99th percentiles); 4th Row: Statistics summary (the box represents the extent from the third quartile, on the top, to the first quartile, on the bottom - the line-mark inside the quartile-box represents the median of the results - the extreme mark on top symbolises the maximum simulated value, while the extreme mark on the bottom indicates the minimum simulated value - the red dashed-line represents the median estimated value of the target values).

presented by the scatter plot of the target versus simulated values, as shown at the second row of Figure C3.4.

Moreover, corroborating the ANN's good modelling performance, the absolute error of the target vs simulated values is low for all studied sub-basins. In numbers, the percentage of the absolute error that falls in the range of -0.15 – 0.15 $m^3 \cdot s^{-1}$ is, approximately: 57.4% (Dese); 75.8% (Zero); 86.8% (Marzenego), and; 88.2%. The same information can be graphically seen as presented by the third row of Figure C3.4.

Finally, the forth row of Figure C3.4 depicts some useful statistics regarding the simulation results of the ANN model, such as the range of the simulated values and their respective first and third quartiles for all the studied watersheds and for each month of the year separately, together with the median value of the target values for comparison purposes. In general, such results indicate that the ANN model does a very good job in reproducing the monthly median external contributions.

Furthermore, although the time intervals considered for each watershed are different (see Table C3.3), it is possible to draw an interesting parallel with the observed bimodal behaviour of the aquifer system located to the north/north-west of the VLW. A first high-flow phase, yet not clear, can be identified around the period ranging from the first to the second trimester. A second high-flow phase, instead, is much easily detectable and can be identified around the period transacting between the third and forth trimesters. Such behaviour can be spotted in both Dese-Zero and Marzenego model results, as those are the watersheds mostly affected by the hydraulic contributions coming from the big external aquifer to the VLW (see Figure C3.1).

No clear sign is identifiable for the Montalbano watershed, instead. This fact can be attributed to the fact that this watershed is not directly affected by the hydraulic contributions coming from the big external aquifer to the VLW, as the Montalbano watershed is somewhat confined in between surrounding river systems, namely: Bacchiglione, to the south and west; Fiumazzo, to the north, and; Brenta, to the east. In spite of this particular characteristic, it is interesting to notice the increasing trend of water demand from external sources during the spring and summer seasons. Being a watershed covered predominantly by agricultural

activities, this change in the signal of total external hydraulic contributions is expected due to the increased water demand for irrigation and losses due to evapotranspiration.

Being identified the total amount of water entering or leaving the studied watersheds, the next step aims at the quantification of the nutrient movement in the study area. This step is performed after the identification of the water movement in order to ensure that the movement of nutrient loadings beyond the watershed boundaries has the same signal and relative magnitude as the estimated amount of hydraulic loadings. The results for this methodological step are shown in Table C3.9.

Table C3.9: ANN model results, for the nutrient variables.

Variable	Sub-basin	Dataset	R2	NSE	PBIAS	MSE
Total N	Dese	Training	0.790	0.788	-2.038	0.203
		Validation	0.922	0.920	-1.208	0.089
		Test	0.799	0.795	-0.215	0.222
	Zero	Training	0.826	0.814	-4.381	0.195
		Validation	0.856	0.822	-7.733	0.120
		Test	0.762	0.758	-2.747	0.241
	Marzenego	Training	0.550	0.549	3.227	0.451
		Validation	0.604	0.599	1.322	0.140
		Test	0.790	0.671	25.178	0.475
	Montalbano	Training	0.923	0.920	-5.626	0.073
		Validation	0.973	0.971	-8.883	0.021
		Test	0.898	0.895	-2.135	0.189
Total P	Dese	Training	0.629	0.618	4.407	0.380
		Validation	0.586	0.586	0.440	0.437
		Test	0.601	0.576	6.205	0.387
	Zero	Training	0.580	0.572	-0.697	0.418
		Validation	0.595	0.573	6.019	0.452
		Test	0.629	0.615	1.366	0.396
	Marzenego	Training	0.472	0.471	0.986	0.525
		Validation	0.429	0.426	0.357	0.478
		Test	0.517	0.492	10.025	0.597
	Montalbano	Training	0.565	0.529	36.950	0.598
		Validation	0.696	0.660	36.042	0.231
		Test	0.637	0.582	73.634	0.333

The results shown in Table C3.9 indicate that the proposed methodology is capable of estimating the total amount of nutrients entering or leaving the area of study, although less accurately than the results shown in Table C3.8. It is interesting to note, however, that the ANN model is better capable of

estimating the total amount of nitrogen compounds (i.e. nitrite, nitrate, ammonia and organic nitrogen compounds) than of phosphorus compounds (i.e. mineral phosphorus and organophosphorus compounds). This behaviour is true for all four studied water basins. Another interesting observation that can be derived from the results shown in Table C3.9 is the fact that, specifically for the Montalbano watershed, the ANN model tends to quite significantly overestimate the amount of phosphorus coming from/going to external sub-basins.

In summary, the results shown in this Sub-Section indicate that the employed ANN model is capable of computing, at a monthly scale, the estimated hydraulic influences not taken into account when running the SWAT model alone. Besides, the ANN model is also capable of satisfactory reproducing the total amount of nitrogen being carried by external hydraulic influences, while the total amount of phosphorus, although not as accurate as the total nitrogen results, are also satisfactory reproduced by the model. Moreover, the results summarised in Figure C3.4 also show indications that the ANN model is somewhat capable of reproducing some of the observed particularities of the studied watersheds, such as the observed bimodal behaviour of the external aquifer system influencing the Dese-Zero and Marzenego watersheds, and the artificial water apportion increase during the spring and summer seasons due to agricultural needs in the Montalbano watershed.

3.3.4 Coupled SWAT-ANN Model

Following the calibration and validation of the ANN model, the next proposed methodological step consists on coupling the SWAT and the ANN models, on re-running the calibration process for the new model, and on re-evaluating the new simulation results. The outcomes of this operation are summarised in Tables C3.10 and C3.11. Figure C3.5, instead, depicts a comparison between the results of the SWAT and the SWAT-ANN models when performing the simulation of streamflow extreme values on a daily basis.

Confronting the results shown in Tables C3.5 and C3.10, it is possible to verify that the mean calibrated values for the majority of the calibrated parameters have not change significantly from the pre-calibrated SWAT model configuration,

Table C3.10: SWAT-CUP/SUFI2 results of the coupled SWAT-ANN model.

		Calibrated Value (min–max)		
Parameter	**Description**	**Dese-Zero**	**Marzenego**	**Montalbano**
CN2	Initial SCS CN II value	73.5 (64.5–82.4)	87.6 (76.9–98.0)	82.3 (70.2–95.0)
ESCO	Soil evaporation compensation factor	0.95	0.72	0.97
EPCO	Plant uptake compensation factor	0.90	0.99	0.93
SURLAG	Surface runoff lag coefficient	7.10	7.18	8.23
OV_N	Manning's 'n' - overland flow	0.18 (0.01–0.41)	0.10 (0.01–0.23)	0.12 (0.01–0.25)
CH_N1	Manning's 'n' - tributary channels	0.12	0.17	0.14
CH_N2	Manning's 'n' - main channel	0.18	0.21	0.15
GW_DELAY	Groundwater delay time	35.80	25.55	28.32
ALPHA_BF	Baseflow alpha factor[1]	0.7758	0.6915	0.9028
GWQMN	Shallow aquifer water depth for return flow to occur	893.43	817.88	902.50
GW_REVAP	Groundwater "revap" coefficient	0.0855	0.1988	0.2000
RCHRG_DP	Deep aquifer percolation fraction	0.0404	0.0702	0.0435
ALPHA_BF_D	Deep aquifer alpha factor	0.0610	0.0639	0.0968
SOL_AWC()	Available water capacity of the soil layer	0.12 (0.03–0.16)	0.14 (0.04–0.19)	0.14 (0.07–0.20)
SOL_K()	Saturated hydraulic conductivity	14.80 (0.10–89.52)	13.17 (0.10–91.31)	12.65 (1.65–89.50)
NPERCO	Nitrate percolation coefficient	0.66	0.67	0.47
PPERCO	Phosphorus percolation coefficient	13.28	15.69	17.50
PHOSKD	Phosphorus soil partitioning coefficient	100	125	100
RS4	Organic N settling rate in reach at 20°C	0.0295	0.0370	0.0564
RS5	Organic P settling rate in reach at 20°C	0.0389	0.0601	0.0366
BC1	Biological oxidation rate (NH4 to NO2) in reach at 20°C	0.4421	0.6089	0.7533
BC2	Biological oxidation rate (NO2 to NO3) in reach at 20°C	1.3247	1.4285	1.7692
BC4	Mineralisation rate (OrgP to SolP) in reach at 20°C	0.2273	0.4812	0.3895

[1] Values are higher for sub-basins located upstream the aquifer recharge area.

Table C3.11: Coupled SWAT-ANN model results.

Variable	Sub-basin	Dataset	Scenario	R2	NSE	PBIAS
Streamflow	Dese-Zero	Calibration	Daily basis	0.635	0.593	17.432
			Monthly basis	0.765	0.662	17.049
		Validation	Daily basis	0.817	0.797	14.171
			Monthly basis	0.905	0.837	14.096
	Marzenego	Calibration	Daily basis	0.634	0.603	-11.371
			Monthly basis	0.759	0.677	-10.209
		Validation	Daily basis	0.580	0.554	-10.693
			Monthly basis	0.595	0.552	-12.361
	Montalbano	Calibration	Daily basis	0.721	0.535	-10.612
			Monthly basis	0.865	0.773	-10.469
		Validation	Daily basis	0.681	0.652	12.688
			Monthly basis	0.853	0.820	12.212
Total N	Dese-Zero	Calibration	Monthly basis	0.564	0.502	17.905
		Validation		0.647	0.490	18.025
	Marzenego	Calibration	Monthly basis	0.651	0.567	0.057
		Validation		0.780	0.755	2.980
	Montalbano	Calibration	Monthly basis	0.847	0.833	-22.928
		Validation		0.914	0.812	3.278
Total P	Dese-Zero	Calibration	Monthly basis	0.747	0.663	10.557
		Validation		0.669	0.440	-8.285
	Marzenego	Calibration	Monthly basis	0.567	0.457	-7.511
		Validation		0.795	0.649	-26.857
	Montalbano	Calibration	Monthly basis	0.831	0.820	-14.801
		Validation		0.923	0.681	-28.724

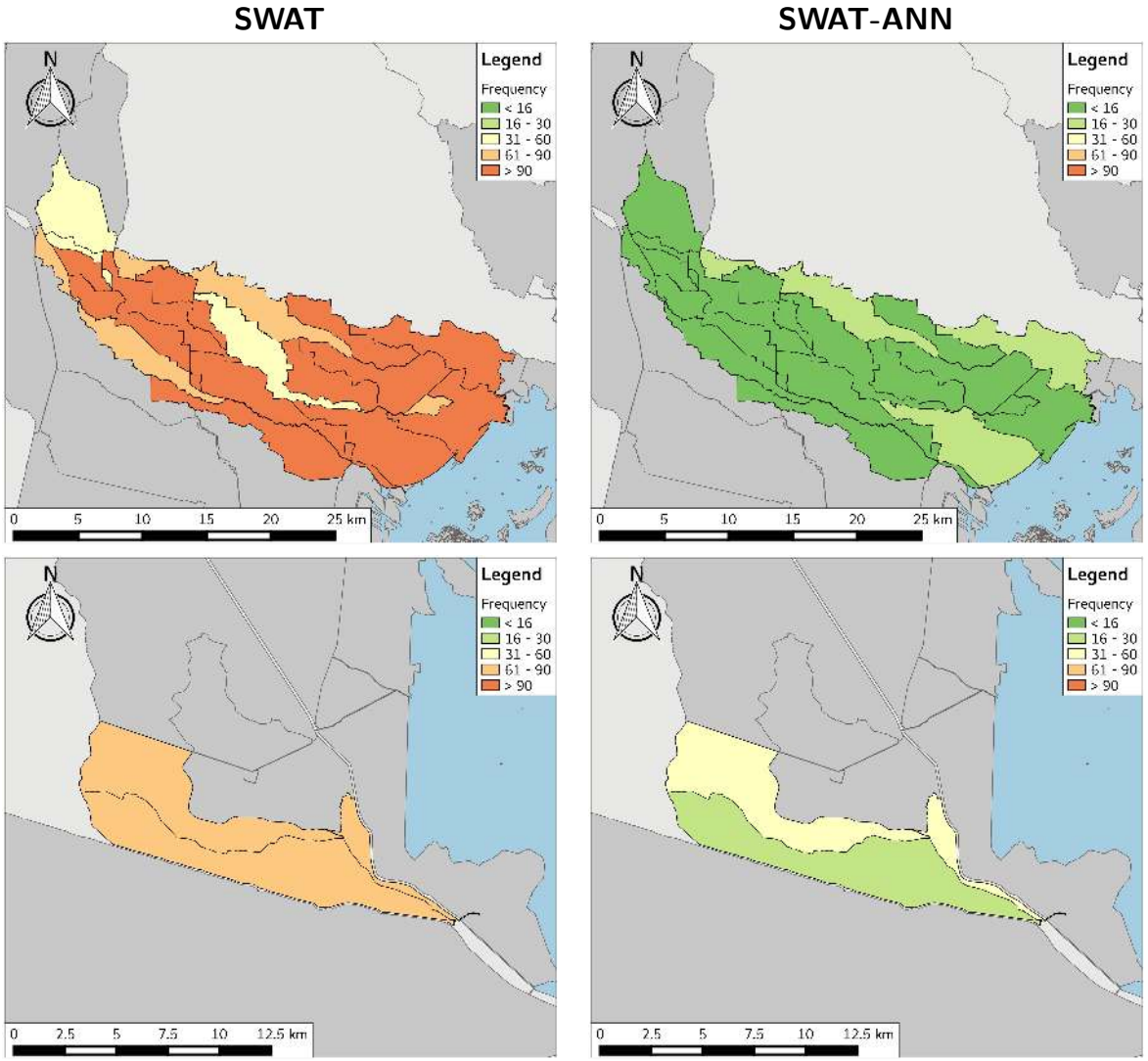

Figure C3.5: Performance comparison between the pre-calibrated SWAT and the coupled SWAT-ANN model results when simulating extreme streamflow values per sub-basin. The classification is based on the simulated values which are lower than the 1st or higher than the 99th percentiles of the observed streamflow database. For sub-basins in which no streamflow data was directly available, the information was extrapolated by taking into account its relative contribution area and surrounding observation data. The simulation period covers the years from 1993 to 2014, while the results are shown as yearly averages for a daily simulation configuration.

indicating a satisfactory SWAT pre-calibration procedure. In fact, considering only the parameters pertinent to the hydraulic balance of the studied watersheds, only one parameter show variations above an absolute threshold value of 50% with respect to the results of the pre-calibrated SWAT model when considering all three watersheds, namely *GW_DELAY*. The increase in the absolute value of the parameter *GW_DELAY* indicates that the period of time that water takes to leave the soil profile and recharge the shallow aquifer is greater in the coupled SWAT-ANN model, signalling that the pre-calibrated SWAT model was possibly over-predicting the magnitude of the return flow in order to cope with the absence of the already mentioned external hydraulic influences.

Similarly, the variation in the *GWQMN* parameter for both Dese-Zero and Marzenego watersheds corroborates this idea. The coupled SWAT-ANN model calibration points to the direction that a deeper threshold of water in the shallow aquifer is necessary for return flow to occur with regards to the results of the pre-calibrated SWAT model. This behaviour is consistent for all three watersheds. Another parameter that shows interesting results it the *SURLAG*. The actual increase in the *SURLAG* parameter among all three studied watersheds indicates that the pre-calibrated SWAT model was over-predicting the amount of surface runoff discharging into the streams for every day of simulation.

In any case, the *GW_DELAY*, *GWQMN*, and *SURLAG* values obtained from the SWAT model pre-calibration procedure indicate a configuration which tried to emulate the observed hydrological behaviour of a system without, however, considering any of the relevant external hydraulic influences to the studied watersheds. Consequently, the automatic calibration of the SWAT model adjusted the intrinsic watershed parametrisation in order to account for such missing information. Ultimately, this has lead to an overestimation of both groundwater and surface runoff contributions to the main channel flow when the relevant external water sources to the studied watersheds are not considered.

Regarding the parameters pertaining the nutrients balance, it is interesting to notice that, by considering the apportion of nutrients entering/leaving the studied watersheds, there is a significant variation in the calibrated values between the SWAT pre-calibrated and the SWAT-ANN models. In general, the rate coefficients for organic nitrogen and organic phosphorus in the reach at 20°C is overestimated

in the SWAT pre-calibrated model, while the parameters *BC1*, *BC2*, and *BC4* are all underestimated by the SWAT pre-calibrated model. Similarly to what is observed for streamflow, the configuration of these parameters indicates that the SWAT pre-calibrated model is overestimating the total loading of nutrients in order to cope with the absence of the aforementioned external influences.

Regarding the modelling capabilities of the coupled SWAT-ANN model, it can be verified a significant improvement of the model's performance, as shown in Table C3.11 and Figure C3.5. Comparing the calibration dataset results of the pre-calibrated SWAT model (see Table C3.6 for reference) with the results shown in Table C3.11, it is possible to verify a huge improvement in the model's performance for all three studied watersheds, especially when considering the simulation under a monthly basis. This improvement is true for both streamflow and nutrient variables. It is interesting to notice, however, that some biases verified during the calibration process of the empirical model are transferred to the SWAT-ANN model. For instance, the large underestimation bias of the ANN model when simulation the external loading of phosphorus to the Montalbano watershed are also verified in Table C3.11, however with an inverted signal due to the predominant artificial deviation of superficial waters during high flow period, which ultimately translates in an overestimation of total phosphorus loadings.

Nevertheless, still considering the calibration dataset, the results presented in Table C3.6 indicate that the proposed coupled SWAT-ANN model is capable of reproducing the overall water and nutrient balances of the studied watersheds. Ratifying the results of the calibration dataset, the results of the validation dataset (shown in Table C3.11) confirm the better simulation capability of the coupled SWAT-ANN model when performing under a monthly basis scenario for all three studied watersheds.

An interesting result attributed to the difference in the composition of the calibration and validation datasets can be verified when analysing the results of the Montalbano watershed. While the coupled SWAT-ANN model exhibits a tendency to overestimation the streamflow for the calibration dataset, it shows the opposite behaviour when applied to the validation dataset. This discrepancy can be attributed to particularities of both calibration and validation datasets, such as the presence of wetter years in the calibration dataset. Anyhow, the results of

the coupled SWAT-ANN model for the Montalbano watershed can be considered to be satisfactory and significantly better than the results of pre-calibrated SWAT model, as verified in Table C3.11.

Indeed, the external hydraulic contributions are extremely important for both the water and nutrient balances of the studies watershed. By applying the methodology described in the Section 3.2, it is possible to quantify these influences. For instance, the mean percentage of the total streamflow of the Dese-Zero that can be attributed to sources external to the watershed varies from 19% during wet weather conditions to 59% during dry weather conditions. Table C3.12 presents a summary of the average percentage of external hydraulic and nutrient loadings to the studied watersheds during a simulation run from 1996 to 2014.

Table C3.12: Summary of the influence of external hydraulic and nutrient loadings when entering the studied watersheds during the simulation period of 1996 to 2014.

Sub-basin	Condition	Streamflow	Total N	Total P
Dese-Zero	High Flow	19.0%	33.2%	12.8%
	Low Flow	59.0%	75.9%	60.9%
Marzenego	High Flow	30.2%	37.6%	35.4%
	Low Flow	81.9%	80.1%	79.8%
Montalbano	High Flow	5.1%	21.3%	3.6%
	Low Flow	63.0%	69.9%	67.2%

3.4 Conclusions

The VLW is characterised for being a very complex catchment. Several modifications in its superficial watercourses throughout the centuries have resulted in a very unique environment, requiring specialised hydraulic management practices. From a number of external hydraulic contributions capable of affecting the water dynamics of the VLW, two stand-out, namely: i. Groundwater entering the VLW from the big unconfined aquifer to the north/north-west of the VLW, and; ii. Artificially controlled superficial waters deviated from/to bordering watersheds that do not discharge into the Lagoon of Venice.

This chapter explored a framework to estimate the total external hydraulic contributions to three particular sub-basins of the VLW, namely: Dese-Zero; Marzenego, and; Montalbano. The proposed methodological framework is built upon the use of a coupled mechanistic-empirical modelling technique based on the hypothesis that the mechanistic model is capable of simulating the hydrological processes and water movement occurring inside boundaries of the studied watersheds, while the empirical model is capable of simulating the total external hydraulic contributions. The mechanistic model used in this research is the SWAT model while the empirical counterpart is an ANN model.

The first step of the proposed methodological frameworks consisted in finding the most relevant information to be exchanged between the two models, including the exogenous weather data. It is found that, among all the studied weather information, temperature and precipitation play a major role in explaining the variability of the input data. However, the consideration of the information such as solar radiation and the simulated external hydraulics contributions from bordering watersheds can aggregate knowledge for the estimation of the total external hydraulic loads to the studied watersheds. Moreover, it is found that the the total external hydraulic loads to the Dese-Zero watershed is essentially a non-linear process, consequently being better reproduced by the non-liner ANN model.

Additionally, the coupling of mechanistic and empirical models has proven to be fruitful, as the coupled SWAT-ANN model is not only capable of satisfactory reproducing the water and nutrient balances of the studied watersheds, but also to increase the hydrological modelling capability of the SWAT model when performing under an intricate and complex environment such as the VLW.

The results obtained from the application of the proposed methodology also confirm the findings of previous studies in the same area, indicating that under ordinary flow conditions and in dry periods, the water and nutrient balances of the VLW are in general highly affected by the water flowing into the watershed from bordering water basins, particularly during the spring and summer seasons and in the northern section of the VLW.

Finally, as some recommendations for further developments in this field of research, it is proposed the consideration of other hydro-meteorological variables, such as snow coverage area, snow depth, and potential snow melt flux in the

pre-alpine region, processes that are capable of affecting the recharge processes of the aquifer system, and, consequently, the water table depth of the aquifer system in the vicinities of the VLW. Moreover, the use of more robust modelling tools, such as the coupled SWAT-MODFLOW model could also lead to better simulation results, specially in what concerns the simulation of groundwater dynamics and the IGF process. Lastly, the consideration of a more robust method to perform the dimensionality reduction of the input data range and to identify the most relevant input variables to be exchanged from the mechanistic component to the empirical models is welcomed, such as the use of Independent Component Analysis – ICA [7, 25, 33].

Acknowledgements

The work presented in this chapter was possible due to the possibility of performing some calculations on the *Sistema per Calcolo Scientifico di Ca' Foscari* – SCSCF computer cluster (www.dais.unive.it/scscf), a multiprocessor system owned by Ca' Foscari University of Venice and running under a GNU/Linux operating system.

A special thank is given to all the people who have directly or indirectly contributed to the development of this research, in particular: Dr. Arianna Azzellino (Politecnico di Milano, Italy), notably for providing specific data and technical information, without which would make the research presented in this chapter not possible; Dr. Stefan Julich, Filipa Tavares Wahren, and Daniel Hawtree (Institute of Soil Science and Site Ecology, TU Dresden, Germany), for providing theoretical support regarding the use of the SWAT model, and; ARPAV - Area Tecnico Scientifica and Consorzio di Bonifica – Acque Risorgiva, for providing specific technical information regarding the management of the VLW.

References

[1] Abbaspour, K. C., 2014. SWAT-CUP 2012: SWAT Calibration and Uncertainty Programs - A User Manual. Tech. rep.

[2] Arnold, J. G., Kiniry, J. R., Srinivasan, R., Williams, J. R., Haney, E. B., Neitsch, S. L., 2012. Soil & Water Assessment Tool: Input/Output Documentation. Version 2012. Tech. rep., Texas A&M AgriLife, USDA Agricultural Rsearch Service, College Station, TX, USA.

[3] Arnold, J. G., Srinivasan, R., Muttiah, R. S., Williams, J. R., 1998. Large Area Hydrologic Modeling and Assessment Part I: Model Development. Journal of the American Water Resources Association 34 (1), 73–89.

[4] ARPAV, 2015. ARPAV - Dati Meteorologici.
URL http://www.arpa.veneto.it/temi-ambientali/meteo/dati

[5] ARPAV, Veneto, R., 2008. Le acque sotterranee della pianura veneta: I risultati del Progetto SAMPAS. Tech. rep., Regione Veneto, ARPAV, Iniziativa cofinanziata dall'Unione Europea - FESR - DOCUP Ob. 2 anno 2000-2005 - Progetto SAMPAS, Padova, PD, Italy.

[6] Azzellino, A., Carpani, M., Cevirgen, S., Giupponi, C., Parati, P., Ragusa, F., Salvetti, R., 2013. Managing the nutrient loads of the Venice Lagoon Watershed: are the loads external to the watershed relevant under the WFD River Basin District framework? Journal of Coastal Research (1, 65), 25–30.

[7] Beverina, F., Palmas, G., Silvoni, S., Piccione, F., Giove, S., 2003. User adaptive BCIs: SSVEP and P300 based interfaces. PsychNology Journal 1 (4), 331–354.

[8] Bixio, V., Celegon, E. A., Fanton, P., Fiume, A., Vazzoler, C., Zanetti, S., Bixio, A. C., Rech, F., 2009. Documento Propedeutico ai Piani Generali di Bonifica e Tutela del Territorio dei Consorzi di Bonifica del Veneto: Caratteri fisici e climatici dei comprensori di bonifica del Veneto. Tech. rep., Regione Veneto, Piazzola sul Brenta.

[9] Bixio, V., Celegon, E. A., Fanton, P., Fiume, A., Vazzoler, C., Zanetti, S., Bixio, A. C., Rech, F., 2009. Documento Propedeutico ai Piani Generali di Bonifica e Tutela del Territorio dei Consorzi di Bonifica del Veneto: La Bonifica idraulica nella Regione Veneto. Tech. rep., Regione Veneto, Piazzola sul Brenta.

[10] Bixio, V., Celegon, E. A., Fanton, P., Fiume, A., Vazzoler, C., Zanetti, S., Bixio, A. C., Rech, F., 2009. Documento Propedeutico ai Piani Generali di Bonifica e Tutela del Territorio dei Consorzi di Bonifica del Veneto: L'irrigazione nella Regione Veneto. Tech. rep., Regione Veneto, Piazzola sul Brenta.

[11] Çevirgen, S., Azzellino, A., Giupponi, C., Parati, P., Ragusa, F., Salvetti, R., 2015. SWAT meta-modeling as support of the management scenario analysis in large watersheds. Water Science and Technology 72 (12), 2103–2111.

[12] Eckelmann, H. W., Sponagel, R. H., Grottenthaler, W., Hartmann, K.-J., Hartwich, R., Janetzko, P., Joisten, H., Kühn, D., Sabel, K.-J., Traidl, R., Boden, H. A.-h.-A., 2006. Bodenkundliche Kartieranleitung. KA5. Schweizerbart Science Publishers, Stuttgart, Germany.

[13] Essenfelder, A. H., Giove, S., Giupponi, C., 2016. Identifying the Factors Influencing the Total External Hydraulic Loads to the Dese-Zero Watershed. In: 8th International Congress on Environmental Modelling and Software. Vol. 3. Toulouse, France, pp. 731–738.

[14] Giupponi, C., Azzellino, A., Salvetti, R., Parati, P., Carpani, M., 2012. Water Quality Assessment in the Venice Lagoon Watershed with Multiple Modelling Approaches. In: Proceedings - 2012 International Congress on Environmental Modelling and Software. pp. 1–8.

[15] Hsieh, W. W., Tang, B., 1998. Applying Neural Network Models to Prediction and Data Analysis in Meteorology and Oceanography. Bulletin of the American Meteorological Society 79 (9), 1855–1870.

[16] Kassambara, A., Mundt, F., 2017. factoextra: Extract and Visualize the Results of Multivariate Data Analyses.
URL https://cran.r-project.org/package=factoextra

[17] Krause, P., Boyle, D. P., 2005. Advances in Geosciences Comparison of different efficiency criteria for hydrological model assessment. Advances In Geosciences 5 (89), 89–97.

[18] Legates, D. R., McCabe, G. J., 1999. Evaluating the use of "goodness-of-fit" measures in hydrologic and hydroclimatic model validation. Water Resources Research 35 (1), 233–241.

[19] Maraun, D., Wetterhall, F., Chandler, R. E., Kendon, E. J., Widmann, M., Brienen, S., Rust, H. W., Sauter, T., Themeßl, M., Venema, V. K. C., Chun, K. P., Goodess, C. M., Jones, R. G., Onof, C., Vrac, M., Thiele-Eich, I., 2010. Precipitation downscaling under climate change: Recent developements to bridge the gap between dynamical models and the end user. Reviews of Geophysics 48 (2009RG000314), 1–38.

[20] Moriasi, D. N., Arnold, J. G., Van Liew, M. W., Binger, R. L., Harmel, R. D., Veith, T. L., 2007. Model evaluation guidelines for systematic quantification of accuracy in watershed simulations. Transactions of the ASABE 50 (3), 885–900.

[21] Neitsch, S. L., Arnold, J. G., Kiniry, J. R., Williams, J. R., 2011. Soil & Water Assessment Tool Theoretical Documentation. Version 2009. Tech. Rep. TR-406, Texas A&M AgriLife, USDA Agricultural Rsearch Service, College Station, TX, USA.

[22] Noori, N., Kalin, L., 2016. Coupling SWAT and ANN models for enhanced daily streamflow prediction. Journal of Hydrology 533 (February), 141–151.

[23] Nyeko, M., 2014. Hydrologic Modelling of Data Scarce Basin with SWAT Model: Capabilities and Limitations. Water Resources Management 29 (1), 81–94.

[24] Orientali, A., 2010. Subunità Idrografica Bacino Scolante, Laguna di Venezia e Mare Antistante. Tech. rep., Venezia VE.

[25] Piccione, F., Giorgi, F., Tonin, P., Priftis, K., Giove, S., Silvoni, S., Palmas, G., Beverina, F., 2006. P300-based brain computer interface: Reliability and performance in healthy and paralysed participants. Clinical Neurophysiology 117 (3), 531–537.

[26] Podolak, I. T., 1999. Feedforward neural network's sensitivity to input data representation. Computer Physics Communications 117, 181–188.

[27] Praus, P., 2010. Principal Component Analysis of Hydrological Data. In: Gasmelseid, T. M. (Ed.), Handbook of Research on Hydroinformatics: Technologies, Theories and Applications. Information Science Reference, New York, NY, USA, Ch. 18, p. 364.

[28] R, C. T., 2016. R: A Language and Environment for Statistical Computing. URL https://www.r-project.org/

[29] Salvetti, R., Acutis, M., Azzellino, A., Carpani, M., Giupponi, C., Parati, P., Vale, M., Vismara, R., 2008. Modelling the point and non-point nitrogen loads to the Venice Lagoon (Italy): the application of water quality models to the Dese-Zero basin. Desalination 226 (1-3), 81–88.

[30] Salvetti, R., Azzellino, A., Gardoni, D., Vismara, R., Carpani, M., Giupponi, C., Acutis, M., Vale, M., Parati, P., 2007. Application of SWAT Model on Three Watersheds within the Venice Lagoon Watershed (Italy): Source Apportionment and Scenario Analysis. In: Proceedings - 4th International SWAT Conference Application. pp. 408–417.

[31] Veneto, R., 2000. Piano Direttore 2000 - Piano per la prevenzione dell'inquinamento e il risanamento delle acque del Bacino Idrografico immediatamente sversante nella Laguna di Venezia. Tech. rep., Regione Veneto, Segreteria Regionale All'Ambiente, Direzione Tutela Dell'Ambiente, Venezia VE.

[32] Veneto, R., 2014. Infrastruttura dei Dati Territoriali del Veneto - Catalogo dei Dati.
URL http://idt.regione.veneto.it/app/metacatalog/

[33] Wang, J., Chang, C. I., 2006. Independent component analysis-based dimensionality reduction with applications in hyperspectral image analysis. IEEE Transactions on Geoscience and Remote Sensing 44 (6), 1586–1600.

[34] Zhang, G. P., Savenije, H. H. G., 2005. Rainfall-runoff modelling in a catchment with a complex groundwater flow system: application of the Representative Elementary Watershed (REW) approach. Hydrology and Earth System Sciences Discussions 2 (3), 639–690.

Chapter 4

On Impacts & Climate Change

The VLW Case Study

Abstract

Climate change is no longer a question of *"if"* but of *"how"*. In a world where climatic changes are certain to occur but how and when these changes might occur is still uncertain, the consideration of possible future climate trajectories is fundamental for building a holistic perspective of possible future adaptation strategies. A key concern to follow in the next decades is whether the agricultural sector will be able to continue providing food to meet human demands as the competition for specific resources increases, such as freshwater resources for irrigation. This chapter builds-upon the utilisation of the coupled SWAT-ANN as a tool capable of translating both climate change effects (e.g. CO_2 fertilization effect) and specific artificial hydraulic management actions (e.g. water utilised for irrigation) under future hydro-meteorological conditions, while evaluating different irrigation efficiency scenarios as alternative adaptation strategies to cope with the possible negative impacts of climate change in the agricultural sector of the VLW. Results suggest an increased dependency on irrigation water coming from external sources to the VLW, while investments in improved irrigation systems can offset some of this demand.

4.1 Introduction

Currently, human demand of RFWRs represents only 10% of its total availability at a global scale [33]. However, as the availability of this resource is variable both in space and time, demand is not always met and pressures worldwide tend to increase as population and economy grow [19, 43]. In fact, it is estimated that by 2050 Earth's population will increase by two to three billion people, adding pressure to a higher demand for and, consequently, production of food. A higher demand for food results in a higher demand for RFWRs. Moreover, demand for RFWRs may also increase due to a development of socio-economic conditions worldwide [23], ultimately resulting in a higher competition for this resource [41]. Consequently, the relationship between current and future effects of climate change and irrigation practices is of crucial interest to farmers as irrigation plays a fundamental role in the sustainability of crop production and RFWRs availability and consumption [3].

The agricultural sector is by far the largest consumer of RFWRs worldwide. As a matter of fact, approximately 70% of the world's RFWRs withdrawn from superficial water bodies and groundwater sources is consumed directly by the agricultural sector by means of irrigation [24]. Indeed, irrigation plays a central role in increasing agricultural yields, enhancing the quality of crops, and providing means for the management of water resources against undesired climate conditions, such as droughts [17, 9, 25]. Additionally, farmers that make use of irrigation as a management tool have better means of pursuing the plantation of economically attractive high-yield seed varieties and to better supply crop's demand, thus giving room for boosts in yields [24].

Ideally, irrigation should be applied only when plants do not meet their water requirements, aiming at closing the gap between a crop's optimal water needs and the natural availability of water resources [31]. Irrigation scheduling is then required, as there is the need to match the often varying crop requirements during the growing season, hence minimising water losses due to evaporation, runoff, and/or percolation [28]. By better managing RFWRs, farmers often can use sparing resources to increase food production by expanding irrigated land

or by converting to higher-value, higher-profit crop variants [35, 29]. However, several factors affect the efficiency[1] of irrigation operations, ranging from climatic conditions to the methods employed for irrigation.

Indeed, irrigation is just one of the several examples of how agriculture has adapted to adverse climatic conditions. While rain-fed crops have access only to the water available in the soil's root zone, irrigated crops have access to a much more diverse source of water, such as groundwater and rivers. This advantage may prove useful in a context of climate change. As the main source of water for rain-fed crops is precipitation, changes in the patterns of precipitation due to climate change can potentially affect the yields of rain-fed crops more intensively than the yields of irrigated crops [22, 29]. Even if irrigated crops are more resilient to changing precipitation patterns than rain-fed crops, climate change effects can severely impact irrigation systems worldwide by reducing water availability and increasing plant's water needs, thereby potentially reducing crop yields [16, 36, 18]. Hence, it is not a surprise that the IPCC identifies low access to irrigation water as a key risk of loss of rural livelihoods and income [21], as insufficient access to irrigation water can result in reduced agricultural productivity.

The impacts of climate change on agricultural irrigation depends mainly on two main factors, namely: i. The intensity and frequency of adverse effects coming from changing climatic conditions, and; ii. The adaptive capacity of the agricultural sector [29]. While climate change effects depend on how the climate system responds to perturbations, the agricultural sector's adaptive capacity depends on adaptation strategies, such as the improvement of irrigation conveyance systems to reduce the amount of water losses in irrigation systems. Adaptation strategies, hence, have the potential of offsetting some of the negative impacts of climate change in irrigated agriculture while, at the same time, providing additional WRM benefits [12].

While irrigation demand can be relaxed by adopting adequate adaptation strategies, the availability of water for irrigation depends strongly on climate conditions and water demand from other sectors. In fact, rising water demand

[1] Water use efficiency is an indicator used to express the level of performance of irrigation systems from the source to the crop: it is the ratio between estimated plant requirements and the actual water withdrawal from source [24].

from competing sectors can potentially be more significant than direct climate change effects in defining the amount of water available to irrigation in the short term [43]. In Europe, is is estimated that climate change and socio-economic factors will increase irrigation needs [21]. Hence, European regions that are vulnerable to water scarcity will have to adapt to new configurations of water availability versus demand [18]. One way of reducing water demand for irrigation is through implementation of water efficient technologies [27].

This chapter, then, explores how climate change may impact the agricultural sector of the VLW in terms of availability of water for irrigation. Two possible future irrigation efficiency scenarios are considered: i. The first considers a baseline scenario, where irrigation efficiencies are kept constant throughout the simulation period and at a pre-defined reference value, and; ii. The second explores an evolutionary scenario, where irrigation efficiencies are considered to improve consistently through time until the end of the simulation period. Aiming at better capturing the possible changes in future climate, data from six different GCMs is considered. The work developed in this chapter relies on the use of the coupled SWAT-ANN model as a tool capable of capturing and translating the dynamic nature of human-decision actions in the management of the availability of water resources for irrigation systems, as described in Chapter 1, Sub-Section 1.2.1, and Chapter 3, Sub-Section 3.2.5. Moreover, the utilised model also incorporates the dynamic CO_2 fertilization effect and the reviewed irrigation procedure code modifications, both described in Chapter 1, Sub-Section 1.2.2.

4.2 Methodology

4.2.1 Irrigation and the SWAT Model

The SWAT model allows the configuration of a specific irrigation schedule and operation for each HRU in a watershed [32]. The model allows irrigation water to come from five distinct sources, namely: reach, reservoir, shallow aquifer, deep aquifer, and unlimited outside source. A deeper description of how the SWAT model considers irrigation operations and the proposed code modifications[2]

regarding this topic can be found in Chapter 1, Sub-Section 1.2.2. A full description of the model parametrisation regarding irrigation operations can be found in Neitsch et al. [32] and Arnold et al. [1].

Crop type is a major factor affecting irrigation water needs. Each crops has unique water requirements, which, in turn, varies depending on meteorological and growing stage conditions. In general, the crops that require more water are crops with long total growing season and high daily water needs. During early growing stages, the general water requirement of annual crops is usually about 50% lower than water needs at mid-season growing stages. Consequently, irrigation scheduling helps eliminate or reduce instances where too little or too much water is applied to crops [31]. The spatial distribution of the crops considered in the study area covered by this chapter is shown in Figure C4.1, while Table C4.1 brings some quantified information regarding the land-use in the VLW.

Table C4.1: Land-use classification in the VLW – Coverage areas.

SWAT LU Class	LU Description	Area [km^2]	Percentage [%]
CORN[1]	Maize	812.03	38.00%
URLD	Urban Low Density	322.24	15.08%
SGBT[1]	Sugarbeet	181.80	8.51%
SOYB[1]	Soybean	158.70	7.43%
URHD	Urban High Density	153.23	7.17%
AGRL	Generic Agricultural Land	147.39	6.90%
WWHT	Wheat	130.61	6.11%
GRAP	Vineyard	128.66	6.02%
FRSD	Forest	35.33	1.65%
PAST	Pasture	27.34	1.28%
WATR	Water	25.09	1.17%
RNGE	Range-Grasses	13.14	0.61%
WETL	Wetland	1.22	0.06%
	Total	**2,136.78**	**100.00%**

[1] Irrigated crops considered in this study.
Data source: Veneto [42]

Acknowledging the fact that crops have unique water requirements, the work presented in this chapter relies on the idea that farmers know when to apply irrigation water to crops according to their perception of water needs by the crops. This process is simulated by the SWAT model as an *auto-irrigation* procedure, where irrigation water is applied to the field only when the crop reach a certain

[2]The work presented in this chapter relies on the use of the modified irrigation version of the SWAT model (see Chapter 1, Sub-Section 1.2.2 for reference).

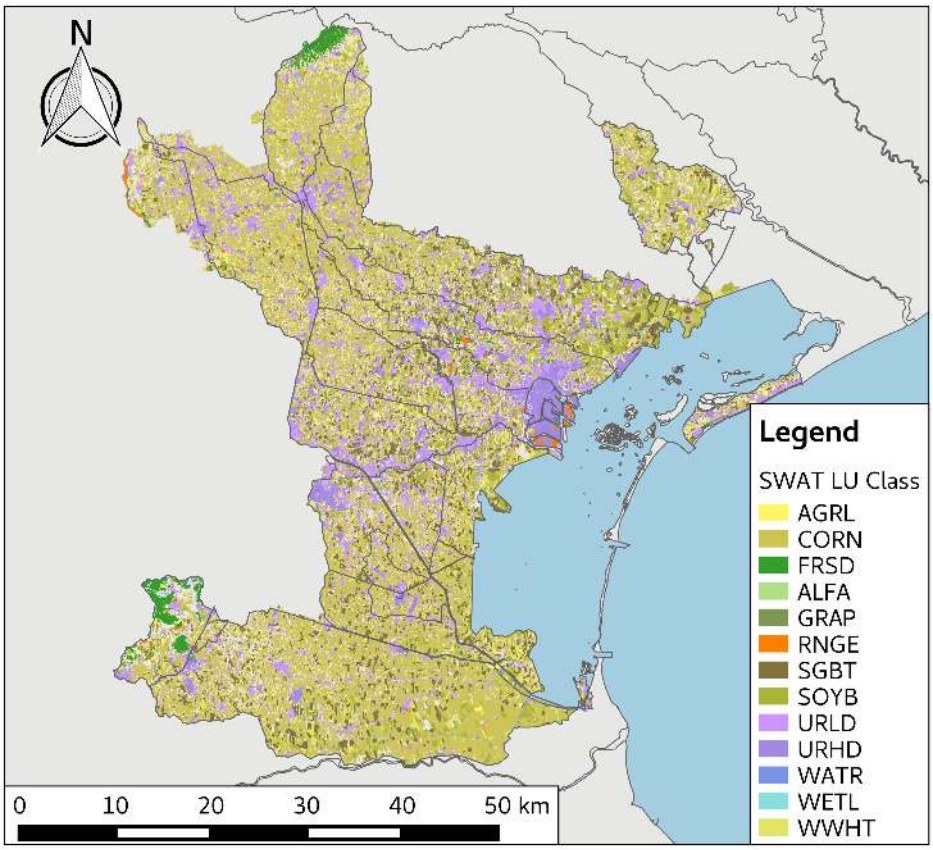

Data source: Veneto [42]

Figure C4.1: Land-use classification in the VLW – SWAT Classes.

water stress threshold value [1]. The amount of water that is taken from the source, in turn, depends on the amount of water available in the source and on the amount of water that farmers are allowed/able/willing to take. Not all water removed from the source reaches the field, as some losses may occur during the transportation of water from the source to the field. Similarly, different irrigation methods can be more or less efficient in applying irrigation water to the field. Generally, there exists three main irrigation methods, namely [7, 31]:

1. Surface (or gravity) irrigation;
2. Sprinkler irrigation, and;
3. Drip irrigation.

Surface irrigation is an irrigation method characterised by the application of water by gravity flow to the surface of a field. This type of irrigation method can be sub-divided into two basic groups: i. Basin irrigation, and; ii. Furrow irrigation. Basin irrigation consists in applying water to the whole field and flooding it with water. Furrow irrigation, on the other hand, consists in utilising small channels or strips of land to transport water from a source the field. Surface irrigation is the cheapest irrigation method, but is generally highly inefficient [31].

The sprinkler irrigation method is more efficient than the surface irrigation method, consisting in spraying water onto crops through rotating sprinkler heads. The concept behind a sprinkler irrigation system is to emulate the effects of a light precipitation event. Although more efficient, these systems are also more costly, both in terms of installation and in maintenance due to the need of a pressurised water-pipe system [7].

Finally, drip irrigation systems are similar to sprinkler systems in the sense that they also utilise pressurised water-pipes to transport water from the source to the field. The difference, however, relies on the way irrigation water is applied to the field. In these systems, water drippers running close to the soil surface or underneath ground are utilised, offering the advantage of eliminating possible water losses due to evaporation, rendering this method highly efficient [31].

The SWAT models allows the quantification of irrigation efficiency by introducing two parameters: *IRR_EFF* and *IRR_ASQ*. *IRR_EFF* is the irrigation

efficiency of the irrigation method at a particular HRU. *IRR_ASQ*, instead, is a parameter indicating the amount of total irrigation water that is converted to surface runoff [1]. It makes necessary, then, the estimation of both parameters in order to accurately simulate irrigations practices in the study area. Brouwer et al. [6] suggest a simple formulation for estimating the irrigation efficiency of an irrigation operation, as follows[3]:

$$irr_{eff} = \frac{E_c \cdot E_a}{100} \tag{C4.1}$$

where E_c is the conveyance efficiency[4] [%]; E_a is the field application efficiency[5] [%], and; irr_{eff} is the irrigation efficiency of the whole irrigation system [%].

While field application efficiency depends mainly on the irrigation method, conveyance efficiency depends mainly on how water is transported from the source to the field and on soil properties and characteristics. Table C4.2 shows some indicative values of conveyance efficiency with respect to the dominant texture of the soil and on the canal length responsible for the transportation of water from the source to the field. Figure C4.2, instead, depicts the spatial distribution of the dominant soil textures found in the VLW.

Table C4.2: Conveyance irrigation efficiency – Indicative values.

	Soil Texture		
Canal Length	**Sand**[1,2]	**Loam**[1,2]	**Clay**[1,2]
Long (> 2,000m)	60%	70%	80%
Medium (200-2,000m)	70%	75%	85%
Short (< 2000m)	80%	85%	90%

[1] Values for earthen canals only.
[2] Values for adequately maintained canals only.
Data source: Brouwer et al. [6]

As discussed, some irrigation methods are more efficient than others in terms of how much water actually is available to crops if compared to the total amount

[3] Text here exaplaining the limitattions of the equation.
[4] Conveyance efficiency represents the efficiency of transportation of water from the source to the field.
[5] Field application efficiency represents the efficiency of water applications by a specific irrigation method in the field.

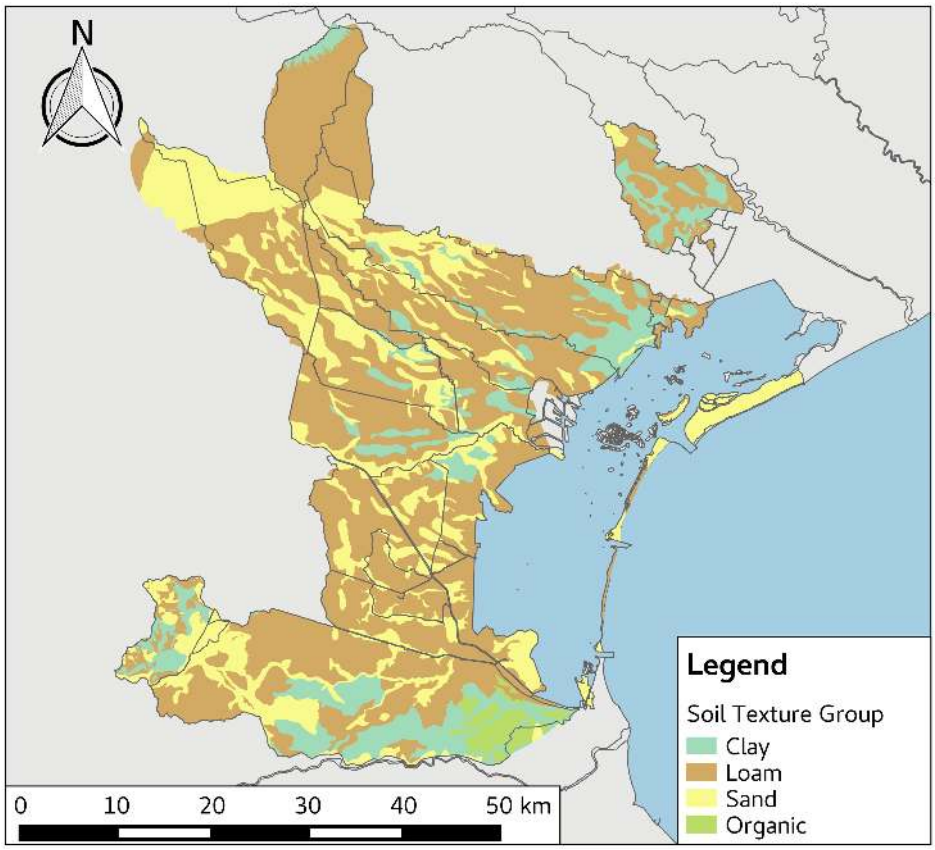

Data source: Veneto [42], ARPAV [2], Eckelmann et al. [15]

Figure C4.2: Predominant soil texture classification in the VLW.

of water that is taken from the source. Table C4.3 presents an estimate of the average irrigation efficiency of the most common irrigation methods in Italy and an indicative value of the field application efficiency as given by Brouwer et al. [6].

Table C4.3: Irrigation and field application efficiencies.

Irrigation Method	Irrigation Efficiency Italy[1]	Field Application Efficiency Indicative Value[2]
Surface	30%	60%
Sprinkler	58%	75%
Drip	70%	90%

[1] Approximate values. Data source: Ignaciuk and Mason-D'Croz [29].
[2] Data source: Brouwer et al. [6].

4.2.2 Irrigation in the VLW

The VLW is a watershed shaped in great part due to the crucial role that irrigation played and still plays in promoting the economic development in the region [4]. Due to intensive land-use for agricultural practices, the VLW is characterised by a very complex network of irrigation channels [11], many of which are managed by specific hydraulic devices. Many of the most important VLW's hydraulic devices are operated, among other factors, to sustain an optimal water availability for irrigation [34].

Currently, the general water infrastructure in the VLW is composed mainly of open canals and the majority of installed irrigation systems utilises a sprinkler system as irrigation method [46, 3]. The main exception is the region located to the north-west of the VLW, in the region comprised between the Piave and Brenta river systems. In this area a significant fraction of crops is irrigated by gravity due to the fact that the terrain in this region is adequate for this kind of irrigation method. Some areas of the same region, though, utilise either a sprinkler or drip irrigation method that differs from the rest of the VLW due to the fact that the water source comes from either groundwater or from outside the VLW's area. This last irrigation system is relatively new in the VLW, and imports water from mainly the Brenta river system[6] to supply water for irrigation

systems in the VLW [5].

Figure C4.3 depicts the spatial distribution of the dominant irrigation methods in the VLW as well as information regarding the source of the irrigation water.

Taken into consideration all the information described so far, it is possible to estimate an initial irrigation efficiency for each HRU in the VLW. Table C4.4 summarises this processing by presenting the average irrigation efficiency of irrigated crops by irrigation method.

Table C4.4: Estimated irrigation efficiency in the VLW.

	Irrigation Method		
Crop	**Gravity**	**Sprinkler**	**Sprinkler/Drip**
Maize	37.6%	53.0%	69.3%
Sugarbeet	39.0%	52.1%	70.1%
Soybean	39.0%	53.2%	69.9%

Building from the methodological framework presented in the previous chapters and recognising the fact that the consideration of the dynamics between human and water systems is required when performing the long-term analysis of water cycle dynamics [38, 37], the work presented in this chapter relies on the utilisation of the coupled SWAT-ANN model for the simulation of the complex hydraulic management in the VLW as a dynamic process capable of affecting the water balance of the VLW. The utilisation of this methodological framework allows for the consideration of variations in both climatic and crop management conditions as factors capable of affecting the way river basin managers sustain an optimal superficial water flow and water availability for irrigation purposes.

In order to capture the adaptation potential of farmers to climate change with regards to the use o water for irrigation, this chapter explores two distinct irrigation efficiency scenarios. The first, named baseline scenario, assumes that irrigation efficiencies are to remain constant in each HRU throughout the simulation period. The second scenario, named adaptive, considers that irrigation efficiencies improves over time. Specifically, the irrigation efficiencies are updated at the beginning of each simulation year until reaching a maximum value at the last simulated year.

[6] A detailed description of the external hydraulic influences to the VLW can be found in Chapter 1, Section 1.3. A case study exploring a framework to model these external influences is presented in Chapter 3.

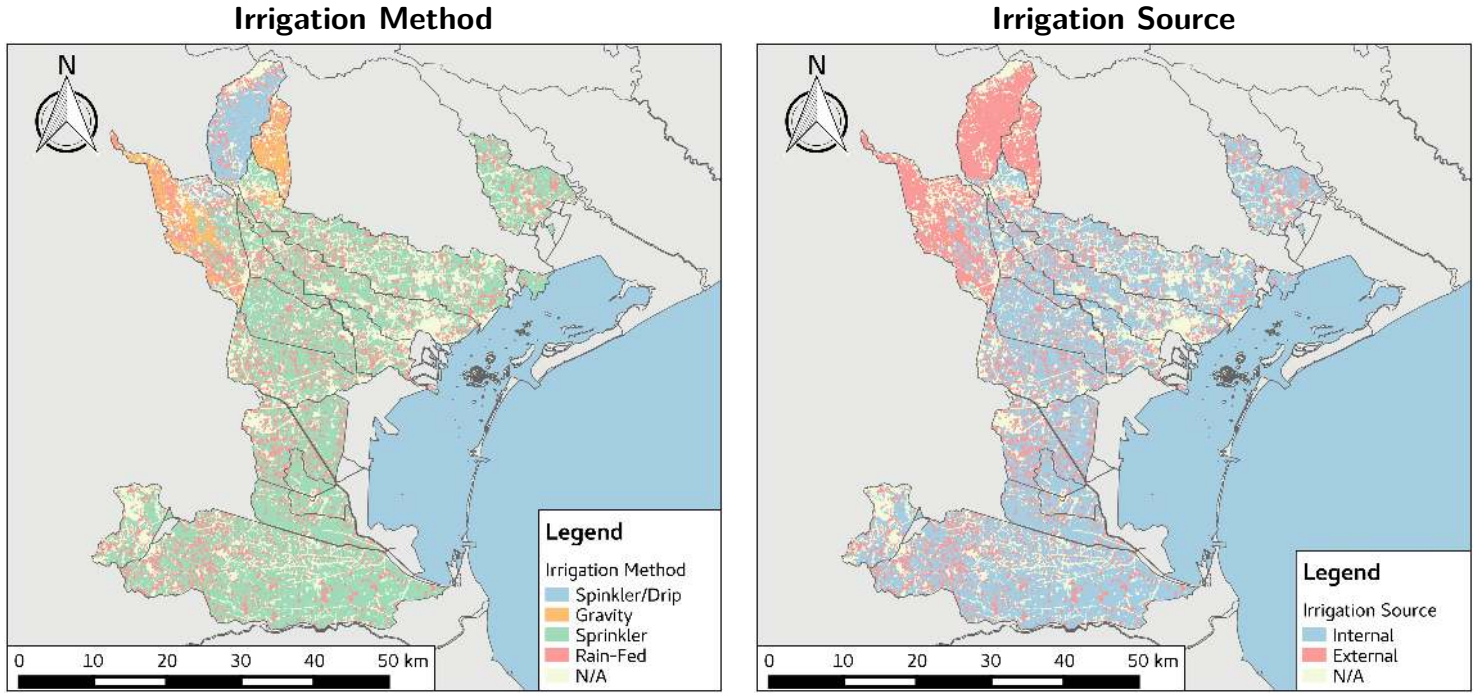

Data source: del Veneto [13]

Figure C4.3: The irrigation in the VLW.

The maximum allowed value for a single irrigation system is assumed to be the indicative field application efficiency as shown in Table C4.3. Irrigation methods are allowed to be upgraded in case the maximum theoretical irrigation efficiency is restricting further development. The initial values of both scenarios are the same and are summarised in Table C4.4[7].

In summary, both scenarios assume the total irrigated area to remain constant throughout the simulation period, while the adaptive scenario considers an ever-increasing irrigation efficiency as the simulation progresses. Figure C4.4 depicts how the irrigation efficiency is considered to evolve in the adaptive irrigation scenario.

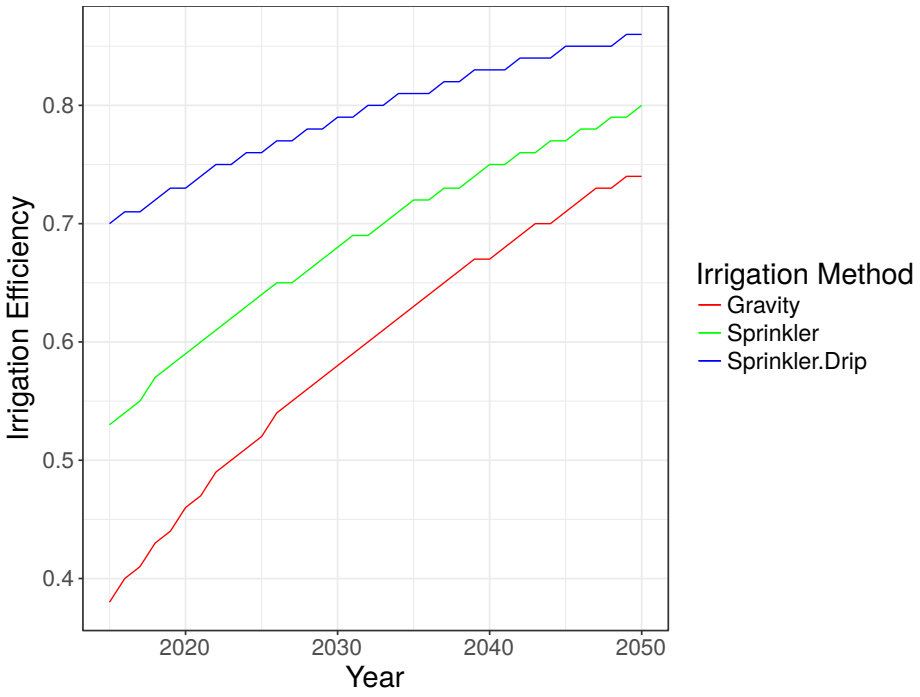

Figure C4.4: Irrigation Efficiency - Adaptive Scenario.

[7]The values shown in Table C4.4 are just a summary of the overall irrigation efficiencies in the VLW. The work presented in this chapter considers an unique irrigation efficiency for each HRU as a result of the combination between irrigation methods, soil properties, and conveyance efficiencies.

4.2.3 Climate Change

The consideration of multi-model ensemble in climate change offers the possibility of better understanding future plausible climate pathways [40, 26, 20]. The work presented in this chapter, then, relies on the use of different climate projections as forced by six different GCMs as a way of better capturing the diversity of predictions coming from different models [14]. Table C4.5 presents a summary of the considered simulated future climate data.

The selected RCP scenario is the 4.5 [10, 39, 44] and covers the period from 2006 to 2050. This climatic pathway is selected as it represents a close-to-average concentration trajectory of GHGs in the atmosphere among the available RCPs scenarios[8]. The selected meteorological variables are show in Table C4.6. Figure C4.5 depicts the evolution of the average near-surface air temperature and precipitation during the simulation period for the VLW.

In summary, two different irrigation management scenarios were simulated under nine different future climatic conditions, resulting in a total of 18 simulations for each sub-basin of the VLW and covering the period from 2010 to 2050.

4.3 Results and Discussions

This sections presents the summary of the most relevant results[9] obtained after the application of the methodological framework as discussed in Section 4.2. The evolution of the total amount of water withdraw from the source to irrigation purposes per year is depicted in Figure C4.6. Figure C4.7, instead, depicts the total amount of irrigation water that is made available for crops after counting the efficiency of the irrigation system. All this information is presented individually for each crop and irrigation scenario, while each plot presents the results of all considered future climate pathways coming from the combinations of GCM/RCM

[8] Due to data availability restrictions, as the EURO-CORDEX project does not include regionalisations of the RCP 6.0 scenario [30], only the RCP 4.5 was considered in the work presented in this chapter.

Table C4.5: List of considered GCMs and related data.

Project	RCM	GCM	Experiment	Spatial Resolution	Frequency
COSMO-CLM[1]	COSMO-CLM	CMCC-CM	rcp45	0.0715°	daily
EURO-CORDEX EUR-11[2]	SMHI-RCA4 v1	CNRM-CERFACS-CNRM-CM5	rcp45	0.11°	daily
EURO-CORDEX EUR-11[2]	SMHI-RCA4 v1	ICHEC-EC-EARTH	rcp45	0.11°	daily
EURO-CORDEX EUR-11[2]	SMHI-RCA4 v1	IPSL-IPSL-CM5A-MR	rcp45	0.11°	daily
EURO-CORDEX EUR-11[2]	SMHI-RCA4 v1	MOHC-HadGEM2-ES	rcp45	0.11°	daily
EURO-CORDEX EUR-11[2]	SMHI-RCA4 v1	MPI-M-MPI-ESM-LR	rcp45	0.11°	daily
EURO-CORDEX EUR-11[2]	CCLM4-8-17 v1	CNRM-CERFACS-CNRM-CM5	rcp45	0.11°	daily
EURO-CORDEX EUR-11[2]	CCLM4-8-17 v1	MOHC-HadGEM2-ES	rcp45	0.11°	daily
EURO-CORDEX EUR-11[2]	CCLM4-8-17 v1	MPI-M-MPI-ESM-LR	rcp45	0.11°	daily

[1] Data source: Bucchignani et al. [8], Zollo et al. [45]
[2] Data source: Jacob et al. [30]

Table C4.6: Weather variables information and ID codes.

Variable Code	Description	Unit
huss	Near-Surface Specific Humidity	$-$
pr	Precipitation	$kg \cdot m^{-2} \cdot s^{-1}$
rsds	Surface Downwelling Shortwave Radiation	$W \cdot m^{-2}$
sfcWind	Near-Surface Wind Speed	$m \cdot s^{-1}$
tasmax	Maximum Near-Surfcace Air Temperature	K
tasmin	Minimum Near-Surfcace Air Temperature	K

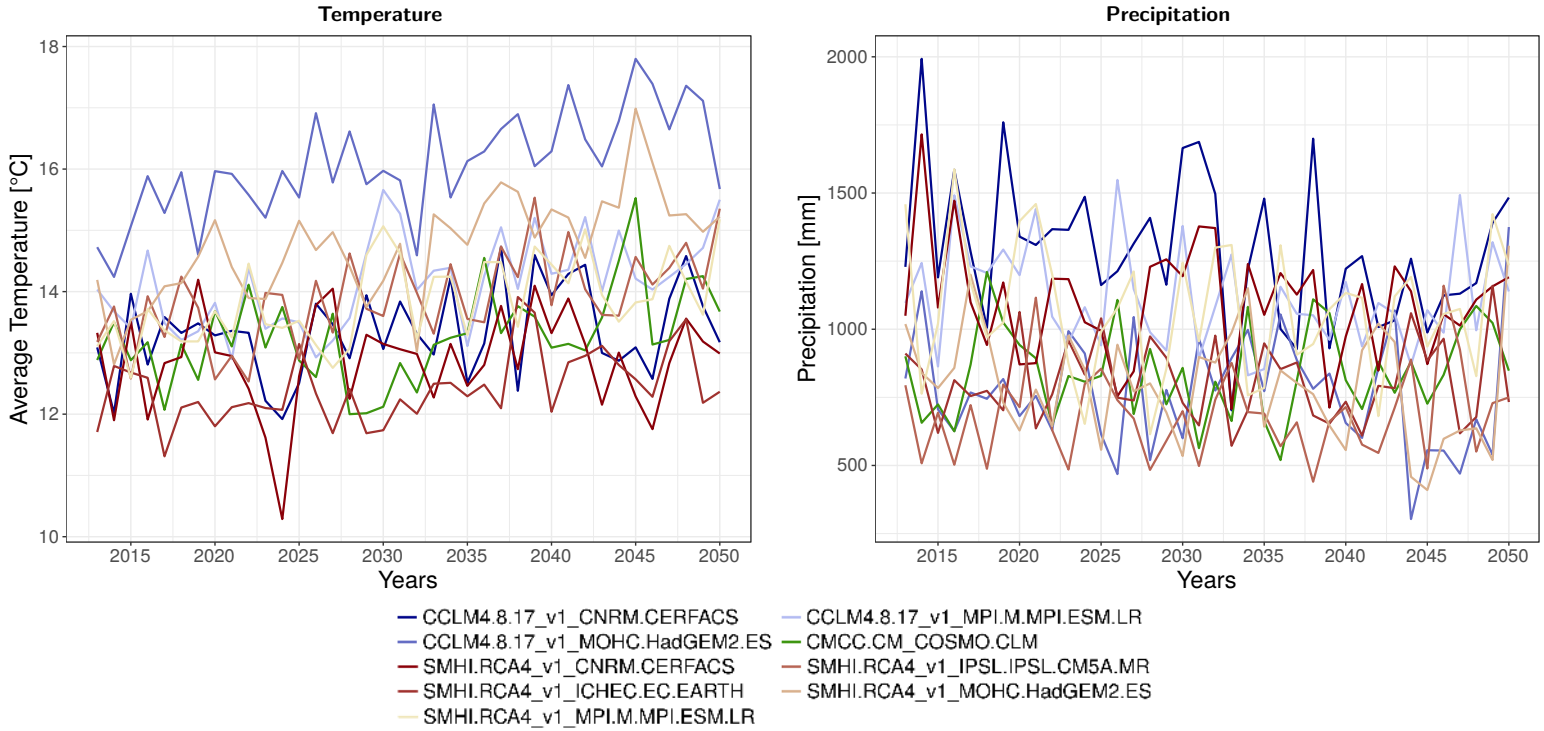

Figure C4.5: Temperature and Precipitation pathways.

as displayed in Table C4.5.

From the results shown in Figures C4.6 and C4.7, it is possible to verify that the increase in the overall efficiency of irrigation systems in the VLW can significantly affect the amount of water that is withdraw from source. This results is consistent for all considered future climate pathways. Indeed, the difference between the two assessed irrigation efficiency scenarios can be significantly large during the last decade of simulation, as the irrigation efficiency between the two scenarios tends to get larger. In numbers, a consistent investment in irrigation systems in the VLW can reduce yearly water withdrawals for just the Dese-Zero sub-basin and for the area covered by maize by up to 10 millions m^3 yearly. This value represents a saving of approximately 30% of the total water withdrawals for irrigation for the same sub-basin and crop.

A consistent improvement of irrigation systems in the VLW can not only reduce the total amount of water that is withdrawn from the source, but also increase the total amount of water that can be made available to crops. This is graphically shown by Figures C4.6 and C4.7. While a noticeable reduction of total water withdrawals can be seen in Figure C4.6 when comparing the baseline against the adaptive irrigation scenario, an increase in the total amount of water that is not lost due to inefficiencies of the irrigation systems can be verified in Figure C4.7.

More interestingly, however, is the fact that both irrigation scenarios point in the direction that, as the climate changes in the VLW region, an increased number of years with extraordinary water requirements is verified. In general, the improvement of irrigation systems can ease the agricultural demand for RFWRs, possibly offsetting this demand to other sectors, such as human consumption. In particular, the installation of efficient pressurised irrigation systems, such as drip and sprinklers irrigation methods, can potentially decrease climate-extreme-related risks by providing a reliable source of water for crops. In any case, the use of efficient irrigation technologies contributes not only to an improvement of physical water productivity, but also to a potential increase in crops productivity. Figure C4.8 shows the evolution of both water and temperature stresses for the

[9] As this chapter is a work in progress, the results shown and discussed upon in this section cover only the Dese-Zero sub-basin of the VLW.

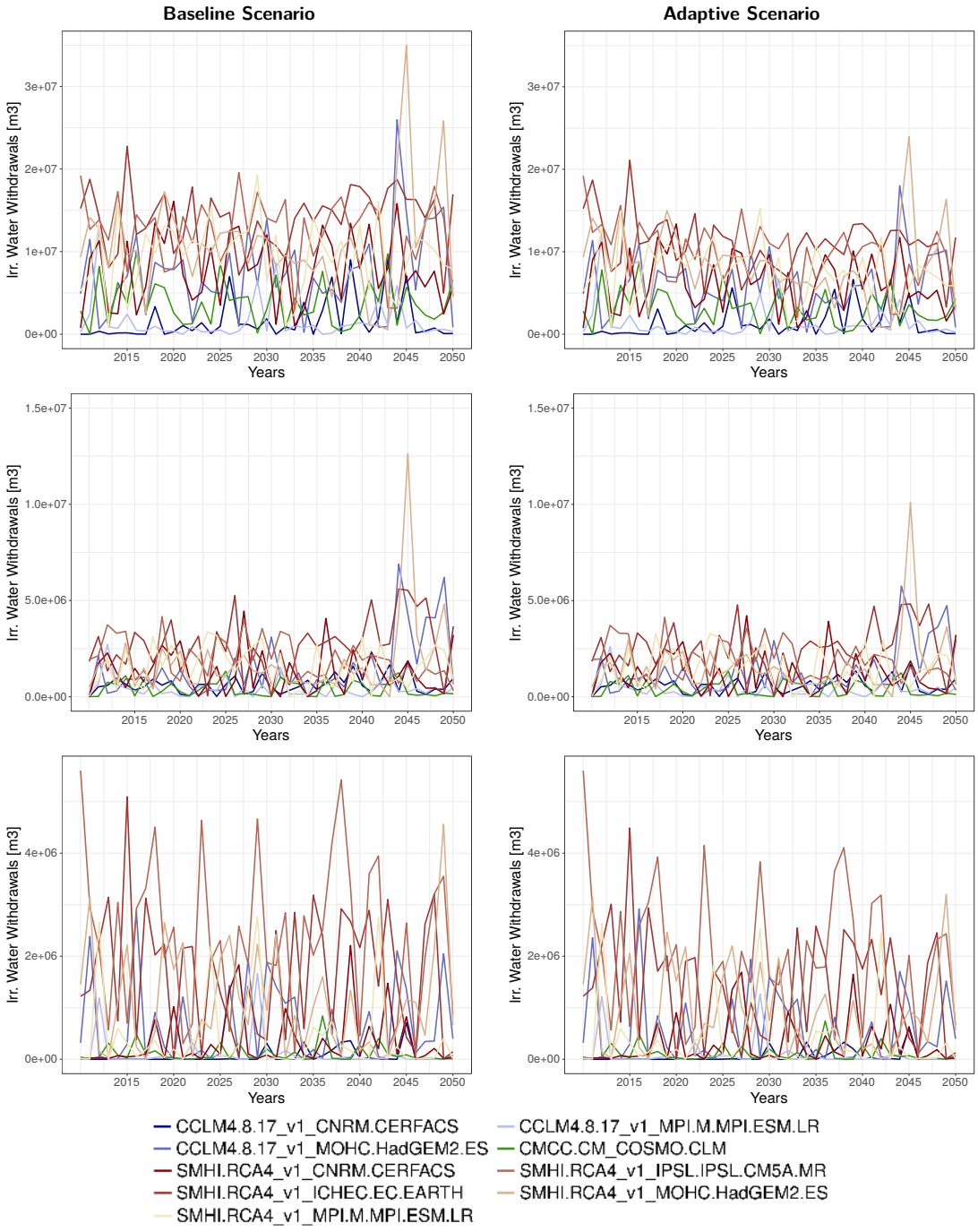

Figure C4.6: Total irrigation water withdrawals per crop type. From left to right: 1st Column: Baseline irrigation scenario; 2nd Column: Adaptive irrigation scenario. From top to bottom: 1st Row: Maize; 2nd Row: Soybean; 3rd Row: Sugarbeet.

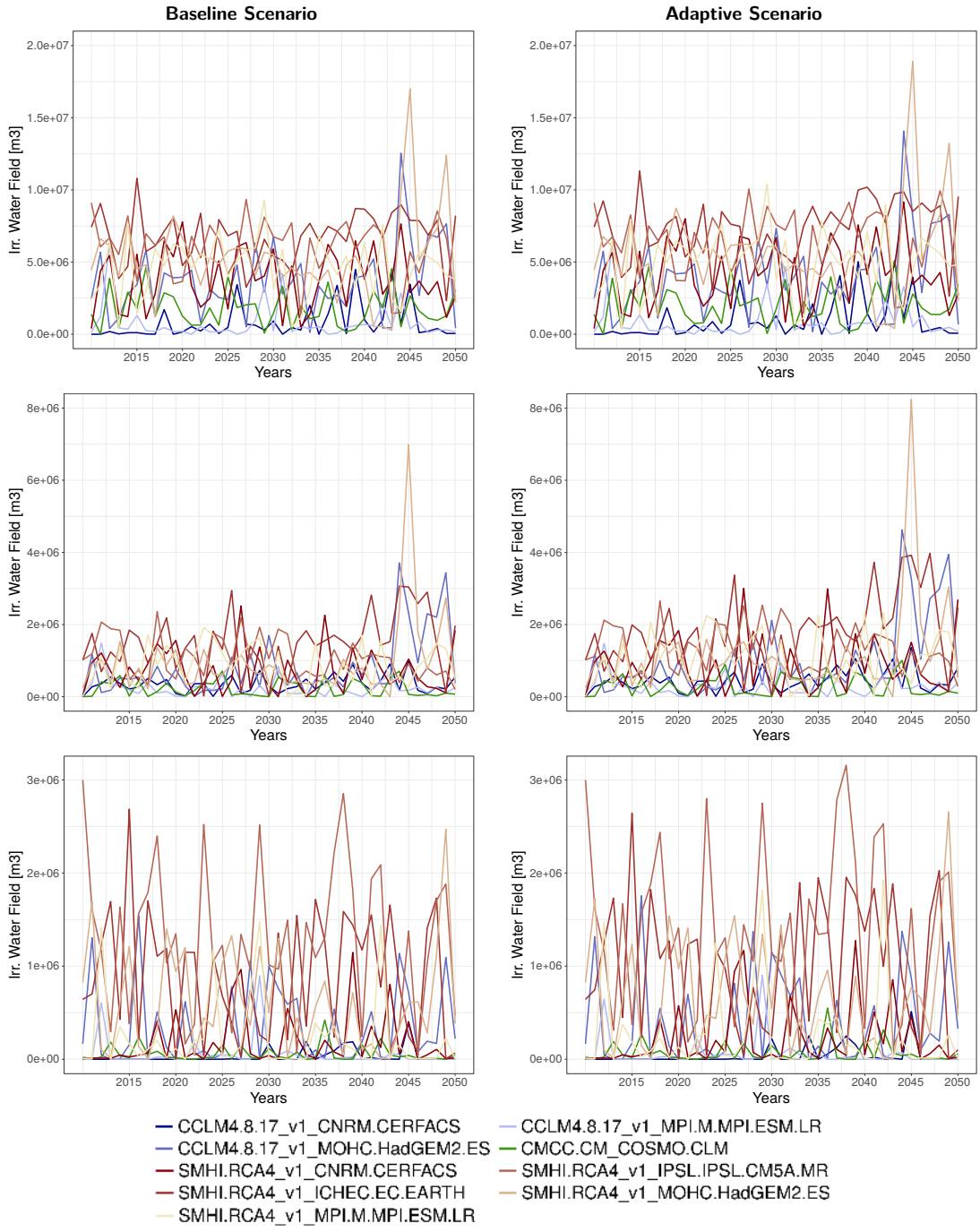

Figure C4.7: Total irrigation water available to crops. From left to right: 1st Column: Baseline irrigation scenario; 2nd Column: Adaptive irrigation scenario. From top to bottom: 1st Row: Maize; 2nd Row: Soybean; 3rd Row: Sugarbeet.

two considered irrigation efficiencies scenarios.

In theory, the improvement of irrigation systems can contribute to a reduction in plant waters stress by increasing the availability of water to crops per irrigation operation. In practice, however, this increase in productivity is only verified under water shortage circumstances. The SWAT accounts for this behaviour by restraining plant's growth with respect to the most significant stress factor on a single day. Hence, some interesting results can be drawn from the data shown in Figure C4.8, as follows:

1. Temperature stress is generally more important as a restraining stress factor for crops' growth than water stress throughout the simulation period;

2. Temperature stress increases significantly during the last decade of the considered simulation period;

3. Water stress can be slightly reduced by investing in more efficient irrigation systems, and;

4. Water stress remains somehow constant throughout the simulation period.

As expected, the temperature stress is equal for both irrigation scenarios due to the fact that temperature stress is calculated by the SWAT model by considering only near-surface air temperature and plant characteristics that bear no direct relation with water requirements. The effects of limiting growing factors such as water and temperature stresses directly affects the growing of crops, and, consequently, their yield. Figure C4.9.

By analysing the results shown in Figure C4.9, it is possible to verify that the yield of the considered crops does not vary significantly between the two different irrigation scenarios. Instead, the yield varies quite significantly under different climatic pathways, as verified by the extent of the boxplots in Figure C4.9. Both these results are consistent with the results shown in Figure C4.8, as temperature is the main factor limiting crops' growth. In any case, the increase in the efficiency of irrigation systems slightly increases the volume of agricultural production. However, significant changes are only verified in circumstances of water shortage. In essence, irrigation is a technology that can increase yields, but is primarily

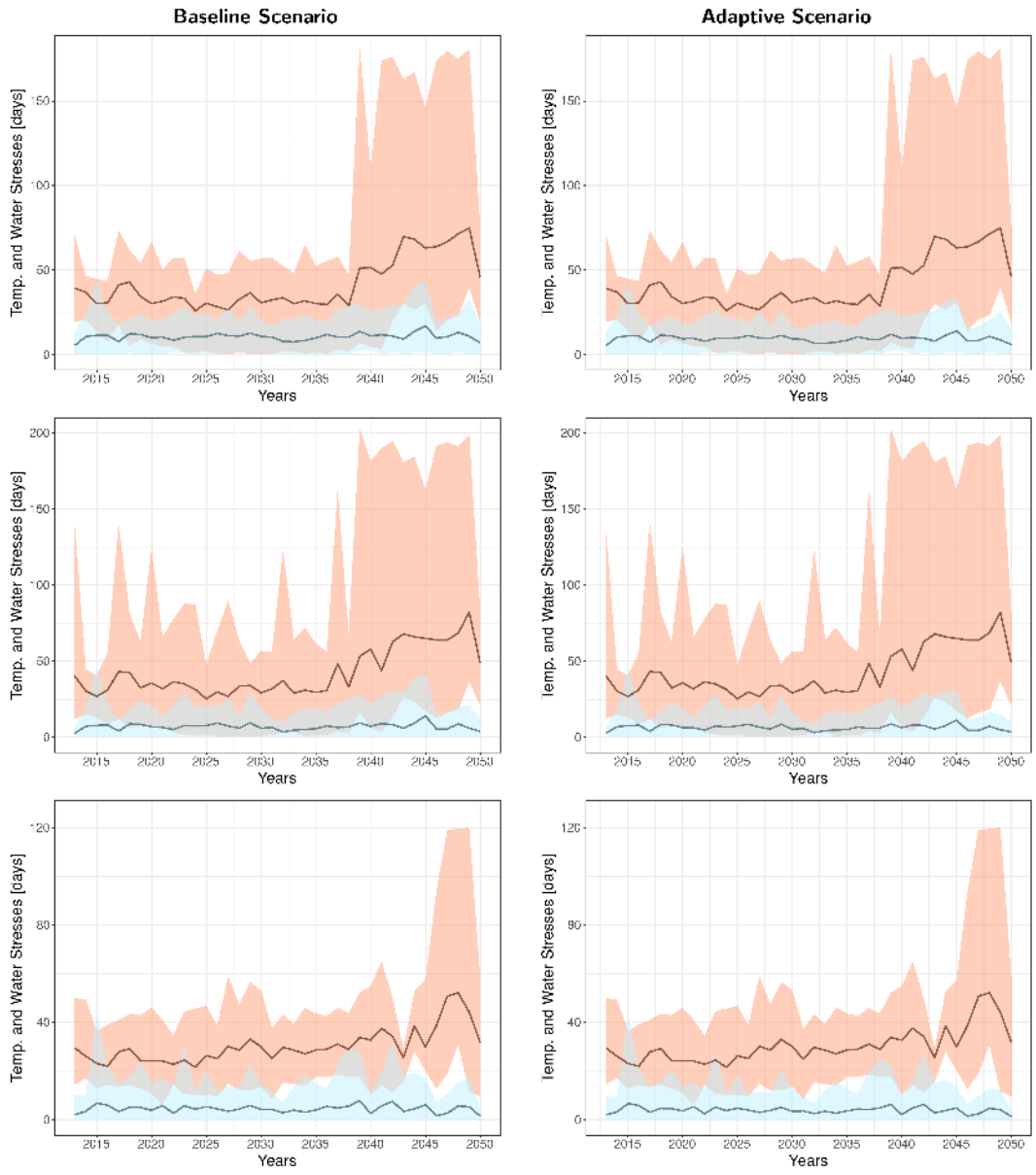

Figure C4.8: Evolution of crops' water and temperature stresses during the simulation period. From left to right: 1st Column: Baseline irrigation scenario; 2nd Column: Adaptive irrigation scenario. From top to bottom: 1st Row: Maize; 2nd Row: Soybean; 3rd Row: Sugarbeet. The elements of this plot are: The elements in shades of red represents Temperature Stress, while the elements in shades of blue represents Water Stress; The shaded area represents the range of simulated values (min-max), and; The solid lines represents the mean value of all simulations.

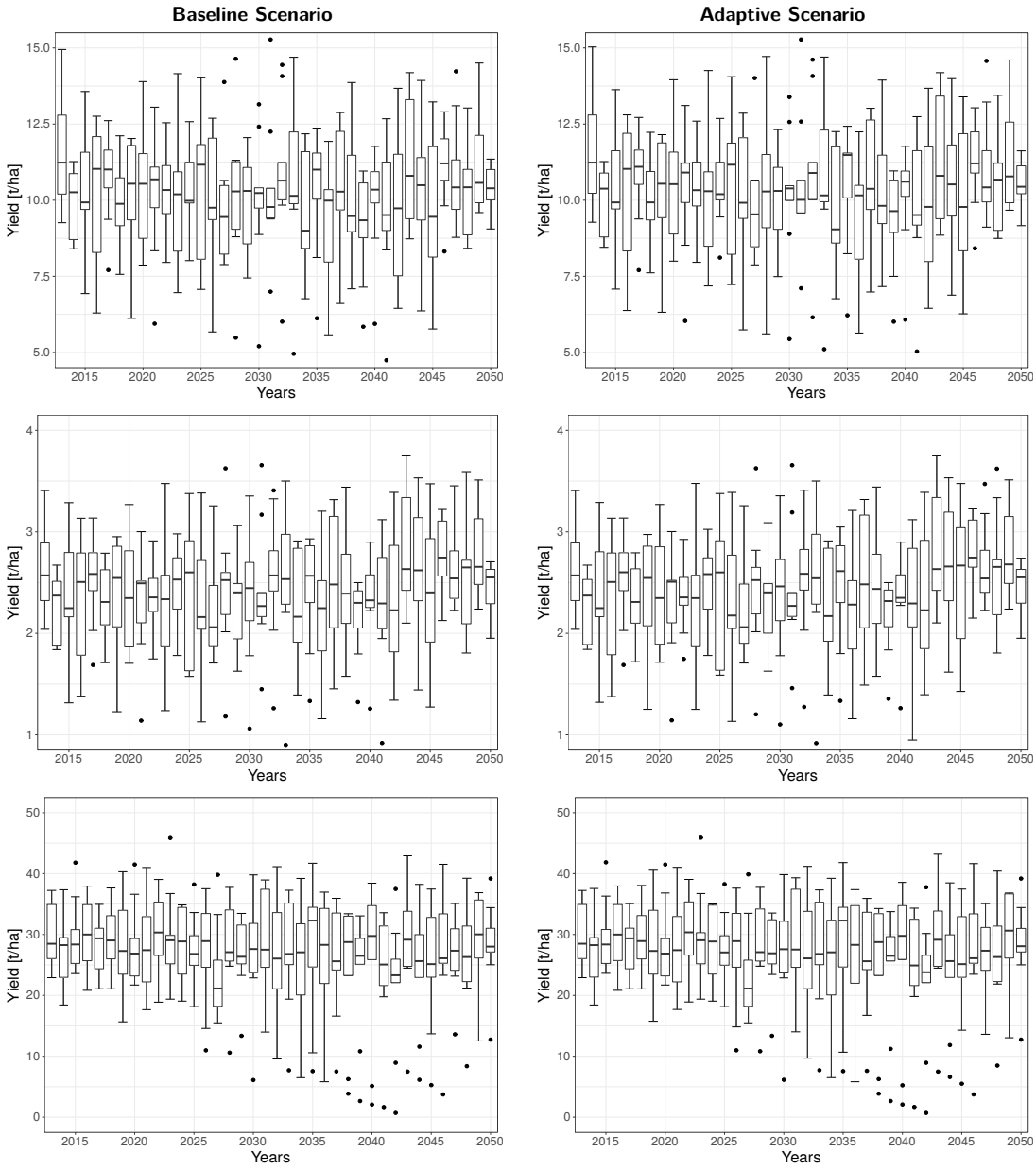

Figure C4.9: Yield [kg/ha] of selected crops during the simulation period. From left to right: 1st Column: Baseline irrigation scenario; 2nd Column: Adaptive irrigation scenario. From top to bottom: 1st Row: Maize; 2nd Row: Soybean; 3rd Row: Sugarbeet.

focused on increasing water reliability and reducing the risks associated with water scarcity and extreme events.

Still, the application of the proposed methodology allows the study of how the total external hydraulic influences entering the VLW might be affected under future climate conditions. Figure C4.10 depicts the summary of these calculations.

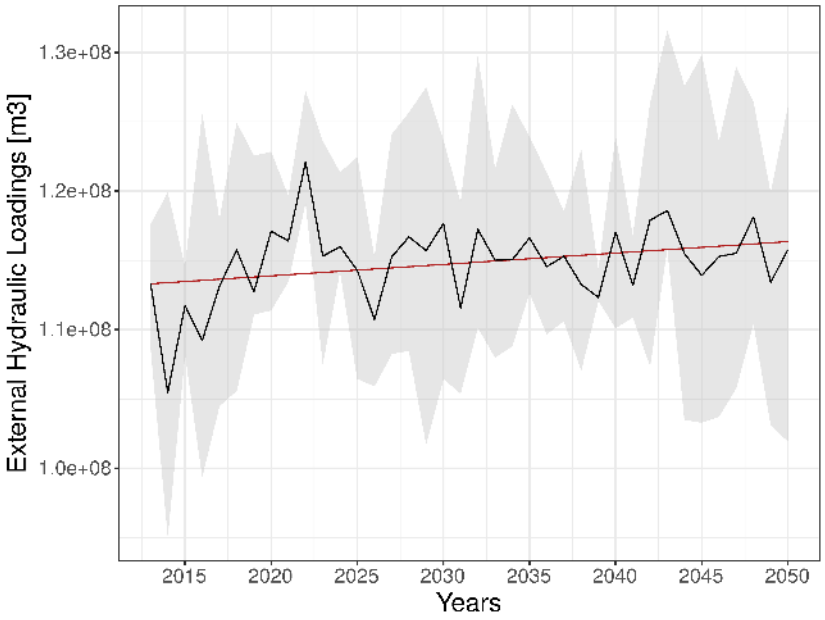

Figure C4.10: Evolution of total external hydraulic loadings for the adaptive irrigation scenario. The elements of this plot are: The shaded area represents the range of simulated values (1st Quartile - 3rd Quartile); The solid black line represents the mean simulated values, and; The solid red line indicates the linear regression of the mean simulated values.

The results shown in Figure C4.10 indicate a slight increase in the total amount of external hydraulic loadings coming from outside sources to the Dese-Zero sub-basin. As the coupled SWAT-ANN model is the tool utilised to simulate such dynamics, hence relying on the usage of both temperature and precipitation information to perform the estimation of the total external hydraulic loadings to the VLW (see Chapter 3), this result can be partially attributed to the fact that, due to a expected warmer and dryer climate in the VLW's region (see Figure C4.5), there is an increased demand for external hydraulic loadings to the VLW in order to maintain an optimal flow and supply of superficial water resources in the

Dese-Zero sub-basin. Moreover, as climate change effects become clearer on the climate system, resulting in an increased variability of climate data, an increased variability on the amount of total external hydraulic loadings to the Dese-Zero is also verified, as depicted in Figure C4.10.

However, not only climate plays a role in explaining the increased dependency of the Dese-Zero watershed on external water sources, as the reduction of both baseflow and percolation processes are also expected to affect the artificial hydraulic management of that watershed. Figure C4.11 depicts the evolution of both total percolation water passing through the bottom of the soil profile, and total baseflow for the simulation period, both under the adaptive irrigation scenario.

As the irrigation efficiency increases and less water is applied to the field due to an overall reduction of water losses, a series of consequent hydrologic events can be expected. First, less water will percolate past the bottom of the soil profile, meaning that less water will recharge the shallow aquifer systems of the Dese-Zero watershed. As a direct consequence, less water will flow back from the aquifers to the superficial stream network (i.e. baseflow), ultimately leading to an increased demand of water sources that are external to the Dese-Zero watershed's are, resulting in an intensification in the amount of water imported from bordering watersheds.

Finally, it is also possible to assess the effects of the dynamic CO_2 atmospheric concentration on crop's growth and water budget in the study area (see Chapter 1, Sub-Section 1.2.2.1 for reference). Figure C4.12 summarises these results.

By analysing the results shown in Figure C4.12 it is possible to verify that, based on the equations built in the SWAT model and discussed in Chapter 1, the effects of dynamic concentration of CO_2 in the atmosphere is not only important to determine the final maximum yield of crops, but also their rate of evaporation. If this is the case, a higher concentration of CO_2 in the atmosphere can offset some of the total amount of irrigation water required by crops. In practice, however, the total amount of water required by crops depends not only on the concentration of CO_2 in the atmosphere, but also on other factors such as air temperature and water vapour deficit. In any case, the consideration of a dynamic behaviour of CO_2 concentration in the atmosphere is relevant when performing

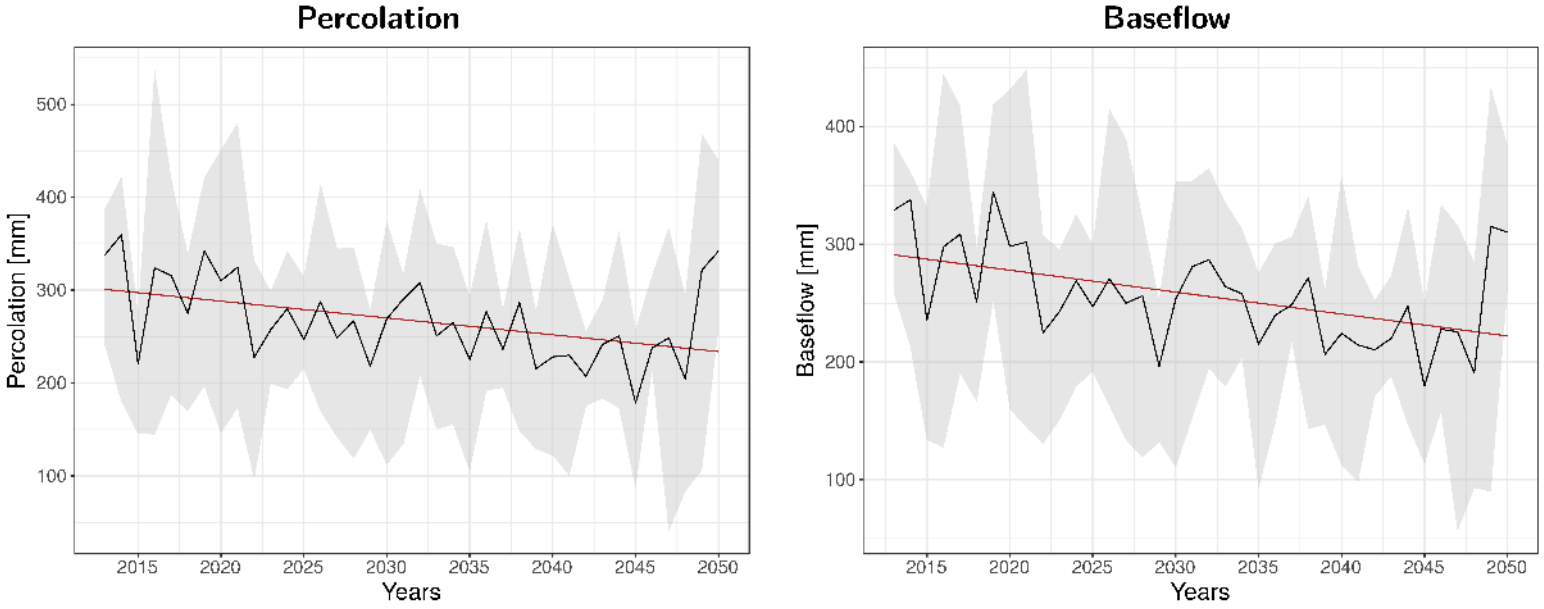

Figure C4.11: Evolution of percolation water passing through the bottom of the soil profile and total baseflow for the adaptive irrigation scenario. The elements of this plot are: The shaded area represents the range of simulated values (1^{st} Quartile - 3^{rd} Quartile); The solid black line represents the mean simulated values, and; The solid red line indicates the linear regression of the mean simulated values.

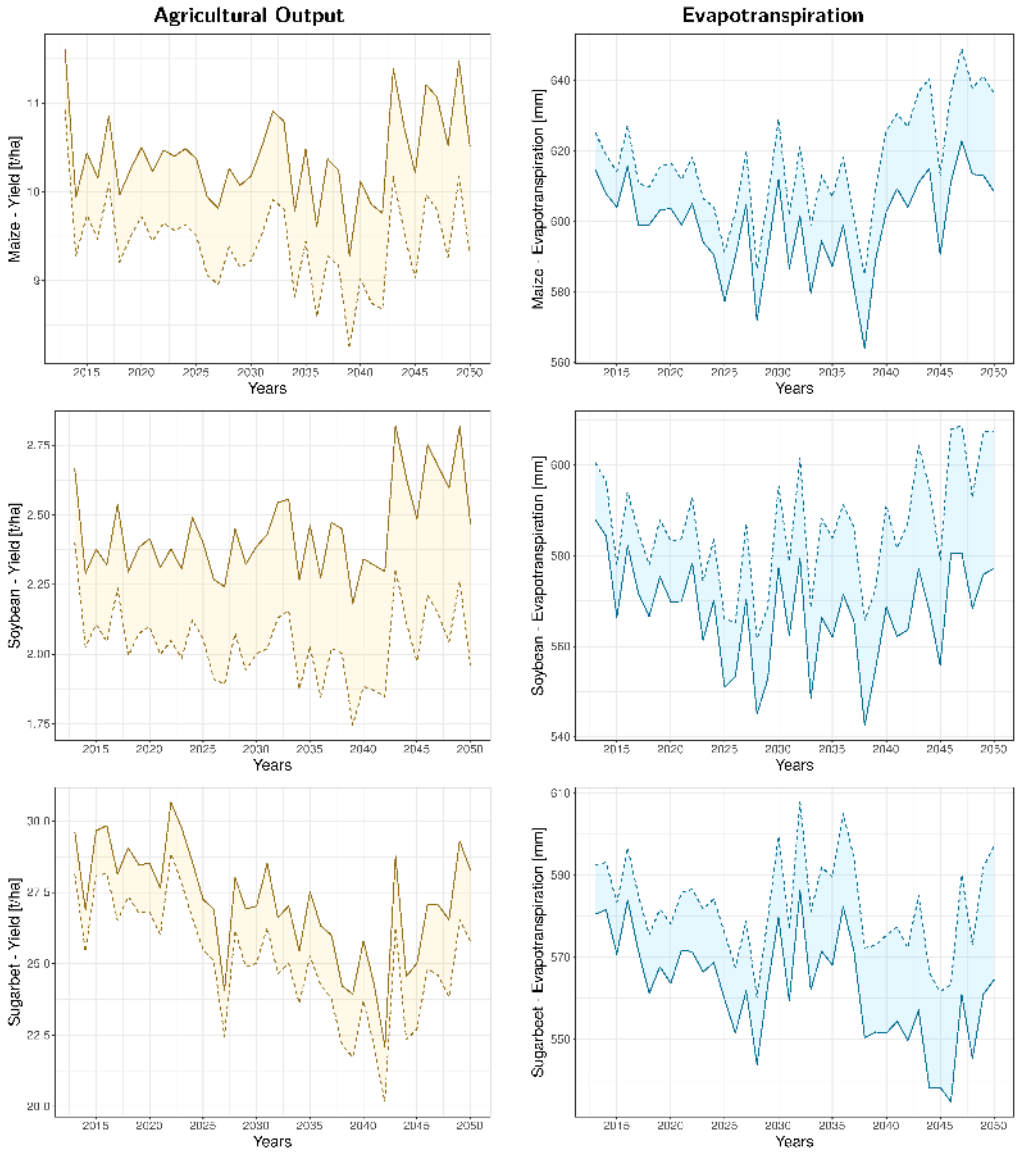

Figure C4.12: Agricultural production comparison between the original SWAT model and the dynamic atmospheric CO_2 concentration SWAT model. From left to right: 1st Column: Crop yields; 2nd Column: Evapotranspiration. From top to bottom: 1st Row: Maize; 2nd Row: Soybean; 3rd Row: Sugarbeet. The elements of this plot are: The solid lines represent the mean values of all simulations when the effects of dynamic atmospheric CO_2 concentration are taken into account; The dashed lines represent the mean values of all simulations when the atmospheric CO_2 concentration is fixed at the standard value of 330 p.p.m.v., and; The shaded area highlights the differences between the two mean values.

long-term hydrological simulations. In fact, the total mean difference between the two scenarios shown in Figure C4.12 for the evapotranspiration variable by 2050 is of 26 mmH_2O for the whole Dese-Zero sub-basin, a value that represents, approximately, 6.5 million m^3 of water. This value, for instance, if fully directed to irrigation applications, could possibly sustain the irrigation water requirements of all the area covered by maize in the same sub-basin during the whole growing season.

4.4 Conclusions

This study has explored how climate change impacts might affect the irrigation process in the VLW's area in the long-term by proposing the evaluation of an evolutionary irrigation efficiency scenario as an alternative adaptation strategy for which farmers can adopt in order to increase crops resilience against adverse climatic impacts. The results obtained by the work developed in this chapter indicate that improved irrigation systems can reduce the overall water withdrawals from source while, at the same time, increase the amount of water that is made available to crops, thus increasing the general efficiency of irrigation systems. Moreover, the improvement of efficiency in irrigation systems can increase the availability of RFWRs by reducing the demand from the agricultural sector, thus offsetting the demand for this resource to other sectors, such as human consumption.

Investments in more efficient irrigation systems can not only reduce the total amount of water that is used during irrigation operations, but also increase the resilience of irrigated crops to adverse climatic conditions. The climatic pathways evaluated in this chapter point to the direction of an increasing pressure on crops due to an increase of near-surface temperatures and a decrease in the total amount of precipitation falling over the VLW's as a result from changing climate patterns. Indeed, under these circumstances, the results obtained in this study indicate that crops' temperature stress is expected to be the dominant physical factor limiting the grow of crops during the next decades, while water stress can affect the growth of irrigated crops only during droughts or periods of low

availability of water for irrigation.

Due to the complex hydraulic management system currently implemented in the VLW that is responsible for supporting a close-to-optimal water supply to irrigation systems, the yield of crops is expected to be slightly affected by the increase of irrigation efficiencies in the watershed. Instead, direct climatic factors, such as changing patterns of precipitation and temperature, are expected to play a much larger role in determining the productivity of crops in the VLW. Still, the results suggest a consistent increased dependency on the amount of irrigation water coming from sources outside of the VLW during the next decades, a result that can be partially attributed to the effects of climate change on the regional hydrologic cycle of the Dese-Zero watershed, ultimately diminishing the rate of hydrologic processes such as baseflow and percolation. The explored alternative adaptation strategy of increasing investments for the improvement of irrigation systems can offset some of the increased demand of water imported from bordering watersheds.

As a guideline for improving further research in the topic, some recommendations can be made. First, in some cases, improvements in irrigation systems can result in the expansion of irrigated areas. Moreover, with a general higher availability of water for irrigation due to an increased efficiency of irrigation systems, farmers may opt to switch to higher-value, higher-profit crop variants that previously were not a viable option. Similarly, when farmers need to reduce the irrigated area, it is common the adoption of different crop variants that require less water than traditional crops. These considerations results in a dynamic land-use, that was not incorporated in the work presented in this chapter. A way of determining the best options available to farmers or group of farmers (i.e. agents) could be the coupling of a hydrologic model (e.g. SWAT) with a micro-economics model capable of revealing the preferences of agents with regards to economic, climatic, and water availability constraints, the latter coming from the hydrologic model.

Acknowledgements

A special thank is given to all the people who have directly or indirectly contributed to the development of this research, in particular: Dr. Paola Mercogliano (Euro-Mediterranean Center on Climate Change – CMCC; Italian Aerospace Research Centre – CIRA), Myriam Montesarchio (CMCC; CIRA), and Luigi Cattaneo (CMCC; CIRA), notably for providing specific data and technical information regarding the COSMO-CLM and CMCC-CM models. Also, the author is thankful and acknowledge the fact that work presented in this chapter would have not be possible without the climate data provided by the EURO-CORDEX project, a branch of the international CORDEX initiative that is sponsored by the World Climate Research Program – WRCP.

References

[1] Arnold, J. G., Kiniry, J. R., Srinivasan, R., Williams, J. R., Haney, E. B., Neitsch, S. L., 2012. Soil & Water Assessment Tool: Input/Output Documentation. Version 2012. Tech. rep., Texas A&M AgriLife, USDA Agricultural Rsearch Service, College Station, TX, USA.

[2] ARPAV, 2015. ARPAV - Dati Meteorologici.
URL http://www.arpa.veneto.it/temi-ambientali/meteo/dati

[3] Balbi, S., Bhandari, S., Gain, A. K., Giupponi, C., 2013. Multi-agent agro-economic simulation of irrigation water demand with climate services for climate change adaptation. Italian Journal of Agronomy 8 (e23), 175–185.

[4] Bixio, V., Celegon, E. A., Fanton, P., Fiume, A., Vazzoler, C., Zanetti, S., Bixio, A. C., Rech, F., 2009. Documento Propedeutico ai Piani Generali di Bonifica e Tutela del Territorio dei Consorzi di Bonifica del Veneto: L'irrigazione nella Regione Veneto. Tech. rep., Regione Veneto, Piazzola sul Brenta.

[5] Brenta, C. d. B., 2016. Inaugurazione Nuovo Impianto Pluvirriguo Bassano del Grappa.
URL http://www.consorziobrenta.it/news-iniziative/InaugurazioneBassano-8ottobre2016.pdf

[6] Brouwer, C., Prins, K., Heibloem, M., 1989. Training Manual No. 4 - Irrigation Scheduling. Tech. Rep. 4, Food and Agriculture Organization of the United Nations, Rome, Italy.

[7] Brouwer, C., Prins, K., Kay, M., Heibloem, M., 1990. Training Manual No. 5 - Irrigation Methods. Tech. Rep. 5, Food and Agriculture Organization of the United Nations, Rome, Italy.

[8] Bucchignani, E., Montesarchio, M., Zollo, A. L., Mercogliano, P., 2015. High-resolution climate simulations with COSMO-CLM over Italy: Performance evaluation and climate projections for the 21st century. International Journal of Climatology.

[9] Cetin, O., Bilgel, L., 2002. Effects of different irrigation methods on shedding and yield of cotton. Agricultural Water Management 54 (1), 1–15.

[10] Clarke, L. E., Jacoby, H., Pitcher, H., Reilly, J., Richels, R., 2007. Scenarios of Greenhouse Gas Emissions and Atmospheric Concentrations. Sub-report 2.1A of Synthesis and Assessment Product 2.1 by the U.S. Climate Change Science Program and the Subcommittee on Global Change Research. Tech. Rep. July, Department of Energy, Office of Biological & Environmental Research, Washington, DC, USA.

[11] CMCC, E.-M. C. o. C. C., EIA-UATLANTICA, E. I. e. A. S. U. A. d. P., UPV, U. P. d. V., 2012. ICARUS - IWRM for Climate Change Adaptation in Rural Social Ecosystems in Southern Europe. Tech. Rep. January.

[12] da Cunha, D. A., Coelho, A. B., Féres, J. G., 2014. Irrigation as an adaptive strategy to climate change: an economic perspective on Brazilian agriculture. Environment and Development Economics 20 (01), 57–79.

[13] del Veneto, C. R., 2009. Piano di Tutela delle Acque. Art. 121 D.Lgs. 3/04/2006 n. 152. Tech. rep., Consiglio Regionale del Veneto. VIII Legislatura, Venezia VE.

[14] Duan, Q., Ajami, N. K., Gao, X., Sorooshian, S., 2007. Multi-model ensemble hydrologic prediction using Bayesian model averaging. Advances in Water Resources 30 (5), 1371–1386.

[15] Eckelmann, H. W., Sponagel, R. H., Grottenthaler, W., Hartmann, K.-J., Hartwich, R., Janetzko, P., Joisten, H., Kühn, D., Sabel, K.-J., Traidl, R., Boden, H. A.-h.-A., 2006. Bodenkundliche Kartieranleitung. KA5. Schweizerbart Science Publishers, Stuttgart, Germany.

[16] Elliott, J., Deryng, D., Müller, C., Frieler, K., Konzmann, M., Gerten, D., Glotter, M., Flörke, M., Wada, Y., Best, N., Eisner, S., Fekete, B. M., Folberth, C., Foster, I., Gosling, S. N., Haddeland, I., Khabarov, N., Ludwig, F., Masaki, Y., Olin, S., Rosenzweig, C., Ruane, A. C., Satoh, Y., Schmid, E., Stacke, T., Tang, Q., Wisser, D., 2014. Constraints and potentials of future irrigation water availability on agricultural production under climate change. Proceedings of the National Academy of Sciences of the United States of America 111 (9), 3239–44.

[17] Ercoli, L., Mariotti, M., Masoni, A., Bonari, E., 1999. Effect of irrigation and nitrogen fertilization on biomass yield and efficiency of energy use in crop production of Miscanthus. Field Crops Research 63 (1), 3–11.

[18] Esteve, P., Varela-Ortega, C., Blanco-Gutiérrez, I., Downing, T. E., 2015. A hydro-economic model for the assessment of climate change impacts and adaptation in irrigated agriculture. Ecological Economics 120, 49–58.

[19] Falkenmark, M., Widstrand, C., 1992. Population and water resources: a delicate balance. Population bulletin 47 (3), 1–36.

[20] Falloon, P., Challinor, A., Dessai, S., Hoang, L., Johnson, J., Koehler, A.-K., 2014. Ensembles and uncertainty in climate change impacts. Frontiers in Environmental Science 2 (July), 1–7.

[21] Field, C., Barros, V., Mach, K., Mastrandrea, M., van Aalst, M., Adger, W., Arent, D., Barnett, J., Betts, R., Bilir, T., Birkmann, J., Carmin, J., Chadee, D., Challinor, A., Chatterjee, M., Cramer, W., Davidson, D., Estrada, Y., Gattuso, J.-P., Hijioka, Y., Hoegh-Guldberg, O., Huang, H., Insarov, G., Jones, R., Kovats, R., Romero-Lankao, P., Larsen, J., Losada, I., Marengo, J., McLean, R., Mearns, L., Mechler, R., Morton, J., Niang, I., Oki, T., Olwoch, J., Opondo, M., Poloczanska, E., Pörtner, H.-O., Redsteer, M., Reisinger, A., Revi, A., Schmidt, D., Shaw, M., Solecki, W., Stone, D., Stone, J., Strzepek, K., Suarez, A., Tschakert, P., Valentini, R., Vicuña, S., Villamizar, A., Vincent, K., Warren, R., White, L., Wilbanks, T., Wong, P., Yohe, G., 2014. Technical Summary. In: Field, C., Barros, V., Dokken, D., Mach, K., Mastrandrea, M., Bilir, T., Chatterjee, M., Ebi, K., Estrada, Y., Genova, R., Girma, B., Kissel, E., Levy, A., MacCracken, S., Mastrandrea, P., White, L. (Eds.), Climate Change 2014: Impacts, Adaptation, and Vulnerability. Part A: Global and Sectoral Aspects. Contribution of Working Group II to the Fifth Assessment Report of the Intergovernmental Panel on Climate Change. Cambridge University Press, Cambridge, United Kingdom and New York, NY, USA., Ch. Tec. Summ., pp. 35–94.

[22] Fischer, G., Tubiello, F. N., van Velthuizen, H., Wiberg, D. A., 2007. Climate change impacts on irrigation water requirements: Effects of mitigation, 1990-2080. Technological Forecasting and Social Change 74 (7), 1083–1107.

[23] Foley, J. A., 2011. Can We Feed the World & Sustain the Planet? Scientific American 305 (5), 60–65.

[24] Food and Agriculture Organization of the United Nations - FAO, 2003. Agriculture, food and water. A contribution to the World Water Development Report. Tech. rep., Food and Agriculture Organization of the United Nations, FAO. A contribution to the World Water Development Report, Rome, Italy.

[25] Foudi, S., Erdlenbruch, K., 2011. The role of irrigation in farmer's risk management strategies in France. European Review of Agricultural Economics (jbr024), 1–21.

[26] Fowler, H. J., Ekström, M., 2009. Multi-model ensemble estimates of climate change impacts on UK seasonal precipitation extremes. International Journal of Climatology 29 (January 2009), 385–416.

[27] Gleick, P. H., 2000. The Changing Water Paradigm - A Look at Twenty-first Century Water Resources Development. Water International 25 (1), 127–138.

[28] Gomez-Macpherson, H., 2015. Water & Agriculture: Adaptive strategies at farm level. Tech. Rep. Version 17, June.

[29] Ignaciuk, A., Mason-D'Croz, D., 2014. Modelling adaptation to climate change in agriculture. OECD Food, Agriculture and Fisheries Papers (70), 58.

[30] Jacob, D., Petersen, J., Eggert, B., Alias, A., Christensen, O. B., Bouwer, L. M., Braun, A., Colette, A., Déqué, M., Georgievski, G., Georgopoulou, E., Gobiet, A., Menut, L., Nikulin, G., Haensler, A., Hempelmann, N., Jones, C., Keuler, K., Kovats, S., Kröner, N., Kotlarski, S., Kriegsmann, A., Martin, E., van Meijgaard, E., Moseley, C., Pfeifer, S., Preuschmann, S., Radermacher, C., Radtke, K., Rechid, D., Rounsevell, M., Samuelsson, P., Somot, S., Soussana, J. F., Teichmann, C., Valentini, R., Vautard, R., Weber, B., Yiou, P., 2014. EURO-CORDEX: New high-resolution climate change projections for European impact research. Regional Environmental Change 14 (2), 563–578.

[31] Mirata, M., Emtairah, T., 2010. Water Efficiency Handbook.

[32] Neitsch, S. L., Arnold, J. G., Kiniry, J. R., Williams, J. R., 2011. Soil & Water Assessment Tool Theoretical Documentation. Version 2009. Tech. Rep. TR-406, Texas A&M AgriLife, USDA Agricultural Rsearch Service, College Station, TX, USA.

[33] Oki, T., Kanae, S., 2006. Global Hydrological Cycles and World Water Resources. Science 313 (5790), 1068–1072.

[34] Orientali, A., 2010. Subunità Idrografica Bacino Scolante, Laguna di Venezia e Mare Antistante. Tech. rep., Venezia VE.

[35] Pfeiffer, L., Lin, C. Y. C., 2014. Does efficient irrigation technology lead to reduced groundwater extraction? Empirical evidence. Journal of Environmental Economics and Management 67 (2), 189–208.

[36] Rosenzweig, C., Elliott, J., Deryng, D., Ruane, A. C., Müller, C., Arneth, A., Boote, K. J., Folberth, C., Glotter, M., Khabarov, N., Neumann, K., Piontek, F., Pugh, T. a. M., Schmid, E., Stehfest, E., Yang, H., Jones, J. W., 2014. Assessing agricultural risks of climate change in the 21st century in a global gridded crop model intercomparison. Proceedings of the National Academy of Sciences of the United States of America 111 (9), 3268–73.

[37] Sivapalan, M., Konar, M., Srinivasan, V., Chhatre, A., Wutich, A., Scott, C. A., Wescoat, J. L., 2014. Socio-hydrology: Use-inspired water sustainability science for the Anthropocene. Earth's Future 2, 225–230.

[38] Sivapalan, M., Savenije, H. H. G., Blöschl, G., 2012. Socio-hydrology: A new science of people and water. Hydrological Processes 26 (8), 1270–1276.

[39] Smith, S. J., Wigley, T., 2006. Multi-Gas Forcing Stabilization with Minicam. The Energy Journal 27, 373–391.

[40] Tebaldi, C., Knutti, R., Allen, M., Stott, P., Mitchell, J., Schnur, R., Delworth, T., Andronova, N., Schlesinger, M., Annan, J., Hargreaves, J., Edwards, N., Marsh, R., Annan, J., Hargreaves, J., Ohgaito, R., Abe-Ouchi, A., Emori, S., Benestad, R., Berger, J., Bryan, F., Danabasoglu, G., Nakashiki, N., Yoshida, Y., Kim, D.-H., Tsutsui, J., Cantelaube, P., Terres, J.-M., Collins, M., Booth, B., Harris, G., Murphy, J., Sexton, D., Webb, M., Dettinger, M., Doblas-Reyes, F., Pavan, V., Stephenson, D., Evensen, G., Evensen, G., Forest, C., Stone, P., Sokolov, A., Allen, M., Webster, M., Forest, C., Stone, P., Sokolov, A., Frame, D., Booth, B., Kettleborough, J., Stainforth, D., Gregory, J., Collins, M., Allen, M., Gates, W., Gent, P., McWilliams, J., Gent, P., Willebrand, J., McDougall, T., McWilliams, J., Gillett, N., Zwiers, F., Weaver, A., Hegerl, G., Allen, M., Stott, P., Giorgi, F.,

Francisco, R., Giorgi, F., Mearns, L., Giorgi, F., Mearns, L., Goldstein, M., Rougier, J., Greene, A., Goddard, L., Lall, U., Hagedorn, R., Doblas-Reyes, F., Palmer, T., Hegerl, G., Crowley, T., Hyde, W., Frame, D., Houghton, J., Ding, Y., Griggs, D., Noguer, M., van der Linden, P., Xiaosu, D., Dai, X., Maskell, K., Johnson, C., Kiehl, J., Shields, C., Knutti, R., Stocker, T., Joos, F., Plattner, G.-K., Knutti, R., Stocker, T., Joos, F., Plattner, G.-K., Knutti, R., Joos, F., Müller, S., Plattner, G.-K., Stocker, T., Knutti, R., Meehl, G., Allen, M., Stainforth, D., Krishnamurti, T., Kishtawal, C., Zhang, Z., Larow, T., Bachiochi, D., Williford, E., Gadgil, S., Surendran, S., Lambert, S., Boer, G., Lopez, A., Tebaldi, C., New, M., Stainforth, D., Allen, M., Kettleborough, J., Luo, Q., Jones, R., Williams, M., Bryan, B., Bellotti, W., Meehl, G., Boer, G., Covey, C., Latif, M., Stouffer, R., Meinshausen, M., Min, S.-K., Hense, A., Murphy, J., Sexton, D., Barnett, D., Jones, G., Webb, M., Collins, M., Stainforth, D., Nakićenović, N., Nychka, D., Tebaldi, C., Otto-Bliesner, B., Brady, E., Clauzet, G., Tomas, R., Levis, S., Kothavala, Z., Palmer, T., Palmer, T., Räisänen, J., Palmer, T., Shutts, G., Hagedorn, R., Doblas-Reyes, F., Jung, T., Leutbecher, M., Palmer, T., Doblas-Reyes, F., Hagedorn, R., Weisheimer, A., Piani, C., Frame, D., Stainforth, D., Allen, M., Räisänen, J., Räisänen, J., Palmer, T., Redi, M., Robertson, A., Lall, U., Zebiak, S., Goddard, L., Schneider, S., Stainforth, D., Stott, P., Kettleborough, J., Tebaldi, C., Mearns, L., Nychka, D., Smith, R., Tebaldi, C., Smith, R., Nychka, D., Mearns, L., Thomson, M., Doblas-Reyes, F., Mason, S., Hagedorn, R., Connor, S., Phindela, T., Morse, A., Palmer, T., von Deimling, T., Held, H., Ganopolski, A., Rahmstorf, S., Wigley, T., Raper, S., Wild, M., Wild, M., Long, C., Ohmura, A., Yun, W., Stefanova, L., Krishnamurti, T., 2007. The use of the multi-model ensemble in probabilistic climate projections. Philosophical transactions of the Royal Society. Series A, Mathematical, physical, and engineering sciences 365 (1857), 2053–75. URL http://www.ncbi.nlm.nih.gov/pubmed/17569654

[41] Van Emmerik, T. H. M., Li, Z., Sivapalan, M., Pande, S., Kandasamy, J., Savenije, H. H. G., Chanan, A., Vigneswaran, S., 2014. Socio-hydrologic modeling to understand and mediate the competition for water between

agriculture development and environmental health: Murrumbidgee River basin, Australia. Hydrology and Earth System Sciences 18 (10), 4239–4259.

[42] Veneto, R., 2014. Infrastruttura dei Dati Territoriali del Veneto - Catalogo dei Dati.
URL http://idt.regione.veneto.it/app/metacatalog/

[43] Vörösmarty, C. J., Green, P., Salisbury, J., Lammers, R. B., 2000. Global Water Resources: Vulnerability from Climate Change and Population Growth. Science 289 (July), 284–288.

[44] Wise, M., Calvin, K., Thomson, A., Clarke, L., Bond-Lamberty, B., Sands, R., Smith, S. J., Janetos, A., Edmonds, J., 2009. Implications of Limiting CO2 Concentrations for Land Use and Energy. Science 324 (May), 1183–1186.

[45] Zollo, A. L., Rillo, V., Bucchignani, E., Montesarchio, M., Mercogliano, P., 2015. Extreme temperature and precipitation events over Italy: Assessment of high-resolution simulations with COSMO-CLM and future scenarios. International Journal of Climatology.

[46] Zucaro, R., Furlani, A., 2009. Programma Interregionale: Monitoraggio dei Sistemi Irrigui delle Regioni Centro Settentrionali. Rapporto Sullo Stato dell'Irrigazione in Veneto. Tech. rep., Istituto Nazionale di Economia Agraria INEA, Rome, Italy.

Chapter 5

On Risks & Climate Change

The IRW Case Study

Abstract

River floods are one of the most common yet devastating natural hazards. The total damage of a flood event depends on its core elements: hazard, vulnerability, and exposure. The quantification of each risk's core element is an essential step for disaster risk management. Currently, the consideration of dynamic human adaptation actions and their linkages with physical processes is a challenge in quantifying flood hazards when performing long-term analysis of hydrologic systems. Building upon the SREX and the KULTURisk framework, this chapter proposes a methodological framework tailored to account for the effects of both natural and non-natural factors on the water balance of watersheds by proposing the use of the coupled SWAT-ANN model to simulate the hydrological processes of a watershed and to compute the dynamic behaviour of managing flood control reservoirs as a function of these processes. The IRW, a watershed historically prone to river flood events, is chosen as a case study. Results suggest that the incorporation of an ANN module in the SWAT model to account for the dynamic management of reservoirs is a useful instrument for linking hydrologic process and flood risk reduction under a context of climate change and long-term analysis.

5.1 Introduction

River floods are one of the most common yet most devastating natural hazards worldwide [35, 29], resulting in billions of dollars being spent globally each year [6]. In Europe, river floods are among the most important weather-related loss events and have the potential to cause severe economic damage. According to the European Environment Agency – EEA, from the years 2000 to 2009, Europe as a whole has spent more than 55 billion euros to cope with impacts of floods [13]. Similarly, in the other side of the Atlantic ocean, a report prepared by the NOAA indicated that during the year of 2013, the United Stated has had 2.15 billion dollars of total costs coming from only direct flood-related damages [44]. In Brazil, the economic losses due to floods are estimated to be around 0.75 billion dollars yearly between the years of 2008 and 2012 [11].

Not all damages coming from river floods can be quantified in monetary terms, however. Flood damages that cannot be measured by monetary terms are classified as intangible. Examples are the number of human lives lost after a flood episode or the ecosystem services indirectly affected by an inundation event. Still, the damage caused by a river flood episode can be further categorised into direct and indirect effects [39, 57]. Direct impacts can be understood as the impacts which have as only cause the flood itself, not being mediated by any other factor such as material damages to property or the environment in flooded areas (e.g. damage to buildings, infrastructure, etc.). Indirect impacts are classified as a subsequent effects of direct impacts, such as losses of industrial productivity or transportation disruption. Table C5.1 summarises these classifications of flood damages.

Table C5.1: Flow partition estimates in the VLW.

		Damage Measurement	
		Tangible	**Intangible**
Damage Type	**Direct**	E.g. Damage to infrastructure	E.g. Loss of life
	Indirect	E.g. Loss of industrial productivity	E.g. Increased vulnerability to water-borne diseases

Adapted from: Messner and Meyer [39], Thieken et al. [57]

Although flood events result from excessive precipitation and hydro-meteorological extreme events [6], the damage caused by floods depends on the degree to which a flood hazard can affect population and assets [50, 25, 28]. Due the ease of access to fresh water resources and environmental services provided by rivers, a great number of cities and settlements around the globe are located close to or inside flood prone areas, increasing their exposure to possible negative effects to flood hazards [12]. However, not only exposure determines the magnitude of damages resulting from flood events, but also the vulnerability to which population and assets can be adversely affected by a flood hazard. This is evident when comparing similar hazard events that happened in contrasting socio-economic realities (e.g. [9, 7, 37, 17]). Indeed, the combination of hazard, vulnerability, and exposure leads to the concept of risk [25]. Not by accident, then, risk management present itself as a way of managing and reducing the damages caused by river floods.

At this point, the definition of some concepts related to risk management is fundamental for the characterisation of flood related damages. This work relies on the definition of hazard, exposure, and vulnerability as given by the IPCC Special Report on Managing the Risks of Extreme Events and Disasters to Advance Climate Change Adaptation – SREX [25], as follows:

- **Hazard:** The potential occurrence of a natural or human-induced physical event that may cause loss of life, injury, or other health impacts, as well as damage and loss to property, infrastructure, livelihoods, service provision, and environmental resources;
- **Vulnerability:** The propensity or predisposition to be adversely affected, and;
- **Exposure:** The presence of people; livelihoods; environmental services and resources; infrastructure; or economic, social, or cultural assets in places that could be adversely affected.

From the definitions above, hazard can be understood as the physical component of risk, while vulnerability is closely related to socio-economics characteristics of assets[1]. Exposure, instead, provides the linkage between the two components. If one of these components is missing, there is no risk. Hence, risk is the result of

a complex, often non-linear, combination of its components. Similarly to IWMPs, flood risk management, then, should be the result of an integrated approach, based on multidisciplinary research and including contributions ranging from physical to socio-economic sciences [22]. In mathematical terms, the concept of risk can be defined as follows:

$$R = f\left(H, V, E\right) \tag{C5.1}$$

where H is the characterisation of the hazard; V is the characterisation of the vulnerability; E is the characterisation of the exposure, and; R is the risk[2].

Although floods are mainly the result of hydro-meteorological conditions, human activities can directly and indirectly affect the magnitude and frequency of flood episodes over time. For instance, the conversion of natural vegetated areas to agricultural lands and/or the expansion of impermeable surface areas on a watershed can result in decreased rated of infiltration and intensification of surface runoff [6]. Indirectly, human may alter the circulation process of water in the atmosphere, resulting in changing patters of precipitation and ultimately affecting the rainfall-runoff process at a watershed-level scale [54].

Indeed, climate change can potentially increase the risk of floods by altering the distribution, frequency, and/or intensity of precipitation events over land, ultimately resulting in an intensification of the hydrologic cycle and affecting the intensity and/or frequency of flood episodes [25, 23]. Economically, the costs of river flood related episodes are estimated to go up to 46 billion euros annually in whole Europe by 2050, while the number of people affected by floods is estimated to reach 290 thousand people annually in whole Europe by the same period [18]. In the context of climate change, the concept of risk can be illustrated as shown in Figure C5.1.

[1]Although hazard can be seen as the physical component and vulnerability as the socio-economic component of risk, this does not mean that hazard is isolated from the socio-economic system or that vulnerability is isolated from the physical system. On the contrary, as extensively discussed in this dissertation's Introduction and in Chapter 1, the notion of isolated physical or socio-economic systems is no longer feasible as they are interconnected and interdependent among themselves, especially under long-term analysis [3, 53].

[2]It is important to notice that, from the definition of risk as given by Eq. C5.1, risk is not simply the result of a multiplication between its components, but instead the result of a function, often complex and non-linear, among its components.

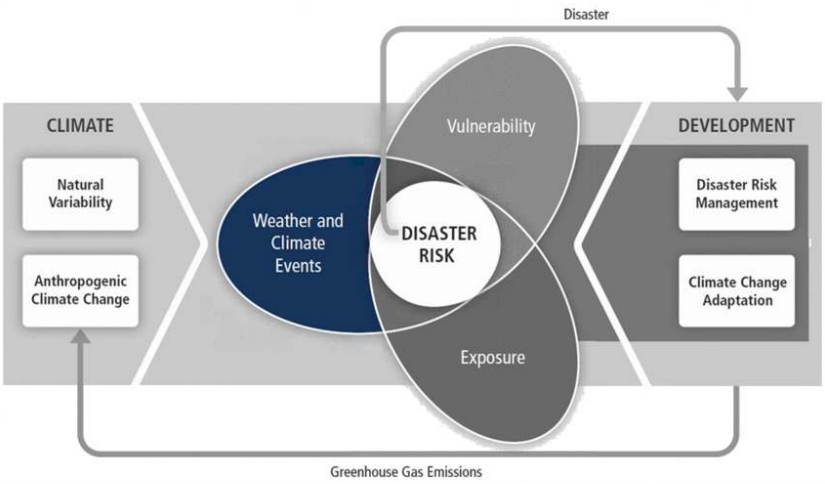

Source: IPCC [25]

Figure C5.1: Schematic representation of risk and its components.

Following the definition of risk as shown in Figure C5.1 and as already previously discussed, there is no risk if there is no hazard. Hence, the characterisation of the hazard is fundamental for a successful assessment of risk. With regards to flood hazards, flood events are usually specified by the probability analysis of flood peaks [52]. However, a flood hazard is a composition of several properties that characterise a specific flood event, the most common being the flood extension area, the flood depth, and the flow velocity [51, 14, 15, 57]. Hence, flood properties should not be estimated only by the correlation with statistical probabilities of flood peaks [52], but instead be considered as individual factors contributing to the characterisation of the hazard. Under such circumstances, the coupling of hydrologic and hydraulic models provide an interesting and useful framework to characterise river flood hazards [38].

Rivera et al. [48] proposed the study of hydrologic modelling to determine flood prone areas in the Aguán river basin, in Honduras, by relying on the use of the SWAT model to estimate discharge values, while using the Hydrological Engineering Center - River Analysis System – HEC-RAS hydraulic model to estimate flood characteristics, such as flood extension and flood depth. The authors concluded that the proposed methodology is useful for the identification

of flood prone area, being capable of indicating areas where an early flood warning system could be more effective. Knebl et al. [30], in turn, proposed a methodological framework based on the use of both Hydrological Engineering Center - Hydrologic Modeling System – HEC-HMS and HEC-RAS models to simulate regional-scale flood dynamics at the San Antonio River Basin, in Central Texas, USA. The authors conclude that, although the hydrological model tends to overestimate the magnitude of runoff, the proposed methodological framework is capable of producing reasonable good results. Several other studies can be shown as examples of different modelling techniques successfully applied to flood forecasting and characterisation (e.g. [8, 61, 27]).

In a context of climate change, however, the physical properties that characterise a flood event are not static. For instance, some concepts that define exposure can also affect the hazard component of risk, such as land-use. In fact, LCLUCs resulting from people's activities can determine the extent to which flood events might impact human life and welfare [6]. As not only human actions but also global and regional climatic responses are uncertain under a context of long-term analysis, it becomes more relevant the identification of changes in flooding patterns rather than the accurate representation of how and when a single flood event might occur. In other words, under a climate change perspective, the characterisation of the stochastic nature of flood events surpass in importance the characterisation of single-flood events [54]. Hence, a key concept brought by the schematic representation of risk as depicted in Figure C5.1 is the notion that not only disaster risk management can help reduce the risk, but also adaptation actions.

Adaptation is a concept that can be applied to both human and natural systems, consisting in the notion of adjustment to new climatic conditions in order to cope with harmful situations [25]. Human adaptation options can be classified as structural (e.g. flood control dam) and non-structural (e.g. flood warning system), being identified according to a variety of factors, such as site-specific characteristics, socio-economic constraints, and technological progress. Due to this fact, the modelling of adaptation options and their feedbacks to the climate system is a limitation of the current generation of GCMs [45]. While the identification of novel adaptation options is rather challenging, the understanding

of how already implemented adaptation actions might be affected or managed under future climate conditions is evenly complex. In a context of regional hydrologic modelling, one example is how flood control dams might be operated under different climatic conditions.

The work presented in this chapter, then, acknowledges the above discussed background and proposes the use of modelling techniques capable of simulating the regional hydrologic cycle at a watershed-level scale and under long-term analysis. Based on the methodology subsequently discussed, this chapter proposes a methodological framework for the characterisation of river flood hazards by relying on the use of a coupled SWAT-ANN model capable of simulating the hydrological processes of a watershed under a context of climatic changes and able to characterise the dynamic management of flood control reservoirs, while proposing the use of the hydraulic HEC-RAS model to translate the hydrological outputs into features that characterise flood hazard events. For the characterisation of river flood hazards, the proposed methodological frameworks build upon the Knowledge-based approach to develop a cULTUre of Risk prevention – KULTURisk – KULTURisk framework.

Aiming at the assessment of the validity of the proposed methodological framework, this chapter explores the first part of the proposed methodological framework by introducing the IRW as a case for the verification of the applicability of the coupled SWAT-ANN model as a tool capable of simulating the hydrologic processes and dynamic management of flood control reservoirs under long-term analysis. In terms of objectives, this chapter has two main goals: i. To verify the applicability of the coupled SWAT-ANN models in reproducing the overall hydrologic behaviour of the IRW and in capturing the management behaviour of the controlled flood control dams in the IRW as subject to hydro-meteorological conditions, and; ii. To assess how climate change may affect the rainfall-runoff process of the IRW, aiming at the stochastic characterisation of changes in the hazard component of river flood risk of this watershed.

5.2 Methodology

5.2.1 River Floods Modelling

There are several ways to characterise a flood event, ranging from remote sensing techniques (e.g. [66], [47], and [34]) to mathematical modelling techniques (e.g. [60], [30], and [46]). Similarly, most studies can be divided into global or regional assessments (e.g. [64]). This sub-section, then, introduces the concepts required in order to build the foundation of a conceptual flood hazard characterisation at a regional scale and relying on the use of mathematical models. Still, the presented framework is heavily based and built upon the KULTURisk framework [22, 49].

5.2.1.1 The Case Study Area

The watershed selected as case study for this chapter is the IRW[3], as shown in Figure C1.7. Figure C5.2, instead, shows the location of the three major flood control reservoirs in the study area, as well as the location of the stream gauges used for calibration purposes.

5.2.1.2 The SWAT Model

The SWAT model is an eco-hydrological watershed-scale model which offers the capability of assessing different watershed-related management processes and operations[4] [5]. While it is true that the the SWAT model lacks the ability to simulate detailed, single event flood events [42] as it was designed to be a support tool to assist water resource managers in assessing the impacts of different land management operations on water supply and related processes [5], it is also true that the model is capable of simulating and capturing changing patterns of hydrological and hydrological-related processes in long-term analysis due to its capability of considering changes in both climate and land-use and management [62, 26, 65, 21, 31, 36].

[3] A detailed description of the whole IRW is covered in Chapter 1, Section 1.4.

[4] A more detailed description of the SWAT model can found in Chapter 1, Section 1.2, along with all the proposed code modifications.

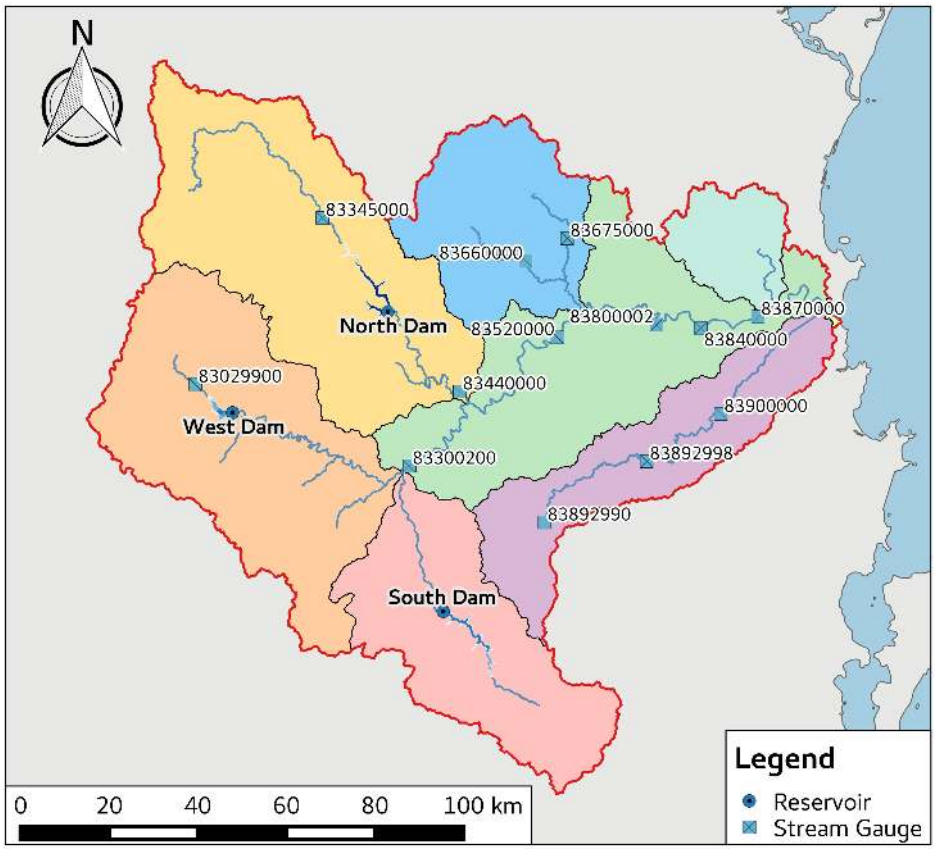

Data source: ANA [4]

Figure C5.2: The IRW case study.

Indeed, even if operating on a daily time-step, the SWAT model is efficient and robust enough to simulate long periods of time [5], which, in turn, is a fundamental requirement for any kind of long-term quantitative analysis. In fact, the SWAT model acknowledges the fact that an accurate representation of the water balance is the driving force behind every hydrologic-related process occurring in a watershed [42]. Consequently, the accurate representation of the rainfall-runoff process is a core process of the model.

Perhaps the most relevant capability of the SWAT model is that it is not only capable of simulating long periods of time, but also of incorporating the representation of a variety of dynamic processes during its simulation phase. For instance, the model takes into account a variety of land management options (e.g. crop rotation, tillage operations, etc.) that, ultimately, are capable of affecting the water balance of a watershed [42]. Indeed, long-term analysis (especially if the focus is floods) without the consideration of an evolving natural-human system is not feasible [53, 10].

Based on what has been discussed so far, and based on the concept that, under a perspective of long-term analysis, the capture of variations in the rainfall-runoff process is far more relevant than the accurate representation of single event flood routing, the methodological framework presented in this chapter assumes the SWAT model to be a tool capable of capturing dynamic changes capable of affecting hydrologic process in a watershed (e.g. land-use changes) and translate them to the rainfall-runoff process.

5.2.1.3 The HEC-RAS Model

The HEC-RAS model was developed by the Hydrologic Engineering Center, a subdivision of the Institute of Water Resources of the US Army Crop of Engineers, and being a product of the Corps' Civil Works System Wide Water Resources Research Program [59]. The model has been designed perform one-dimensional and two-dimensional, steady and unsteady hydraulic calculations for a network of channels. The model offers four distinct river analysis possibilities, yet the one of interest for the methodological framework presented in this chapter is the simulation of steady flow systems for the estimation of flood characteristics.

The steady flow simulation component of HEC-RAS model is the module intended to estimate water surfaces with respect to steady gradually varied flow [59]. Two terms coming from this last statement are fundamental for the characterisation of a flood event: i, First, the term *steady state* means that flow conditions are non-variant over time, so the depth and velocity of a particular flood event are constant at a given channel location and for a specific flow condition, and; ii. Second, the term *gradually varied flow* means that a continuous variation of the characteristics of a specific flood event are verified from cross-section to cross-section of a channel [55, 24].

Finally, the computation of the spatial dimension of a flood event can be done by utilising the HEC-geoRAS extension [2], ultimately enabling the mapping and characterisation of a particular flood event.

5.2.2 Climate Change

Much like the work presented and discussed in Chapter 4, the quantification of climate change effects is an uncertain science, a concept that is fundamental for the discussion presented in the current chapter. Thereby, the consideration of multi-model ensembles in a context of climate change offers the possibility of assessing plausible future climatic pathways while enabling the accounting of errors and uncertainties in climate projections [56, 19, 16]. Hence, this chapter relies on the use of different climate projections downscaled by the NEX-DCP30 project [58] and forced by four different GCMs, as shown in Table C5.2. Table C5.3, instead, list the variables considered in this study.

Following the discussion presented both in Chapter 1, Section 1.4, and in the current sub-subsection, the selection of of the GCMs listed in Table C5.2 was based on a literature review indicating which family of GCMs (among the list of available models) is able to capture effects associated with ENSO on the global hydrologic cycle [43, 32, 33], as this is a factor contributing to the characterisation of floods in the IRW [41, 20, 40, 63].

Table C5.2: List of considered GCMs and related data.

Project	RCM	GCM	Experiments	Spatial Resolution	Frequency
NEX-DCP30[1]	BCSD – NEX-DCP30	CCSM4	rcp45	30 arcseconds	daily
NEX-DCP30[1]	BCSD – NEX-DCP30	CSIRO-Mk3-6-0	rcp45	30 arcseconds	daily
NEX-DCP30[1]	BCSD – NEX-DCP30	GFDL-ESM2M	rcp45	30 arcseconds	daily
NEX-DCP30[1]	BCSD – NEX-DCP30	MPI-ESM-MR	rcp45	30 arcseconds	daily

[1] Data source: Trasher et al. [58]

Table C5.3: Weather variables information and ID codes.

Variable Code	Description	Unit
pr	Precipitation	$kg \cdot m^{-2} \cdot s^{-1}$
tasmax	Maximum Near-Surfcace Air Temperature	K
tasmin	Minimum Near-Surfcace Air Temperature	K

5.2.3 The KULTURisk Framework

The KULTURisk framework is a flexible Regional Risk Assessment – RRA methodology for water-related natural hazards developed within the FP7-KULTURisk Project [22, 49]. Building on the definition of risk summarised in Figure C5.1 and based on the understanding that interdisciplinary knowledge is a requirement for flood risk assessments, the KULTURisk framework was developed as a tool capable of supporting the assessment of alternative risk reduction measures while taking into consideration not only physical and economic dimensions of risk but also social and cultural elements [22]. The KULTURisk framework when applied to flood risk is shown by Figure C5.3.

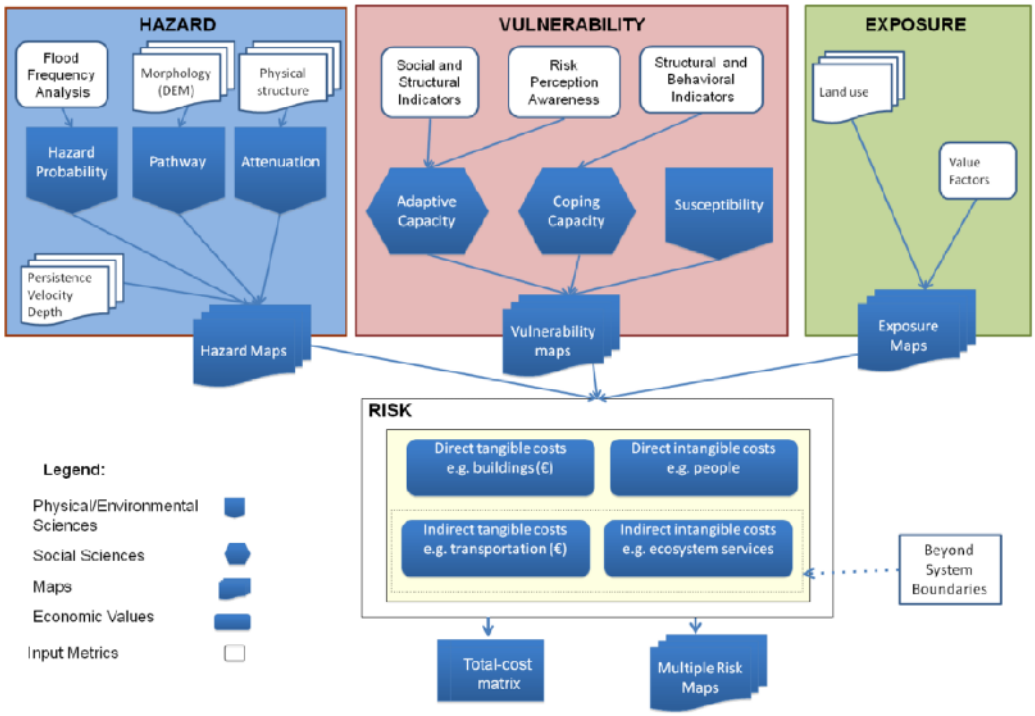

Source: Giupponi et al. [22]

Figure C5.3: The KULTURisk framework applied to the characterisation of flood risk.

As shown in Figure C5.3, the KULTURisk framework considers risk to be a function of the hazard, vulnerability, and exposure, in compliance with the

definition of risk given by Figure C5.1. Moreover, as defined by Ronco et al. [49], the KULTURisk framework *"integrates the outputs of hydrodynamic models with site-specific biogeophysical and socio-economic indicators to develop tailored risk indexes and Geographical Information System – GIS-based maps for each of the selected receptors in the considered region"*. From this definition, two new concepts are introduced, which are and can be defined as follows:

- **Indicator:** Measure variable capable of providing specific quantified information about a particular receptor (e.g. population density, population income, land-cover, slope, etc.), and;
- **Receptor:** A physical entity, with a specified geographical extent, that is characterised by particular features (e.g. people, buildings, infrastructure, agriculture, natural and semi-natural systems, sites of cultural relevance, etc.).

While receptors are closely related to the focus to which a risk assessment is being performed, biogeophysical indicators can be related also to the characterisation of the hazard. For instance, vegetation cover area may be an indicator of a vegetation cover receptor, while also influencing the characterisation of the hazard by affecting the rainfall-runoff process of a watershed. Being the hazard a physical process in essence (although affected by human factors, as discussed in the introductory section), the identification of physical and environmental characteristics that define a hazardous event is fundamental. As shown in Figure C5.3, four main inputs characterise a flood hazard event, namely: flood return period; pathway; attenuation factors, and; flood characteristics.

The flood return period can be estimated by means of data-series analysis (for observed periods) and hydrologic modelling (for future or alternative scenarios). The definition of a flood return period (e.g. 10-years return period) is dependent on specific requirements of stakeholders, while the consideration of different flood return periods enables the characterisation of diverse hazard maps. In a context of climate change, the contemplation of future scenarios is necessary, thus requiring the consideration of future conditions and factors capable of affecting the rainfall-runoff process of watersheds, such as climatic and land-use changes.

Pathway is a concept deriving from site-specific characteristics of a watershed. In essence, it consists of a set of factors that are particular to a watershed and that directly affect the characterisation of a flood hazard. Examples are terrain characteristics (in a context of hydrologic modelling, represented by the DEM), soil attributes, land-cover characteristics, and land-use and management practices.

Attenuation factors are features that have been implemented specifically to diminish the magnitude or decrease the frequency of a hazard. In a context of flood risk, attenuation factors are closely related to structural adaptation measures, such as the building of flood control dams, the rectification of channels, and the implementation of flood pumping stations.

Finally, flood characteristics are a set of properties that defines a particular flood event and that is dependent on all previous features that characterise a flood hazard event, i.e.: flood return period, pathway, and attenuation factors. The flood characteristics, hence, summarise the features of a flood event, being the direct input of flood hazard maps.

5.2.4 The Methodological Framework

Based on the discussion presented so far, this chapter proposes a methodological framework to characterise flood hazards under long-term analysis through the use of both SWAT-ANN and HEC-RAS models. The proposed methodological framework is depicted in Figure C5.4.

From the methodological framework depicted in Figure C5.4, it is possible to verify that the general flow of information shown in this figure is very similar to the framework shown in Figure C5.3. However, apart from the obvious difference that the methodological framework depicted in Figure C5.4 is developed to accommodate the inclusion of both SWAT-ANN and HEC-RAS models, some differences can be highlighted.

The first difference is the split of the morphology map input into two separate categories: static and dynamic. The static branch considers fixed, non-variable site-specific features, such as the DEM and soil properties[5]. The dynamic branch, on the other hand, embraces site-specific features that are considered to evolve

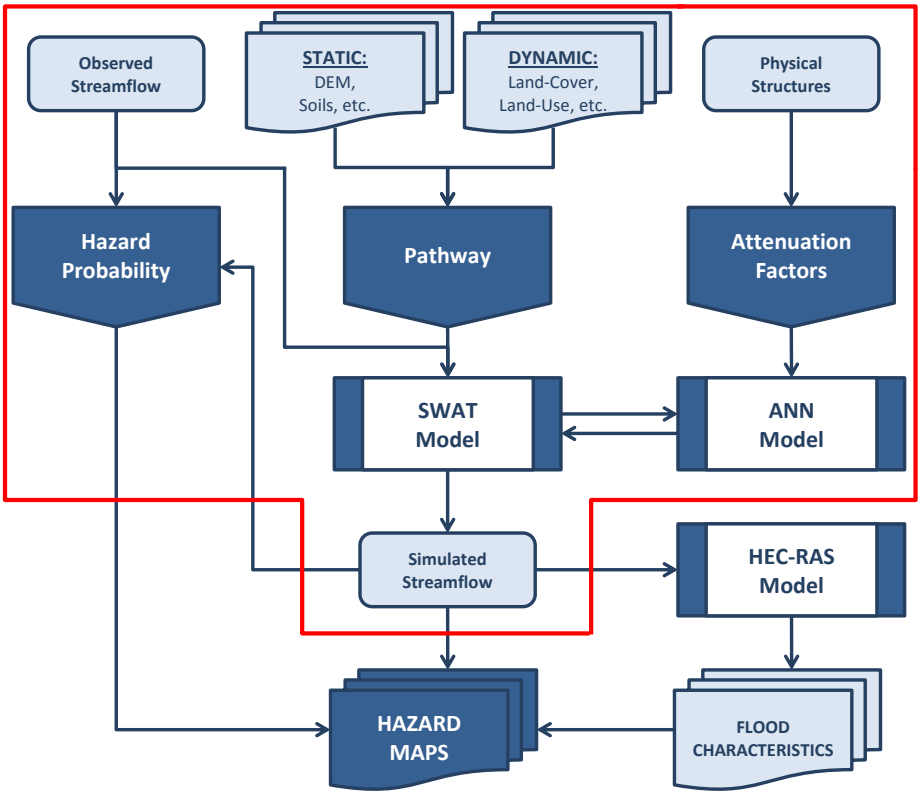

Figure C5.4: Flowchart depicting the proposed methodological framework.

over time, such as LCLUCs and changes in land-use management conditions.

A second difference between the frameworks depicted in Figures C5.4 and C5.3 is the fact that physical structures are not considered as a map input, but rather as an input metric. The reason for this change relies on the fact that, although the spatial location of physical structures serving as attenuation factors to floods is important and should in fact be considered during the flood routing phase of the SWAT model, this information is not passed to the model as a map layer, but rather as an input metric that characterises the physical structure (e.g. reservoirs).

The last major difference between the two frameworks is the fact that both the pathway and attenuation factors are not directly linked to the final result, i.e. hazard maps. Instead, both processes assumed to directly influence the characterisation of single flood events, which, in turn, define the hazard maps.

It is important to emphasise the fact that the final product of the proposed framework depicted in Figure C5.4 is defined as *hazard maps*, in its plural form. This is so due to the fact that, differently from the the deterministic approach considered in Chapters 3 and 4, this chapter relies on the concept of stochastic modelling of hydrologic systems as a way of characterising flood hazard events, much like the work discussed in Chapter 2. Hence, both the SWAT and the ANN models are assumed to be an ensemble of physically-valid models, thus recognising the errors and uncertainties related to the simulation of the system being modelled [38, 1]. Stochasticity, then, is added as a core concept in the characterisation of river flood hazard when performed under a context of climate change and long-term analysis.

Under a context of climate change, it makes necessary the identification of how climate change might affect river floods, in particularly to its effects on the probability of flood hazard in a watershed. One way of achieving such objective is through flood frequency analysis [23]. By utilising statistical techniques, it is possible to estimate the probability of the occurrence of a particular flood event and to determine specific flood return periods. A Probability Distribution Function – PDF that is particularly useful to study the distribution of extreme

[5]While it is true that both DEM and soil properties can (and in fact do) change over time, it is also true that the rate of change of these features is much slower than the rate of LCLUCs.

values is the Gumbel distribution, which can be computed as follows:

$$F_G(x) = \frac{1}{\sigma} \cdot exp\left(-\frac{x-\mu}{\sigma}\right) \cdot exp\left(-exp\left(-\frac{x-\mu}{\sigma}\right)\right) \tag{C5.2}$$

where μ is the location parameter and σ is the scale parameter of the Gumbel distribution.

Building upon the work developed in the previous chapters, the work presented in this chapter makes use of the coupled SWAT-ANN model as a tool capable of simulating the streamflow of a river, hence solving the first step required for the characterisation of flood events. The methodological work carried-out in this chapter, then, is inserted in the methodological framework presented in Figure C5.4, being highlighted by the red polygon.

5.3 Results and Discussions

As discussed in Section 5.1, the case study covered in this chapter studies the impacts of climate change on the rainfall-runoff process of the IRW, hence implementing the first part of the proposed methodological framework (see Figure C5.4). This section is sub-divided into three sub-sections, namely: ANN Model, SWAT-ANN Model, and Climate Change. The first sub-section brings the main results pertaining to the calibration of the ANN model in simulating the artificially-controlled discharge of the three main flood control reservoirs located in the IRW. The second sub-section summarises the main results from the calibration procedure of the coupled SWAT-ANN. Finally, the third and final sub-section presents the main results and a pertinent discussion regarding the long-term analysis of climate change impacts in the rainfall-runoff process of the IRW.

5.3.1 ANN Model

As the first step for the training of the ANN model for the simulation of the artificially-controlled outflow of the main reservoirs in the IRW, some information were selected coming from the physically-based hydrologic model and passed the

ANN as explanatory variables. The full list of variables that are exchanged between the two modules is shown in Table C5.4. The direction in which information is exchanged is from the SWAT model to the ANN model, so variables of type *"Input"* are understood as output information from the SWAT model and as input information to the ANN model. The information is exchanged on-line between the models, and the calibration of both model is done interactively until convergence. Still, the outputs of the ANN model are limited downwards by zero, meaning that no negative outflow is allowed, and upwards by the maximum daily outflow discharge feasible for each particular dam. The final results of training procedure of the ANN model are presented in Table C5.5, while Figure C5.5 displays the scatter plot for the training dataset for all three reservoirs.

The results shown in Table C5.5 and Figure C5.5 indicates that the ANN model is capable of accurately simulating the controlled outflow of the three major reservoir located in the IRW. An interesting observation relies on the fact that the ANN model generally underestimates the observed reservoir's outflow values, as indicated by a positive PBIAS. With the exception of the validation dataset for the North reservoir, this result is consistent throughout all three reservoirs and datasets. This same behaviour is graphically depicted in Figure C5.5, as indicated by the linear regression between the simulated and observed outflow values. As explored in Chapter 2, this result is expected due to the nature of ANN models, as this technology uses observed data as a target training value and adjusts the weight connection values between the neuron to minimise the errors of the predictions. As a consequence, since most of the observations are by definition not extreme values, ANN models are usually less capable of learning the behaviour of the system under extreme conditions due to the lack of training examples. In any case, the results shown in this sub-sections point in the direction of ANNs as being valid tools for the estimation of artificially-controlled reservoir's outflow under different hydro-meteorological conditions in the IRW area.

5.3.2 SWAT-ANN Model

Building upon the expertise acquired by the work developed in both Chapters 3 and 4, the calibration of the SWAT model is performed in parallel with the

Table C5.4: List of variables exchanged between the SWAT and ANN models.

Variable	Unit	Definition	Type[1]
ressa	ha	Surface area of reservoir on day	Input
res_vol	$m^3 H_2O/day$	Reservoir volume on day	Input
resflwi	$m^3 H_2O/day$	Water entering reservoir on day	Input
respcp	$m^3 H_2O/day$	Precipitation on reservoir for day	Input
resev	$m^3 H_2O/day$	Evaporation from reservoir on day	Input
ressep	$m^3 H_2O/day$	Seepage from reservoir on day	Input
flw	$m^3 H_2O/day$	Observed reservoir outflow on day	Target
resflwo	$m^3 H_2O/day$	Water leaving reservoir on day	Output

[1] Type of data as considered to the ANN model.

Table C5.5: ANN model calibration results.

Reservoir	Dataset	R2	NSE	PBIAS
North	Training	0.784	0.783	0.395
	Validation	0.791	0.788	-1.501
	Test	0.761	0.759	0.725
West	Training	0.619	0.617	3.632
	Validation	0.598	0.594	2.423
	Test	0.647	0.645	5.554
South	Training	0.646	0.645	5.291
	Validation	0.773	0.765	2.740
	Test	0.687	0.675	4.113

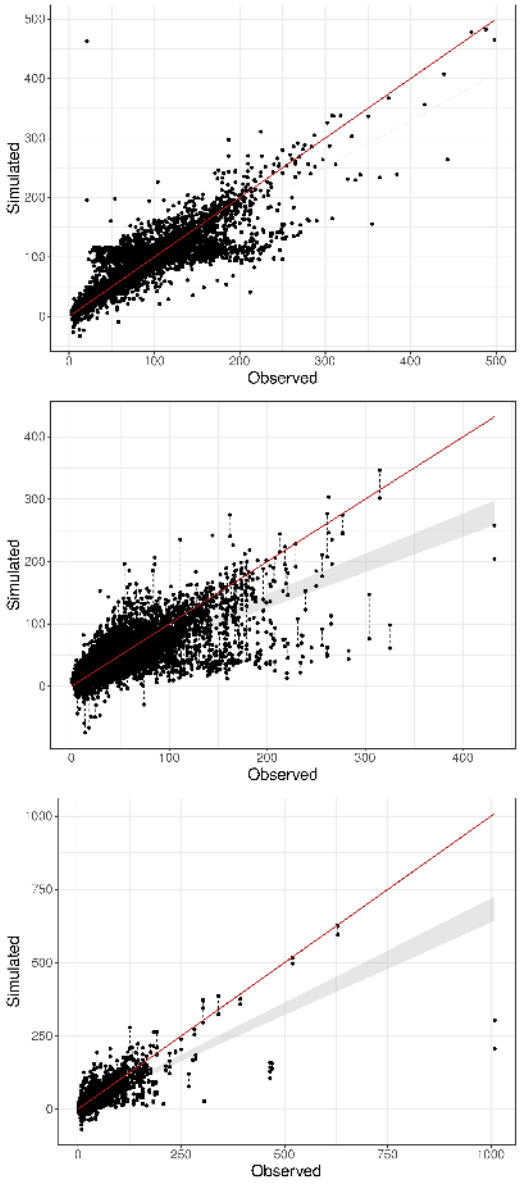

Figure C5.5: ANN model calibration scatter plots for the average water leaving reservoir on day, in m^3/s. From top to bottom: 1st Row: North reservoir; 2nd Row: West reservoir; 3rd Row: South reservoir. The elements of this plot are: The black dots represent the simulated (y-axis) versus observed (x-axis) values; The black dashed lines are the range of simulated values; The red solid line indicates a perfect of observed values, and; The shaded area represents the range of the linear regression between the simulated and the observed values.

calibration of the ANN model, as both models communicate and exchange information throughout the hydrological simulations. Similarly to the calibration process of the coupled SWAT-ANN model as described in Chapter 3, the worked presented in this chapter makes use of the SWAT-CUP and the SUFI2 algorithm as a support tool for the calibration procedure of the SWAT model [1]. The number of iterations for each calibration cycle ranges from 300 to 500, whereas the first calibration cycle always runs 500 iterations. The final results of calibration procedure of the coupled SWAT-ANN model are presented in Table C5.6.

Table C5.6: SWAT-ANN model calibration results.

Sub-basin	Stream Gauge	Dataset	R2	NSE	PBIAS
01	83345000	Calibration	0.746	0.538	-21.538
		Validation	0.681	0.428	-27.303
02	83675000	Calibration	0.783	0.723	-08.088
		Validation	0.686	0.584	-12.471
04	83660000	Calibration	0.872	0.669	-19.161
		Validation	0.749	0.447	-25.810
13	83800002	Calibration	0.750	0.576	-04.043
		Validation	0.746	0.488	-04.578
14	83840000	Calibration	0.943	0.799	-07.604
		Validation	0.941	0.599	-13.165
15	83870000	Calibration	0.831	0.509	07.698
		Validation	0.866	0.518	07.681
17	83029900	Calibration	0.566	0.363	-20.860
		Validation	0.544	0.292	-23.967
20	83440000	Calibration	0.652	0.576	-14.848
		Validation	0.605	0.514	-15.400
22	83520000	Calibration	0.740	0.648	-13.995
		Validation	0.709	0.599	-15.764
29	83900000	Calibration	0.836	0.760	-06.971
		Validation	0.834	0.745	-07.698
30	83300200	Calibration	0.778	0.715	-05.836
		Validation	0.656	0.569	-06.450
35	83892998	Calibration	0.672	0.525	-08.546
		Validation	0.642	0.475	-09.741
36	83892990	Calibration	0.652	0.585	-04.344
		Validation	0.561	0.503	-04.993

The results shown in Table C5.6 suggest that, apart from a few sub-basins, the coupled SWAT-ANN is capable of reproducing the rainfall-runoff process of the IRW. Some sub-basins, however, fail to achieve a minimum efficiency threshold value for the validation dataset, such as the sub-basin number 17. Most sub-basins

(i.e. 8 out of 13), however, show adequate validation values, while 4 out of 13 sub-basins show results that are relatively close to the validation threshold. In general, when considered as a whole hydrological unit, the calibration of the coupled SWAT-ANN model can be considered as satisfactory, as the overall NSE value is 0.533 and the PBIAS value is -5.282, both in approximate values.

Differently from the under-estimation behaviour of the ANN (see Table C5.5 and Figure C5.5), the calibration results of the coupled SWAT-ANN model clearly indicate a tendency to over-predict the IRW channel's streamflow, as revealed by the negative PBIAS values summarised in Table C5.6. However, even if the coupled SWAT-ANN model systematically over predicts the IRW's streamflow, its overall PBIAS is considered as an acceptable value, reinforcing the notion that the proposed coupled SWAT-ANN model is a valid tool to be applied for the simulation of the rainfall-runoff process in the study area.

5.3.3 Climate Change

Aiming at the identification of how climate change might affect river floods in the IRW and following the proposed methodological framework (see Sub-Section 5.2.4), the next step consists in the performing the flood frequency analysis of the simulation results. Figure C5.6 summarises the results of the fitted Gumbel distribution function to the streamflow data as simulated by the coupled SWAT-ANN model during the period of 1992 and 2012. Table C5.7, instead, presents the comparison between different flood return periods and the considered climate change scenarios, while also displaying the baseline historical scenario for reference.

The results shown in Table C5.7 indicate no clear trend in the rainfall-runoff process of the IRW for the simulation period between 2010 and 2040. However, some results are rather interesting: while the results of the GCM CCSM4 indicates a decrease of, approximately, 28% in the 100-year flood return period for the simulation period of 2010-2030, between the next simulation period (i.e. 2020-2040), the signal is inverted, suggesting an increase of, approximately, 22% in the 100-year flood return period. This behaviour is attributed to the fact that during the decade between 2030 and 2040, the years of 2031 and 2036 are simulated

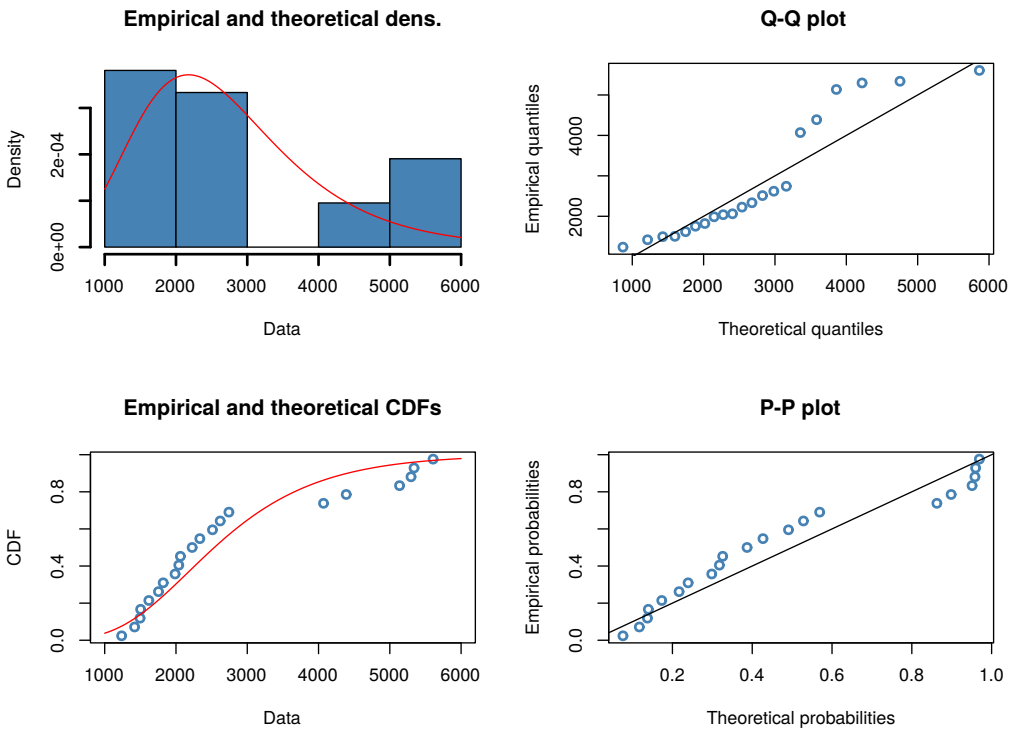

Figure C5.6: Fitted Gumbel distribution to the simulated SWAT flow data, in m^3/s, during the simulation period between the years 1992 and 2012. The resulting parameters of the fitted distribution are: $\mu = 2174.9$ and $\sigma = 990.3$, where μ is the location parameter and σ is the scale parameter of the Gumbel distribution.

Table C5.7: Flood return period for the IRW, for RCP 4.5.

		Flood Return Period			
Simulation Scenario	**Period**	**100 years**	**50 years**	**10 years**	**5 years**
Historical	1992-2012	6730.3	6038.9	4403.4	3660.3
CCSM4	2010-2030	4874.1	4389.5	3243.3	2722.4
	2020-2040	8242.5	7296.3	5058.4	4041.5
CSIRO-Mk3-6-0	2010-2030	5743.3	5109.7	3611.0	2930.0
	2020-2040	5128.3	4556.7	3204.8	2590.5
GFDL-ESM2M	2010-2030	6664.4	5864.6	3972.7	3113.0
	2020-2040	5862.3	5198.9	3629.5	2916.5
MPI-ESM-MR	2010-2030	5626.1	4991.8	3491.3	2809.5
	2020-2040	7107.7	6294.0	4369.1	3494.6

as very wet years, resulting in large streamflow forecasts. The same behaviour is observed for the GCM MPI-ESM-MR, predicting a decrease 100-year flood return period for the simulation period of 2010-2030, while suggesting an increased 100-year flood return period for the next 2 decades period. The results for the other two GCMs, however, suggest a slight decrease in the intensity of flood events in the IRW for the whole simulation period (i.e. 2010-2040).

5.4 Conclusions

River floods are one of the most devastating natural hazards worldwide, being also one of the main concerns of river basin managers. Several structural measures have been implement in watersheds around the globe to manage the risks of flood events, such as flood control dams and destination of specific areas to attenuate flood hazards. Structural measures aim at the reduction of flood hazards by managing the streamflow in rivers and streams in a watershed, hence affecting the rainfall-runoff process of a river basin. One of the main challenge of river basin managers pertains to how quantify the management of these structures on the long-term, such as under the effects of climate change. Based on such motivation, this chapter has proposed a methodological framework, based on the definition of risk as provided by the SREX and on the KULTURisk framework, to quantify and characterise river flood hazards. Moreover, exploring the expertise acquired from the previous chapters, the proposed framework relies on the usage of the coupled SWAT-ANN model for the computation of the rainfall-runoff processes under dynamic hydro-meteorological conditions, while expanding the framework to incorporate an hydraulic model aiming at the spatial characterisation of flood events. In order to verify the validity of the assumptions behind the drawing of the proposed methodological framework, this chapter explores the applicability of the coupled SWAT-ANN model to simulate the rainfall-runoff process of the IRW. Specifically, the ANN model is utilised as a tool capable of simulating the dynamic artificially-controlled outflow of the three major flood control dams in the study area, while the SWAT model accounts for the physical basis of the rainfall-runoff process.

The results obtained in this chapter suggest that the coupling of both modelling techniques provides a very useful instrument for the long-term analysis of dynamic watershed management actions under varying hydro-meteorological conditions. The physically-based information passed from the SWAT model to the ANN enables the latter to accurately estimate the outflows of the three major flood control dams in the study area, while, at the same time, maintaining physical consistency due to the direct coupling with a physically-based hydrological model. The ANN model, however, consistently under-predicts the outflows of the considered flood control dams, a behaviour that is attributed to the nature of ANN models, as these models require a large amount of data for their training, resulting in a general lack of training examples for extreme conditions. This same behaviour is verified and explored in Chapter 2.

The results obtained from the flood frequency analysis under future climate conditions indicate no clear trends in the flood intensity and frequency in the study area. The results obtained point in the direction of an increased range of possibilities as further in the future the simulation goes, however. While all results suggest a decrease in the intensity of flood episodes in the IRW during the decades between 2010 and 2030, two out of four GCMs indicate the opposite behaviour for the simulation period between 2020 and 2040. This result is attributed to the fact that during this period, two year are predicted to be exceptionally wet, intensifying the rainfall-runoff process in the study area.

As a recommendation for further studies, it is proposed the consideration of the incorporation of the socio-economic dimension in the long-term analysis of climate change impacts over the study area. As socio-economic drivers can determine the preference of people or groups of people, the consideration of the socio-economic dimension can add depth to a similar research, allowing the computation of effects on the regional hydrologic cycle as coming from dynamic land-cover and land-use. Moreover, the socio-economic dimension might also play a significant role in the management of the outflow from the three studied flood control dams, as secondary usage of water stored in flood control reservoirs is to supply water for crops in irrigation schemes. Another recommendation would be the consideration of another RCP scenario, such as the 8.5, to increase the range of possible future hydro-meteorological conditions. Moreover, a larger future

simulation period is also welcomed.

Acknowledgements

The author is thankful and acknowledge the fact that the work presented in this chapter was only possible due to the utilisation of the climate data provided by the NEX-DCP30 database, a climate database prepared by the Climate Analytics Group and NASA Ames Research Center using the NASA Earth Exchange, and distributed by the NASA Center for Climate Simulation – NCCS.

References

[1] Abbaspour, K. C., 2014. SWAT-CUP 2012: SWAT Calibration and Uncertainty Programs - A User Manual. Tech. rep.

[2] Ackerman, P. E. C. T., 2009. HEC-GeoRAS: GIS Tools for Support of HEC-RAS using ArcGIS®. Tech. Rep. September, US Army Corps of Engineers. Hydrologic Engineering Center.

[3] Alcamo, J., Vörösmarty, C. J., Naiman, R. J., Lettenmaier, D. P., Pahl-Wostl, C., 2008. A grand challenge for freshwater research: understanding the global water system. Environmental Research Letters 3 (1), 010202.

[4] ANA, A. N. d. Á., 2014. HidroWeb - Sistema de Informações Hidrológicas. URL http://hidroweb.ana.gov.br/default.asp

[5] Arnold, J. G., Srinivasan, R., Muttiah, R. S., Williams, J. R., 1998. Large Area Hydrologic Modeling and Assessment Part I: Model Development. Journal of the American Water Resources Association 34 (1), 73–89.

[6] Brooks, K. N., Ffolliott, P. F., Magner, J. A., 2013. Hydrology and the Management of Watersheds, 4th Edition. John Wiley & Sons, Inc., Iowa, USA.

[7] Brouwer, R., Akter, S., Brander, L., Haque, E., 2007. Socioeconomic vulnerability and adaptation to environmental risk: A case study of climate change and flooding in Bangladesh. Risk Analysis 27 (2), 313–326.

[8] Campolo, M., Soldati, A., Andreussi, P., 2003. Artificial neural network approach to flood forecasting in the River Arno. Hydrological Sciences Journal 48 (June), 381–398.

[9] Cutter, S. L., Boruff, B. J., Shirley, W. L., 2003. Social vulnerability to environmental hazards. Social Science Quarterly 84 (2), 242–261.

[10] Di Baldassarre, G., Viglione, A., Carr, G., Kuil, L., Salinas, J. L., Blöschl, G., 2013. Socio-hydrology: Conceptualising human-flood interactions. Hydrology and Earth System Sciences 17 (8), 3295–3303.

[11] dos Santos, E. T., 2013. Impactos Econômicos de Desastres Naturais e Megacidades: O Caso dos Alagamentos em São Paulo. Msc. thesis, University of São Paulo.

[12] Douben, K. J., 2006. Characteristics of river floods and flooding: A global overview, 1985-2003. Irrigation and Drainage 55 (SUPPL. 1), 25–27.

[13] EEA, E. E. A., 2010. Mapping the impacts of natural hazards and technological accidents in Europe. An overview of the last decade. Tech. Rep. 13.

[14] EU, T. E. P., the Council of the European Union, 2007. Directive 2007/60/EC of the European Parliament and of The Council of 23 October 2007 on the Assessment and Management of Flood Risks. Official Journal of the European Union L 288/27 (2455), 1–8.

[15] EXCIMAP, E. E. C. o. F. M., 2007. Handbook on good practices for flood mapping in Europe. Tech. rep.

[16] Falloon, P., Challinor, A., Dessai, S., Hoang, L., Johnson, J., Koehler, A.-K., 2014. Ensembles and uncertainty in climate change impacts. Frontiers in Environmental Science 2 (July), 1–7.

[17] Fankhauser, S., McDermott, T. K. J., 2014. Understanding the adaptation deficit: Why are poor countries more vulnerable to climate events than rich countries? Global Environmental Change 27 (1), 9–18.

[18] Feyen, L., Watkiss, P., 2011. Technical Policy Briefing Note 3. The Impacts and Economic Costs of River Floods in Europe, and the Costs and Benefits of Adaptation. Summary of Sector Results from the ClimateCost Project, funded by the European Community's Seventh Framework Programme. Tech. Rep. 4.

[19] Fowler, H. J., Ekström, M., 2009. Multi-model ensemble estimates of climate change impacts on UK seasonal precipitation extremes. International Journal of Climatology 29 (January 2009), 385–416.

[20] Garcia, S. R., 2006. O Fenômeno El Niño/Oscilação Sul e seus Efeitos na América do Sul. Trabalho do curso Evolução dos Conceitos Meteorológicos ministrado pelo Prof. Dr. Vadlamudi Brahmananda Rao. Tech. rep., Ministério Da Ciência e Tecnologia, Instituto Nacional de Pesquisas Espaciais - INPE.

[21] Githui, F., Gitau, W., Mutuab, F., Bauwens, W., 2009. Climate change impact on SWAT simulated streamflow in western Kenya. International Journal of Climatology 29, 1823–1834.

[22] Giupponi, C., Mojtahed, V., Gain, A. K., Balbi, S., 2013. Integrated Assessment of Natural Hazards and Climate Change Adaptation: I . The KULTURisk Methodological Framework.

[23] Hirabayashi, Y., Mahendran, R., Koirala, S., Konoshima, L., Yamazaki, D., Watanabe, S., Kim, H., Kanae, S., 2013. Global flood risk under climate change. Nature Climate Change 3 (June), 816–821.

[24] Horner, C., 2016. Introduction to HEC-RAS. Colorado State University College of Engineering.
URL http://www.engr.colostate.edu/{~}pierre/ce{_}old/classes/CIVE401/GuestLectures2016/IntroductiontoHEC-RAS.pdf

[25] IPCC, 2012. Summary for Policymakers. No. November. Cambridge University Press, Cambridge, United Kingdom and New York, NY, USA.

[26] Jha, M., Arnold, J. G., Gassman, P. W., Giorgi, F., Gu, R. R., 2006. Climate change sensitivity assessment on Upper Mississippi River Basin streamflows using SWAT. Journal of the American Water Resources Association 42 (4), 997–1016.

[27] Jongman, B., Kreibich, H., Apel, H., Barredo, J. I., Bates, P. D., Feyen, L., Gericke, A., Neal, J., Aerts, J. C. J. H., Ward, P. J., 2012. Comparative flood damage model assessment: Towards a European approach. Natural Hazards and Earth System Science 12 (12), 3733–3752.

[28] Jongman, B., Ward, P. J., Aerts, J. C. J. H., 2012. Global exposure to river and coastal flooding: Long term trends and changes. Global Environmental Change 22 (4), 823–835.

[29] Jonkman, S. N., 2005. Global Perspectives on Loss of Human Life Caused by Floods. Natural Hazards 34 (2), 151–175.

[30] Knebl, M. R., Yang, Z. L., Hutchison, K., Maidment, D. R., 2005. Regional scale flood modeling using NEXRAD rainfall, GIS, and HEC-HMS/ RAS: A case study for the San Antonio River Basin Summer 2002 storm event. Journal of Environmental Management 75 (4 SPEC. ISS.), 325–336.

[31] Li, Z., Liu, W.-z., Zhang, X.-c., Zheng, F.-l., 2009. Impacts of land use change and climate variability on hydrology in an agricultural catchment on the Loess Plateau of China. Journal of Hydrology 377 (1-2), 35–42.

[32] Lin, J. L., 2007. Interdecadal variability of ENSO in 21 IPCC AR4 coupled GCMs. Geophysical Research Letters 34 (12), 1–6.

[33] Llopart, M., Coppola, E., Giorgi, F., da Rocha, R. P., Cuadra, S. V., 2014. Climate change impact on precipitation for the Amazon and La Plata basins. Climatic Change 125 (1), 111–125.

[34] Long, S., Fatoyinbo, T. E., Policelli, F., 2014. Flood extent mapping for Namibia using change detection and thresholding with SAR. Environmental Research Letters 9 (3), 035002.

[35] Lugeri, N., Kundzewicz, Z. W., Genovese, E., Hochrainer, S., Radziejewski, M., 2010. River flood risk and adaptation in Europe—assessment of the present status. Mitigation and Adaptation Strategies for Global Change 15 (7), 621–639.

[36] Mango, L. M., Melesse, A. M., McClain, M. E., Gann, D., Setegn, S. G., 2011. Land use and climate change impacts on the hydrology of the upper Mara River Basin, Kenya: Results of a modeling study to support better resource management. Hydrology & Earth System Sciences 15 (7), 2245–2258.

[37] Masozera, M., Bailey, M., Kerchner, C., 2007. Distribution of impacts of natural disasters across income groups: A case study of New Orleans. Ecological Economics 63 (2-3), 299–306.

[38] Merwade, V., Olivera, F., Arabi, M., Edleman, S., 2008. Uncertainty in Flood Inundation Mapping: Current Issues and Future Directions. Journal of Hydrologic Engineering 13, 608–620.

[39] Messner, F., Meyer, V., 2006. Flood Damage, Vulnerability and Risk Perception: Challenges for Flood Damage Research. In: Schanze, J., Zeman, E., Marsalek, J. (Eds.), Flood Risk Management: Hazards, Vulnerability and Mitigation Measures. Springer Netherlands, Dordrecht, NL, Ch. 13, pp. 149–167.

[40] Mitterstein, M. R., Severo, D. L., 2007. Análise de variabilidade intrasazonal e interanual da precipitação no vale do Itajaí com a transformada de ondaletas. Dynamis Revista Tecno-Científica 13 (1), 1–10.

[41] Neiff, J. J., Mendiondo, E. M., Depettris, C. a., 2000. ENSO floods on river ecosystems: from catastrophes to myths. In: Proceedings - 1st International Symposium on Flood Defence. pp. 1–12.

[42] Neitsch, S. L., Arnold, J. G., Kiniry, J. R., Williams, J. R., 2011. Soil & Water Assessment Tool Theoretical Documentation. Version 2009. Tech. Rep. TR-406, Texas A&M AgriLife, USDA Agricultural Rsearch Service, College Station, TX, USA.

[43] Nijssen, B., O'Donnell, G. M., Hamlet, A. F., Lettenmaier, D. P., 2001. Hydrologic Sensitivity of Global Rivers to Climate Change. Climatic Change 50, 143–175.

[44] NOAA, 2013. United States Flood Loss Report - Water Year 2011. Tech. rep.

[45] Palmer, P. I., Smith, M. J., 2014. Model human adaptation to climate change. Nature 512 (August), 365–366.

[46] Pistocchi, A., Mazzoli, P. a., 2002. Use of HEC-RAS and HEC-HMS models with ArcView for hydrologic risk management. In: Proceedings - 2012 International Congress on Environmental Modelling and Software. pp. 305–310.

[47] Pourali, S. H., Arrowsmith, C., Chrisman, N., Matkan, A. A., Mitchell, D., 2014. Topography Wetness Index Application in Flood-Risk-Based Land Use Planning. Applied Spatial Analysis and Policy.

[48] Rivera, S., Hernandez, A. J., Ramsey, R. D., 2007. Predicting flood hazard areas: A SWAT and HEC-RAS simulations conducted in Aguan river basin of Honduras, Central America. In: ASPRS 2007 Annual Conference. No. May 2007. Tampa, FL, US, p. 11.

[49] Ronco, P., Gallina, V., Torresan, S., Zabeo, A., Semenzin, E., Critto, A., Marcomini, A., 2014. The KULTURisk Regional Risk Assessment methodology for water-related natural hazards - Part 1: Physical-environmental assessment. Hydrology and Earth System Sciences 18 (12), 5399–5414.

[50] Ruin, I., Creutin, J. D., Anquetin, S., Lutoff, C., 2008. Human exposure to flash floods - Relation between flood parameters and human vulnerability

during a storm of September 2002 in Southern France. Journal of Hydrology 361 (1-2), 199–213.

[51] Scawthorn, C., Flores, P., Blais, N., Seligson, H., Tate, E., Chang, S., Mifflin, E., Thomas, W., Murphy, J., Jones, C., Lawrence, M., 2006. HAZUS-MH Flood Loss Estimation Methodology. I: Overview and Flood Hazard Characterization. Natural Hazards Review 7 (2), 72–81.

[52] Schumann, A. H., 2011. Flood risk assessment and management: How to specify hydrological loads, their consequences and uncertainties. Springer Science, Business Media, Bochum, Germany.

[53] Sivapalan, M., Savenije, H. H. G., Blöschl, G., 2012. Socio-hydrology: A new science of people and water. Hydrological Processes 26 (8), 1270–1276.

[54] Stocker, T. F., Dahe, Q., Plattner, G.-K., Alexander, L. V., Allen, S. K., Bindoff, N. L., Bréon, F.-M., Church, J. A., Cubash, U., Emori, S., Forster, P., Friedlingstein, P., Talley, L. D., Vaughan, D. G., Xie, S.-P., 2013. Technical Summary. In: Stocker, T., Qin, D., Plattner, G.-K., Tignor, M., Allen, S., Boschung, J., Nauels, A., Y. Xia, V. B., Midgley, P. (Eds.), Climate Change 2013: The Physical Science Basis. Contribution of Working Group I to the Fifth Assessment Report of the Intergovernmental Panel on Climate Change. Cambridge University Press, Cambridge, United Kingdom and New York, NY, USA., Ch. Tec. Summ., pp. 33–115.

[55] Tate, E., 1999. Introduction to HEC-RAS. Department of Civil, Architectural and Environmental Engineering. The University of Texas at Austin.
URL http://www.ce.utexas.edu/prof/maidment/grad/tate/research/RASExercise/webfiles/hecras.html

[56] Tebaldi, C., Knutti, R., Allen, M., Stott, P., Mitchell, J., Schnur, R., Delworth, T., Andronova, N., Schlesinger, M., Annan, J., Hargreaves, J., Edwards, N., Marsh, R., Annan, J., Hargreaves, J., Ohgaito, R., Abe-Ouchi, A., Emori, S., Benestad, R., Berger, J., Bryan, F., Danabasoglu, G., Nakashiki, N., Yoshida, Y., Kim, D.-H., Tsutsui, J., Cantelaube, P., Terres, J.-M., Collins, M., Booth, B., Harris, G., Murphy, J., Sexton, D., Webb,

M., Dettinger, M., Doblas-Reyes, F., Pavan, V., Stephenson, D., Evensen, G., Evensen, G., Forest, C., Stone, P., Sokolov, A., Allen, M., Webster, M., Forest, C., Stone, P., Sokolov, A., Frame, D., Booth, B., Kettleborough, J., Stainforth, D., Gregory, J., Collins, M., Allen, M., Gates, W., Gent, P., McWilliams, J., Gent, P., Willebrand, J., McDougall, T., McWilliams, J., Gillett, N., Zwiers, F., Weaver, A., Hegerl, G., Allen, M., Stott, P., Giorgi, F., Francisco, R., Giorgi, F., Mearns, L., Giorgi, F., Mearns, L., Goldstein, M., Rougier, J., Greene, A., Goddard, L., Lall, U., Hagedorn, R., Doblas-Reyes, F., Palmer, T., Hegerl, G., Crowley, T., Hyde, W., Frame, D., Houghton, J., Ding, Y., Griggs, D., Noguer, M., van der Linden, P., Xiaosu, D., Dai, X., Maskell, K., Johnson, C., Kiehl, J., Shields, C., Knutti, R., Stocker, T., Joos, F., Plattner, G.-K., Knutti, R., Stocker, T., Joos, F., Plattner, G.-K., Knutti, R., Joos, F., Müller, S., Plattner, G.-K., Stocker, T., Knutti, R., Meehl, G., Allen, M., Stainforth, D., Krishnamurti, T., Kishtawal, C., Zhang, Z., Larow, T., Bachiochi, D., Williford, E., Gadgil, S., Surendran, S., Lambert, S., Boer, G., Lopez, A., Tebaldi, C., New, M., Stainforth, D., Allen, M., Kettleborough, J., Luo, Q., Jones, R., Williams, M., Bryan, B., Bellotti, W., Meehl, G., Boer, G., Covey, C., Latif, M., Stouffer, R., Meinshausen, M., Min, S.-K., Hense, A., Murphy, J., Sexton, D., Barnett, D., Jones, G., Webb, M., Collins, M., Stainforth, D., Nakićenović, N., Nychka, D., Tebaldi, C., Otto-Bliesner, B., Brady, E., Clauzet, G., Tomas, R., Levis, S., Kothavala, Z., Palmer, T., Palmer, T., Räisänen, J., Palmer, T., Shutts, G., Hagedorn, R., Doblas-Reyes, F., Jung, T., Leutbecher, M., Palmer, T., Doblas-Reyes, F., Hagedorn, R., Weisheimer, A., Piani, C., Frame, D., Stainforth, D., Allen, M., Räisänen, J., Räisänen, J., Palmer, T., Redi, M., Robertson, A., Lall, U., Zebiak, S., Goddard, L., Schneider, S., Stainforth, D., Stott, P., Kettleborough, J., Tebaldi, C., Mearns, L., Nychka, D., Smith, R., Tebaldi, C., Smith, R., Nychka, D., Mearns, L., Thomson, M., Doblas-Reyes, F., Mason, S., Hagedorn, R., Connor, S., Phindela, T., Morse, A., Palmer, T., von Deimling, T., Held, H., Ganopolski, A., Rahmstorf, S., Wigley, T., Raper, S., Wild, M., Wild, M., Long, C., Ohmura, A., Yun, W., Stefanova, L., Krishnamurti, T., 2007. The use of the multi-model ensemble in probabilistic climate projections. Philosophical transactions of the Royal Society. Series

A, Mathematical, physical, and engineering sciences 365 (1857), 2053–75. URL http://www.ncbi.nlm.nih.gov/pubmed/17569654

[57] Thieken, a. H., Ackermann, V., Elmer, F., Kreibich, H., Kuhlmann, B., Kunert, U., Maiwald, H., Merz, B., Müller, M., Piroth, K., Schwarz, J., Schwarze, R., Seifert, I., Seifert, J., 2009. Methods for the evaluation of direct and indirect flood losses. In: RIMAX Contributions at the 4th International Symposium on Flood Defence (ISFD4). pp. 1–10.

[58] Trasher, B., Xiong, J., Wang, W., Melton, F., Michaelis, A., Nemani, R., 2013. New downscaled climate projections suitable for resource management in the U.S. NEX-DCP30: Downscaled 30 Arc-Second CMIP5 Climate Projections for Studies of Climate Change Impacts in the United States 1 . Intent of This Document and POC.

[59] US Army Corps of Engineers, 2010. HEC-RAS River Analysis System. Tech. Rep. January, Institute for Water Resources, Davis, CA.

[60] Van Der Knijff, J. M., De Roo, A., 2008. LISFLOOD - Distributed Water Balance and Flood Simulation Model - Revised User Manual. Tech. rep., JRC Scientific and Technical Reports.

[61] Van Der Knijff, J. M., Younis, J., De Roo, a. P. J., 2010. LISFLOOD: a GIS-based distributed model for river basin scale water balance and flood simulation. International Journal of Geographical Information Science 24 (2), 189–212.

[62] Varanou, E., Gkouvatsou, E., Baltas, E., Mimikou, M., 2002. Quantity and Quality Integrated Catchment Modeling under Climate Change with use of Soil and Water Assessment Tool Model. Journal of Hydrologic Engineering 7 (3), 228–244.

[63] Ward, P. J., Eisner, S., Flo Rke, M., Dettinger, M. D., Kummu, M., 2014. Annual flood sensitivities to El Niño-Southern Oscillation at the global scale. Hydrology and Earth System Sciences 18, 47–66.

[64] WRI, W. R. I., 2017. AQUEDUCT Global Flood Analyzer. Partners: Deltares, VU IVM Institute for Environmental Studies, Universiteit Utrecht, PBI, Netherlands Environmental Assessment Agency.
URL http://floods.wri.org/{#}

[65] Zhang, X., Srinivasan, R., Hao, F., 2007. Predicting hydrologic response to climate change in the Luohe river Basin using the SWAT model. American Society of Agricultural and Biological Engineers 500 (3), 901–310.

[66] Zwenzner, H., Voigt, S., 2008. Improved estimation of flood parameters by combining space based SAR data with very high resolution digital elevation data. Hydrology and Earth System Sciences Discussions 5 (5), 2951–2973.

Conclusions

Anthropogenic activities are a major forcing capable of shaping and altering regional and global processes. Indeed, the Anthropocene, the era in which we are all currently living in, is the result of unprecedented human actions on the natural environment, and the idea of integration has never been more contemporary. Human and natural systems are not isolated compartments, linked only by flow of material and energy among them, but instead components of an evolving, integrated entity. This a relatively new concept in the scientific community, thereby requiring the development of new concepts and sciences. In hydrology, for instance, the new concept of *global water systems* has been developed, while the new science of *socio-hydrology* has been proposed. Interesting to notice is the fact that, although born inside a community of predominantly hydrologists, both novel terms move away from their pure-hydrologic background, shifting closer to an interdisciplinary and integrative approach.

Hence, based on such background, the work presented in this dissertation has, in general terms, explored the possibility of using technologies deriving from machine learning coupled with physically-based hydrologic models as a way of better capturing possible effects coming from dynamic human-nature systems capable of affecting the regional hydrologic cycle of a watershed, and, ultimately, supporting the development of WMPs. Specifically, specific human management actions are considered to be interlinked and interdependent with the hydrologic and climatic systems, following the notion of WRSs, resulting in the contemplation of the relationships among these processes as a fundamental factor to be considered when stressed by hydro-meteorological and under long-term analysis. Mathematically, this is translated in the computationally coupling of

both modelling techniques, resulting in a hybrid model founded by physically-representative concepts, coming directly from the physically-based model, while, at the same time, capable of learning, as the result of a contribution from the machine learning module. The selected models utilised throughout this dissertation are the SWAT model, as the physically-based component, and an ANN model, as the machine learning module, resulting in a model referred to as SWAT-ANN model.

The first step taken in order to implement the proposed overall methodology was on exploring the current limitations of both models, i.e. the SWAT model and the ANN technology. Chapter 1, then, reviewed basic concepts related to IWM in general and hydrologic modelling in particular, moving to an introduction of the SWAT model. Three limitations were identified coming from the application of the SWAT model in a context of long-term analysis and climate change, namely: i. The lacking ability to account for a dynamic effect of increased atmospheric CO_2 concentration on the regional hydrologic cycle and on plant growth; ii. The inaccurate account of irrigation efficiency, particularly with regards to the amount of water that is extracted from the source, and; iii. The inability to dynamically account for alternative adaptive management actions under pressures coming from diverse hydro-meteorological conditions and under long-term considerations. Each identified SWAT model's limitation is then individually addressed by specific modifications proposed in the SWAT source code. The chapter concludes by presenting an overall description of the two case study sites that are explored throughout this dissertation.

Moving on to evaluate the possibility of coupling the SWAT and the ANN models, Chapter 2 focused on introducing the capabilities of the developed ANN model and on exploring the intrinsic uncertainties of ANNs in general when applied in a context of regional hydrologic modelling. Applied for the short-term forecasting of the stream stage of the IRW, the work presented in Chapter 2 concludes that the developed ANN performs well for the specific hydrologic problem to which it was applied, while identifying that a significant parcel of the overall uncertainties affecting the performance capability of ANN models comes from the composition and quality of the input data. Moreover, the initialisation of ANN models, the model structure, and the model architecture

also play a significant role in determining the overall performance of ANN models. Specifically for the proposed case study, it is found that precipitation is the main exogenous variable driving the forecasting of the stream stage in the study area, while endogenous information (i.e. observed stream stage) is capable of adding consistency to the process of forecasting the stream stage of the IRW. As a way of handling uncertainties, this chapter proposed the utilisation of an ensemble of best-calibrated ANN models, thereby accounting for errors and uncertainties that are intrinsic to the ANN model and also to the process being simulated.

Even if actions are taken to manage the uncertainties of ANN models (as proposed in Chapter 2), in essence this modelling technique is still a *"black-box"*. This issue grows larger as the uncertainties of different processes are summed up with the intrinsic uncertainties of ANN models, such as in a context of climate change and long-term analysis. Hence, building upon the introductory discussion in Chapter 1 and on the applicability of ANN models as demonstrated in Chapter 2, Chapter 3 proposed the use of physically-based modelling techniques coupled with ANN models as a way of reducing the degree of empiricism of ANN models, while, at the same time, exploring its utilisation as a method capable of simulating complex dynamic hydraulic management operations in a highly modified watershed, the VLW. Taking advantage of the interesting scenery offered by the Italian case study, the framework proposed in this chapter seeks to address one of the main challenges in conducting hydrologic simulations in the VLW area: the total external hydraulic contributions affecting the overall hydrology of the VLW. Two are the main sources of external hydraulic loadings considered in the study presented in this chapter: IGF and artificially controlled superficial streamflow deviated from/to bordering watersheds. Based on the results presented in this chapter, it is concluded that the coupling of the SWAT model (as a tool capable of simulating the hydrologic process occurring in a watershed) with the ANN model (as a tool capable of dynamically simulating the management of artificial hydraulic devices with respect to specific hydro-meteorological conditions) results in a useful and powerful instrument for supporting hydrologic modelling and IWM in general, such as for the management of artificial structures in a watershed.

Chapter 4, then, builds upon the discussions and results obtained in Chapter 3 and moves to a situation of climate change and long-term analysis. This chapter

explored the possible impacts of climate change on the agricultural sector of the VLW by evaluating, specifically, the consequences on water availability to irrigated crops in the area during the period of 2013-2050 and under the RCP 4.5. Two different irrigation scenarios are evaluated: a baseline and an adaptive. It is found that, for some crops, climate change might impacts the total amount of water required by crops yearly. Still, it is argued that improved irrigation systems can reduce the overall water withdrawals from the considered water sources while, at the same time, increase the amount of water that is made available to crops, thus increasing the general efficiency of irrigation systems. More importantly, however, is the consideration that improved irrigation systems can increase the resilience of irrigated crops to adverse climatic conditions. The work presented in Chapter 4 also strengthens the notion that the limitations of the SWAT model as introduced in Chapter 1 must be addressed before performing any kind of long-term analysis under climate change conditions. Specifically, the consideration of dynamic concentrations of CO_2 in the atmosphere is not only important to determine the final maximum yield of crops, but also their rate of evaporation, hence affecting the overall water balance of the watershed. Still, the results obtained in this chapter also point in the direction of an increased dependency on the amount of irrigation water coming from external sources to the VLW during the simulation period of 2015 to 2050. This result is attributed to two main factors, namely: the increased efficiency of irrigation applications, and the impacts of climate change on the regional hydrologic cycle of the studied watershed. Combined, both processes ultimately diminishes the rate of hydrologic processes such as baseflow and percolation, thus reducing the storage of water internal to the studied watershed. Interestingly, the explored alternative adaptation strategy of increasing investments for the improvement of irrigation systems can also offset some of the increased demand of water imported from bordering watersheds.

Finally, Chapter 5 targeted the study of how river flood risk might be affected by changing climatic conditions. Specifically, this chapter proposed a conceptual methodological framework, based on both the SREX and the KULTURisk framework, to characterise river flood hazards in a context of climate change and long-term analysis. The proposed framework is tailored for the utilisation of the coupled SWAT-ANN model (to account for the simulation of hydrologic processes

and for dynamically quantifying artificial hydraulic management actions, such as the controlled outflow of reservoirs) and the HEC-RAS model (to compute the characteristics of river flood hazard events). A main consideration of the proposed methodological framework relies on the fact that the characterisation of flood events should be stochastic rather than deterministic. To achieve such requirement, the framework proposed in Chapter 5 assumed the outputs of the SWAT-ANN model comes from an ensemble of physically-valid models, thus recognising the errors and acknowledging the uncertainties related to the simulation of the system being modelled. In order to verify the validity of the proposed methodological framework, a case study exploring how climate change might affect the rainfall-runoff process of the IRW is proposed. The results suggest that not only the developed ANN model is capable of simulating the dynamic management of the flood control dams, but that the coupling of the SWAT and the ANN models is capable of accurately simulating the rainfall-runoff process of the IRW. Still, it is not found a clear trend coming from the analysis of climate change impacts in the rainfall-runoff period in the study area.

Some final general recommendations can be made at this point, the first pertaining to the idea of improving the chosen machine learning method, particularly with regards to the training method of the ANN model. Currently, the model utilises the Levenberg-Marquardt as the supervised training algorithm. Although efficient if compared to other training algorithms, such as the steepest-descent training procedure, the Levenberg-Marquardt may become impracticable due to the computation of the inverse of the approximate Hessian matrix. Consequently, if the resulting dimension of the approximate Hessian matrix is somewhat large, the computational costs of performing this operation may render the Levenberg-Marquardt inefficient. An alternative would be the utilisation of a novel training procedure known as Neuron-By-Neuron training algorithm (see *"Wilamowski, B. M. & Irwin, J. D. The Industrial Electronics Handbook: Intelligent Systems. (CRC Press, Inc., 2011)"* for further reference).

A second recommendation pertains to the idea of incorporating the concept of stochastic hydrologic modelling also to the physically-based component (i.e.e SWAT model) in the case studies presented in Chapters 3 and 4. Indeed, as the this dissertation relies on the usage of the SWAT model as the physically-based

model responsible for the computation of most of the processes pertaining to the hydrologic cycle, the utilisation of the SWAT-CUP can provide the means required to move from a deterministic to a stochastic hydrologic modelling. The ANN model, on the other hand, is already implemented to work as a stochastic model, as shown in Chapter 2.

A last recommendation regards the possibility of interconnecting the socio-economic sphere within the hydrologic simulations. This consideration is especially relevant for the work carried out in Chapter 4 and Chapter 5, in particular due to their long-term analysis nature. For instance, a consideration of how farmers might adapt when stressed by diverse climatic conditions can be determined by using a micro-economics model capable of revealing the preferences of farmers with respect to a variety of constraints (e.g. economic and climatic).

Appendix 1 – SWAT Model

Proposed Code Modifications

This appendix chapter describes the proposed changes implemented in the SWAT model. Some changes were made in already existing SWAT sub-routines and are displayed only as differences between the original and updated files, while other changes were implemented as completely new sub-routines. As the SWAT model is developed in Fortran language, the new sub-routines were written using either the *.f* or *.f95* file extensions for compatibility purposes. This appendix chapter is sub-divided into three sections, each covering a specific proposed modification theme.

The CO_2 Fertilization Effect

ALLOCATE_PARMS.F

```
354c354
<       !!allocate (co2(msub)) !!Removed by Essenfelder, 06/10/15
---
>       allocate (co2(msub))
359,361d358
< !!    array to account for different CO2 conc. in atm. for each year
<       allocate (co2(myr)) !!Added by Essenfelder, 06/10/15
<
1810c1807
<       end
---
>       end
```

```
\ No newline at end of file
```

ETPOT.F

```
229c229
<            rc = 49. / (1.4 - 0.4 * co2(curyr) / 330.)
                                    !!Modified by Essenfelder, 06/10/15
---
>            rc = 49. / (1.4 - 0.4 * co2(hru_sub(j)) / 330.)
295,296c295,296
<      &                           * (1.4 - 0.4 * co2(curyr) / 330.))
                                    !!Modified by Essenfelder, 06/10/15
<
                                    !!to account for CO2 fert. effect
                                      due to climate change
---
>      &                           * (1.4 - 0.4 * co2(hru_sub(j)) / 330.))
>
329c329
<       end
---
>       end
\ No newline at end of file
```

GROW.F

```
194,196c194,196
<           if (co2(curyr) > 330.) then !!Modified by Essenfelder, 06/10/15
<             beadj = 100. * co2(curyr) / (co2(curyr) +
<      &              Exp(wac21(idp) - co2(curyr) * wac22(idp)))
---
>           if (co2(hru_sub(j)) > 330.) then
>             beadj = 100. * co2(hru_sub(j)) / (co2(hru_sub(j)) +
>      &              Exp(wac21(idp) - co2(hru_sub(j)) * wac22(idp)))
343c343
<       end
---
>       end
\ No newline at end of file
```

READSUB.F

```
216,217c216
<       !!read (101,*) co2(i) !!Removed by Essenfelder, 06/10/15
<       read (101,*)          !!Added by Essenfelder, 06/10/15
---
>       read (101,*) co2(i)
406c405
<       !!if (co2(i) <= 0.) co2(i) = 330. !!Removed by Essenfelder, 06/10/15
---
>       if (co2(i) <= 0.) co2(i) = 330.
473c472
<       end
---
>       end
\ No newline at end of file
```

READCO2.F

```
      subroutine readco2

!!    ~ ~ ~ PURPOSE ~ ~ ~
!!    reads in the input data for the yearly CO2 concentration

!!    ~ ~ ~ INCOMING VARIABLES ~ ~ ~
!!    name          |units          |definition
!!    ~ ~ ~ ~ ~ ~ ~ ~ ~ ~ ~ ~ ~ ~ ~ ~ ~ ~ ~ ~ ~ ~ ~ ~ ~ ~ ~ ~ ~ ~ ~ ~
!!    iyr           |year           |beginning year of simulation
!!    nbyr          |none           |number of years simulated
!!    ~ ~ ~ ~ ~ ~ ~ ~ ~ ~ ~ ~ ~ ~ ~ ~ ~ ~ ~ ~ ~ ~ ~ ~ ~ ~ ~ ~ ~ ~ ~ ~

!!    ~ ~ ~ OUTGOING VARIABLES ~ ~ ~
!!    name          |units          |definition
!!    ~ ~ ~ ~ ~ ~ ~ ~ ~ ~ ~ ~ ~ ~ ~ ~ ~ ~ ~ ~ ~ ~ ~ ~ ~ ~ ~ ~ ~ ~ ~ ~
!!    co2(:)        |ppmv           |atmospheric CO2 concentration
!!    ~ ~ ~ ~ ~ ~ ~ ~ ~ ~ ~ ~ ~ ~ ~ ~ ~ ~ ~ ~ ~ ~ ~ ~ ~ ~ ~ ~ ~ ~ ~ ~

!!    ~ ~ ~ LOCAL DEFINITIONS ~ ~ ~
!!    name          |units          |definition
!!    ~ ~ ~ ~ ~ ~ ~ ~ ~ ~ ~ ~ ~ ~ ~ ~ ~ ~ ~ ~ ~ ~ ~ ~ ~ ~ ~ ~ ~ ~ ~ ~
!!    i             |none           |counter
!!    iyear         |none           |current year being read
!!    ~ ~ ~ ~ ~ ~ ~ ~ ~ ~ ~ ~ ~ ~ ~ ~ ~ ~ ~ ~ ~ ~ ~ ~ ~ ~ ~ ~ ~ ~ ~ ~

!!    ~ ~ ~ ~ ~ ~ END SPECIFICATIONS ~ ~ ~ ~ ~ ~

      use parm
      implicit none
```

```
      integer :: ii, iyear


!!    initialize variables
      ii = 0
      iyear = 0

!!    open co2.dat file
      open (330,file="co2.txt")

!!    skip first line
      read (330,*)

!!    read co2.dat file and attribute co2 concentrations to co2(:) array
      do
        read (330,3301) iyear, co2(1)
                !! check if year is = to beginning year of simulation
          if (iyear == iyr) then
                    do ii = 2, nbyr
                          read (330,3301) iyear, co2(ii)
                        end do
                        exit
                  end if
      end do

!!    close the co2.dat file
      close (330)

3301  format (i4,f6.2)

      return

      end
```

The Irrigation Process

ALLOCATE_PARMS.F

```
230,231d229
<       allocate (lird(mhru))  !!Included by Essenfelder, 01/10/15
<       allocate (tird(mhru))  !!Included by Essenfelder, 01/10/15
886,888d883
<       allocate (alirr(mhru)) !!Included by Essenfelder, 01/10/15
<       allocate (aqirr(mhru)) !!Included by Essenfelder, 01/10/15
<       allocate (atirr(mhru)) !!Included by Essenfelder, 01/10/15
```

```
1812c1807
<       end
---
>       end
\ No newline at end of file
```

IRRIGATE.F

```
1c1
<       subroutine irrigate(flag, j, volmm)
---
>       subroutine irrigate(jj,volmm)
10,17c10
< !!                                    |applied to HRU that sums up to sol_sw
< !!    alirr(:)     |mm H2O            |average annual amount of irrigation H2O
< !!                                    |applied to HRU that is lost due to
< !!                                    |application efficiency
< !!    aqirr(:)     |mm H2O            |average annual amount of irrigation H2O
< !!                                    |applied to HRU that returns to runoff
< !!    tird(:)      |mm H2O            |total average annual amount of irr.
< !!                                    |water applied to HRU on current day
---
> !!                                    |applied to HRU
21,26d13
< !!    irrefm(:)    |none              |irrigation efficiency - schedule irr
< !!    irr_eff(:)   |none              |irrigation efficiency - auto-irr.
< !!    irrsq(:)     |none              |fraction of total applied irr water
< !!                                    |that is lost as runoff - schedule irr
< !!    irr_asq(:)   |none              |fraction of total applied irr water
< !!                                    |that is lost as runoff - auto-irrigation
29d15
< !!    shallst(:)   |mm H2O            |depth of water in shallow aquifer
35c21
< !!    hrumono(22,:)|mm H2O            |amount of irr. water applied to HRU
---
> !!    hrumono(22,:)|mm H2O            |amount of irr. water applied to HRU
43,59c29,31
< !!                                    |applied to HRU that sums up to sol_sw
< !!    alirr(:)     |mm H2O            |average annual amount of irr. water
< !!                                    |applied to HRU that is lost due to
< !!                                    |application efficiency
< !!    aqirr(:)     |mm H2O            |average annual amount of irr. water
< !!                                    |applied to HRU that returns to runoff
< !!    tird(:)      |mm H2O            |total average annual amount of irr.
< !!                                    |water applied to HRU on current day
< !!    aird(:)      |mm H2O            |amount of irrigation water applied to
< !!                                    |HRU on curr. day that sums up to sol_sw
```

```
< !!    iird(:)      |mm H2O          |amount of irrigation water applied to
< !!                                 |HRU on current day that is lost due to
< !!                                 |application efficiency
< !!    qird(:)      |mm H2O          |amount of irrigation water applied to
< !!                                 |HRU on curr. day that returns to runoff
< !!    tird(:)      |mm H2O          |total amount of irr. water applied
< !!                                 |to HRU on current day
---
> !!                                 |applied to HRU
> !!    aird(:)      |mm H2O          |amount of water applied to HRU on curr.
> !!                                 |day
62d33
< !!    shallst(:)   |mm H2O          |depth of water in shallow aquifer
67,69c38
< !!    sq_rto       |none            |fraction of total applied irr water
< !!                                 |that is lost as runoff
< !!    hrumono(22,:)|mm H2O          |amount of irr. water applied to HRU
---
> !!    hrumono(22,:)|mm H2O          |amount of irr. water applied to HRU
76,81c45,50
< !!    flag         |none            |irrigation flag:
< !!                                 |0 no irrigation operation on current day
< !!                                 |1 scheduled irrigation
< !!                                 |2 auto irrigation
< !!    irreff       |none            |irrigation application efficiency
< !!    k            |none            |HRU number
---
> !!    fcx          |mm H2O          |amount of H2O stored in soil layer when
> !!                                 |moisture content is at field capacity
> !!    jj           |none            |HRU number
> !!    k            |none            |counter (soil layers)
> !!    stx          |mm H2O          |amount of water stored in soil layer on
> !!                                 |current day
82a52
> !!    yy           |mm H2O          |amount of water added to soil layer
88d57
<       implicit none
90c59
<       integer, intent (in) :: j
---
>       integer, intent (in) :: jj
92,93c61,62
<       integer :: flag
<       real :: irreff
---
>       integer :: k
>       real :: fcx, stx, yy
95,101c64,66
<       irreff = 0.
<       sq_rto = 0.
```

```
<
< !! Check if it is a scheduled or auto-irrigation operation
<       if (flag == 0) then
<         return                          !! If no flag is active, exit
<       end if
---
> !! initialize variable for HRU
> !! (because irrigation can be applied in different command loops
> !! the variable is initialized here)
103,127c68,71
< !! Get irrigation efficiency and runoff return parameters
<                       if (flag == 1) then      !! If scheduled irrigation
<                         irreff = irrefm(j)
<                         sq_rto = irrsq(j)
<                       elseif (flag == 2) then  !! If auto-irrigation
<                         irreff = irr_eff(j)
<                         sq_rto = irr_asq(j)
<                       end if
<
< !! Calculate the amount of irrigation applied to soil and irr losses
<       qird(j) = volmm * sq_rto
<       aird(j) = volmm * irreff
<       lird(j) = volmm - (aird(j) + qird(j))
<       tird(j) = volmm
<
< !! Check if lird is negative due to invalid irreff and sq_rto inputs
      (i.e. irreff + sq_rto > 1.0)
<       if (lird(j) < 0.) then
<         lird(j) = 0.
<         qird(j) = volmm - aird(j)
<       end if
<
< !! Add the irrigation water losses to shallow aquifer storage
<       shallst(j) = shallst(j) + lird(j)
<
< !! Summary calculations
---
>       aird(jj) = volmm * (1. - sq_rto)
>       qird(jj) = volmm * sq_rto
>
> !! summary calculations
129,134c73,75
<         irn(j) = irn(j) + 1
<         aairr(j) = aairr(j) + aird(j)
<         aqirr(j) = aqirr(j) + qird(j)
<         alirr(j) = alirr(j) + lird(j)
<         atirr(j) = atirr(j) + tird(j)
<         hrumono(22,j) = hrumono(22,j) + tird(j)
---
>         irn(jj) = irn(jj) + 1
```

```
>          aairr(jj) = aairr(jj) + aird(jj)
>          hrumono(22,jj) = hrumono(22,jj) + aird(jj)
139c80
<        end
---
>        end
\ No newline at end of file
```

MODPARM.F

```
317c317
<        real, dimension (:), allocatable :: aird, lird, qird, tird
           !!Included by Essenfelder, 01/10/15
---
>        real, dimension (:), allocatable :: qird
507c507
<        real, dimension (:), allocatable :: anano3,t_ov,sol_sumfc
           !Edited by Essenfelder, 01/10/15
---
>        real, dimension (:), allocatable :: anano3,aird,t_ov,sol_sumfc
509,510c509
<        real, dimension (:), allocatable :: cht,u10,rhd
           !!Edited by Essenfelder, 01/10/15
<        real, dimension (:), allocatable :: aairr, alirr, aqirr, atirr
           !!Included by Essenfelder, 01/10/15
---
>        real, dimension (:), allocatable :: aairr,cht,u10,rhd
911c910
<        end module parm
---
>        end module parm
\ No newline at end of file
```

REWIND_INIT.F

```
14,16d13
<        alirr = 0. !!Included by Essenfelder, 01/10/15
<        aqirr = 0. !!Included by Essenfelder, 01/10/15
<        atirr = 0. !!Included by Essenfelder, 01/10/15
267,269d263
<        lird = 0.  !!Included by Essenfelder, 01/10/15
<        qird = 0.  !!Included by Essenfelder, 01/10/15
<        tird = 0.  !!Included by Essenfelder, 01/10/15
505c499
```

```
<       end
---
>       end
\ No newline at end of file
```

ROUTE.F

```
226,229c226
<       !! call irr_rch !!Removed by Essenfelder, 02/12/2015
<       do k = 1, nhru
<         call irrigation(2, 1, k)  !! Auto-irr - Source reach only - k HRU
<       end do
---
>       call irr_rch
238c235
<       end
---
>       end
\ No newline at end of file
```

ROUTRES.F

```
238,241c238
<         !! call irr_res             !!Removed by Essenfelder, 02/12/2015
<         do k = 1, nhru
<               call irrigation(2, 2, k)  !! Auto-irr - Source res. only
<         end do
---
>         call irr_res
438c435
<       end
---
>       end
\ No newline at end of file
```

SCHED__MGT.F

```
72c72
<                 irr_flag(ihru) = 1
---
>             irr_flag(ihru) = 1
78,80c78,79
```

```
<              if (irr_sc(ihru) > 2) then
<                !! call irrsub !!Removed by Essenfelder, 02/12/2015
<                    call irrigation(1, irr_sc(j), j)  !! Schd-irrigation
---
>              if (irr_sc(ihru) > 2) then    !! reach and res flags
>                call irrsub
83,91c82,90
< !!             if (imgt ==1) then
< !!               write (143, 1002) subnum(j), hruno(j), iyr, i_mo,
< !!     *         iida, hru_km(j), "        ",
< !!     *         "IRRIGATE", phubase(j), phuacc(j), sol_sw(j),bio_ms(j),
< !!     *         sol_rsd(1,j), sol_sumno3(j),sol_sumsolp(j),irramt(j),
< !!     *         irr_sc(j), irr_no(j)
< !!1002  format (a5,1x,a4,3i6,1x,e10.5,1x,2a15,7f10.2,10x,f10.2,70x,2i7)
< !!
< !!             end if
---
>              if (imgt ==1) then
>                write (143, 1002) subnum(j), hruno(j), iyr, i_mo,
>      *         iida, hru_km(j), "        ",
>      *         "IRRIGATE", phubase(j), phuacc(j), sol_sw(j),bio_ms(j),
>      *         sol_rsd(1,j), sol_sumno3(j),sol_sumsolp(j),irramt(j),
>      *         irr_sc(j), irr_no(j)
> 1002  format (a5,1x,a4,3i6,1x,e10.5,1x,2a15,7f10.2,10x,f10.2,70x,2i7)
>
>              end if
336c335
<       end
---
>       end
\ No newline at end of file
```

SUBBASIN.F

```
218,221c218
<         !!if (auto_wstr(j) > 1.e-6 .and. irrsc(j) > 2) call autoirr
            !!Removed by Essenfelder, 02/12/2015
<         if (auto_wstr(j) > 1.e-6 .and. irr_sca(j) > 2) then
<           call irrigation(2, irr_sca(j), j)  !! Auto-irrigation
<         end if
---
>         if (auto_wstr(j) > 1.e-6 .and. irrsc(j) > 2) call autoirr
541c538
<       end
---
>       end
\ No newline at end of file
```

IRRIGATION.F

```
      subroutine irrigation(irr_type, irr_scode, irr_hru)

!!    ~ ~ ~ PURPOSE ~ ~ ~
!!    this subroutine controls the irrigation process

!!    ~ ~ ~ INCOMING VARIABLES ~ ~ ~
!!    name            |units          |definition
!!    ~ ~ ~ ~ ~ ~ ~ ~ ~ ~ ~ ~ ~ ~ ~ ~ ~ ~ ~ ~ ~ ~ ~ ~ ~ ~ ~ ~ ~ ~ ~ ~ ~ ~ ~ ~
!!    auto_wstr(:)    |none or mm    |H2O stress threshold that triggers irr
!!    irr_hru         |none           |HRU number
!!    irr_no(:)       |none           |irrigation source location (auto-irr)
!!                                    |if IRR=1, IRRNO is the number of the
!!                                    |          reach
!!                                    |if IRR=2, IRRNO is the number of the
!!                                    |          reservoir
!!                                    |if IRR=3, IRRNO is the number of the
!!                                    |          subbasin
!!                                    |if IRR=4, IRRNO is the number of the
!!                                    |          subbasin
!!                                    |if IRR=5, not used
!!    irr_sc(:)       |none           |irr. source code (auto-irrigation):
!!                                    |1 divert water from reach
!!                                    |2 divert water from reservoir
!!                                    |3 divert water from shallow aquifer
!!                                    |4 divert water from deep aquifer
!!                                    |5 divert water from unlimited source
!!    irr_scode       |none           |irr. source code (auto-irr.):
!!                                    |0 any of the below:
!!                                    |1 divert water from reach
!!                                    |2 divert water from reservoir
!!                                    |3 divert water from shallow aquifer
!!                                    |4 divert water from deep aquifer
!!                                    |5 divert water from unlimited source
!!    irr_noa(:)      |none           |irr. source location (auto-irr.)
!!                                    |if IRR=1, IRRNO is the number of the
!!                                    |          reach
!!                                    |if IRR=2, IRRNO is the number of the
!!                                    |          reservoir
!!                                    |if IRR=3, IRRNO is the number of the
!!                                    |          subbasin
!!                                    |if IRR=4, IRRNO is the number of the
!!                                    |          subbasin
!!                                    |if IRR=5, not used
!!    irr_sca(:)      |none           |irrigation source code (auto-irr):
!!                                    |1 divert water from reach
!!                                    |2 divert water from reservoir
!!                                    |3 divert water from shallow aquifer
```

```
!!                                  |4 divert water from deep aquifer
!!                                  |5 divert water from unlimited source
!!    irr_type        |none         |irrigation flag:
!!                                  |0 no irr. operation on curr. day
!!                                  |1 scheduled irrigation
!!                                  |2 auto irrigation
!!    ~ ~ ~ ~ ~ ~ ~ ~ ~ ~ ~ ~ ~ ~ ~ ~ ~ ~ ~ ~ ~ ~ ~ ~ ~ ~ ~ ~ ~ ~ ~ ~ ~ ~ ~ ~

!!    ~ ~ ~ OUTGOING VARIABLES ~ ~ ~
!!    name          |units          |definition
!!    ~ ~ ~ ~ ~ ~ ~ ~ ~ ~ ~ ~ ~ ~ ~ ~ ~ ~ ~ ~ ~ ~ ~ ~ ~ ~ ~ ~ ~ ~ ~ ~ ~ ~ ~ ~
!!    irrno(:)      |none          |irrigation source location
!!                                |if IRR=1, IRRNO is the number of the
!!                                |          reach
!!                                |if IRR=2, IRRNO is the number of the
!!                                |          reservoir
!!                                |if IRR=3, IRRNO is the number of the
!!                                |          subbasin
!!                                |if IRR=4, IRRNO is the number of the
!!                                |          subbasin
!!                                |if IRR=5, not used
!!    irrsc(:)      |none          |irrigation source code:
!!                                |1 divert water from reach
!!                                |2 divert water from reservoir
!!                                |3 divert water from shallow aquifer
!!                                |4 divert water from deep aquifer
!!                                |5 divert water from unlimited source
!!    sol_sumfc(:)|mm H2O          |amount of H2O held in the soil profile
!!                                |at field capacity
!!    sol_sw(:)     |mm H2O         |amount of H2O stored in soil profile on
!!                                |any given day
!!    strsw(:)      |none          |fraction of potential plant growth
!!                                |achieved on the day where the
!!                                |reduction is caused by water stress
!!    wstrs_id(:)   |none          |water stress identifier:
!!                                |1 plant water demand
!!                                |2 soil water deficit
!!    ~ ~ ~ ~ ~ ~ ~ ~ ~ ~ ~ ~ ~ ~ ~ ~ ~ ~ ~ ~ ~ ~ ~ ~ ~ ~ ~ ~ ~ ~ ~ ~ ~ ~ ~ ~

!!    ~ ~ ~ LOCAL DEFINITIONS ~ ~ ~
!!    name          |units          |definition
!!    ~ ~ ~ ~ ~ ~ ~ ~ ~ ~ ~ ~ ~ ~ ~ ~ ~ ~ ~ ~ ~ ~ ~ ~ ~ ~ ~ ~ ~ ~ ~ ~ ~ ~ ~ ~
!!    flag          |none          |irrigation flag:
!!                                |0 no irrigation operation on current day
!!                                |1 scheduled irrigation
!!                                |2 auto irrigation
!!    j             |none          |HRU number
!!    ~ ~ ~ ~ ~ ~ ~ ~ ~ ~ ~ ~ ~ ~ ~ ~ ~ ~ ~ ~ ~ ~ ~ ~ ~ ~ ~ ~ ~ ~ ~ ~ ~ ~ ~ ~

!!    ~ ~ ~ SUBROUTINES/FUNCTIONS CALLED ~ ~ ~
```

```
!!    Intrinsic:
!!    SWAT: irr_source

!!    ~ ~ ~ ~ ~ ~ END SPECIFICATIONS ~ ~ ~ ~ ~ ~

      use parm
      implicit none

      integer :: irr_type, irr_scode, irr_hru
      integer :: flag, j

!! Get current hru number
      j = 0
      j = irr_hru

!! Check if it is a scheduled or auto-irrigation operation
      flag = 0
      if (irr_flag(j) == 1) flag = 1   !! If scheduled irriation = 1
      if (irra_flag(j) == 1) flag = 2  !! If auto-irriation = 2
      if (flag == 0) return            !! If no flag is active, exit

!! Check if current irrigation type is the same as the one requested
      if (flag /= irr_type) return

!! Get irrigation source code and irrigation source location
                        if (flag == 1) then      !! If scheduled irrigation
                          irrsc(j) = irr_sc(j)
        irrno(j) = irr_no(j)
                        elseif (flag == 2) then  !! If auto-irrigation
                          irrsc(j) = irr_sca(j)
        irrno(j) = irr_noa(j)
                        end if

!! Check if current HRU irrsc is the same as the one requested
      if (irr_scode /= 0 .and. irrsc(j) /= irr_scode) return

!! Proceed with irrigation operation
      if (flag == 1) then      !! Scheduled irrigation
        call irr_source(flag, j)
        irr_flag(j) = 0        !! Set the irr flag to 0
      elseif (flag == 2) then  !! If auto-irrigation
   !! Check if auto-irrigation is triggered
        if (((wstrs_id(j) == 1) .and. (strsw(j) < auto_wstr(j))) .or.
     &   ((wstrs_id(j)==2).and.((sol_sumfc(j)-sol_sw(j))>auto_wstr(j))))
     &  then
          call irr_source(flag, j)
        end if
      end if

      return
```

```
      end
```

IRR_SOURCE.F

```
      subroutine irr_source(flag, j)

!!    ~ ~ ~ PURPOSE ~ ~ ~
!!    this subroutine selects the irrigation source and performs the
!!    subtraction of irrigation water from source

!!    ~ ~ ~ INCOMING VARIABLES ~ ~ ~
!!    name            |units          |definition
!!    ~ ~ ~ ~ ~ ~ ~ ~ ~ ~ ~ ~ ~ ~ ~ ~ ~ ~ ~ ~ ~ ~ ~ ~ ~ ~ ~ ~ ~ ~ ~ ~ ~ ~ ~ ~
!!    aird(:)         |mm H2O         |amount of irrigation water applied to
!!                                    |HRU on curr. day that sums up to sol_sw
!!    auto_wstr(:)    |none or mm     |H2O stress threshold that triggers irr
!!    deepst(:)       |mm H2O         |depth of water in deep aquifer
!!    flowmin(:)      |m^3/s          |minimum instream flow for irrigation
!!                                    |diversions when IRR=1, irrigation water
!!                                    |will be diverted only when streamflow
!!                                    |is at or above FLOWMIN.
!!    hru_sub(:)      |none           |subbasin in which HRU is located
!!    inum1           |none           |reach or reservoir number
!!    irramt(:)       |mm H20         |depth of irr. water applied to HRU
!!    irrno(:)        |none           |irrigation source location
!!                                    |if IRR=1, IRRNO is the number of the
!!                                    |          reach
!!                                    |if IRR=2, IRRNO is the number of the
!!                                    |          reservoir
!!                                    |if IRR=3, IRRNO is the number of the
!!                                    |          subbasin
!!                                    |if IRR=4, IRRNO is the number of the
!!                                    |          subbasin
!!                                    |if IRR=5, not used
!!    irrsc(:)        |none           |irrigation source code:
!!                                    |1 divert water from reach
!!                                    |2 divert water from reservoir
!!                                    |3 divert water from shallow aquifer
!!                                    |4 divert water from deep aquifer
!!                                    |5 divert water from unlimited source
!!    irr_mx(:)       |mm H2O         |maximum irr amount per auto application
!!    nhru            |none           |number of HRUs in watershed
!!    nirr(:)         |none           |sequence number of irr application
!!                                    |within the year
!!    res_vol(:)      |m^3            |reservoir volume
!!    rchstor(:)      |m^3            |water stored in reach
!!    rtwtr           |m^3            |water leaving reach on day
```

```
!!    shallst(:)      |mm H2O          |depth of water in shallow aquifer
!!    sol_sumfc(:)    |mm H2O          |amount of H2O held in the soil profile
!!                                     |at field capacity
!!    sol_sw(:)       |mm H2O          |amount of H2O stored in soil profile on
!!                                     |given day
!!    ~ ~ ~ ~ ~ ~ ~ ~ ~ ~ ~ ~ ~ ~ ~ ~ ~ ~ ~ ~ ~ ~ ~ ~ ~ ~ ~ ~ ~ ~ ~ ~ ~ ~ ~ ~ ~

!!    ~ ~ ~ OUTGOING VARIABLES ~ ~ ~
!!    name            |units          |definition
!!    ~ ~ ~ ~ ~ ~ ~ ~ ~ ~ ~ ~ ~ ~ ~ ~ ~ ~ ~ ~ ~ ~ ~ ~ ~ ~ ~ ~ ~ ~ ~ ~ ~ ~ ~ ~ ~
!!    deepirr(:)      |mm H2O          |amount of water removed from deep aquifer
!!                                     |for irrigation
!!    deepst(:)       |mm H2O          |depth of water in deep aquifer
!!    nirr(:)         |none            |sequence number of irrigation application
!!                                     |within the year
!!    rchstor(:)      |m^3             |water stored in reach
!!    res_vol(:)      |m^3             |reservoir volume
!!    rtwtr           |m^3             |water leaving reach on day
!!    shallirr(:)     |mm H2O          |amount of H2O removed from shall. aq.
!!                                     |for irrigation
!!    shallst(:)      |mm H2O          |depth of water in shallow aquifer
!!    ~ ~ ~ ~ ~ ~ ~ ~ ~ ~ ~ ~ ~ ~ ~ ~ ~ ~ ~ ~ ~ ~ ~ ~ ~ ~ ~ ~ ~ ~ ~ ~ ~ ~ ~ ~ ~

!!    ~ ~ ~ LOCAL DEFINITIONS ~ ~ ~
!!    name            |units          |definition
!!    ~ ~ ~ ~ ~ ~ ~ ~ ~ ~ ~ ~ ~ ~ ~ ~ ~ ~ ~ ~ ~ ~ ~ ~ ~ ~ ~ ~ ~ ~ ~ ~ ~ ~ ~ ~ ~
!!    cnv             |none            |conversion factor (mm/ha => m^3)
!!    flag            |none            |irrigation flag:
!!                                     |0 no irrigation operation on current day
!!                                     |1 scheduled irrigation
!!                                     |2 auto irrigation
!!    j               |none            |HRU number
!!    jrch            |none            |reach number
!!    jres            |none            |reservoir number
!!    k               |none            |counter
!!    str_irr         |string          |Stores the string for sched. or auto-irr
!!    vmm             |mm H2O          |amount of irr. water applied to HRU
!!    vmma            |mm H2O          |max amount of water available in source
!!    vol             |m^3             |volume of irr. water applied to HRU
!!    wtr_avail       |m^3             |volume of water available from reach
!!    wtrin           |m^3             |H2O outflow from reach prior to
!!                                     |subtracting irr. diversions
!!    xx              |???             |temporary variable to store temp results
!!    ~ ~ ~ ~ ~ ~ ~ ~ ~ ~ ~ ~ ~ ~ ~ ~ ~ ~ ~ ~ ~ ~ ~ ~ ~ ~ ~ ~ ~ ~ ~ ~ ~ ~ ~ ~ ~

!!    ~ ~ ~ SUBROUTINES/FUNCTIONS CALLED ~ ~ ~
!!    Intrinsic: Abs, Max, Min
!!    SWAT: irrigate

!!    ~ ~ ~ ~ ~ ~ END SPECIFICATIONS ~ ~ ~ ~ ~ ~
```

```
      use parm
      implicit none

      integer :: flag, ii, j, jrch, jres, k
      real :: cnv, vmma, vmm, vol, wtr_avail, wtrin, xx
      character(len=8) :: str_irr

!! Clear variables
      cnv = 0.
      vmma = 0.
      vmm = 0.
      vol = 0.
      wtr_avail = 0.
      xx = 0.

!! Get identifier numbers
      jrch = 0
      jres = 0
      if (irrsc(j) == 1) jrch = inum1 !! If source = reach, get reach number
      if (irrsc(j) == 2) jres = inum1 !! If source = res., get res number

!! Fill the string for scheduled or auto-irrigation
      if (flag == 1) str_irr = "SCHD_IRR"
      if (flag == 2) str_irr = "AUTO_IRR"

     !! Calculate maximum irrigation amount ==========================
      select case (irrsc(j))    !! Select irrigation source
        case (1)    !! Source --> Reach ------------------------------
          if (irrno(j) == jrch) then  !! Check if remove water from reach
                      if (rtwtr > (flowmin(j) * 86400.)) then
                        cnv = 0.
                        cnv = hru_ha(j) * 10.
                        wtr_avail = 0.
                        wtr_avail = rtwtr + rchstor(jrch)
                        vmma = 0.  !! Max water available in source
                        vmma = (wtr_avail - flowmin(j) * 86400.) *
     *                   flowfr(j) / cnv
                        if (divmax(j) < 0.) then !! Convert unit to mmH2O
                          xx = (Abs(divmax(j)) * 10000.) / cnv
                        else  !! If unit is mm H2O, get divmax
                          xx = divmax(j)
                        endif
                        vmma = Min(xx, vmma)   !! Max irr water to apply
                        xx = 0.  !! Clear temporary variable
                      end if
                    end if
        !! ------------------------------------------------------------

        case (2)    !! Source --> Reservoir --------------------------
```

```
          if (irrno(j) == jres) then  !! Check if remove water from res
                        cnv = 0.
                        cnv = hru_ha(j) * 10.
                        vmma = 0.
                        vmma = res_vol(jres) / cnv !! Max water in source
          end if
        !! ------------------------------------------------------------------

        case (3)    !! Source --> Shallow aquifer ------------------------------
          vmma = 0.
          do k = 1, nhru !! Loop HRUs to get water available shall. aq.
            if (hru_sub(k) == irrno(j)) then
              cnv = 0.
              cnv = hru_ha(k) * 10.
              vmma = vmma + shallst(k) * cnv !! Get max water in source
            end if
          end do
          cnv = 0.
          cnv = hru_ha(j) * 10.
          vmma = vmma / cnv              !! Max irr water to apply
        !! ------------------------------------------------------------------

        case (4)   !! Source --> Deep aquifer ----------------------------------
          vmma = 0.
          do k = 1, nhru !! Loop HRUs to get water available deep aq.
            if (hru_sub(k) == irrno(j)) then
              cnv = 0.
              cnv = hru_ha(k) * 10.
              vmma = vmma + deepst(k) * cnv  !! Max water in source
            end if
          end do
          cnv = 0.
          cnv = hru_ha(j) * 10.
          vmma = vmma / cnv              !! Max irr water to apply
        !! ------------------------------------------------------------------

         case (5)   !! Source - Unlimited ---------------------------------------
          vmma = 0.
          vmma = sol_sumfc(j)             !! Max irr water to apply
         !! ------------------------------------------------------------------

      end select !! ================================================================



!! Check if water is available from source and, if so, apply irr
      if (vmma > 0.) then
        vmm = 0.
        vmm = Min(sol_sumfc(j), vmma)  !! If avail. water from source is
                                       !!   < than amount of water in soil
```

```
                                    !!   profile at field capacity
!! Check if available water from source < maximum irrigation amount
   if (flag == 1) vmm = Min(vmm, irramt(j))  !! Scheduled irrigation
   if (flag == 2) vmm = Min(vmm, irr_mx(j))  !! Auto-irrigation

!! Subtract irrigation water applied from source ========================
   select case (irrsc(j))     !! Select irrigation source
     case (1)    !! Source --> Reach ------------------------------------
       if (irrno(j) == jrch) then  !! Check if remove water from reach
                    wtrin = 0.
                    wtrin = rtwtr + rchstor(jrch) !! Outflow reach
                    cnv = 0.
                    cnv = hru_ha(j) * 10.
                    vol = 0.
                    vol = vmm * cnv           !! Irr. in m^3/d
                    vol = Min(vol, wtr_avail) !! If irr>water avail.
                    if (rchstor(jrch) > vol) then !! Use from rchstor
                      xx = 0.
                      rchstor(jrch) = rchstor(jrch) - vol
                    else !! If rchstor is not enough,
                      xx = vol - rchstor(jrch) !! use from rtwrt
                      vol = rchstor(jrch)
                      rchstor(jrch) = 0.
                      rtwtr = rtwtr - xx
                      if (rtwtr < 0.) then !! If vol. < 0, fix it
                          xx = xx + rtwtr
                          rtwtr = 0.
                      end if
                   !! Subtract irrigation from reach outflow
                      if (ievent > 0) then
                        do ii = 1, nstep
                          hrtwtr(ii) = hrtwtr(ii) - xx
                          hrtwtr(ii) = Max(0., hrtwtr(ii))
                        end do
                      end if
                    end if
                    vol = vol + xx
                    vmm = vol / cnv
                    xx = 0.  !! Clear temporary variable
       end if
     !! ------------------------------------------------------------------

     case (2)    !! Source --> Reservoir --------------------------------
       if (irrno(j) == jres) then  !! Check if remove water from res.
                    cnv = 0.
                    cnv = hru_ha(j) * 10.
                    vol = 0.
                    vol = vmm * cnv    !! Irrigation amount in m^3/d
                    res_vol(jres) = res_vol(jres) - vol
                    if (res_vol(jres) < 0.) then !! If vol. < 0, fix it
```

```
                        vol = vol + res_vol(jres)
                        res_vol(jres) = 0.
                      end if
                      vmm = vol / cnv
        end if
      !! ------------------------------------------------------------------

      case (3)     !! Source --> Shallow aquifer ----------------------
        do k = 1, nhru !! Loop HRUs to get water avail. from shall. aq.
          if (hru_sub(k) == irrno(j)) then
            shallst(k) = shallst(k) - vmm
            if (shallst(k) < 0.) then     !! If vol. < 0, fix it
              vmm = vmm + shallst(k)
              shallst(k) = 0.
            end if
            shallirr(k) = shallirr(k) + vmm
          end if
        end do
      !! ------------------------------------------------------------------

      case (4)    !! Source --> Deep aquifer -------------------------
        do k = 1, nhru   !! Loop HRUs to get water avail. from deep aq.
          if (hru_sub(k) == irrno(j)) then !! If vol. < 0, fix it
            deepst(k) = deepst(k) - vmm
            if (deepst(k) < 0.) then
              vmm = vmm + deepst(k)
              deepst(k) = 0.
            end if
            deepirr(k) = deepirr(k) + vmm
          end if
        end do
      !! ------------------------------------------------------------------

    end select !! ===================================================

  !! Calculate the irrigation amount in m^3/d
    cnv = 0.
    cnv = hru_ha(j) * 10.
    vol = 0.
    vol = vmm * cnv     !! Irrigation amount in m^3/d

  !! Calculate the irrigation amount and losses
    call irrigate(flag, j, vmm)

  !! Check if HRU is a pothole
    if (pot_fr(j) > 1.e-6) then
      pot_vol(j) = pot_vol(j) + aird(j) / (10. * potsa(j))
    end if

  !! Advance irrigation operation number
```

```
        nirr(j) = nirr(j) + 1

      !! Write the outputs to 'output.mgt' file
        if (imgt == 1) then
          write (143, 1000) subnum(j), hruno(j), iyr, i_mo, iida,
     *    hru_km(j), "          ", str_irr, phubase(j), phuacc(j),
     *    sol_sw(j), bio_ms(j), sol_rsd(1,j),sol_sumno3(j),
     *    sol_sumsolp(j), aird(j), irrsc(j), irrno(j)
        end if

      !! If irrigation source is reach, update reach specific parameters
                    if (irrsc(j) == 1) then
                      if (wtrin /= rtwtr .and. wtrin > 0.01) then
                        sedrch  = sedrch  * rtwtr / wtrin
                        rch_san = rch_san * rtwtr / wtrin
                        rch_sil = rch_sil * rtwtr / wtrin
                        rch_cla = rch_cla * rtwtr / wtrin
                        rch_sag = rch_sag * rtwtr / wtrin
                        rch_lag = rch_lag * rtwtr / wtrin
                        rch_gra = rch_gra * rtwtr / wtrin
                        if (sedrch  < 1.e-6) then
                          sedrch  = 0.
                          rch_san = 0.
                          rch_sil = 0.
                          rch_cla = 0.
                          rch_sag = 0.
                          rch_lag = 0.
                          rch_gra = 0.
                        end if
                        if (ievent > 0) then
                          do ii = 1, nstep
                            hsedyld(ii) = hsedyld(ii) * rtwtr / wtrin
                          end do
                        end if
                      end if
                    end if

       end if

1000   format (a5,1x,a4,3i6,1x,e10.5,1x,2a15,7f10.2,10x,f10.2,70x,i10,
     *         10x,i10)

       return
       end
```

Coupling with ANN Model

ALLOCATE_PARMS.F

```
50,55c50,51
<       use parm
<
<       !! Added by Essenfelder
<       logical :: filecheck
<       integer :: IOstatus
<
---
>       use parm
>
1802,1839c1798,1799
<       !! ============================
<
<       !! Added by Essenfelder
<       allocate(vol_annet(9,msub))
<       vol_annet = 0.
<       inquire(file="Xsim.csv", exist=filecheck)
<       if (filecheck) then
<         open(unit=101,file="Xsim.csv",iostat=IOstatus,status='old')
<         if (IOstatus == 0) close(101, status='delete')
<       endif
<       inquire(file="Xsim_db.csv", exist=filecheck)
<       if (filecheck) then
<         open(unit=102,file="Xsim_db.csv",iostat=IOstatus,status='old')
<         if (IOstatus == 0) close(102, status='delete')
<       endif
<       inquire(file="XwtrQlty.csv", exist=filecheck)
<       if (filecheck) then
<         open(unit=103,file="XwtrQlty.csv",iostat=IOstatus,status='old')
<         if (IOstatus == 0) close(103, status='delete')
<       endif
<       inquire(file="XwtrQlty_db.csv", exist=filecheck)
<       if (filecheck) then
<       open(unit=104,file="XwtrQlty_db.csv",iostat=IOstatus,status='old')
<         if (IOstatus == 0) close(104, status='delete')
<       endif
<       inquire(file="ySim.csv", exist=filecheck)
<       if (filecheck) then
<         open(unit=105,file="ySim.csv",iostat=IOstatus,status='old')
<         if (IOstatus == 0) close(105, status='delete')
<       endif
<       inquire(file="ySim_db.csv", exist=filecheck)
<       if (filecheck) then
```

```
<          open(unit=106,file="ySim_db.csv",iostat=IOstatus,status='old')
<          if (IOstatus == 0) close(106, status='delete')
<        endif
<
<
<
---
>        !! ============================
>
1845c1805
<
---
>
1847c1807
<        end
---
>        end
\ No newline at end of file
```

COMMAND.F

```
134,136c134,135
<            case (2)
<              call route
<              if (inum4 == 1) call annet !! compute external/artificial
                                              sources (Essenfelder)
---
>            case (2)
>              call route
141c140
<            case (3)
---
>            case (3)
144c143
<            case (4)
---
>            case (4)
146c145
<            case (5)
---
>            case (5)
150c149
<            case (6)
---
>            case (6)
154c153
<            case (7)
```

```
---
>            case (7)
157c156
<            case (8)
---
>            case (8)
160c159
<            case (9)
---
>            case (9)
162c161
<            case (10)
---
>            case (10)
165c164
<            case (11)
---
>            case (11)
170c169
<            case (13)
---
>            case (13)
187c186
<        end
---
>        end
\ No newline at end of file
```

MODPARM.F

```
907,909d906
<
<        !! Added by Essenfelder for annet calculation
<        real, dimension(:,:), allocatable :: vol_annet
912c909,910
<        end module parm
---
>
>        end module parm
\ No newline at end of file
```

READFIG.F

```
205,208c205,207
```

```
<                nrch = nrch + 1
<                inum4s(idum) = inum3s(idum) !! Store inum3s as inum4s
< !!             assume subbasin is the same number as the reach (if zero)
<                !!if (inum3s(idum) == 0) then
---
>                nrch = nrch + 1
> !!             assume subbasin is the same number as the reach (if zero)
>                if (inum3s(idum) == 0) then
210c209
<                !!end if
---
>                end if
\ No newline at end of file
```

ROUTE.F

```
95,105d94
<
< !! compute contribution of H2O from artificial sources (vol_annet)
<       varoute(2,inum2)  = varoute(2,inum2)  + vol_annet(1,inum1)*86400
<       varoute(4,inum2)  = varoute(4,inum2)  + vol_annet(2,inum1) !! orgN
<       varoute(14,inum2) = varoute(14,inum2) + vol_annet(3,inum1) !! NH3
<       varoute(15,inum2) = varoute(15,inum2) + vol_annet(4,inum1) !! NO2
<       varoute(6,inum2)  = varoute(6,inum2)  + vol_annet(5,inum1) !! NO3-N
<       varoute(5,inum2)  = varoute(5,inum2)  + vol_annet(6,inum1) !! orgP
<       varoute(7,inum2)  = varoute(7,inum2)  + vol_annet(7,inum1) !! minP
<       varoute(16,inum2) = varoute(16,inum2) + vol_annet(8,inum1) !! CBOD
<       varoute(17,inum2) = varoute(17,inum2) + vol_annet(9,inum1) !! DO
\ No newline at end of file
```

ANNET_PREDATA.F95

```
      subroutine annet_predata

!!    ~ ~ ~ PURPOSE ~ ~ ~ ~ ~ ~ ~ ~ ~ ~ ~ ~ ~ ~ ~ ~ ~ ~ ~ ~ ~ ~ ~ ~ ~ ~
!!    this subroutine prepares the input data to be read by the annet
!!    model
!!    Author: Arthur Hrast Essenfelder
!!    E-mail: arthur.essenfelder@unive.it
!!
!!    Version: 1.0
!!    Last update on: 07/11/2016
!!
!!    ~ ~ ~ INCOMING VARIABLES  ~ ~ ~ ~ ~ ~ ~ ~ ~ ~ ~ ~ ~ ~ ~ ~ ~ ~ ~
```

```
!!    name            |units          |definition
!!    ------------------------------------------------------------
!!    i               |none           |day of the year, integer
!!    inum1           |none           |subbasin id number
!!    hru1            |none           |HRU id number
!!    hru_ra(:)       |MJ/m^2         |solar radiation for the day in HRU
!!    rhd(:)          |none           |relative humidity for the day in HRU
!!    subp(:)         |mm H2O         |precipitation for the day in HRU
!!    tmpav(:)        |deg C          |avg air temp. on current day in HRU
!!    u10(:)          |m/s            |wind speed for the day in HRU
!!    ~ ~ ~ ~ ~ ~ ~ ~ ~ ~ ~ ~ ~ ~ ~ ~ ~ ~ ~ ~ ~ ~ ~ ~ ~ ~ ~ ~ ~ ~ ~ ~
!!
!!    ~ ~ ~ OUTGOING VARIABLES ~ ~ ~ ~ ~ ~ ~ ~ ~ ~ ~ ~ ~ ~ ~ ~ ~ ~ ~
!!    name            |units          |definition
!!    ------------------------------------------------------------
!!    arrXsim(1)      |m^3/s          |flow out of reach on day
!!    arrXsim(2)      |none           |relative humidity for the day in HRU
!!    arrXsim(3)      |mm H2O         |precipitation for the day in HRU
!!    arrXsim(4)      |MJ/m^2         |solar radiation for the day in HRU
!!    arrXsim(5)      |deg C          |avg air temp. on current day in HRU
!!    arrXsim(6)      |m/s            |wind speed for the day in HRU
!!    arrXsim(7)      |boolean        |spring season
!!    arrXsim(8)      |boolean        |summer season
!!    arrXsim(9)      |boolean        |autumn season
!!    arrXsim(10)     |boolean        |winter season
!!    ~ ~ ~ ~ ~ ~ ~ ~ ~ ~ ~ ~ ~ ~ ~ ~ ~ ~ ~ ~ ~ ~ ~ ~ ~ ~ ~ ~ ~ ~ ~ ~
!!
!!    ~ ~ ~ LOCAL DEFINITIONS ~ ~ ~ ~ ~ ~ ~ ~ ~ ~ ~ ~ ~ ~ ~ ~ ~ ~ ~
!!    name            |units          |definition
!!    ------------------------------------------------------------
!!    ii              |none           |generic counter
!!    arrSize         |none           |stores the size of the data array
!!    iseason         |none           |stores the results of funseason
!!    ~ ~ ~ ~ ~ ~ ~ ~ ~ ~ ~ ~ ~ ~ ~ ~ ~ ~ ~ ~ ~ ~ ~ ~ ~ ~ ~ ~ ~ ~ ~ ~
!!
!!    ~ ~ ~ SUBROUTINES/FUNCTIONS CALLED ~ ~ ~ ~ ~ ~ ~ ~ ~ ~ ~ ~ ~ ~
!!    name            |type           |definition
!!    ------------------------------------------------------------
!!    funseason()     |function       |functions for the seasons of year:
!!                                    |0 = error
!!                                    |1 = winter
!!                                    |2 = spring
!!                                    |3 = summer
!!                                    |4 = autumn
!!
!!    ~ ~ ~ ~ ~ ~ END SPECIFICATIONS ~ ~ ~ ~ ~ ~ ~ ~ ~ ~ ~ ~ ~ ~ ~ ~

      !! Initial declarations ------------------------------------------
      use parm
      implicit none
```

```
!! ------------------------------------------------------------------

!! Declaring Variables ---------------------------------------------
character(16) :: filename1,filename2,filename3,filename4
character(4) :: subcode
logical :: filecheck
integer :: ii, kk, icl, arrSize = 14
integer :: funseason, iseason, IOstatus
real, allocatable :: arrXsim(:), arrWtrQlty(:)
real :: cnv
!! ------------------------------------------------------------------

!! Preparing the inputs for the array data -------------------------
!! Initialising the arrXsim
allocate(arrXsim(arrSize))
arrXsim = 0.

!! Loading the data to the arrXsim
!! Reach variables
arrXsim(1) = rchdy(1,inum1)       !!flow in (m^3/s)

!! Weather variables
arrXsim(2) = rhd(hru1(inum1))     !!relative humidity
arrXsim(3) = subp(hru1(inum1))    !!precipitation
arrXsim(4) = hru_ra(hru1(inum1)) !!solar radiation
arrXsim(5) = tmpav(hru1(inum1))   !!average air temperature
arrXsim(6) = u10(hru1(inum1))     !!wind speed

!! Temporal variables
iseason = funseason(i)
select case (iseason)
  case (1) !! winter
      arrXsim(10) = 1.
  case (2) !! spring
      arrXsim(7) = 1.
  case (3) !! summer
      arrXsim(8) = 1.
  case (4) !! autumn
      arrXsim(9) = 1.
  case default
      arrXsim(7)  = 0.     !! Spring
      arrXsim(8)  = 0.     !! Summer
      arrXsim(9)  = 0.     !! Autumn
      arrXsim(10) = 0.     !! Winter
end select

!! Watershed variables
arrXsim(11) = wshddayo(7)     !!actual evapotranspiration (mmH2O)
arrXsim(12) = wshddayo(104)   !!gwq to streamflow (mmH2O)
arrXsim(13) = wshddayo(35)    !!H2O stored in soil profile (mmH2O)
```

```
      kk = 0     !!Counter for irrigated HRUs
      do ii=1, nhru
        if ((aird(ii)+qird(ii))>0.) then
            arrXsim(14) = arrXsim(14) + aird(ii)+qird(ii)
            kk = kk + 1
        endif
      end do
      if (kk > 0) then
        arrXsim(14) = arrXsim(14)/kk  !!Irrigation water applied (mmH2O)
      endif
      !! ------------------------------------------------------------------

      !! Preparing the inputs for the arrWtrQlty ------------------------
      allocate(arrWtrQlty(9))
      arrWtrQlty = 0.
      arrWtrQlty(1) = rchdy(1,inum1)       !!flow in (m^3/s)
      arrWtrQlty(2) = rchdy(8,inum1)       !!orgN in (kg N)
      arrWtrQlty(3) = rchdy(14,inum1)      !!NH4 in (kg)
      arrWtrQlty(4) = rchdy(16,inum1)      !!NO2 in (kg)
      arrWtrQlty(5) = rchdy(12,inum1)      !!NO3 in (kg N)
      arrWtrQlty(6) = rchdy(10,inum1)      !!orgP in (kg P)
      arrWtrQlty(7) = rchdy(18,inum1)      !!solP in (kg P)
      arrWtrQlty(8) = rchdy(22,inum1)      !!CBOD in (kg)
      arrWtrQlty(9) = rchdy(24,inum1)      !!dis O2 in (kg)
      !! ------------------------------------------------------------------

      !! Preparaing the name of the output files ------------------------
      filename1 = "Xsim.csv"
      filename2 = "Xsim_db.csv"
      filename3 = "XwtrQlty.csv"
      filename4 = "XwtrQlty_db.csv"
      !! ------------------------------------------------------------------

      !! Writing the data to .csv file ----------------------------------
      !! Checking if file exists, otherwise create it (Xsim)
      inquire(file=filename1, exist=filecheck)
      if (filecheck) then
        open(9970, file=filename1, action='write', status='old', &
             access='append')
      else
        open(9970, file=filename1, action='write', status='replace')
        write(9970, 1011)
      end if
      !! Write the data to the file
      do ii=1,arrSize
        write(9970, 1002, advance = 'no') arrXsim(ii)
        if (ii /= arrSIZE) then
            write (9970, 1003, advance = 'no') ","
        end if
      end do
```

```
      write(9970, *)
      close(9970)
      !! Checking if file exists, otherwise create it (WtrQlty)
      inquire(file=filename3, exist=filecheck)
      if (filecheck) then
        open(9980, file=filename3, action='write', status='old', &
             access='append')
      else
        open(9980, file=filename3, action='write', status='replace')
        write(9980, 2011)
      end if
      !! Write the data to the file
      do ii=1,9
        write(9980, 1002, advance = 'no') arrWtrQlty(ii)
        if (ii /= 9) then
            write (9980, 1003, advance = 'no') ","
        end if
      end do
      write(9980, *)
      close(9980)
      !! ------------------------------------------------------------------

      !! Writing the data to .csv database file ---------------------------
      !! Checking if file exists, otherwise create it (Xsim)
      inquire(file=filename2, exist=filecheck)
      if (filecheck) then
        open(9971, file=filename2, action='write', status='old', &
             access='append')
      else
        open(9971, file=filename2, action='write', status='replace')
        write(9971, 1001)
      end if
      !! Write the data to the file
      write(9971, 1004, advance = 'no') inum1
      write(9971, 1003, advance = 'no') ","
      write(9971, 1004, advance = 'no') i_mo
      write(9971, 1003, advance = 'no') ","
      write(9971, 1004, advance = 'no') icl(iida)
      write(9971, 1003, advance = 'no') ","
      write(9971, 1004, advance = 'no') iyr
      write(9971, 1003, advance = 'no') ","
      do ii=1,arrSize
        write(9971, 1002, advance = 'no') arrXsim(ii)
        if (ii /= arrSIZE) then
            write (9971, 1003, advance = 'no') ","
        end if
      end do
      write(9971, *)
      close(9971)
      !! Checking if file exists, otherwise create it (WtrQlty)
```

```
      inquire(file=filename4, exist=filecheck)
      if (filecheck) then
        open(9981, file=filename4, action='write', status='old', &
             access='append')
      else
        open(9981, file=filename4, action='write', status='replace')
        write(9981, 2001)
      end if
      !! Write the data to the file
      write(9981, 1004, advance = 'no') inum1
      write(9981, 1003, advance = 'no') ","
      write(9981, 1004, advance = 'no') i_mo
      write(9981, 1003, advance = 'no') ","
      write(9981, 1004, advance = 'no') icl(iida)
      write(9981, 1003, advance = 'no') ","
      write(9981, 1004, advance = 'no') iyr
      write(9981, 1003, advance = 'no') ","
      do ii=1,9
        write(9981, 1002, advance = 'no') arrWtrQlty(ii)
        if (ii /= 9) then
            write (9981, 1003, advance = 'no') ","
        end if
      end do
      write(9981, *)
      close(9981)
      !! ------------------------------------------------------------------

1001  format ("RCH,MO,DA,YR,FLOW.SWAT,HMD,PCP,SLR,TMP,WND,&
␣␣␣␣␣␣␣␣␣␣␣␣␣␣␣Spring,Summer,Autumn,Winter,&
␣␣␣␣␣␣␣␣␣␣␣␣␣␣␣ACT.EVAPT,GWQ,SOL.SW,IRR")
1002  format (f10.4)
1003  format (a1)
1004  format (i4)
1011  format ("FLOW.SWAT,HMD,PCP,SLR,TMP,WND,&
␣␣␣␣␣␣␣␣␣␣␣␣␣␣␣Spring,Summer,Autumn,Winter,&
␣␣␣␣␣␣␣␣␣␣␣␣␣␣␣ACT.EVAPT,GWQ,SOL.SW,IRR")
2001  format ("RCH,MO,DA,YR,FLOW.SWAT,ORGN,NH4,NO2,NO3,&
␣␣␣␣␣␣␣␣␣␣␣␣␣␣␣ORGP,MINP,BOD,DO")
2011  format ("FLOW.SWAT,ORGN,NH4,NO2,NO3,&
␣␣␣␣␣␣␣␣␣␣␣␣␣␣␣ORGP,MINP,BOD,DO")

      return
      end
```

ANNET.F95

```
      subroutine annet
```

```
!!    ~ ~ ~ PURPOSE ~ ~ ~ ~ ~ ~ ~ ~ ~ ~ ~ ~ ~ ~ ~ ~ ~ ~ ~ ~ ~ ~ ~ ~ ~
!!    this subroutine controls the call of the annet function
!!    Author: Arthur Hrast Essenfelder
!!    E-mail: arthur.essenfelder@unive.it
!!
!!    Version: 1.0
!!    Last update on: 07/11/2016
!!
!!    ~ ~ ~ INCOMING VARIABLES ~ ~ ~ ~ ~ ~ ~ ~ ~ ~ ~ ~ ~ ~ ~ ~ ~ ~ ~
!!    name            |units          |definition
!!    ------------------------------------------------------------
!!
!!    ~ ~ ~ ~ ~ ~ ~ ~ ~ ~ ~ ~ ~ ~ ~ ~ ~ ~ ~ ~ ~ ~ ~ ~ ~ ~ ~ ~ ~ ~ ~ ~
!!
!!    ~ ~ ~ OUTGOING VARIABLES ~ ~ ~ ~ ~ ~ ~ ~ ~ ~ ~ ~ ~ ~ ~ ~ ~ ~ ~
!!    name            |units          |definition
!!    ------------------------------------------------------------
!!
!!    ~ ~ ~ ~ ~ ~ ~ ~ ~ ~ ~ ~ ~ ~ ~ ~ ~ ~ ~ ~ ~ ~ ~ ~ ~ ~ ~ ~ ~ ~ ~ ~
!!
!!    ~ ~ ~ LOCAL DEFINITIONS ~ ~ ~ ~ ~ ~ ~ ~ ~ ~ ~ ~ ~ ~ ~ ~ ~ ~ ~
!!    name            |units          |definition
!!    ------------------------------------------------------------
!!
!!    ~ ~ ~ ~ ~ ~ ~ ~ ~ ~ ~ ~ ~ ~ ~ ~ ~ ~ ~ ~ ~ ~ ~ ~ ~ ~ ~ ~ ~ ~ ~ ~
!!
!!    ~ ~ ~ SUBROUTINES/FUNCTIONS CALLED ~ ~ ~ ~ ~ ~ ~ ~ ~ ~ ~ ~ ~ ~
!!    name            |type           |definition
!!    ------------------------------------------------------------
!!    annet_predata   |subroutine     |prepares input data to annet function
!!    annet_posdata   |subroutine     |reads output data from annet function
!!
!!    ~ ~ ~ ~ ~ ~ END SPECIFICATIONS ~ ~ ~ ~ ~ ~ ~ ~ ~ ~ ~ ~ ~ ~ ~ ~

      !! Initial declarations
      use parm
      implicit none

      !! Declaring Variables
      character(32) :: filename, filename1, filename2
      character(4) :: subcode
      character(2024) :: command1, command2
      logical :: filecheck
      integer :: XsimRows

      !! Preparing the input data for the ANnet model
      call annet_predata

      !! Preparing the name of the files
```

```
      filename = "ANnet_Simulate_Run"
      write(subcode, '(i4)') inum1
!      write(filename1, '(a32)') trim(filename) // &
!                                trim(adjustl(subcode)) // ".R"
!      write(filename2, '(a32)') trim("Xsim") // &
!                                trim(adjustl(subcode)) // ".csv"
      write(filename1, '(a32)') trim(filename) // ".R"
      write(filename2, '(a32)') trim("Xsim") // ".csv"
      filename1 = trim(adjustl(filename1))
      filename2 = trim(adjustl(filename2))

      !! Checking if ANnet model exists
      inquire(file=filename1, exist=filecheck)
      if (filecheck) then

        !! Check if number of rows in Xsim file is enough to call R
        command1 = "wc␣-l␣<␣" // trim(adjustl(filename2)) &
                   // "␣>␣XsimRows.txt"
        command1 = trim(adjustl(command1))
        call EXECUTE_COMMAND_LINE(command1, wait=.TRUE.)
        open(510,file='XsimRows.txt')
        read(510,*) XsimRows
        close(510, status='delete')

        !! If number of rows is equal to 30 days (1 month)
        if (XsimRows == (30+1)) then
            command2 = "Rscript␣--vanilla␣--default-packages='methods,&
␣␣␣␣␣␣␣␣␣␣␣␣␣␣␣␣␣␣␣␣␣␣␣␣stats,utils'␣" // trim(adjustl(filename1))
            command2 =trim(adjustl(command2))
            call EXECUTE_COMMAND_LINE(command2, wait=.TRUE.)
        end if

        !! Reading the output of the ANnet model and importing to SWAT
        call annet_posdata

      end if

      return
      end
```

ANNET_POSDATA.F95

```
      subroutine annet_posdata

!!    ~ ~ ~ PURPOSE ~ ~ ~ ~ ~ ~ ~ ~ ~ ~ ~ ~ ~ ~ ~ ~ ~ ~ ~ ~ ~ ~ ~ ~ ~ ~
!!    this subroutine reads the output data created by the annet
!!    model and inputs it to the SWAT model
```

```
!!    Author: Arthur Hrast Essenfelder
!!    E-mail: arthur.essenfelder@unive.it
!!
!!    Version: 1.0
!!    Last update on: 07/11/2016
!!
!!    ~ ~ ~ INCOMING VARIABLES ~ ~ ~ ~ ~ ~ ~ ~ ~ ~ ~ ~ ~ ~ ~ ~ ~ ~
!!    name              |units          |definition
!!    ------------------------------------------------------------
!!    inum1             |none           |subbasin id number
!!    ~ ~ ~ ~ ~ ~ ~ ~ ~ ~ ~ ~ ~ ~ ~ ~ ~ ~ ~ ~ ~ ~ ~ ~ ~ ~ ~ ~ ~ ~ ~
!!
!!    ~ ~ ~ OUTGOING VARIABLES ~ ~ ~ ~ ~ ~ ~ ~ ~ ~ ~ ~ ~ ~ ~ ~ ~ ~
!!    name              |units          |definition
!!    ------------------------------------------------------------
!!    vol_annet(:)      |m^3/day        |calculated flow in for the day
!!    arrData(1)        |m^3/s          |calculated flow in (cms)
!!    ~ ~ ~ ~ ~ ~ ~ ~ ~ ~ ~ ~ ~ ~ ~ ~ ~ ~ ~ ~ ~ ~ ~ ~ ~ ~ ~ ~ ~ ~ ~
!!
!!    ~ ~ ~ LOCAL DEFINITIONS ~ ~ ~ ~ ~ ~ ~ ~ ~ ~ ~ ~ ~ ~ ~ ~ ~ ~
!!    name              |units          |definition
!!    ------------------------------------------------------------
!!    ii                |none           |generic counter
!!    kk                |none           |generic counter
!!    arrSize           |none           |stores the size of the data array
!!    checkComma        |none           |counter number of "," in csv file
!!    csvLine           |none           |string to store the csv data
!!    ~ ~ ~ ~ ~ ~ ~ ~ ~ ~ ~ ~ ~ ~ ~ ~ ~ ~ ~ ~ ~ ~ ~ ~ ~ ~ ~ ~ ~ ~ ~
!!
!!    ~ ~ ~ SUBROUTINES/FUNCTIONS CALLED ~ ~ ~ ~ ~ ~ ~ ~ ~ ~ ~ ~ ~
!!    name              |type           |definition
!!    ------------------------------------------------------------
!!    funseason()       |function       |fun for the season of the year:
!!                                      |0 = error
!!                                      |1 = winter
!!                                      |2 = spring
!!                                      |3 = summer
!!                                      |4 = autumn
!!
!!    ~ ~ ~ ~ ~ ~ END SPECIFICATIONS ~ ~ ~ ~ ~ ~ ~ ~ ~ ~ ~ ~ ~ ~ ~

      !! Initial declarations ------------------------------------------
      use parm
      implicit none
      !! --------------------------------------------------------------

      !! Declaring Variables --------------------------------------------
      character(16) :: filename, filename1, filename2
      character(4) :: subcode
      character(2024) :: csvLine
```

```
      logical :: filecheck
      integer :: IOstatus
      integer :: ii, kk, icl, arrSize, checkComma
      real, allocatable :: arrData(:), arrPart(:)
      !! ------------------------------------------------------------------

      !! Preparaing the name of the output files ------------------------
      filename = "ySim"
      write(subcode, '(i4)') inum1
!      write(filename1, '(a16)') trim(filename) // &
!                                trim(adjustl(subcode)) // ".csv"
!      write(filename2, '(a16)') trim(filename) // "_" // &
!                                trim(adjustl(subcode)) // ".csv"
      write(filename1, '(a16)') trim(filename) // ".csv"
      write(filename2, '(a16)') trim(filename) // "_" // ".csv"
      filename1 = "ySim.csv"
      filename2 = "ySim_db.csv"
      !! ------------------------------------------------------------------

      !! Reading the data from the .csv file ----------------------------
      !! Checking if file exists
      inquire(file=filename1, exist=filecheck)
      if (filecheck) then
        open(115, file=filename1, action='read', status='old')
        read(115, *)
        read(115, '(a2024)') csvLine
        close(115)
      else
        csvLine = "0,0,0,0,0,0,0,0,0"
      end if
      csvLine = trim(csvLine)
      !! ------------------------------------------------------------------

      !! Counting the number of variables -------------------------------
      arrSize = 1
      checkComma = 0
      do
        if (index(csvLine(checkComma:len(csvLine)), ',') == 0) then
            exit
        end if
        checkComma = checkComma + &
                     index(csvLine(checkComma:len(csvLine)), ',')
        arrSize = arrSize + 1
      end do
      allocate(arrData(arrSize))
      !! ------------------------------------------------------------------

      !! Getting the data values ----------------------------------------
      !! Checking if file exists
      inquire(file=filename1, exist=filecheck)
```

```
      if (filecheck) then
        open(115, file=filename1, action='read', status='old')
        read(115, *)
        read(115, *) arrData
        close(115)
      else
        arrData = 0.
      end if
      !! ------------------------------------------------------------------

      !! Partitioning the total flow per resurgence sub-basin ------------
      !! Reading the file containing the partitioning information
      inquire(file="file_annet.csv", exist=filecheck)
      if (filecheck) then
        allocate(arrPart(2))
        arrPart = 0.
        open(120, file="file_annet.csv", action='read', status='old')
        read(120, *)
        !! Importing the data from the ANnet model ----------------------
        do
            read(120, *, IOSTAT=IOstatus) arrPart
            if (IOstatus < 0) then
                exit
            else
                kk = INT(arrPart(1))
                do ii=1, 9
                    vol_annet(ii,kk) = arrData(ii) * arrPart(2)
                end do
            endif
        end do
        close(120)
        !! ------------------------------------------------------------------
      else
        arrPart = 0.
      end if
      !! ------------------------------------------------------------------

      !! Writting results to file ----------------------------------------
      !! Checking if file exists, otherwise create it
      inquire(file=filename2, exist=filecheck)
      if (filecheck) then
        open(9980, file=filename2, action='write', status='old', &
             access='append')
      else
        open(9980, file=filename2, action='write', status='replace')
        write(9980, 1001)
      end if
      !! Write the data to the file
      do kk=1,msub
        write(9980, 1004, advance = 'no') kk
```

```
        write(9980, 1003, advance = 'no') ","
        write(9980, 1004, advance = 'no') i_mo
        write(9980, 1003, advance = 'no') ","
        write(9980, 1004, advance = 'no') icl(iida)
        write(9980, 1003, advance = 'no') ","
        write(9980, 1004, advance = 'no') iyr
        write(9980, 1003, advance = 'no') ","
        do ii=1,9
            write(9980, 1002, advance = 'no') vol_annet(ii,kk)
            if (ii /= arrSIZE) then
                write(9980, 1003, advance = 'no') ","
            end if
        end do
        write(9980, *)
      end do
      close(9980)
      !! ------------------------------------------------------------------

1001  format ("RCH,MO,DA,YR,FLOW,ORGN,NH4,NO2,NO3,ORGP,MINP,BOD,DO")
1002  format (f10.4)
1003  format (a1)
1004  format (i4)

      return
      end
```

FUNSEASON.F95

```
      function funseason(iday) result(iseason)

!!    ~ ~ ~ PURPOSE ~ ~ ~ ~ ~ ~ ~ ~ ~ ~ ~ ~ ~ ~ ~ ~ ~ ~ ~ ~ ~ ~ ~ ~ ~ ~
!!    given the day and the month, this function returns the season
!!
!!    ~ ~ ~ INCOMING VARIABLES  ~ ~ ~ ~ ~ ~ ~ ~ ~ ~ ~ ~ ~ ~ ~ ~ ~ ~ ~
!!    name         |units          |definition
!!    ------------------------------------------------------------
!!    iday         |none           |day of the year, integer
!!    ~ ~ ~ ~ ~ ~ ~ ~ ~ ~ ~ ~ ~ ~ ~ ~ ~ ~ ~ ~ ~ ~ ~ ~ ~ ~ ~ ~ ~ ~ ~ ~
!!
!!    ~ ~ ~ OUTGOING VARIABLES  ~ ~ ~ ~ ~ ~ ~ ~ ~ ~ ~ ~ ~ ~ ~ ~ ~ ~ ~
!!    name         |units          |definition
!!    ------------------------------------------------------------
!!    iseason      |none           |season of the year, integer:
!!                                 |0 = error
!!                                 |1 = winter
!!                                 |2 = spring
!!                                 |3 = summer
```

```
!!                                  |4 = autumn
!!    ~ ~ ~ ~ ~ ~ ~ ~ ~ ~ ~ ~ ~ ~ ~ ~ ~ ~ ~ ~ ~ ~ ~ ~ ~ ~ ~ ~ ~ ~ ~ ~ ~ ~ ~
!!
!!    ~ ~ ~ LOCAL DEFINITIONS ~ ~ ~ ~ ~ ~ ~ ~ ~ ~ ~ ~ ~ ~ ~ ~ ~ ~ ~ ~ ~
!!    name          |units          |definition
!!    ------------------------------------------------------------
!!                  |               |
!!    ~ ~ ~ ~ ~ ~ ~ ~ ~ ~ ~ ~ ~ ~ ~ ~ ~ ~ ~ ~ ~ ~ ~ ~ ~ ~ ~ ~ ~ ~ ~ ~ ~ ~ ~
!!
!!    ~ ~ ~ SUBROUTINES/FUNCTIONS CALLED  ~ ~ ~ ~ ~ ~ ~ ~ ~ ~ ~ ~ ~ ~ ~
!!    none
!!
!!    ~ ~ ~ ~ ~ ~ END SPECIFICATIONS  ~ ~ ~ ~ ~ ~ ~ ~ ~ ~ ~ ~ ~ ~ ~ ~ ~

      implicit none

      integer :: iday, iseason

      if (iday <= 79) then
        iseason = 1 !! winter
      elseif (iday <= 171) then
        iseason = 2 !! spring
      elseif (iday <= 265) then
        iseason = 3 !! summer
      elseif (iday <= 355) then
        iseason = 4 !! autumn
      elseif (iday <= 366) then
        iseason = 1 !! winter
      else
        iseason = 0 !! error
      end if

      end function funseason
```

Appendix 2 – ANnet Model

Model Description

This appendix chapter describes the theory behind the developed ANN model. This chapter is largely based on consolidated knowledge regarding the implementation and use of ANN models. The following publications were used as key references for the writing of this appendix chapter:

1. Haykin, S., 2001. Neural Networks: A Comprehensive Foundation, 2nd Edition. Prentice Hall, Inc., Upper Saddle River, NJ, USA.

2. Hsieh, W. W., 2009. Machine Learning Methods in the Environmental Sciences: Neural Networks and Kernels. Cambridge University Press, New York, NY, USA.

3. Wilamowski, B. M., Irwin, J. D., 2011. The Industrial Electronics Handbook: Intelligent Systems, 2nd Edition. CRC Press, Inc., New York, NY, USA.

The developed model ANN consists of a MLP neural networks model and can be configured to accommodate one or two hidden layers of neurons, each having a varying number of neurons. Any neuron from a specific layer is connected to all neurons of the subsequent layer, but neurons of a same layer are never connected among themselves. In such a way, the information is propagated forward from the input layer to the output layer, resulting in an ANN model type known as *feedforward*. Figure A3.1 depicts an example of a neuron model in a feedforward ANN model.

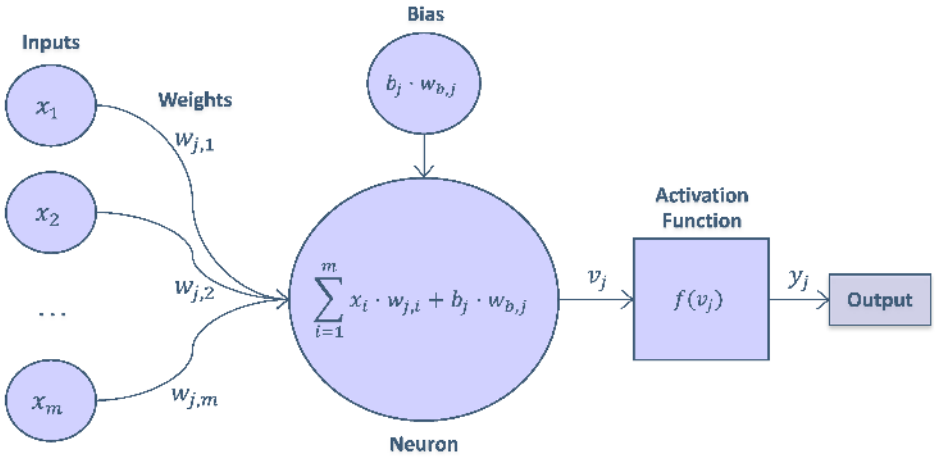

Figure A3.1: An example of a neuron model.

The developed ANN model is capable of being configured as a simple Input-Output – I-O model, as a Delayed Input-Output – I-O.d model, as Non-Linear Autoregressive – NAR, or as a Non-Linear Autoregressive with Exogenous Inputs – NARX model variants. When the model type NAR or NARX is selected, it is possible to run the model as open-loop or close-loop variants[6]. The Section Model Type Variants describes in details the available model type variants.

Regarding the training process, the developed ANN model is built upon the use of a supervised training methodology known as *backpropagation*. Two training algorithms are available, namely: i. The Steepest-Descent algorithm, and; ii. The Levenberg-Marquardt algorithm. During the training procedure, the model evaluates the evolution of the SSE of the calculated outputs with regards to previously known targets as a way of assessing the generalisation property of the resulting neural networks model. Finally, the model was developed in R language and is capable of running in multi-core cluster systems.

[6]An open-loop variant means that autoregressive information of the model comes from direct user feedback inputs during the whole simulation period, while a close-loop variant replaces the feedback inputs with a direct connection between the output and input layers.

Model Type Variants

The developed ANN model can be configured as four distinct variants, each of which is described in this Section. As the developed ANN model is based upon a MLP neural networks model, the way the information is propagated throughout the network is similar in all available model type variants. The general equations which describe this process are presented below:

$$u_{k,j} = \sum_{i=1}^{n} x_{k,i} \cdot w_{i,j} \tag{A3.1}$$

$$v_{k,j} = u_{k,j} + b_j \cdot wb_j \tag{A3.2}$$

$$y_{k,j} = f\left(v_{k,j}\right) \tag{A3.3}$$

where i is the index of a neuron in the previous layer; j is the index of a neuron in the current layer; k is the index of input-output patterns; n is the total number of neurons in the previous layer; $x_{k,i}$ is the input signal of a neuron i from a previous layer to a neuron j in the current layer for an input-output patter k; $w_{i,j}$ is the weight connection value between a neuron i from a previous layer with a neuron j in the current layer; $u_{k,j}$ is the linear output of neuron j for an input-output pattern k; b_j is the neuron j bias signal; wb_j is the bias weight connection with neuron j; $v_{k,j}$ is the activation potential of neuron j for input-output pattern k; $f\left(.\right)$ is the activation function, and; $y_{k,j}$ is the real neuron output of neuron j for input-output pattern k.

Input-Output

The developed I-O model type variant is a MLP ANN model consisting of one input layer with a varying number of input nodes, one or two hidden layer with a varying number of neurons per layer, and one output layer with a single output neuron[7]. An example of a I-O ANN model type variant is depicted in Figure A3.2, whileFigure A3.1 depicts the flow of information in a neuron model.

In mathematical terms, the information is propagated forward as follows:

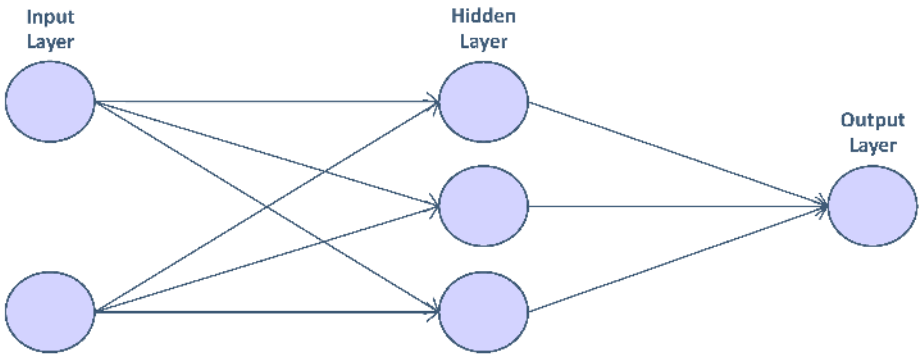

Figure A3.2: Example of an I-O ANN model.

In the I-O model type variant, the information in the input layer is not processed, meaning that x_i and y_j are equal for this layer. This information is used as input signals for the neurons in the first hidden layer, being processed and propagated forward in the network until reaching the output layer.

Delayed Input-Output

The I-O.d model type variant is very similar to the I-O model type variant, working using the same set of equations and information flow. The only difference is that each neuron in the input layer can be delayed by a positive integer number of times, and the variable x_i would also depend on a time dimension. In essence, this modification increases the quantity of input information. For instance, considering the example in Figure A3.2 where the input layer has 2 neurons and supposing a time delay of 3 steps, the input layer of this I-O.d model would then be equivalent to an I-O model type variant of 8 input neurons, which is the result of the original 2 (i.e. not time delayed information) plus 6 delayed neurons (i.e. 3 for each input neuron). Figure A3.3 depicts how a model configured in such a way would look like.

The I-O.d model type variant has some advantages over the I-O model type variant, the most significant one being the fact that the ANN model has now

[7] The developed model is constrained to a single neuron in the output layer.

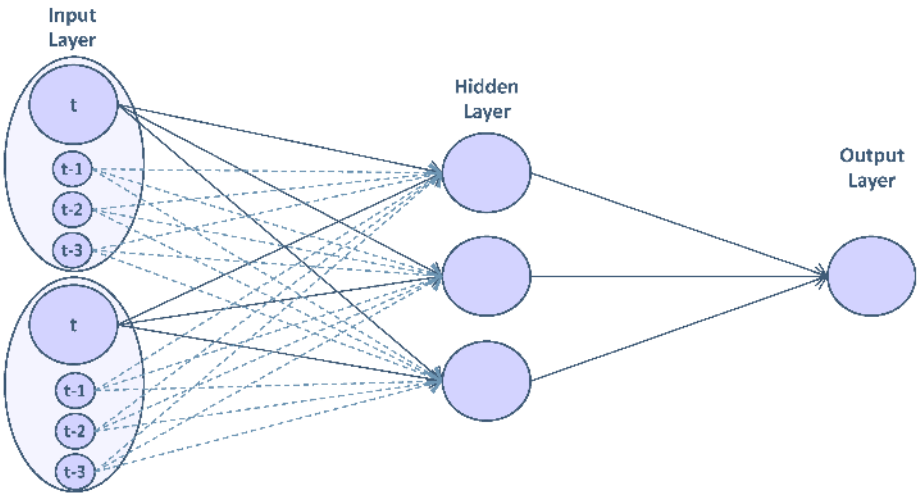

Figure A3.3: Example of an I-O.d ANN model.

a memory of previous input patterns by considering information coming from previous time steps. Besides the need of more computational requirements due to a larger network, another disadvantage of this approach is the fact that all the input information must be continuous for the desired delay time step, otherwise the notion of memory is invalid.

Non-Linear Autoregressive

The principles behind the NAR model type variant are similar to the I-O.d model type variant, the difference being the fact that the inputs to the NAR model type variant are actually the information coming from the output layer itself. Mathematically, the inputs of the input layer (e.g. x_i) are equal to the information coming from the output layer (i.e. $y_{k,j}$ if close-cloop or $t_{k,j}$ if open-loop, where $t_{k,j}$ is the target value of neuron j for input-output pattern k, an information required by the model during the supervised training procedure). An example of a NAR model type variant is shown in Figure A3.4.

A NAR ANN model is a good choice for time-series prediction problems, requiring, however, a larger dataset in order to avoid the over-fitting problem of ANN models.

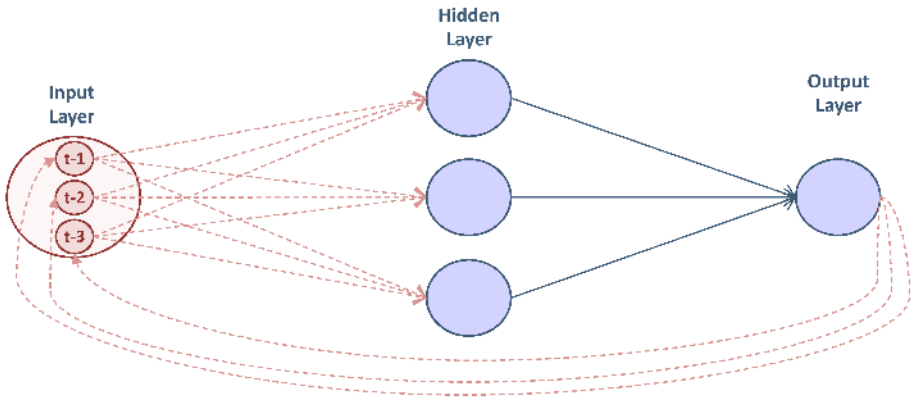

Figure A3.4: Example of a NAR ANN model.

Non-Linear Autoregressive with Exogenous Inputs

Finally, the last model type variant available is known as NARX. This type of ANN model is, in essence, a mix between the I-O.d and NAR model type variants. Mathematically, the exogenous inputs are treated as a I-O.d model type, thereby taking time into consideration, while the autoregressive nature of the model is processed as a NAR model, meaning that the autoregressive inputs of the model (e.g. x_i) are be equal to the information coming from the output layer (i.e. y_j if close-cloop or t_j if open-loop). Figure A3.5 depicts an example of this model.

The NARX ANN model type variant carries both the advantages and disadvantages of the I-O.d and NAR model type variants. It is, however, the most powerful tool in a scenario where input information availability and computational processing power is not an issue.

Training Procedure

The developed ANN model utilises a supervised learning procedure known as backpropagation. A supervised learning procedure consists in performing the training procedure of an ANN by using a teacher. In a conceptual approach,

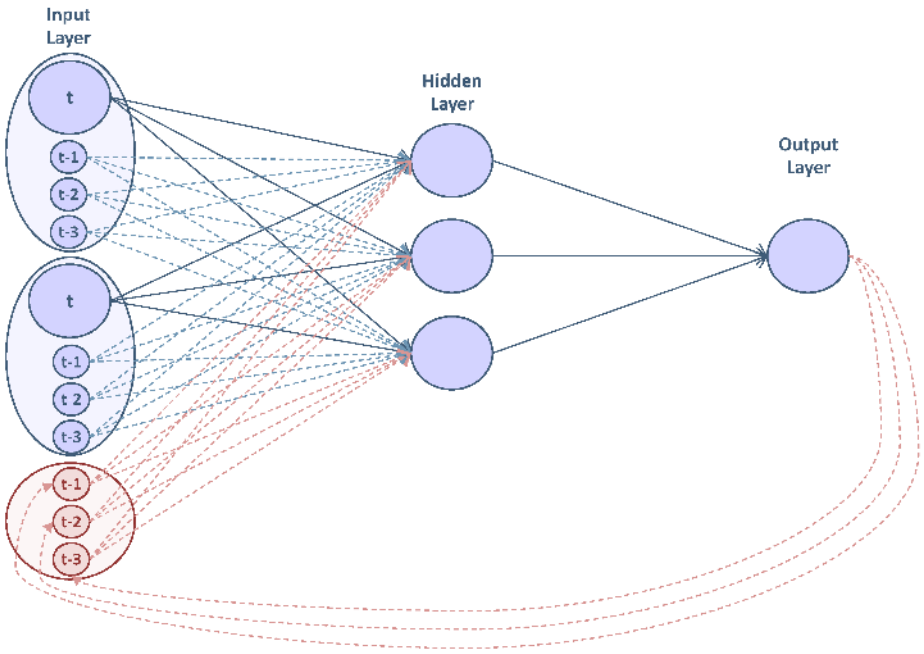

Figure A3.5: Example of a NARX ANN model.

a teacher is someone who has knowledge of the environment of interest. The teacher, in an ANN model, is basically a set of input-output patterns which are the optimal solution for the specific problem to which the ANN model is being applied. The backpropagation procedure can be understood as the process in which the ANN model is able to learn from the knowledge shared by the teacher. Mathematically, the problem can be seen as an optimisation problem, where objective function is the total error in the output layer subject to the weight connections plan. Hence, it consists in calculating a correction in the weight connections between the neurons of the model with respect to the errors observed in the output layer, which are propagated backwards to previous layers, hence the name backpropagation. The training process is repeated until a satisfactory training state. The total error in the output layer, calculated here as the SSE, is calculated as follows:

$$e_{k,m_j} = l_{k,m_j} - y_{k,m_j} \tag{A3.4}$$

$$E(\mathbf{x}, \mathbf{w}) = \frac{1}{2} \cdot \sum_{k=1}^{K} \sum_{m_j=1}^{m} e_{k,m_j}^2 \tag{A3.5}$$

where k is the index of input-output patterns; K is total number of input-output patterns; m_j is the index of a neuron in the output layer; m is the total number of neurons in the output layer; t_{k,m_j} is the output target of neuron m_j for an input-output pattern k; e_{k,m_j} is the absolute error between the real output and the target of neuron m_j for for an input-output pattern k; $\mathbf{x}$ is the input vector; $\mathbf{w}$ is the weight vector, and; $E(\mathbf{x}, \mathbf{w})$ is the total SSE of the model's outputs.

Steepest Descent

The steepest descent algorithm relies on the calculation of the first order derivatives of the total error function $E(\mathbf{x}, \mathbf{w})$ in order to find the closest minima error in the error space. The corrections are made with respect to a gradient vector g. In order to be applicable, the steepest descent algorithm requires the ANN model to be configured utilising activation functions that are differentiable. A list of functions that can be used as activation functions is shown in the following Section. The calculation of g and respective weight connections update is done as follows:

$$\mathbf{g} = \frac{\partial E(\mathbf{x}, \mathbf{w})}{\partial \mathbf{w}} = \left[\frac{\partial E}{\partial w_1}, \frac{\partial E}{\partial w_2}, \ldots, \frac{\partial E}{\partial w_N} \right] \tag{A3.6}$$

$$\mathbf{w_{t+1}} = \mathbf{w_t} - \alpha \cdot \mathbf{g_t} \tag{A3.7}$$

where t is the index of training iterations; N is the total number of weight connections in the network (i.e. the number of all i and j weight connections); α is the learning constant[8]; $\mathbf{w_t}$ is the current weight vector, and; $\mathbf{w_{t+1}}$ is the updated weight vector.

The steepest descent algorithm is know to be a stable training algorithm and relatively easy to be implemented. However, this procedure is also known to be

[8] The learning constant is a value that varies between 0 and 1, controlling the rate of learning.

of slow convergence. Besides, due to the curvature of the error surface, solutions found when using the steepest descent algorithm may not be the best solution globally.

Levenberg-Marquardt

The Levenberg-Marquardt training algorithm provides another option to numerically solve the problem of minimising the non-linear error function of ANN models. Basically, this algorithm blends the previously introduced steepest descent and the Gauss-Newton algorithms altogether. The Gauss-Newton algorithm, in turn, is an approximation of the Newton's Method, introducing the concept of the Jacobian matrix $\mathbf{J}$ as a way to approximate the calculation of the Hessian matrix $\mathbf{H}$. Mathematically, the Levenberg-Marquardt algorithm approximates $\mathbf{H}$ as follows:

$$\mathbf{H} \approx \mathbf{J}^T \cdot \mathbf{J} + \mu \cdot \mathbf{I} \tag{A3.8}$$

where:

$$\mathbf{J} = \begin{bmatrix} \frac{\partial e_{1,1}}{\partial w_1} & \frac{\partial e_{1,1}}{\partial w_2} & \cdots & \frac{\partial e_{1,1}}{\partial w_N} \\ \frac{\partial e_{1,2}}{\partial w_1} & \frac{\partial e_{1,2}}{\partial w_2} & \cdots & \frac{\partial e_{1,2}}{\partial w_N} \\ \vdots & \vdots & \ddots & \vdots \\ \frac{\partial e_{1,m}}{\partial w_1} & \frac{\partial e_{1,m}}{\partial w_2} & \cdots & \frac{\partial e_{1,m}}{\partial w_N} \\ \vdots & \vdots & \ddots & \vdots \\ \frac{\partial e_{K,m}}{\partial w_1} & \frac{\partial e_{K,m}}{\partial w_2} & \cdots & \frac{\partial e_{K,m}}{\partial w_N} \end{bmatrix} \tag{A3.9}$$

and:

$$\frac{\partial e_{k,m_j}}{\partial w_{i,j}} = -s_{k,j} \cdot F\left(y_{k,j}\right)'_{m_j,j} \cdot x_{k,i} \tag{A3.10}$$

where k is the index of input-output patterns; K is total number of input-output patterns; m_j is the index of a neuron in the output layer; m is the total number of neurons in the output layer; i is the index of a neuron in the previous layer; j is the index of a neuron in the current layer; N is the total number of

weight connections (i.e. the number of all i and j weight connections); $s_{k,j}$ is the slope of the activation function $f(.)$ of neuron j for input-output pattern k; $y_{k,j}$ is the real neuron output of neuron j for an input-output pattern k; $x_{k,i}$ is the input signal of a neuron i from a previous layer to a neuron j in the current layer for an input-output patter k; $F(y_{k,j})'_{m_j,j}$ is the derivative of non-linear function between neuron m_j output and neuron j output; μ is the combination coefficient[9], and; $\mathbf{I}$ is the identity matrix.

Finally, the weight updates can be computed as follows:

$$\mathbf{w_{t+1}} = \mathbf{w_t} - \left(\mathbf{J}_t^T \cdot \mathbf{J}_t + \mu \cdot \mathbf{I}\right)^{-1} \cdot \mathbf{J}_t \cdot \mathbf{e}_t \tag{A3.11}$$

where t is the index of training iterations; $\mathbf{e_t}$ is the error vector of the outputs; $\mathbf{w_t}$ is the current weight vector, and; $\mathbf{w_{t+1}}$ is the updated weight vector.

The Levenberg-Marquardt algorithm is a very stable and fast training algorithm if compared to the steepest descent. However, because it involves the computation of the Jacobian matrix (Eq. A3.9) and the calculation of the inverse of a matrix (Eq. A3.7), it is usually applied only to problems with relatively small patterns due to the huge computational demand in more complex problems.

Auxiliary Functions

This section brings a collection of auxiliary functions that may or may no be used by the developed ANN model. This section is sub-divided in two sub-sections: i. The first sub-section displays the equations that may be utilised to perform the normalisation of the input data, and; ii. The second sub-section brings all the available activation functions.

[9] The parameter μ controls the training process of the Levenberg-Marquardt algorithm. When μ is very small, Eq. A3.7 resembles the Gauss-Newton algorithm; when μ is very large, Eq. A3.7 resembles the steepest descent algorithm.

Normalisation Functions

The developed ANN model can normalise the input data if requested. The following normalisation functions are available:

$$x_{norm} = \frac{x - x_{min}}{x_{max} - x_{min}} \tag{A3.12}$$

$$x_{norm} = \frac{x - x_{mean}}{x_{stDev}} \tag{A3.13}$$

where x is the information to be normalised; x_{min} is the minimum value of the $\mathbf{x}$ data vector; x_{max} is the maximum value of the $\mathbf{x}$ data vector; x_{mean} is the mean value of the $\mathbf{x}$ data vector; x_{stDev} is the standard deviation of the $\mathbf{x}$ data vector, and; x_{norm} is the normalised value.

If input data normalisation is applied, the developed ANN will denormalise the data after the data processing is finished. The denormalisation equations are shown below:

$$x_{denorm} = x_{norm} \cdot (x_{max} - x_{min}) + x_{min} \tag{A3.14}$$

$$x_{denorm} = x_{norm} \cdot x_{stDev} + x_{mean} \tag{A3.15}$$

where x_{denorm} is the denormalised value.

Neuron Activation Functions

The available activation functions are:

$$f(x) = x \tag{A3.16}$$

$$f(x) = \frac{1}{1 + e^{-a \cdot x}} \tag{A3.17}$$

$$f(x) = a \cdot tanh(b \cdot x) \tag{A3.18}$$

where x is the input variable for the activation function; a and b are shape coefficients, and; $f(.)$ is the activation function.

The derivatives of the activation functions are:

$$f(x)' = 1 \tag{A3.19}$$

$$f(x)' = \frac{a \cdot e^{-a \cdot x}}{(1 + e^{-a \cdot x})^2} \tag{A3.20}$$

$$f(x)' = a \cdot b \cdot \left(1 - tanh(b \cdot x)^2\right) \tag{A3.21}$$

where $f(.)'$ is the first derivative of the activation function.

Appendix 3 – ANnet Model

Source Code

This appendix chapter brings the source code of the implemented ANN model, called ANnet. The model is written in R language and is implemented as a function. The ANnet function is split in several modules and three main sections: i. The first section presents the main ANnet function, which is responsible for receiving the inputs from the user, calling the auxiliary functions and model variants, and returning the results to the user; ii. The second section presents the two ANN model architecture variants; iii. The third section presents the auxiliary functions.

ANnet Function

ANnet – Main Function

```
################################################################################
############### ANnet - ARTIFICIAL NEURAL NETWORKS PROGRAM ###############
################################################################################
#
# This source code is the main function to call the other ANnet
#  program/function variants (e.g. 1-or-2-hidden layered, training
#  methods, optimisation algorithms, etc.)
#
# default option = DEF
#
# Specifications:
# NAME                  | CLASS/TYPE   | DESCRIPTION
```

```
#-------------------------------------------------------------------------------
# Input                | data.frame   | Input data.frame (row data)
# Target               | data.frame   | Target data.frame (row data)
# Model.Type           | character    | One of the following:
#                      |              |   "Input-Output" (DEF)
#                      |              |   "Delayed Input-Output"
#                      |              |   "NAR"
#                      |              |   "NARX"
# Model.Type.Variant   | character    | One of the following:
#                      |              |   "Open-Loop" (DEF)
#                      |              |   "Close-Loop"
#                      |              | OBS: Used only for NAR/NARX types
# Time.Delay           | integer      | Number of time step delays
#                      |              | *** Not used when Model.Type is
#                      |              |     "Input-Output"
#                      |              |   DEF: 0
# Data.Normalisation   | logical      | Toggles data normalisation
#                      |              |   DEF: TRUE
# Normalisation.Method | character    | One of the following:
#                      |              |   "Feature scaling [0:1]" (DEF)
#                      |              |   "Feature scaling [-1:1]"
#                      |              |   "Standard Score"
# Model.Structure      | character    | One of the following:
#                      |              |   "1-Hidden-Layered" (DEF)
#                      |              |   "2-Hidden-Layered"
# Hidden.Layer.Neurons | integer(:)   | Number of neurons-hidden layer(s)
#                      |              |   c(h) OR c(h1,h2)
#                      |              |   DEF: (i+j)*2/3 OR
#                      |              |   DEF: (i+j)*2/3 && (h1+j)*2/3
# ActFun.Names         | character(:) | Act. function names per layer
#                      |              | One of the following:
#                      |              |   "signum"
#                      |              |   "linear"
#                      |              |   "logsig"
#                      |              |   "tanh"
#                      |              |   DEF: c("tanh","linear") OR
#                      |              |   DEF: c("tanh","tanh","linear")
# ActFun.Parameter.a   | numeric(:)   | Act. function parameter a
#                      |              |   Must be of double type
#                      |              |   DEF: c(1.7159,1.0) OR
#                      |              |   DEF: c(1.7159,1.7159,1.0)
# ActFun.Parameter.b   | numeric(:)   | Act. function parameter b
#                      |              |   Must be of double type
#                      |              |   DEF: c(0.6667,1.0) OR
#                      |              |   DEF: c(0.6667,0.6667,1.0)
# Training.Function    | character    | One of the following:
#                      |              |   "Levenberg-Marquardt" (DEF)
#                      |              |   "Steepest-Descent"
# Dataset.Division.    | numeric(3)   | Fraction of training, validation
#   Factors            |              |   and test datasets
```

```
#                          |             |   Must be of double type
#                          |             |   DEF: c(0.70, 0.20, 0.10)
# Max.Ensemble.Objects|  integer      | Max number ANnet objects to save
#                          |             |   default = 1
# Max.Training.          | integer      | Maximum number training attempts
#   Attempts               |             |   default = 1
# Max.Training.          | integer      | Maximum number training epochs
#   Epochs                 |             |   default = 100
# Bias.Factor            | double       | Bias factor influence (-1 to 1)
#                          |             |   default = 1.
# Preload.Weights        | logical      | Check for load pre-configured net
#                          |             |   default = FALSE
# Preload.ANnet.Object| character    | Name of saved ANnet object to load
#                          |             |   the weight data from
#                          |             |   default = "net.RData"
# Print.Results          | logical      | Write numerical results on console
#                          |             |   default = TRUE
# Plot.Results           | logical      | Plot a series of graphical results
#                          |             |   default = TRUE
# Save.Results           | logical      | Save results to file
#                          |             |   default = TRUE
# Parallel.Processing | logical      | Enables parallelisation of tasks
#                          |             |   default = TRUE
# Number.Cores           | integer      | Maximum number of cores to use
#                          |             |   default = 1
#-------------------------------------------------------------------------
#
# Author: Arthur Hrast Essenfelder
# E-mail: arthur.essenfelder@gmail.com
#
# Version: 1.0
# Last update on: 18/11/2016
# Last modified by: Arthur Hrast Essenfelder
##############################################################################
##############################################################################

# Pre-Loading Libraries & Functions ==========================================
# Functions
source("ANnet-ModelTypeFunctions.R");
# ============================================================================

# ============================================================================
#### ========================= MAIN FUNCTION ========================= #####
# ============================================================================

# Initialising the ANnet Main Program ========================================
ANnet = function(Input, Target,
                 Model.Type, Model.Type.Variant, Time.Delay,
                 Data.Normalisation, Normalisation.Method,
                 Model.Structure, Hidden.Layer.Neurons,
```

```
                ActFun.Names,
                ActFun.Parameter.a, ActFun.Parameter.b,
                Training.Function, Dataset.Division.Factors,
                Max.Ensemble.Objects, Max.Training.Attempts,
                Max.Training.Epochs,
                Bias.Factor,
                Preload.Weights, Preload.ANnet.Object,
                Print.Results, Plot.Results, Save.Results,
                Parallel.Processing, Number.Cores) {

# Checking for missing parameters ------------------------------------
# Model Type related parameters --------------------------
if (missing(Model.Type)) { Model.Type = "Input-Output"; }
if (missing(Model.Type.Variant)) { Model.Type.Variant = "Open-Loop"; }
if (Model.Type == "Input-Output" ||
    Model.Type == "Delayed Input-Output" ||
    Model.Type == "NARX") {
  if (missing(Input))   { stop("Missing Input data.frame"); }
  if (missing(Target))  { stop("Missing Target data.frame"); }
} else if (Model.Type == "NAR") {
  if (missing(Target))  { stop("Missing Target data.frame"); }
  if (missing(Input))   { Input = Target; }
}
if (missing(Time.Delay)) { Time.Delay = as.integer(0); }
else { Time.Delay = as.integer(Time.Delay); }
# Data Normalisation related parameters ------------------
if (missing(Data.Normalisation)) { Data.Normalisation = TRUE; }
if (missing(Normalisation.Method)) {
  Normalisation.Method = "Feature scaling [0:1]";
}
# Model structure related paramteres ---------------------------
if (missing(Model.Structure)) {
  Model.Structure = "1-Hidden-Layered";
}
if (missing(Hidden.Layer.Neurons)) {
  i = ncol(fTimeDelayData(Input,Target,Model.Type,Time.Delay));
  j = ncol(Target);
  if       (Model.Structure == "1-Hidden-Layered") {
    Hidden.Layer.Neurons = as.integer(round(2/3*(i+j)));
  } else if (Model.Structure == "2-Hidden-Layered") {
    Hidden.Layer.Neurons    = c(0,0);
    Hidden.Layer.Neurons[1] = as.integer(round(2/3*(i+j)));
    Hidden.Layer.Neurons[2] = as.integer(round(2/3*
                                      (Hidden.Layer.Neurons[1]+j)));
  }
}
Hidden.Layer.Neurons = as.integer(Hidden.Layer.Neurons);
# Activation Function related parameters -----------------
if (missing(ActFun.Names)) {
  if       (Model.Structure == "1-Hidden-Layered") {
```

```
    ActFun.Names = c("tanh","linear");
  } else if (Model.Structure == "2-Hidden-Layered") {
    ActFun.Names = c("tanh","tanh","linear");
  }
}
if (missing(ActFun.Parameter.a)) {
  a = as.vector(array(0., dim=length(ActFun.Names)));
  for (i in 1:length(ActFun.Names)) {
    if (ActFun.Names[i] == "signum") { a[i] = 1.; }
    if (ActFun.Names[i] == "linear") { a[i] = 1.; }
    if (ActFun.Names[i] == "logsig") { a[i] = 1.; }
    if (ActFun.Names[i] == "tanh")   { a[i] = 1.7159; }
  }
  ActFun.Parameter.a = a;
  rm(i,a);
}
if (missing(ActFun.Parameter.b)) {
  b = as.vector(array(0., dim=length(ActFun.Names)));
  for (i in 1:length(ActFun.Names)) {
    if (ActFun.Names[i] == "signum") { b[i] = 1.; }
    if (ActFun.Names[i] == "linear") { b[i] = 1.; }
    if (ActFun.Names[i] == "logsig") { b[i] = 1.; }
    if (ActFun.Names[i] == "tanh")   { b[i] = 0.6667; }
  }
  ActFun.Parameter.b = b;
  rm(i,b);
}
# Training Function related parameter ----------------------
if (missing(Training.Function)) {
  Training.Function = "Levenberg-Marquardt";
}
if (missing(Dataset.Division.Factors)) {
  Dataset.Division.Factors = c(0.7, 0.20, 0.10);
}
if (missing(Max.Ensemble.Objects)) {
  Max.Ensemble.Objects = as.integer(1)
} else {
  Max.Ensemble.Objects = as.integer(Max.Ensemble.Objects);
}
if (missing(Max.Training.Attempts)) {
  Max.Training.Attempts = as.integer(1)
} else {
  Max.Training.Attempts = as.integer(Max.Training.Attempts);
}
if (missing(Max.Training.Epochs)) {
  Max.Training.Epochs   = as.integer(100)
}
else {
  Max.Training.Epochs = as.integer(Max.Training.Epochs);
}
```

```
# Bias Factor ------------------------------------------------
if (missing(Bias.Factor)) { Bias.Factor = 1.0; }
# Preload Weight Data ----------------------------------------
if (missing(Preload.Weights))       {Preload.Weights=FALSE;}
if (missing(Preload.ANnet.Object)) {Preload.ANnet.Object="net.RData";}
# Print Results ----------------------------------------------
if (missing(Print.Results)) { Print.Results = TRUE; }
if (missing(Plot.Results))  { Plot.Results  = TRUE; }
if (missing(Save.Results))  { Save.Results  = TRUE; }
# Parallelisation and Multitasking ---------------------------
if (missing(Parallel.Processing)) {
  Parallel.Processing = TRUE;
}
if (Parallel.Processing) { suppressMessages(library(parallel)); }
if (missing(Number.Cores)) {
  if (Parallel.Processing) {
    Number.Cores = as.integer(detectCores(TRUE));
  }
  else {
    Number.Cores = as.integer(1);
  }
} else { Number.Cores = as.integer(Number.Cores); }
#------------------------------------------------------------------

# Checking if input data class and type are correct ----------------
CheckClass = TRUE; # Classes are OK if TRUE
# Input and Target data.frames -------------------------------
CheckClass = fCheckClass(Input,  "data.frame", CheckClass);
CheckClass = fCheckClass(Target, "data.frame", CheckClass);
# Model Type and Time Delay related parameters ----------------
CheckClass = fCheckClass(Model.Type,         "character", CheckClass);
CheckClass = fCheckClass(Model.Type.Variant, "character", CheckClass);
CheckClass = fCheckClass(Time.Delay,         "integer",   CheckClass);
# Data Normalisation related parameters ----------------------
CheckClass = fCheckClass(Data.Normalisation,  "logical",  CheckClass);
CheckClass = fCheckClass(Normalisation.Method,"character",CheckClass);
# Model structure related paramteres -------------------------
CheckClass = fCheckClass(Model.Structure,     "character",CheckClass);
CheckClass = fCheckClass(Hidden.Layer.Neurons,"integer",  CheckClass);
# Activation Function related parameters ---------------------
CheckClass = fCheckClass(ActFun.Names,
                         "character", CheckClass);
CheckClass = fCheckClass(ActFun.Parameter.a, "numeric", CheckClass);
CheckClass = fCheckClass(ActFun.Parameter.b, "numeric", CheckClass);
# Training Function related parameter ------------------------
CheckClass = fCheckClass(Training.Function, "character", CheckClass);
CheckClass = fCheckClass(Dataset.Division.Factors,
                         "numeric", CheckClass);
CheckClass = fCheckClass(Max.Ensemble.Objects,
                         "integer", CheckClass);
```

```
CheckClass = fCheckClass(Max.Training.Attempts,
                         "integer", CheckClass);
CheckClass = fCheckClass(Max.Training.Epochs,
                         "integer", CheckClass);
# Bias Factor ------------------------------------------------
CheckClass = fCheckClass(Bias.Factor, "numeric", CheckClass);
# Preload Weight Data ----------------------------------------
CheckClass = fCheckClass(Preload.Weights,     "logical",  CheckClass);
CheckClass = fCheckClass(Preload.ANnet.Object,"character",CheckClass);
# Print Results ----------------------------------------------
CheckClass = fCheckClass(Print.Results, "logical", CheckClass);
CheckClass = fCheckClass(Plot.Results,  "logical", CheckClass);
CheckClass = fCheckClass(Save.Results,  "logical", CheckClass);
# Parallelisation and Multitasking ---------------------------
CheckClass = fCheckClass(Parallel.Processing, "logical", CheckClass);
CheckClass = fCheckClass(Number.Cores,        "integer", CheckClass);
# Check if any class is incorrect ----------------------------
if (CheckClass == FALSE) {
  rm(CheckClass);
  stop("ANnet program is terminating due to errors");
} else { rm(CheckClass); }
#-------------------------------------------------------------------

# If running on a cluster, prepare the cluster ---------------------
if (Parallel.Processing) {
  # Checking if Number.Cores is <= 0 -------------------------
  if (Number.Cores <= 0) { Number.Cores = as.integer(1); }
  # Updating the number of cores to optimise core usage
  while ((Max.Training.Attempts/Number.Cores) < 1.) {
    Number.Cores = Number.Cores - 1;
  }
  # Checking, again, if Number.Cores is <= 0 -----------------
  if (Number.Cores <= 0) { Number.Cores = as.integer(1); }
  # Creating the cluster, only if Number.Cores > 1 ----------
  if (Number.Cores > 1) {
    cl = makePSOCKcluster(Number.Cores);
    # Updating the Max.Training.Attempts to a vector
    tmp = integer(length = Number.Cores);
    for (i in 1:Number.Cores) {
      if (i < Number.Cores) {
        tmp[i] = as.integer(round(Max.Training.Attempts/Number.Cores,
                                  digits = 0));
      } else {
        tmp[i] = as.integer(Max.Training.Attempts - sum(tmp));
      }
    }
    Max.Training.Attempts = tmp;
    rm(tmp);
    # Message number of cores to use ---------------------------
    message("ANnet fuction will use", Number.Cores, " cores");
```

```
  }
}
#-------------------------------------------------------------------------

# Checking for possible user errors in the input data ------------------
CheckInputs = TRUE; # Inputs are OK if TRUE
CheckInputs = fCheckInputs(Input, Target,
                           Model.Type, Model.Type.Variant, Time.Delay,
                           Normalisation.Method,
                           Model.Structure, Hidden.Layer.Neurons,
                           ActFun.Names,
                           ActFun.Parameter.a, ActFun.Parameter.b,
                           Training.Function, Dataset.Division.Factors,
                           Max.Ensemble.Objects, Max.Training.Attempts,
                           Max.Training.Epochs,
                           Bias.Factor,
                           Preload.Weights, Preload.ANnet.Object,
                           CheckInputs);
# Check if any class is incorrect ------------------------------
if (CheckInputs == FALSE) {
  rm(CheckInputs);
  stop("ANnet program is terminating due to errors");
} else { rm(CheckInputs); }
#-------------------------------------------------------------------------

# Calling the ANnet function -------------------------------------------
#Printing progress ----------------------------------------
cat("Progress: ");
progressBar = txtProgressBar(0, Max.Ensemble.Objects, style=3);
progressCount = 0;
# Preparing the list object to store the results-----------
ANnetListHeader = paste(rep("net", Max.Ensemble.Objects),
                        c(1:Max.Ensemble.Objects), sep = "");
ANnetList = vector("list", Max.Ensemble.Objects);
names(ANnetList) = ANnetListHeader;
rm(ANnetListHeader);
# Calling the ANnet function -------------------------------
for (iEnsemble in 1:Max.Ensemble.Objects) {
  source("ANnet-Training.R");
  if (Parallel.Processing && Number.Cores > 1) {
    clusterEvalQ(cl, {source("ANnet-Training.R")});
    netcl = parLapply(cl, Max.Training.Attempts, ANnetTraining,
                  Input=Input, Target=Target,
                  Model.Structure=Model.Structure,
                  Model.Type=Model.Type,
                  Model.Type.Variant=Model.Type.Variant,
                  Time.Delay=Time.Delay,
                  Data.Normalisation=Data.Normalisation,
                  Normalisation.Method=Normalisation.Method,
                  Hidden.Layer.Neurons=Hidden.Layer.Neurons,
```

```
                    ActFun.Names=ActFun.Names,
                    ActFun.Parameter.a=ActFun.Parameter.a,
                    ActFun.Parameter.b=ActFun.Parameter.b,
                    Training.Function=Training.Function,
                    Dataset.Division.Factors=Dataset.Division.Factors,
                    Max.Training.Epochs=Max.Training.Epochs,
                    Bias.Factor=Bias.Factor,
                    Preload.Weights=Preload.Weights,
                    Preload.ANnet.Object=Preload.ANnet.Object);
  } else {
    net = tryCatch({ANnetTraining(Max.Training.Attempts,
                            Input, Target,
                            Model.Structure, Model.Type,
                            Model.Type.Variant, Time.Delay,
                            Data.Normalisation, Normalisation.Method,
                            Hidden.Layer.Neurons,
                            ActFun.Names,
                            ActFun.Parameter.a, ActFun.Parameter.b,
                            Training.Function,
                            Dataset.Division.Factors,
                            Max.Training.Epochs,
                            Bias.Factor,
                            Preload.Weights, Preload.ANnet.Object)},
                   error=function(e) {
                     message("An␣error␣occurred␣while␣calling␣the␣",
                             "function␣ANnetTraining");
                     message(e);
                     stop("The␣program␣is␣terminating");
                   });
  }
  # If running on a cluster, extract best result ----------
  if (Parallel.Processing && Number.Cores > 1) {
    for (i in 1:length(netcl)) {
      if (i == 1) {
        net = netcl[[i]];
      } else {
        if (min(slot(net,         "TrainingResults")$SSE[2,]) >
            min(slot(netcl[[i]], "TrainingResults")$SSE[2,])) {
          net = netcl[[i]];
        }
      }
    }
    rm(netcl);
  }
  # Store best result in an ANnet Ensemble Object ----------
  options(warn=-1);
  ANnetList[iEnsemble] = net;
  options(warn=0);
  rm(net);
  # Updating the progress ----------------------------------
```

```
    progressCount = progressCount + 1;
    setTxtProgressBar(progressBar, progressCount);
  }
  # If running on a cluster, stop it ------------------------
  if (Parallel.Processing && Number.Cores > 1) { stopCluster(cl); }
  #-------------------------------------------------------------

  # Save user defined results -------------------------------------
  if (Print.Results) { fWriteResults(ANnetList); }
  if (Plot.Results)  {
    fPlotScatter(ANnetList);
    fPlotErrorHistogram(ANnetList);
    fPlotTimeSeries(ANnetList);
    fPlotSSE(ANnetList);
  }
  if (Save.Results)  {
    save(ANnetList, file='net.RData');
    fPlotScatter(ANnetList, Save.Results);
    fPlotErrorHistogram(ANnetList, Save.Results);
    fPlotTimeSeries(ANnetList, Save.Results);
    fPlotSSE(ANnetList, Save.Results);
  }
  #-------------------------------------------------------------

  # Returning the calculated ANnet object ------------------------
  rm(list=setdiff(lsf.str(), "ANnet"));
  gc(); # Release memory
  return(ANnetList)
  #-------------------------------------------------------------
}
#=============================================================

#=============================================================
#### ================== AUXILIARY FUNCTIONS ================== ####
#=============================================================
# fCheckClass Function ------------------------------------------
fCheckClass = function(Object, Class, CheckClassState) {
  if (class(Object) != Class) {
    message("ERROR: Wrong class of ",
            deparse(substitute(Object)),
            " parameter");
    message("       Got class '", class(Object),
            "' while required class is '", Class, "'");
    return(FALSE);
  }
  if (CheckClassState == FALSE) { # Proceed to check for errors
    return(FALSE);
  } else {
    return(TRUE)
  }
```

```
}
# ------------------------------------------------------------------------------

# fCheckInputs Function --------------------------------------------------------
fCheckInputs = function(Input, Target,
                        Model.Type, Model.Type.Variant, Time.Delay,
                        Normalisation.Method,
                        Model.Structure, Hidden.Layer.Neurons,
                        ActFun.Names,
                        ActFun.Parameter.a, ActFun.Parameter.b,
                        Training.Function, Dataset.Division.Factors,
                        Max.Ensemble.Objects, Max.Training.Attempts,
                        Max.Training.Epochs,
                        Bias.Factor,
                        Preload.Weights, Preload.ANnet.Object,
                        CheckInputsState) {
  # Initializing CheckInputs ---------------------------------
  CheckInputs = TRUE;
  # Input and Target data.frames -----------------------------
  i  = ncol(Input);
  j  = ncol(Target);
  k  = nrow(Input);
  kt = nrow(Target);
  if (k != kt) {
    message("ERROR: Invalid Input/Target input");
    message("        Different row dimensions of Input and Target ",
            "Data.Frames");
    CheckInputs = FALSE;
  }
  rm(kt);
  if (j != 1) {
    message("ERROR: Invalid Input/Target input");
    message("        Currently, the ANnet function works with only one ",
            "output variable");
    CheckInputs = FALSE;
  }
  # Model Type and Time Delay related parameters -------------
  if (Model.Type != "Input-Output" &&
      Model.Type != "Delayed Input-Output" &&
      Model.Type != "NAR" &&
      Model.Type != "NARX") {
    message("ERROR: Invalid Model.Type input");
    message("        Must be one of the following:");
    message("          'Input-Output'");
    message("          'Delayed Input-Output'");
    message("          'NAR'");
    message("          'NARX'");
    CheckInputs = FALSE;
  }
  if (Model.Type.Variant != "Open-Loop" &&
```

```
    Model.Type.Variant != "Close-Loop") {
  message("ERROR: Invalid Model.Type.Variant input");
  message("        Must be one of the following:");
  message("            'Open-Loop'");
  message("            'Close-Loop'");
  CheckInputs = FALSE;
}
if (Model.Type.Variant == "Close-Loop") {
  if (Model.Type != "NAR" &&
      Model.Type != "NARX") {
    message("WARNING: Invalid selection of Model.Type.Variant");
    message("          Changing Model.Type.Variant to 'Open-Loop'");
    Model.Type.Variant = "Open-Loop";
  }
}
if (Time.Delay <= 0) {
  if (Model.Type == "Delayed Input-Output" ||
      Model.Type == "NAR" ||
      Model.Type == "NARX") {
    message("ERROR: Invalid Time.Delay input");
    message("       Must be a positive integer value");
    CheckInputs = FALSE;
  }
}
# Data Normalisation related parameters ----------------------
if (Normalisation.Method != "Feature scaling [0:1]" &&
    Normalisation.Method != "Feature scaling [-1:1]" &&
    Normalisation.Method != "Standard Score") {
  message("ERROR: Invalid Normalisation.Method input");
  message("       Must be one of the following:");
  message("           'Feature scaling [0:1]'");
  message("           'Feature scaling [-1:1]'");
  message("           'Standard Score'");
  CheckInputs = FALSE;
}
# Model structure related paramteres -------------------------
if (Model.Structure != "1-Hidden-Layered" &&
    Model.Structure != "2-Hidden-Layered") {
  message("ERROR: Invalid Model.Structure input");
  message("       Must be one of the following:");
  message("           '1-Hidden-Layered'");
  message("           '2-Hidden-Layered'");
  CheckInputs = FALSE;
}
if (Model.Structure == "1-Hidden-Layered") {
  if (length(Hidden.Layer.Neurons) != 1) {
    message("ERROR: Invalid Hidden.Layer.Neurons input");
    message("       Must be of type c(h), where h is the number of ",
            "neurons in the hidden layer");
    CheckInputs = FALSE;
```

```
    }
  } else if (Model.Structure == "2-Hidden-Layered") {
    if (length(Hidden.Layer.Neurons) != 2) {
      message("ERROR: Invalid Hidden.Layer.Neurons input");
      message("       Must be of type c(h1,h2), where h1 is the ",
              "number of neurons in the first hidden layern and h2 is ",
              "the number of neurons in the second hidden layer");
      CheckInputs = FALSE;
    }
  }
  # Activation Function related parameters ------------------
  if (Model.Structure == "1-Hidden-Layered") {
    if (length(ActFun.Names) != 2) {
      message("ERROR: Invalid ActFun.Names input");
      message("       Must be of type c(nam1,nam2), where nam1 is the ",
              "name of the activation function for the connection ",
              "input-hidden layers and nam2 is the name of the ",
              "activation function for the connection hidden-output ",
              "layers");
      CheckInputs = FALSE;
    }
    if (length(ActFun.Parameter.a) != 2) {
      message("ERROR: Invalid ActFun.Parameter.a input");
      message("       Must be of type c(a1,a2), where a1 is the value ",
              "of the parameter a for the selected activation ",
              "function in the connection input-hidden layers and a2 ",
              "is the value of the parameter a for the selected ",
              "activation function in the connection hidden-output ",
              "layers");
      CheckInputs = FALSE;
    }
    if (length(ActFun.Parameter.b) != 2) {
      message("ERROR: Invalid ActFun.Parameter.b input");
      message("       Must be of type c(b1,b2), where b1 is the value ",
              "of the parameter b for the selected activation ",
              "function in the connection input-hidden layers and b2 ",
              "is the value of the parameter b for the selected ",
              "activation function in the connection hidden-output ",
              "layers");
      CheckInputs = FALSE;
    }
  } else if (Model.Structure == "1-Hidden-Layered") {
    if (length(ActFun.Names) != 3) {
      message("ERROR: Invalid ActFun.Names input");
      message("       Must be of type c(nam1,nam2,nam3), where nam1 ",
              "is the name of the activation function for the ",
              "connection input-hidden1 layers , nam2 is the name of ",
              "the activation function for the connection ",
              "hidden1-hidden2 layers , and nam3 is the name of the ",
              "activation function for the connection hidden2-output ",
```

```
            "layers");
    CheckInputs = FALSE;
  }
  if (length(ActFun.Parameter.a) != 3) {
    message("ERROR: Invalid ActFun.Parameter.a input");
    message("        Must be of type c(a1,a2,a3), where a1 is the ",
            "value of the parameter a for the selected activation ",
            "function in the connection input-hidden1 layers, a2 is ",
            "the value of the parameter a for the selected ",
            "activation function in the connection hidden1-hidden2 ",
            "layers, and a3 is the value of the parameter a for the ",
            "selected activation function in the connection ",
            "hidden2-output layers");
    CheckInputs = FALSE;
  }
  if (length(ActFun.Parameter.b) != 3) {
    message("ERROR: Invalid ActFun.Parameter.b input");
    message("        Must be of type c(b1,b2,b3), where b1 is the ",
            "value of the parameter b for the selected activation ",
            "function in the connection input-hidden1 layers, b2 is ",
            "the value of the parameter b for the selected ",
            "activation function in the connection hidden1-hidden2 ",
            "layers, and b3 is the value of the parameter b for the ",
            "selected activation function in the connection ",
            "hidden2-output layers");
    CheckInputs = FALSE;
  }
}
for (i in 1:length(ActFun.Names)) {
  if (ActFun.Names[i] != "signum" &&
      ActFun.Names[i] != "linear" &&
      ActFun.Names[i] != "logsig" &&
      ActFun.Names[i] != "tanh") {
    message("ERROR: Invalid ActFun.Names input");
    message("        Must be one of the following:");
    message("          'signum'");
    message("          'linear'");
    message("          'logsig'");
    message("          'tanh'");
    CheckInputs = FALSE;
  }
}
# Training Function related parameter ----------------------
if (Training.Function != "Levenberg-Marquardt" &&
    Training.Function != "Steepest-Descent") {
  message("ERROR: Invalid Training.Function input");
  message("        Must be one of the following:");
  message("          'Levenberg-Marquardt'");
  message("          'Steepest-Descent'");
  CheckInputs = FALSE;
```

```
  }
  if (sum(Dataset.Division.Factors) != 1.) {
    message("ERROR: Invalid Dataset.Division.Factors input");
    message("       Must be of type c(a,b,c), where a is the factor ",
            "of data to be used for Training, b is the factor of data ",
            "to be used for Validation, and c is the factor of data ",
            "to be used for Testing");
    message("       Also, the resulting sum of a+b+c must equal 1");
    CheckInputs = FALSE;
  }
  for (i in 1:length(Dataset.Division.Factors)) {
    if (Dataset.Division.Factors[i] < 1/k) {
      message("ERROR: Invalid Dataset.Division.Factors input");
      message("       Must be of type c(a,b,c), where a is the factor ",
              "of data to be used for Training, b is the factor of data ",
              "to be used for Validation, and c is the factor of data ",
              "to be used for Testing");
      message("       Also, a, b, and c must be valid positive values");
      CheckInputs = FALSE;
    }
  }
  for (i in 1:length(Max.Training.Attempts)) {
    if (Max.Training.Attempts[i] < 1) {
      message("ERROR: Invalid Max.Training.Attempts input");
      message("       Must be a positive integer value");
      CheckInputs = FALSE;
    }
  }
  if (Max.Ensemble.Objects < 1) {
    message("ERROR: Invalid Max.Ensemble.Objects input");
    message("       Must be a positive integer value");
    CheckInputs = FALSE;
  }
  if (Max.Training.Epochs < 1) {
    message("ERROR: Invalid Max.Training.Epochs input");
    message("       Must be a positive integer value");
    CheckInputs = FALSE;
  }
  # Bias Factor ------------------------------------------------
  if (Bias.Factor < -1. || Bias.Factor > 1.) {
    message("ERROR: Invalid Bias.Factor input");
    message("       Must be a real value ranged between -1. and 1.");
    CheckInputs = FALSE;
  }
  # Preload Weight Data ----------------------------------------
  if (Preload.Weights) {
    if (substr(Preload.ANnet.Object,
               nchar(Preload.ANnet.Object)-5,
               nchar(Preload.ANnet.Object)) != ".RData") {
      message("ERROR: Invalid Preload.ANnet.Object input");
```

```
      message("␣␣␣␣␣␣␣␣Must␣be␣a␣'.RData'␣object");
      CheckInputs = FALSE;
    }
    if (class(get(load(Preload.ANnet.Object))) != "ANnet") {
      message("ERROR:␣Invalid␣Preload.ANnet.Object␣input");
      message("␣␣␣␣␣␣␣␣ObjectmMust␣be␣of␣'ANnet'␣class");
      CheckInputs = FALSE;
    }
  }
  # Check Inputs State ----------------------------------------
  if (CheckInputsState == FALSE) { # Proceed to check for errors
    return(FALSE)
  } else {
    return(CheckInputs)
  }
}
# ----------------------------------------------------------------------
# ======================================================================
```

ANnet Modules

ANnet Activation Functions

```
##############################################################################
############ ANnet - ACTIVATION FUNCTIONS AND 1ST DERIVATIVES ############
##############################################################################
#
# This script contains the activation functions and their derivatives to
#   be used by the ANnet function.
#
# Specifications:
# f()  --> Function: returns the value of the activation function
# fd() --> Function: returns the value of the 1st derivative of the
#                    activation funtion
# fn   --> The activation function name
# a    --> Parameter a (optional)
# b    --> Parameter b (optional)
#
# Author: Arthur Hrast Essenfelder
# E-mail: arthur.essenfelder@gmail.com
#
# Version: 1.0
# Last update on: 18/11/2016
# Last modified by: Arthur Hrast Essenfelder
##############################################################################
```

```
##############################################################################

# Pre-Loading Libraries & Functions ------------------------------------------
# Libraries
suppressMessages(library(pracma));
# ----------------------------------------------------------------------------

# Activation Functions -------------------------------------------------------
f = function(Input, activation.function.name,
             parameter.a, parameter.b) {
  # Getting values ---------------------------------------------
  fn = activation.function.name;
  X  = Input;
  a  = as.double(parameter.a);
  b  = as.double(parameter.b);
  # Computing the activation function --------------------------
  if      (fn == "signum") { f = ifelse(X > 0., X/X, -X/X);
                             f = ifelse(X == 0., 0./X, f); }
  else if (fn == "linear") { f = X; }
  else if (fn == "logsig") { f = 1./(1.+exp(-a*X)); }
  else if (fn == "tanh")   { f = a*tanh(b*X); }
  return(f);
}
#-----------------------------------------------------------------------------

# Activation Functions - First Derivative ------------------------------------
fd = function(Input, activation.function.name,
              parameter.a, parameter.b) {
  # Getting values ---------------------------------------------
  fn = activation.function.name;
  X  = Input;
  a  = as.double(parameter.a);
  b  = as.double(parameter.b);
  # Computing the activation function --------------------------
  if      (fn == "signum") { fd = ifelse(X == 0., X/X, 0./X); }
  else if (fn == "linear") { fd = X/X; }
  else if (fn == "logsig") { fd = a*X*(1.-X); }
  else if (fn == "tanh")   { fd = (b/a)*(a-X)*(a+X); }
  return(fd);
}
#-----------------------------------------------------------------------------
```

ANnet Auxiliary Functions

```
##############################################################################
###################### ANnet - AUXILIARY FUNCTIONS ###########################
##############################################################################
```

```
#
# This script contains a set of auxiliary functions to be used by the
#   ANnet function.
#
# Specifications:
# fFeedforward     --> Function: Performs the feedforward step of an
#                                ANnet 1h or 2h function
# fBackpropagation --> Function: Performs the backpropagation step of an
#                                ANnet 1h or 2h function
#
# Author: Arthur Hrast Essenfelder
# E-mail: arthur.essenfelder@gmail.com
#
# Version: 1.0
# Last update on: 18/11/2016
# Last modified by: Arthur Hrast Essenfelder
################################################################################
################################################################################

# Pre-Loading Libraries & Functions ------------------------------------------
# Libraries
# ----------------------------------------------------------------------------

# Feedforward step Function ==================================================
fFeedforward = function(Input.Data, ActFun.Names,
                        ActFun.Parameter.a, ActFun.Parameter.b,
                        Hidden2.Layer.Weights, Output.Layer.Weights,
                        Hidden2.Layer.Bias, Output.Layer.Bias,
                        Hidden2.Layer.Bias.Weights, Output.Layer.Bias.Weights,
                        Hidden1.Layer.Weights, Hidden1.Layer.Bias,
                        Hidden1.Layer.Bias.Weights) {
  # Loading the data ---------------------------------------------------------
  X       = Input.Data;
  ActFun  = ActFun.Names;
  a       = ActFun.Parameter.a;
  b       = ActFun.Parameter.b;
  Wh2     = Hidden2.Layer.Weights;
  Wo      = Output.Layer.Weights;
  Bh2     = Hidden2.Layer.Bias;
  Bo      = Output.Layer.Bias;
  WBh2    = Hidden2.Layer.Bias.Weights;
  WBo     = Output.Layer.Bias.Weights;
  # Getting useful information -----------------------------------------------
  k  = NROW(X);
  i  = NCOL(X);
  h2 = NROW(Wo);
  j  = NCOL(Wo);
  # Checking if 1 or 2 hidden-layered ANnet ----------------------------------
  if (missing(Hidden1.Layer.Weights) &&
      missing(Hidden1.Layer.Bias) &&
```

```
      missing(Hidden1.Layer.Bias.Weights)) {
    Wh1  = NULL;
    Bh1  = NULL;
    WBh1 = NULL;
    h1   = 0;
  } else if (missing(Hidden1.Layer.Weights) ||
             missing(Hidden1.Layer.Bias)    ||
             missing(Hidden1.Layer.Bias.Weights)) {
    stop("Missing arguments for the feedforward function")
  } else {
    Wh1  = Hidden1.Layer.Weights;
    Bh1  = Hidden1.Layer.Bias;
    WBh1 = Hidden1.Layer.Bias.Weights;
    h1   = ifelse(is.null(Wh1), 0, NCOL(Wh1));
  }
  # Calculating the Feedforward step ----------------------
  if (h1==0) { # If 1-hidden-layered, then -------
    # Hidden layer
    Ah2 = X   %*% Wh2 + Bh2 %*% t(WBh2);
    Yh2 = f(Ah2,  ActFun[1], a[1], b[1]);
    Sh2 = fd(Yh2, ActFun[1], a[1], b[1]);
    # Output layer
    Ao  = Yh2 %*% Wo  + Bo  %*% t(WBo);
    O   = f(Ao,   ActFun[2], a[2], b[2]);
    So  = fd(O,   ActFun[2], a[2], b[2]);
    # Null values
    Yh1 = NULL;
    Sh1 = NULL;
  } else {     # If 2-hidden-layered, then -------
    # Hidden layer 1
    Ah1 = X   %*% Wh1 + Bh1 %*% t(WBh1);
    Yh1 = f(Ah1,  ActFun[1], a[1], b[1]);
    Sh1 = fd(Yh1, ActFun[1], a[1], b[1]);
    # Hidden layer 2
    Ah2 = Yh1 %*% Wh2 + Bh2 %*% t(WBh2);
    Yh2 = f(Ah2,  ActFun[2], a[2], b[2]);
    Sh2 = fd(Yh2, ActFun[2], a[2], b[2]);
    # Output layer
    Ao  = Yh2 %*% Wo + Bo %*% t(WBo);
    O   = f(Ao,   ActFun[3], a[3], b[3]);
    So  = fd(O,   ActFun[3], a[3], b[3]);
  }
  # Creating the results list -----------------------------
  Ff = list(O=O, So=So, Yh2=Yh2, Sh2=Sh2, Yh1=Yh1, Sh1=Sh1);
  return(Ff)
}
# ============================================================

# Backpropagation step Function ==============================
fBackpropagation = function(Training.Method,
```

```
                          Combination.Coefficient, Output.Layer.Error,
                          Output.Layer.Slope, Output.Layer.Input,
                          Output.Layer.Weights,
                          Hidden2.Layer.Slope, Hidden2.Layer.Input,
                          Hidden2.Layer.Weights,
                          Hidden1.Layer.Slope, Hidden1.Layer.Input,
                          Hidden1.Layer.Weights,
                          Previous.Delta) {
# Loading the data ------------------------------------------
u   = Combination.Coefficient;
alp = 0.0;
Eo  = Output.Layer.Error;
So  = Output.Layer.Slope;
Io  = Output.Layer.Input;
Wo  = Output.Layer.Weights;
Sh2 = Hidden2.Layer.Slope;
Ih2 = Hidden2.Layer.Input;
Wh2 = Hidden2.Layer.Weights;
# Getting useful information --------------------------------
k  = NROW(Eo);
h2 = NROW(Wo);
j  = NCOL(Wo);
# Checking if 1 or 2 hidden-layered ANnet -------------------
if (missing(Hidden1.Layer.Slope) &&
    missing(Hidden1.Layer.Input) &&
    missing(Hidden1.Layer.Weights)) {
  Sh1 = NULL;
  Ih1 = NULL;
  h1  = 0;
  i   = NCOL(Ih2);
} else if (missing(Hidden1.Layer.Slope) ||
           missing(Hidden1.Layer.Input) ||
           missing(Hidden1.Layer.Weights)) {
  stop("Missing arguments for the backpropagation function")
} else {
  Sh1 = Hidden1.Layer.Slope;
  Ih1 = Hidden1.Layer.Input;
  h1  = ifelse(is.null(Sh1), 0, NCOL(Sh1));
  if (h1 == 0) { Ih2 = Ih1; Ih1 = NULL; }
  i   = ifelse(is.null(Ih1), NCOL(Ih2), NCOL(Ih1));
}
# Calculating the Weight Corrections ------------------------
E  = as.vector(Eo);                          # Error Vector
dP = fPdeltaW(i, h1, h2, j, Previous.Delta); # Previous deltaW
D  = fdeltaW(i,h1,h2,j,k,So,Sh2,Sh1,Wo,Wh2); # Delta matrix
J  = fJacobian(i,h1,h2,j,k,Io,Ih2,Ih1,D);    # Jacobian matrix
I  = diag(NCOL(J));                          # Identity matrix
Ho = matrix(0., NCOL(J), NCOL(J));           # Null Hessian matrix
H  = tryCatch(chol2inv(chol(((t(J)%*%J)+u*I))), # ~ Hessian matrix
              error = function(e)
```

```
                {tryCatch(solve((t(J)%*%J)+u*I),
                          error = function(e)
                          {Ho;});});
  # Calculating the new deltaW
  if          (Training.Method == "Steepest-Descent") {
    dW = -(alp*dP + (1-alp)*H%*%(t(J)%*%E));
  } else if (Training.Method == "Levenberg-Marquardt") {
    dW = -H %*% (t(J) %*% E);
  }
  dW = fConvertdW(i, h1, h2, j, dW);                    # New deltaW as list
  return(dW);
}
# ============================================================================

#### ================== AUXILIARY FUNCTIONS ================== ####
# ============================================================================
# Calculates delta Function ------------------------------------------------
fdeltaW = function(i, h1, h2, j, k, So, Sh2, Sh1, Wo, Wh2) {
  # Calculating the deltas
  deltaW = NULL;
  idelta = 1;
  if (h1==0) { # If 1-hidden-layered, then ---------------------
    for (m in 1:j) { # For each output
      delta = matrix(0., k, j+h2);
      for (jj in 1:j) { # For each neuron in the output layer
        if (jj == m) {
          delta[,idelta] = So[,m];
        }
        idelta = idelta + 1;
      }
      for (hh2 in 1:h2) { # For each neuron in the hidden layer
        delta[,idelta] = Sh2[,hh2] * (So[,m] * Wo[hh2,m]);
        idelta = idelta + 1;
      }
      deltaW = rbind(deltaW, delta);
    }
  } else { # If 2-hidden-layered, then ----------------------
    for (m in 1:j) { # For each output
      delta = matrix(0., k, j+h2+h1);
      for (jj in 1:j) { # For each neuron in the output layer
        if (jj == m) {
          delta[,idelta] = So[,m];
        }
        idelta = idelta + 1;
      }
      for (hh2 in 1:h2) { # For each neuron in the hidden 2 layer
        delta[,idelta] = Sh2[,hh2] * (So[,m] * Wo[hh2,m]);
        idelta = idelta + 1;
      }
      for (hh1 in 1:h1) { # For each neuron in the hidden 1 layer
```

```
        for (hh2 in 1:h2) { # For each neuron in the hidden 2 layer
          delta[,idelta] = delta[,idelta] + Wh2[hh1,hh2] *
            (Sh2[,hh2] * (So[,m] * Wo[hh2,m]));
        }
        delta[,idelta] = delta[,idelta] * Sh1[,hh1];
        idelta = idelta + 1;
      }
      deltaW = rbind(deltaW, delta);
    }
  }
  return(deltaW);
}
#-------------------------------------------------------------------------

# Computes the Jacobian matrix Function ----------------------------------
fJacobian = function(i, h1, h2, j, k, Io, Ih2, Ih1, deltaW) {
  # Computing the Jacobian matrix
  if (h1==0) { J = matrix(0., k*j, j*h2+h2*i); }
  else {       J = matrix(0., k*j, j*h2+h2*h1+h1*i); }
  iJ = 1;
  if (h1==0) { # If 1-hidden-layered, then ------------------
    for (jj in 1:j) { # For each neuron in the output layer
      for (hh2 in 1:h2) { # For each neuron in the hidden layer
        J[,iJ] = - deltaW[,jj] * Io[,hh2];
        iJ = iJ + 1;
      }
    }
    for (hh2 in 1:h2) { # For each neuron in the hidden layer
      for (ii in 1:i) { # For each neuron in the input layer
        J[, iJ] = - deltaW[,j+hh2] * Ih2[,ii];
        iJ = iJ + 1;
      }
    }
  } else { # If 2-hidden-layered, then ----------------------
    for (jj in 1:j) { # For each neuron in the output layer
      for (hh2 in 1:h2) { # For each neuron in the hidden 2 layer
        J[,iJ] = - deltaW[,jj] * Io[,hh2];
        iJ = iJ + 1;
      }
    }
    for (hh2 in 1:h2) { # For each neuron in the hidden 2 layer
      for (hh1 in 1:h1) { # For each neuron in the hidden 1 layer
        J[, iJ] = - deltaW[,j+hh2] * Ih2[,hh1];
        iJ = iJ + 1;
      }
    }
    for (hh1 in 1:h1) { # For each neuron in the hidden 1 layer
      for (ii in 1:i) { # For each neuron in the input layer
        J[, iJ] = - deltaW[,j+h2+hh1] * Ih1[,ii];
        iJ = iJ + 1;
```

```
      }
    }
  }
  return(J);
}
#-------------------------------------------------------------------------

# Retrieves previous weight correction Function ---------------------------
fPdeltaW = function(i, h1, h2, j, Previous.Delta) {
  # Checking for previous delta
  if (h1==0) { #1-Hidden-layer
    if (is.null(Previous.Delta) || missing(Previous.Delta)) {
      dPWo = matrix(0.,nrow=h2,ncol=j);
      dPWh = matrix(0.,nrow=i, ncol=h2);
    } else {
      dPWo = Previous.Delta$deltaWo;
      dPWh = Previous.Delta$deltaWh;
    }
    dP = c(as.vector(dPWo),as.vector(dPWh));
  } else      { #2-Hidden-layer
    if (is.null(Previous.Delta) || missing(Previous.Delta)) {
      dPWo  = matrix(0.,nrow=h2,ncol=j);
      dPWh2 = matrix(0.,nrow=h1,ncol=h2);
      dPWh1 = matrix(0.,nrow=i, ncol=h1);
    } else {
      dPWo  = Previous.Delta$deltaWo;
      dPWh2 = Previous.Delta$deltaWh2;
      dPWh1 = Previous.Delta$deltaWh1;
    }
    dP = c(as.vector(dPWo),as.vector(dPWh2),as.vector(dPWh1));
  }
  return(dP);
}
#-------------------------------------------------------------------------

# Converts the weight corrections vector to list Function -----------------
fConvertdW = function(i, h1, h2, j, dW) {
  # Returning the Weight update matrices
  if (h1==0) { #1-Hidden-layer
    dWo = matrix(dW[1:(j*h2)],h2,j,byrow=FALSE);
    dWh = matrix(dW[(j*h2+1):(j*h2+h2*i)],i,h2,byrow=FALSE);
    dW  = list(deltaWo=dWo,deltaWh2=dWh,deltaWh1=NULL);
  } else      { #2-Hidden-layer
    dWo  = matrix(dW[1:(j*h2)],h2,j,byrow=FALSE);
    dWh2 = matrix(dW[(j*h2+1):(j*h2+h2*h1)],h1,h2,byrow=FALSE);
    dWh1 = matrix(dW[(j*h2+h2*h1+1):(j*h2+h2*h1+h1*i)],i,h1,byrow=FALSE);
    dW   = list(deltaWo=dWo,deltaWh2=dWh2,deltaWh1=dWh1);
  }
  return(dW);
}
```

```
#-------------------------------------------------------------------------------
# ==============================================================================
```

ANnet Efficiency Criteria Functions

```
################################################################################
################## ANnet - EFFICIENCY CRITERIA FUNCTIONS ######################
################################################################################
#
# This script contains the efficiency criteria functions to be used by
#   the ANnet function.
# The functions are:
#   - Nash-Sutcliffe - fNSE
#   - Percent Bias - fPBIAS
#   - Coefficient of Determination - fR2
#
# Specifications:
# fNSE()   --> Function: returns the value of the NSE function
# fPBIAS() --> Function: returns the value of the PBIAS function
# fR2()    --> Function: returns the value of the R2 function
# O --> The input OBSERVED values (scalar, vector or matrix)
# X --> The input PREDICTED values (scalar, vector or matrix)
#
# Author: Arthur Hrast Essenfelder
# E-mail: arthur.essenfelder@gmail.com
#
# Version: 1.0
# Last update on: 18/11/2016
# Last modified by: Arthur Hrast Essenfelder
################################################################################
################################################################################

# Pre-Loading Libraries & Functions ---------------------------------------
# Libraries
# -------------------------------------------------------------------------

# Nash-Sutcliffe Function -------------------------------------------------
fNSE = function(Input.Observed, Input.Predicted) {
  # Getting values ----------------------------------------------
  O = Input.Observed;
  X = Input.Predicted;
  # Computing the function --------------------------------------
  fNSE = 1 - colSums((O-X)^2)/colSums((O-colMeans(O))^2);
  return(fNSE);
}
#-------------------------------------------------------------------------
```

```
# Percent Bias Function ------------------------------------------------------
fPBIAS = function(Input.Observed, Input.Predicted) {
  # Getting values -----------------------------------------------
  O = Input.Observed;
  X = Input.Predicted;
  # Computing the function ---------------------------------------
  fPBIAS = colSums((O-X)*100)/colSums(O);
  return(fPBIAS);
}
#-------------------------------------------------------------------------------

# Coefficient of Determination Function ------------------------------------
fR2 = function(Input.Observed, Input.Predicted) {
  # Getting values -----------------------------------------------
  O = Input.Observed;
  X = Input.Predicted;
  # Computing the function ---------------------------------------
  fR2 = (colSums((O-colMeans(O))*(X-colMeans(X))) /
           (sqrt(colSums((O-colMeans(O))^2)) *
              sqrt(colSums((X-colMeans(X))^2))))^2;
  return(fR2);
}
#-------------------------------------------------------------------------------
```

ANnet Model Type Functions

```
################################################################################
####### ANnet - SPECIFIC FUNCTIONS DEPENDING ON ANnet Model.Type #######
################################################################################
#
# This script contains a set of functions to be used by the ANnet func.
#   depending on the specific Model.Type
#
# Specifications:
# fTimeDelayData --> Function: returns the delayed input dataset
# fCloseLoopData --> Function: returns the input data for a close-loop net
# Input     --> Original input dataset, with no delay
# Target    --> Original tarhet dataset (optional)
# ModelType --> Type of ANnet model to be considered
# TimeDelay --> Number of time step delays
#
# Author: Arthur Hrast Essenfelder
# E-mail: arthur.essenfelder@gmail.com
#
# Version: 1.0
# Last update on: 18/11/2016
# Last modified by: Arthur Hrast Essenfelder
```

```
##############################################################################
##############################################################################

# Pre-Loading Libraries & Functions ------------------------------------------
# Libraries
#-----------------------------------------------------------------------------

# TimeDelayData Function ======================================================
fTimeDelayData = function(Input, Target, ModelType, TimeDelay) {
  # Loading data ---------------------------------------------------
  X = Input;
  d = TimeDelay;
  i = ncol(X);
  k = nrow(X);
  # Loading Target data if necessary -------------------------------
  if (ModelType == "NAR" || ModelType == "NARX") {
    if (missing(Target)) { stop("Missing Target"); }
    else { y = Target; j = ncol(y); }
  }
  # Check to apply time delay --------------------------------------
  if (d > 0) {
    # Delayed Input-Output -----------------------
    if (ModelType == "Delayed Input-Output") {
      Xtmp = matrix(0., nrow=k-d, ncol=(d+1)*i);
      count = 1
      for (ii in 1:i) { #Data from original Input
        for (dd in d:0) {
          Xtmp[,count] = X[(dd+1):(k+dd-d),ii]
          count = count + 1
        }
      }
    }
    # NAR ----------------------------------------
    else if (ModelType == "NAR") {
      Xtmp = matrix(0., nrow=k-d, ncol=d*j);
      count = 1
      for (jj in 1:j) { #Data from original Target
        for (dd in d:1) {
          Xtmp[,count] = y[(dd):(k+dd-d-1),jj]
          count = count + 1
        }
      }
    }
    # NARX ---------------------------------------
    else if (ModelType == "NARX") {
      Xtmp = matrix(0., nrow=k-d, ncol=((d+1)*i+d*j));
      count = 1
      for (ii in 1:i) { #Data from original Input
        for (dd in d:0) {
          Xtmp[,count] = X[(dd+1):(k+dd-d),ii]
```

```
          count = count + 1
        }
      }
      for (jj in 1:j) { #Data from original Target
        for (dd in d:1) {
          Xtmp[,count] = y[(dd):(k+dd-d-1),jj]
          count = count + 1
        }
      }
    }
    # Others ------------------------------------
    else { stop("Invalid ModelType"); }
  } else { #If not, return the same inputs
    return(X);
  }
  # Returning the time-delayed Input data ------------------
  return(Xtmp);
}
# ============================================================

# CloseLoopData Function ======================================
fCloseLoopData = function(IndexArray, Input, DatasetSplitFactor,
                          ModelType, TimeDelay,
                          ActivationFunctionNames,
                          ActFunParameter.a, ActFunParameter.b,
                          WeightsOutput, WeightBiasOutput, BiasOutput,
                          WeightsHidden2,WeightBiasHidden2,BiasHidden2,
                          WeightsHidden1,WeightBiasHidden1,BiasHidden1){
  # Loading data ------------------------------------------
  id          = IndexArray;
  X           = Input;
  splitFactor = DatasetSplitFactor;
  d           = TimeDelay;
  strActFun   = ActivationFunctionNames;
  a           = ActFunParameter.a;
  b           = ActFunParameter.b;
  Wo          = WeightsOutput;
  WBo         = WeightBiasOutput;
  Bo          = BiasOutput;
  Wh2         = WeightsHidden2;
  WBh2        = WeightBiasHidden2;
  Bh2         = BiasHidden2;
  # Gettig some useful information ------------------------
  i = ncol(X);
  j = ncol(Wo);
  k = nrow(X);
  # Checking if 1 or 2-hidden layered ANnet ---------------
  if        (missing(WeightsHidden1) &&
             missing(WeightBiasHidden1) &&
             missing(BiasHidden1)) {
```

```
  Wh1  = NULL;
  WBh1 = NULL;
  Bh1  = NULL;
} else if (missing(WeightsHidden1) ||
           missing(WeightBiasHidden1) ||
           missing(BiasHidden1)) {
  stop("Missing arguments");
} else {
  Wh1  = WeightsHidden1;
  WBh1 = WeightBiasHidden1;
  Bh1  = BiasHidden1;
}
# Pre-Checks and pre-processing ------------------------------
# Checking if there is a delay
if (d == 0) { return(X); }
# Storing the original index of inputs
idtmp = matrix(1:k, nrow=k, ncol=1);
# Returning the inputs to original id ordering
X     = as.matrix(cbind(id, idtmp, X));
X     = X[order(as.integer(X[, 1]),decreasing=FALSE),];
idtmp = as.matrix(X[,2]);
X     = as.matrix(X[,3:(i+2)]);
# Calculating the Close-Loop Input data ----------------------
for (kk in 1:(k-1)) {
  if (is.null(Wh1)) { #If 1-hidden-layered
    # Hidden Layer 2
    Ah2 = X[kk,] %*% Wh2 + Bh2[kk,] %*% t(WBh2);
    Yh2 = f(Ah2,  strActFun[1], a[1], b[1]);
    # Output Layer
    Ao  = Yh2    %*% Wo  + Bo[kk,]  %*% t(WBo);
    O   = f(Ao,   strActFun[2], a[2], b[2]);
  } else {            #If 2-hidden-layered
    # Hidden Layer 1
    Ah1 = X[kk,] %*% Wh1 + Bh1[kk,] %*% t(WBh1);
    Yh1 = f(Ah1,  strActFun[1], a[1], b[1]);
    # Hidden Layer 2
    Ah2 = Yh1    %*% Wh2 + Bh2[kk,] %*% t(WBh2);
    Yh2 = f(Ah2,  strActFun[2], a[2], b[2]);
    # Output Layer
    Ao  = Yh2    %*% Wo  + Bo[kk,]  %*% t(WBo);
    O   = f(Ao,   strActFun[3], a[3], b[3]);
  }
  # Update the next Input row (for each j) ---------------------
  for (jj in 1:j) {
    # Checking if delay is larger than one time step
    if (d > 1) {
      X[kk+1,(i+d*(jj-j-1)+2):(i+d*(jj-j))] =
        X[kk,(i+d*(jj-j-1)+1):(i+d*(jj-j)-1)];
    }
    X[kk+1,(i+d*(jj-j-1)+1)] = O[jj];
```

```
    }
  }
  # Returning the indexation to the previous order ----------
  X = as.matrix(cbind(idtmp, X));
  X = X[order(as.integer(X[, 1]),decreasing=FALSE),];
  X = as.matrix(X[,2:(i+1)]);
  # Splitting the input data into Cal, Val, and Tst ---------
  Xcal = as.matrix(X[1:as.integer(k*splitFactor[1]),]);
  Xval = as.matrix(X[(1+as.integer(k*splitFactor[1])):
                     (as.integer(k*splitFactor[1]+
                                 k*splitFactor[2])),]);
  Xtst = as.matrix(X[(1+as.integer(k*splitFactor[1]+
                                 k*splitFactor[2])):k,]);
  X = list(Xcal=Xcal, Xval=Xval, Xtst=Xtst);
  # Returning the updated Input close-loop data -------------
  return(X)
}
# ============================================================================
```

ANnet Normalisation Functions

```
##############################################################################
##################### ANnet - NORMALISATION FUNCTIONS ########################
##############################################################################
#
# This script contains the normalisation procedure to be used by the
#   ANnet function.
#
# Specifications:
# norm()      --> Fun: returns the normalised value of a vector
# norm.inv()  --> Fun: returns the normalised inversed value of a vector
# colMax()    --> Fun: returns the maximum value of a matrix by columns
# colMin()    --> Fun: returns the minimum value of a matrix by columns
# X           --> The input (scalar, vector or matrix) to be processed
#
# Possible Normalisation Functions
#   Feature scaling [0:1]
#   Feature scaling [-1:1]
#   Standard Score
#
# Author: Arthur Hrast Essenfelder
# E-mail: arthur.essenfelder@gmail.com
#
# Version: 1.0
# Last update on: 18/11/2016
# Last modified by: Arthur Hrast Essenfelder
##############################################################################
```

```
################################################################################

# Pre-Loading Libraries & Functions ------------------------------------------
# Libraries
# ----------------------------------------------------------------------------

# Normalisation Functions ----------------------------------------------------
fNorm = function(Input.Data, Norm.Method, Data.Statistics) {
  # Getting values -----------------------------------------------------
  X = Input.Data;
  m = NROW(X);
  n = NCOL(X);
  Xmax  = Data.Statistics$max;
  Xmin  = Data.Statistics$min;
  Xmean = Data.Statistics$mean;
  XstDev = Data.Statistics$stDev;
  # Converting to a matrix input ---------------------------------------
  Xmax  = matrix(Xmax,  m, n, byrow=TRUE);
  Xmin  = matrix(Xmin,  m, n, byrow=TRUE);
  Xmean = matrix(Xmean, m, n, byrow=TRUE);
  XstDev = matrix(XstDev, m, n, byrow=TRUE);
  # Calculating the normalised values ----------------------------------
  if       (Norm.Method == "Feature scaling [0:1]") {
    Xnorm = ((X - Xmin) / (Xmax - Xmin));
  } else if (Norm.Method == "Feature scaling [-1:1]") {
    Xnorm = 2. * ((X - Xmin) / (Xmax - Xmin)) - 1.;
  } else if (Norm.Method == "Standard Score") {
    Xnorm = (X - Xmean) / XstDev;
  } else {
    Xnorm = X - X; # ZERO
  }
  # Returning normalised values ----------------------------------------
  Xnorm = as.matrix(Xnorm);
  return(norm);
}
# ----------------------------------------------------------------------------

# Normalisation Functions - Inverse ------------------------------------------
fNormInv = function(Input.Data, Norm.Method, Data.Statistics) {
  # Getting values -----------------------------------------------------
  X     = Input.Data;
  m     = NROW(X);
  n     = NCOL(X);
  Xmax  = Data.Statistics$max;
  Xmin  = Data.Statistics$min;
  Xmean = Data.Statistics$mean;
  XstDev = Data.Statistics$stDev;
  # Converting to a matrix input ---------------------------------------
  Xmax  = matrix(Xmax,  m, n, byrow=TRUE);
  Xmin  = matrix(Xmin,  m, n, byrow=TRUE);
```

```
  Xmean  = matrix(Xmean,   m, n, byrow=TRUE);
  XstDev = matrix(XstDev,  m, n, byrow=TRUE);
  # Calculating the normalised values (inverse) ----------
  if        (Norm.Method == "Feature scaling [0:1]") {
    Xnorm = (X * (Xmax - Xmin)) + Xmin;
  } else if (Norm.Method == "Feature scaling [-1:1]") {
    Xnorm = (((X + 1.) * (Xmax - Xmin)) / (2.)) + Xmin;
  } else if (Norm.Method == "Standard Score") {
    Xnorm = (X * XstDev) + Xmean;
  } else {
    Xnorm = X - X; # ZERO
  }
  # Returning normalised values (inverse) ----------------
  Xnorm = as.matrix(Xnorm);
  return(Xnorm);
}
#-------------------------------------------------------------------

# colMax Function ---------------------------------------------------
colMax = function(Input.Data) {
  X = Input.Data;
  colMax = apply(X, 2, function(x) max(x, na.rm = TRUE));
  return (colMax);
}
#-------------------------------------------------------------------

# colMin Function ---------------------------------------------------
colMin = function(Input.Data) {
  X = Input.Data;
  colMin = apply(X, 2, function(x) min(x, na.rm = TRUE));
  return (colMin);
}
#-------------------------------------------------------------------
```

ANnet Plot Functions

```
###########################################################################
################### ANnet - PLOT AND WRITE FUNCTIONS ######################
###########################################################################
#
# This script contains plot functions to be used by the ANnet function.
#
# Specifications:
# fWriteResults()          --> Fun: Write efficiency criteria results
# fPlotDot()               --> Fun: Dot Plot
# fPlotTargetVsSimulated() --> Fun: Target vs Simulated Plot
# fPlotAbsErrorHistogram() --> Fun: Absolute Error Histogram Plot
```

```
# fPlotSSE()              --> Fun: SSE Training Evolution
# ANnet.Object            --> ANnet object created by an ANnet function
#
# Author: Arthur Hrast Essenfelder
# E-mail: arthur.essenfelder@gmail.com
#
# Version: 1.0
# Last update on: 18/11/2016
# Last modified by: Arthur Hrast Essenfelder
################################################################################
################################################################################

# Pre-Loading Libraries & Functions ------------------------------------------
# Libraries
suppressMessages(library("ggplot2"));
#-------------------------------------------------------------------------------

# Write Efficiency Criteria Results Function ---------------------------------
fWriteResults = function(ANnet.List) {
  # Geting values ------------------------------------------
  net    = ANnet.List;
  n      = length(net);
  j      = NCOL(slot(net[[1]], "Database")$Target);
  R      = array(0., dim=c(n,3,j));
  R2     = array(0., dim=c(n,3,j));
  NSE    = array(0., dim=c(n,3,j));
  PBIAS  = array(0., dim=c(n,3,j));
  epoch  = matrix(0., n, 1);
  SSE    = matrix(0., n, 3);
  for (i in 1:n) {
    R[i,,]     = slot(net[[i]], "TrainingResults")$R;
    R2[i,,]    = slot(net[[i]], "TrainingResults")$R2;
    NSE[i,,]   = slot(net[[i]], "TrainingResults")$NSE;
    PBIAS[i,,] = slot(net[[i]], "TrainingResults")$PBIAS;
    epoch[i,]  = slot(net[[i]], "TrainingResults")$epoch;
    SSE[i,]    = slot(net[[i]], "TrainingResults")$SSE[,epoch[i,]];
  }
  # Printing Results ---------------------------------------
  for (m in 1:j) {
    # Efficiency criteria results
    cat('\n');
    message("Results␣for␣output␣neuron␣", m, ":");
    message("␣␣␣␣␣␣␣␣␣␣␣␣␣␣␣␣␣␣Min␣␣␣␣␣␣␣␣␣␣␣␣Avg␣␣␣␣␣␣␣␣␣␣␣␣Max");
    strDatSet = c("Calibration", "Validation", "Test");
    intDigits = 4L;
    for (i in 1:3) {
      message("␣␣", strDatSet[i]);
      message("␣␣␣␣R:␣␣␣␣␣␣␣␣␣␣", round(min( R[    ,i,m]),intDigits),
              "␣␣␣␣␣␣␣␣"         , round(mean(R[    ,i,m]),intDigits),
              "␣␣␣␣␣␣␣␣"         , round(max( R[    ,i,m]),intDigits));
```

```
      message("␣␣␣␣R2:␣␣␣␣␣␣␣␣␣␣", round(min( R2[   ,i,m]),intDigits),
              "␣␣␣␣␣␣␣␣␣"         , round(mean(R2[   ,i,m]),intDigits),
              "␣␣␣␣␣␣␣␣␣"         , round(max( R2[   ,i,m]),intDigits));
      message("␣␣␣␣NSE:␣␣␣␣␣␣␣␣␣", round(min( NSE[  ,i,m]),intDigits),
              "␣␣␣␣␣␣␣␣␣"         , round(mean(NSE[  ,i,m]),intDigits),
              "␣␣␣␣␣␣␣␣␣"         , round(max( NSE[  ,i,m]),intDigits));
      message("␣␣␣␣PBIAS:␣␣␣␣␣␣␣", round(min( PBIAS[,i,m]),intDigits),
              "␣␣␣␣␣␣␣␣␣"         , round(mean(PBIAS[,i,m]),intDigits),
              "␣␣␣␣␣␣␣␣␣"         , round(max( PBIAS[,i,m]),intDigits));
      message("␣␣␣␣SSE:␣␣␣␣␣␣␣␣␣", round(min( SSE[  ,i])  ,intDigits),
              "␣␣␣␣␣␣␣␣␣"         , round(mean(SSE[  ,i])  ,intDigits),
              "␣␣␣␣␣␣␣␣␣"         , round(max (SSE[  ,i])  ,intDigits));
    }
    message("-------------");
  }
}
#-------------------------------------------------------------------------

# Scatter Plot Function ---------------------------------------------------
fPlotScatter = function(ANnet.List, Save.To.File, Plot.Name,
                        Plot.Width, Plot.Height) {
  # Checking for missing arguments ----------------------------
  if (missing(Save.To.File)) { Save.To.File = FALSE; }
  if (missing(Plot.Width))   { wid = 8; } else { wid = Plot.Width; }
  if (missing(Plot.Height))  { hei = 6; } else { hei = Plot.Height; }
  if (missing(Plot.Name)) {
          Pname = 'Plots-ANnet-Scatter.pdf';
  } else { Pname = Plot.Name; }
  # Getting values --------------------------------------------
  net = ANnet.List;
  n   = length(net);
  j   = NCOL(slot(net[[1]], "Database")$Target);
  k   = NROW(slot(net[[1]], "Database")$Target);
  id  = array(0., dim=c(n,k,2));
  Ot  = matrix(0., k, j);
  O   = array(0., dim=c(n,k,j));
  for (i in 1:n) {
    id[i,,] = slot(net[[i]], "Database")$Indices;
    O[i,,]  = slot(net[[i]], "Database")$Output;
  }
  Ot = slot(net[[1]], "Database")$Target;
  # Scatter plot ----------------------------------------------
  if (Save.To.File) {
    pdf(Pname,width=wid,height=hei,paper='special');
  }
  for (m in 1:j) {
    # Creating the Results Data Frame ---------------
    # Getting data vectors
    Target = Ot[,m];
    min = apply(O, c(2,3), min)[,m];
```

```
    max = apply(O, c(2,3), max)[,m];
    # Calculating the regression vectors
    regressmin = lm(min ~ Target)$coefficients;
    regressmax = lm(max ~ Target)$coefficients;
    regressmin = regressmin[1] + regressmin[2] * Target;
    regressmax = regressmax[1] + regressmax[2] * Target;
    # Creating the data.frame object
    Odf = data.frame(Target, min, max, regressmin, regressmax);
    rm(Target, min, max, regressmin, regressmax);
    # Scatter Plot ---------------------------------
    Pobj = ggplot(Odf, aes(x=Target))+
             geom_ribbon(aes(ymin=regressmin,ymax=regressmax),
                         fill="#C0C0C0")+
             geom_linerange(aes(ymin=min,ymax=max),linetype=2,size=0.2)+
             geom_point(aes(y=min),size=1.2)+
             geom_point(aes(y=max),size=1.2)+
             geom_line(aes(y=Target),size=0.4,color="firebrick")+
             theme_bw()+
             theme(text = element_text(size=18),
               axis.text.x=element_text(size=14),
               axis.text.y=element_text(size=14))+
             labs(x="Observed",y="Simulated")
    plot(Pobj);
  }
  if (Save.To.File) { dev.off() }
}
#-------------------------------------------------------------------

# Time Series Plot Function ---------------------------------------
fPlotTimeSeries = function(ANnet.List, Save.To.File,
                           Plot.Width, Plot.Height, Index.Interval) {
  # Checking for missing arguments ---------------------
  if (missing(Save.To.File)) { Save.To.File = FALSE; }
  if (missing(Plot.Width))   { wid = 8; } else { wid = Plot.Width; }
  if (missing(Plot.Height))  { hei = 6; } else { hei = Plot.Height; }
  if (missing(Index.Interval)){idint = 0.;} else {idint=Index.Interval;}
  # Getting values -------------------------------------
  net = ANnet.List;
  n   = length(net);
  j   = NCOL(slot(net[[1]], "Database")$Target);
  k   = NROW(slot(net[[1]], "Database")$Target);
  if (length(idint)!=2) { idint=c(1, k); }
  id  = array(0., dim=c(n,k,2));
  Ot  = matrix(0., k, j);
  O   = array(0., dim=c(n,k,j));
  for (i in 1:n) {
    id[i,,] = slot(net[[i]], "Database")$Indices;
    O[i,,]  = slot(net[[i]], "Database")$Output;
  }
  Ot = slot(net[[1]], "Database")$Target;
```

```
  # Time Series plot ------------------------------------------
  if (Save.To.File) {
    pdf('Plots-ANnet-TimeSeries.pdf',width=wid,height=hei,
        paper='special');
  }
  for (m in 1:j) {
    # Creating the Results Data Frame ----------
    # Getting data vectors
    Index  = idint[1]:idint[2];
    Target = Ot[idint[1]:idint[2],m];
    min  = apply(O, c(2,3), min )[idint[1]:idint[2],m];
    mean = apply(O, c(2,3), mean)[idint[1]:idint[2],m];
    max  = apply(O, c(2,3), max )[idint[1]:idint[2],m];
    # Creating the data.frame object
    Odf = data.frame(Index, Target, min, mean, max);
    rm(Index, Target, min, max);
    # Time Series Plot -------------------------
    Pojb = ggplot(Odf, aes(x=Index))+
             geom_ribbon(aes(ymin=min,ymax=max),fill="#C0C0C0",
                         color="#C0C0C0",size=0.2)+
             geom_line(aes(y=mean),color="black",size=0.4)+
             geom_point(aes(y=Target),color="firebrick",size=1.2)+
             theme_bw()+
             theme(text = element_text(size=18),
                   axis.text.x=element_text(size=14),
                   axis.text.y=element_text(size=14))+
             labs(x="Days",y="Normalised Stream Gauge");
    plot(Pojb);
  }
  if (Save.To.File) { dev.off(); }
}
#-------------------------------------------------------------------------

# Absolute Error Histogram Plot Function ---------------------------------
fPlotErrorHistogram = function(ANnet.List, Save.To.File,
                               Plot.Width, Plot.Height) {
  # Checking for missing arguments -----------------------
  if (missing(Save.To.File)) { Save.To.File = FALSE; }
  if (missing(Plot.Width))   { wid = 8; } else { wid = Plot.Width; }
  if (missing(Plot.Height))  { hei = 6; } else { hei = Plot.Height; }
  # Getting values ---------------------------------------
  net = ANnet.List;
  n   = length(net);
  j   = NCOL(slot(net[[1]], "Database")$Target);
  k   = NROW(slot(net[[1]], "Database")$Target);
  id  = array(0., dim=c(n,k,2));
  Ot  = matrix(0., k, j);
  O   = array(0., dim=c(n,k,j));
  for (i in 1:n) {
    id[i,,] = slot(net[[i]], "Database")$Indices;
```

```
    O[i,,]  = slot(net[[i]], "Database")$Output;
  }
  Ot  = slot(net[[1]], "Database")$Target;
  # Error Histogram plot ----------------------------------------
  if (Save.To.File) {
    pdf('Plots-ANnet-ErrorHistogram.pdf',width=wid,height=hei,
        paper='special');
  }
  for (m in 1:j) {
    # Creating the Results Data Frame ----------
    # Getting data vectors
    Target = Ot[,m];
    min = apply(O, c(2,3), min)[,m];
    max = apply(O, c(2,3), max)[,m];
    errmin = data.frame(AbsoluteError = min - Target);
    errmax = data.frame(AbsoluteError = max - Target);
    errmin$Range = 'min';
    errmax$Range = 'max';
    # Creating the data.frame object
    Odf = rbind(errmin, errmax);
    rm(Target, min, max, errmin, errmax);
    # Histogram Plot ----------------------------
    Pobj = ggplot(Odf, aes(AbsoluteError, fill=Range))+
              geom_histogram(position="identity",bins=64,alpha=0.2,
                             color="black",size=0.2)+
              theme_bw()+
              theme(text = element_text(size=18),
                    axis.text.x=element_text(size=14),
                    axis.text.y=element_text(size=14))+
              labs(x="Absolute Error",y="Frequency");
    plot(Pobj);
  }
  if (Save.To.File) { dev.off(); }
}
#-------------------------------------------------------------------

# Sum Squared Error - SSE Training Evolution Plot ------------------
fPlotSSE = function(ANnet.List, Save.To.File,
                    Plot.Width, Plot.Height) {

  # Checking for missing arguments -----------------------
  if (missing(Save.To.File)) { Save.To.File = FALSE; }
  if (missing(Plot.Width))   { wid = 8; } else { wid = Plot.Width; }
  if (missing(Plot.Height))  { hei = 6; } else { hei = Plot.Height; }
  # Get values -------------------------------------------
  net   = ANnet.List;
  n     = length(net);
  k     = NROW(slot(net[[1]], "Database")$Target);
  epoch = matrix(0., n, 1);
  for (i in 1:n) {
```

```
    epoch[i,] = slot(net[[i]], "TrainingResults")$epoch;
  }
  SSE   = array(k*100., dim=c(n, 3, max(epoch)));
  for (i in 1:n) {
    SSE[i,,1:epoch[i,]] = slot(net[[i]],
                               "TrainingResults")$SSE[,1:epoch[i,]];
  }
  # SSE evolution ------------------------------------------
  if (Save.To.File) {
    pdf('Plots-ANnet-SSE.pdf',width=wid,height=hei,paper='special');
  }
  # Creating the Results Data Frame ------------
  # Getting data vectors
  Index  = 1:max(epoch);
  SSEmin = t(apply(SSE, c(2,3), min));
  SSE    = replace(SSE, SSE==k*100., 0.); # Workaround to get max
  SSEmax = t(apply(SSE, c(2,3), max));
  # Create the data.frame object
  SSEdf = data.frame(Index=Index,
                     SSEmin1=SSEmin[1:max(epoch),1],
                     SSEmin2=SSEmin[1:max(epoch),2],
                     SSEmin3=SSEmin[1:max(epoch),3],
                     SSEmax1=SSEmax[1:max(epoch),1],
                     SSEmax2=SSEmax[1:max(epoch),2],
                     SSEmax3=SSEmax[1:max(epoch),3]);
  rm(Index, SSEmin, SSEmax);
  # SSE Plot ---------------------------------------
  Pobj = ggplot(SSEdf, aes(x=Index))+
           geom_ribbon(aes(ymin=SSEmin1,ymax=SSEmax1,fill="#CCE5FF"),
                       size=0.2,color="#001933",alpha=0.4)+
           geom_ribbon(aes(ymin=SSEmin2,ymax=SSEmax2,fill="#CCFFCC"),
                       size=0.2,color="#003300",alpha=0.4)+
           geom_ribbon(aes(ymin=SSEmin3,ymax=SSEmax3,fill="#FFCCCC"),
                       size=0.2,color="#330000",alpha=0.4)+
           scale_y_log10()+
           scale_fill_identity(name="Dataset",guide="legend",
                               labels=c("Test","Validation","Training"))+
           theme_bw()+
           theme(text = element_text(size=18),
                 axis.text.x=element_text(size=14),
                 axis.text.y=element_text(size=14))+
           labs(x="Training␣Epoch",y="SSE␣(log10)");
  plot(Pobj);
  if (Save.To.File) { dev.off(); }
}
#-------------------------------------------------------------------------
```

ANnet Simulate

```
##############################################################################
##################### ANnet - SIMULATION FUNCTION ############################
##############################################################################
#
# This script contains the feedforward procedure to be used by the
#   ANnet function.
#
# Specifications:
# fSim()      --> Function: returns the output matrix of a FeedForward
#                           step for the ANnet function
# ANnet.List  --> An ANnet list object created by an ANnet function
# Input.Data  --> The input matrix to be processed
# Target.Data --> The target matrix, used only for NAR and NARX
#
# Author: Arthur Hrast Essenfelder
# E-mail: arthur.essenfelder@gmail.com
#
# Version: 1.0
# Last update on: 18/11/2016
# Last modified by: Arthur Hrast Essenfelder
##############################################################################
##############################################################################

#Pre-Loading Libraries & Functions ------------------------------------------
#Functions
source("ANnet-ActivationFunctions.R");
source("ANnet-AuxiliaryFunctions.R");
source("ANnet-ModelTypeFunctions.R");
source("ANnet-NormalisationFunctions.R");
#-----------------------------------------------------------------------------

#Simulate ANnet Object Function ==============================================
fSim = function(ANnet.List, Input.Data, Target.Data,
                Model.Type.Variant) {

  # Getting all the constant data ---------------------------------------------
  # Getting values from ANnet.List Object -------------------
  net          = ANnet.List;
  n            = length(net);
  j            = NCOL(slot(net[[1]],"Database")$Target);
  Model.Type   = slot(net[[1]],"ModelSpecifications")$ModelType;
  d            = slot(net[[1]],"ModelSpecifications")$TimeDelay;
  splitFactor  = slot(net[[1]],"ModelSpecifications")$DatasetSplitFactor;
  ActFun       = slot(net[[1]],"ModelSpecifications")$ActFunctionName;
  a            = slot(net[[1]],"ModelSpecifications")$ActFunctionPrmA;
  b            = slot(net[[1]],"ModelSpecifications")$ActFunctionPrmB;
  BiasFactor   = slot(net[[1]],"ModelSpecifications")$BiasFactor;
```

```
NormData     = slot(net[[1]],"DataNormalisation")$NormalisationCheck;
NormMethod   = slot(net[[1]],"DataNormalisation")$NormalisationMethod;
Xstat        = slot(net[[1]],"DataNormalisation")$InputStatistics;
Otstat       = slot(net[[1]],"DataNormalisation")$TargetStatistics;
# Getting values passed to the function ------------------
# Getting the Input data
X = Input.Data;
i = NCOL(X);
k = NROW(X);
if (missing(Model.Type.Variant)) {
  Model.Type.Variant = slot(net[[1]],
                            "ModelSpecifications")$ModelTypeVariant;
}
# Getting the Target data
if (missing(Target.Data)) {
  if (Model.Type == "NAR" || Model.Type == "NARX") {
    stop("Missing Target.Data");
  } else { Ot = matrix(0., k, j); }
} else { Ot = Target.Data; }
#-------------------------------------------------------------

# Pre-processing some information ------------------------------
# Checking if retrieved Target data is correct ----------
if (NCOL(Ot) != j) { stop("Invalid Target.Data"); }
if (Model.Type.Variant == "Close-Loop") {
  if (NROW(Ot) != d) { stop("Invalid Target.Data"); }
} else {
  if (Model.Type == "NAR" || Model.Type == "NARX") {
    if (NROW(Ot) != k) { stop("Invalid Target.Data"); }
  }
}
# Pre-processing the input data, if necessary ----------
if (Model.Type != "Input-Output") {
  if (Model.Type.Variant == "Open-Loop") {
    X = fTimeDelayData(X, Ot, Model.Type, d);
    Ot = as.matrix(Ot[(d+1):(k),]);
    i  = NCOL(X);
    k  = NROW(X);
  } else if (Model.Type.Variant == "Close-Loop") {
    Ottmp = matrix(0., nrow=k, ncol=ncol(Ot));
    Ottmp[1:d,] = Ot;
    Ot = Ottmp;
    rm(Ottmp);
    X = fTimeDelayData(X, Ot, Model.Type, d);
    Ot = as.matrix(Ot[(d+1):(k),]);
    i  = NCOL(X);
    k  = NROW(X);
  }
}
if (i != NCOL(slot(net[[1]],"Database")$Input)) {
```

```
    stop("Incorrect nrow Input.Data")
  }
  # Normalising the data, if necessary ----------------------
  if (NormData == TRUE) {
    X  = fNorm(X,  NormMethod, Xstat);
    Ot = fNorm(Ot, NormMethod, Otstat);
  }
  #--------------------------------------------------------------

  # Performing the simulations ------------------------------------
  # Creating the array to store the results
  Osim = array(0., dim=c(n,k,j));
  # Looping through the stored ANnet models
  for (iEnsemble in 1:n) {
    # Getting the weights ---------------------------------------
    Wh1  = slot(net[[iEnsemble]],"Weights")$Wh1;
    Wh2  = slot(net[[iEnsemble]],"Weights")$Wh2;
    Wo   = slot(net[[iEnsemble]],"Weights")$Wo;
    WBh1 = slot(net[[iEnsemble]],"Weights")$WBh1;
    WBh2 = slot(net[[iEnsemble]],"Weights")$WBh2;
    WBo  = slot(net[[iEnsemble]],"Weights")$WBo;
    # Getting information about ANnet structure ----------------
    h1 = ifelse(is.null(Wh1), 0, NCOL(Wh1));
    h2 = NCOL(Wh2);
    # Bias ------------------------------------------------------
    Bh1 = matrix(BiasFactor, k, 1);
    if (is.null(Wh1)) { Bh1 = NULL; }
    Bh2 = matrix(BiasFactor, k, 1);
    Bo  = matrix(BiasFactor, k, 1);
    # FEEDFORWARD -----------------------------------------------
    # Close-Loop data -------------------------------
    if (Model.Type.Variant == "Close-Loop") {
      id = matrix(1:k, nrow=k, ncol=1);
      X  = fCloseLoopData(id, X, splitFactor, Model.Type, d,
                          ActFun, a, b,
                          Wo, WBo, Bo, Wh2, WBh2, Bh2,
                          Wh1, WBh1, Bh1);
      X  = rbind(X$Xcal,X$Xval,X$Xtst);
    }
    # Feedforward the data --------------------------
    Ff = fFeedforward(X, ActFun, a, b, Wh2, Wo,
                      Bh2, Bo, WBh2, WBo,
                      Wh1, Bh1, WBh1);
    #-----------------------------------------------------------
    # Finalising the simulation for current ANnet -------------
    # Reverting normalisation, if necessary
    if (NormData == TRUE) { O = fNormInv(Ff$O, NormMethod, Otstat);
    } else                { O = Ff$O; }
    # Storing the results
    Osim[iEnsemble,,] = O;
```

```
    # ------------------------------------------------------------
  }
  # Returning simulation values ---------------------------------
  return(Osim);
  # ------------------------------------------------------------------
}
# ======================================================================
```

ANnet Training

```
##############################################################################
################ ANnet - 1 and 2 HIDDEN LAYERED VARIANTS #####################
##############################################################################
#
# This function is a Neural Networks program/function (1 or 2 hidden
#  layered), being a MLP Feedforward Neural Network and using
#  Backpropagation as the training procedure.
#
# Specifications:
# i  --> Dimension of the input layer (i.e. number of input neurons)
# h1 --> Dimension of the hidden layer 1 (i.e. number of hidden neurons)
# h2 --> Dimension of the hidden layer 2 (i.e. number of hidden neurons)
# j  --> Dimension of the output layer (i.e. number of output neurons)
# k  --> Dimension of the data set (i.e. number of input-output pairs)
# X  --> Input Matrix - ixk dimensional
# Y  --> Hidden Matrix - hxk dimensional
# A  --> Activation Matrix - hxk or jxk dimensional
# O  --> Output Matrix - jxk dimensional
# Ot --> Target Matrix - jxk dimensional
# W  --> Weight Matrix - ixh or hxj dimensional
# E  --> Error Matrix - hxk or jxk dimensional
# B  --> Bias Vector - kx1 dimensional
# WB --> Bias Weight Vector - hx1 or jx1 dimensional
#
# Author: Arthur Hrast Essenfelder
# E-mail: arthur.essenfelder@gmail.com
#
# Version: 1.0
# Last update on: 18/11/2016
# Last modified by: Arthur Hrast Essenfelder
##############################################################################
##############################################################################

# Pre-Loading Libraries & Functions ==========================================
# Libraries
suppressMessages(library("fBasics"));
# Functions
```

```
source("ANnet-ActivationFunctions.R");
source("ANnet-AuxiliaryFunctions.R");
source("ANnet-EfficiencyCriteriaFunctions.R");
source("ANnet-ModelTypeFunctions.R");
source("ANnet-NormalisationFunctions.R");
source('ANnet-PlotFunctions.R');
source("ANnet-Simulate.R");
source("ANnet-WriteDataset.R");
#=============================================================================

# Initialising the ANnetTraining Function ====================================
ANnetTraining = function(Max.Training.Attempts,
                         Input, Target,
                         Model.Structure, Model.Type,
                         Model.Type.Variant, Time.Delay,
                         Data.Normalisation, Normalisation.Method,
                         Hidden.Layer.Neurons,
                         ActFun.Names,
                         ActFun.Parameter.a, ActFun.Parameter.b,
                         Training.Function, Dataset.Division.Factors,
                         Max.Training.Epochs,
                         Bias.Factor,
                         Preload.Weights, Preload.ANnet.Object) {

  # Defining the parameters ==================================================
  X                = as.matrix(Input);
  Ot               = as.matrix(Target);
  d                = Time.Delay;
  NormData         = Data.Normalisation;
  NormMethod       = Normalisation.Method;
  h                = Hidden.Layer.Neurons;
  if         (Model.Structure == "1-Hidden-Layered") {
    h1 = 0;
    h2 = h[1];
  } else if (Model.Structure == "2-Hidden-Layered") {
    h1 = h[1];
    h2 = h[2];
  } else { stop("ERROR: Invalid Model.Structure"); }
  ActFun           = ActFun.Names;
  a                = ActFun.Parameter.a;
  b                = ActFun.Parameter.b;
  trFun            = Training.Function;
  splitFactor      = Dataset.Division.Factors;
  trainingAttempts = Max.Training.Attempts;
  epochMax         = Max.Training.Epochs;
  #===========================================================================

  # Loading the input information ============================================
  # Getting the dimensions of X and Ot ---------------------
  i = NCOL(X);
```

```
j = NCOL(Ot);
k = NROW(X);
# Preparing the input data, if necessary ----------------------
if (Model.Type == "Input-Output") { d = 0; }
else { X = fTimeDelayData(X, Ot, Model.Type, d) }
# Updating Ot data and Indices --------------------------------
Ot = as.matrix(Ot[(d+1):(k),]);
i  = NCOL(X);
k  = NROW(X);
# Storing the original X and Ot basic statistics --------------
Xstat  = list(max=colMax(X), min=colMin(X),
              mean=colMeans(X), stDev=colStdevs(X));
Otstat = list(max=colMax(Ot), min=colMin(Ot),
              mean=colMeans(Ot), stDev=colStdevs(Ot));
# Normalising the input data ----------------------------------
if (NormData == TRUE) {
  X  = fNorm(X,  NormMethod, Xstat);
  Ot = fNorm(Ot, NormMethod, Otstat);
}
# Consolidating the data into one matrix (id+X+Ot) ------------
idXOt = as.matrix(cbind(1:k, X, Ot));
# ===============================================================

# Defining Common Objects ======================================
# BIAS ----------------------------------------------------------
# Hidden Layer 1 ------------------------------------------------
if (h1 == 0) { # If 1-Hidden Layer ------------
  Bh1    = NULL;
  Bh1cal = NULL;
  Bh1val = NULL;
  Bh1tst = NULL;
} else {       # If 2-Hidden Layer ------------
  Bh1    = matrix(Bias.Factor, k, 1);
  Bh1cal = matrix(Bh1[1:as.integer(k*splitFactor[1]),1],
                  ncol=1, byrow = FALSE);
  Bh1val = matrix(Bh1[(1+as.integer(k*splitFactor[1])):
                      (as.integer(k*splitFactor[1]+
                                  k*splitFactor[2])),1],
                  ncol=1, byrow = FALSE);
  Bh1tst = matrix(Bh1[(1+as.integer(k*splitFactor[1]+
                                  k*splitFactor[2])):k,1],
                  ncol=1, byrow = FALSE);
}
# Hidden Layer 2 ------------------------------------------------
Bh2    = matrix(Bias.Factor, k, 1);
Bh2cal = matrix(Bh2[1:as.integer(k*splitFactor[1]),1],
                ncol=1, byrow = FALSE);
Bh2val = matrix(Bh2[(1+as.integer(k*splitFactor[1])):
                    (as.integer(k*splitFactor[1]+
                                k*splitFactor[2])),1],
```

```
                ncol=1, byrow = FALSE);
Bh2tst = matrix(Bh2[(1+as.integer(k*splitFactor[1]+
                                  k*splitFactor[2])):k,1],
                ncol=1, byrow = FALSE);
# Output Layer ------------------------------------------------
Bo     = matrix(Bias.Factor, k, 1);
Bocal  = matrix(Bo[1:as.integer(k*splitFactor[1]),1],
                ncol=1, byrow = FALSE);
Boval  = matrix(Bo[(1+as.integer(k*splitFactor[1])):
                   (as.integer(k*splitFactor[1]+
                               k*splitFactor[2])),1],
                ncol=1, byrow = FALSE);
Botst  = matrix(Bo[(1+as.integer(k*splitFactor[1]+
                                  k*splitFactor[2])):k,1],
                ncol=1, byrow = FALSE);
#-------------------------------------------------------------------

# Declaring the overall best attempt results matrices ---------------
# Efficiency Criteria - 1-Cal; 2-Val; 3-Test ------------------------
R     = matrix(0.,   3, j);
R2    = matrix(0.,   3, j);
NSE   = matrix(0.,   3, j);
PBIAS = matrix(100., 3, j);
# SSE Generalisation Check ------------------------------------------
SSEvalCheckDim = 6;    # Consecutive training epochs
SSEcheckLimit  = 0.001; # i.e. 0.1% of change
#-------------------------------------------------------------------
#===================================================================

# Initiating the training attempts ==================================
for (nTrainingAttempts in 1:trainingAttempts) {

  # Split the input dataset in Cal, Val, and Tst datasets ------------
  # Randomising the data matrix ---------------------------------------
  tmp = idXOt[sample(NROW(idXOt)),];
  id  = as.matrix(tmp[, 1:1]);           #Index array
  X   = as.matrix(tmp[, 2:(i+1)]);       #Input matrix
  Ot  = as.matrix(tmp[, (i+2):(i+j+1)]); #Target matrix
  # Creating the Cal, Val, and Tst datasets ---------------------------
  idcal = as.matrix(id[1:as.integer(k*splitFactor[1]),]);
  idval = as.matrix(id[(1+as.integer(k*splitFactor[1])):
                       (as.integer(k*splitFactor[1]+
                                   k*splitFactor[2])),]);
  idtst = as.matrix(id[(1+as.integer(k*splitFactor[1]+
                                   k*splitFactor[2])):k,]);
  Xcal  = as.matrix(X[1:as.integer(k*splitFactor[1]),]);
  Xval  = as.matrix(X[(1+as.integer(k*splitFactor[1])):
                      (as.integer(k*splitFactor[1]+
                                  k*splitFactor[2])),]);
  Xtst  = as.matrix(X[(1+as.integer(k*splitFactor[1]+
```

```
                                        k*splitFactor[2])):k,]);
    Otcal = as.matrix(Ot[1:as.integer(k*splitFactor[1]),]);
    Otval = as.matrix(Ot[(1+as.integer(k*splitFactor[1])):
                         (as.integer(k*splitFactor[1]+
                                     k*splitFactor[2])),]);
    Ottst = as.matrix(Ot[(1+as.integer(k*splitFactor[1]+
                                     k*splitFactor[2])):k,]);
    # Clearing variables ------------------------------------
    rm(tmp, X, Ot);
    #-------------------------------------------------------------------

    # Declaring the attempts-specific matrices ------------------------
    # Weights ---------------------------------------------
    if (h1 == 0) { # If 1-Hidden Layer ----------
      # Neuron weights
      Wh1 = NULL;
      Wh2 = matrix(runif(i*h2, -1., 1.), i, h2);
      Wo  = matrix(runif(h2*j, -1., 1.), h2, j);
      # Bias weights
      WBh1 = NULL;
      WBh2 = matrix(runif(h2, -1., 1.), h2, 1);
      WBo  = matrix(runif(j,  -1., 1.), j,  1);
    } else {      # If 2-Hidden Layer ----------
      # Neuron weights
      Wh1 = matrix(runif(i*h1,  -1., 1.), i,  h1);
      Wh2 = matrix(runif(h1*h2, -1., 1.), h1, h2);
      Wo  = matrix(runif(h2*j,  -1., 1.), h2, j);
      # Bias weights
      WBh1 = matrix(runif(h1, -1., 1.), h1, 1);
      WBh2 = matrix(runif(h2, -1., 1.), h2, 1);
      WBo  = matrix(runif(j,  -1., 1.), j,  1);
    }
    # Check Preload Weights control
    if (Preload.Weights) {
      tmp    = load(Preload.ANnet.Object);
      nettmp = get(tmp);
      n      = length(net);
      if (n > 1) { message("WARNING: Loading weights from 1st
                           object only"); }
      if (NCOL(slot(net[[1]], "Database")$Input)  == i &&
          NCOL(slot(net[[1]], "Database")$Target) == j) {
        Wh2  = slot(net[[1]], "Weights")$Wh2;
        Wo   = slot(net[[1]], "Weights")$Wo;
        WBh2 = slot(net[[1]], "Weights")$WBh2;
        WBo  = slot(net[[1]], "Weights")$WBo;
        if (h1 == 0) { # If 1-Hidden Layer ----------
          Wh1  = NULL;
          WBh1 = NULL;
        } else {      # If 2-Hidden Layer ----------
          Wh1  = slot(net[[1]], "Weights")$Wh1;
```

```
      WBh1 = slot(net[[1]], "Weights")$WBh1;
    }
  } else {
    stop("Cannot preload weights. Different dimensions.")
  }
}
# Training specific ------------------------------------
Wh1TR  = Wh1;
Wh2TR  = Wh2;
WoTR   = Wo;
WBh1TR = WBh1;
WBh2TR = WBh2;
WBoTR  = WBo;
deltaW = NULL;
SSEoTR = array(0, dim=c(3));
OptimalSolution = FALSE; # Optimal solution control check
u = 1.;                  # Combination coefficient
# Errors -----------------------------------------------
# SSE
SSEocal = matrix(k*100., epochMax, 1);
SSEoval = matrix(k*100., epochMax, 1);
SSEotst = matrix(k*100., epochMax, 1);
SSEBestAttempt = matrix(k*100., 3, epochMax);
# SSE Generalisation Check
SSEvalCheckCounter = 1;
SSEvalCheck        = array(0, dim=c(SSEvalCheckDim));
SSEcheck           = 1.;
#-------------------------------------------------------------------
# ==================================================================

# Initiate training epochs ========================================
for (epoch in 1:epochMax) {

  # FEEDFORWARD ----------------------------------------------------
  # Close-Loop Data ------------------------------------
  if (Model.Type.Variant == "Close-Loop") {
    X = rbind(Xcal, Xval, Xtst);
    X = fCloseLoopData(id, X, splitFactor, Model.Type, d,
                       ActFun, a, b,
                       Wo, WBo, Bo, Wh2, WBh2, Bh2,
                       Wh1, WBh1, Bh1);
    Xcal = as.matrix(X$Xcal);
    Xval = as.matrix(X$Xval);
    Xtst = as.matrix(X$Xtst);
  }
  # Calibration ----------------------------------------
  Ffcal = fFeedforward(Xcal, ActFun, a, b, Wh2, Wo,
                       Bh2cal, Bocal, WBh2, WBo,
                       Wh1, Bh1cal, WBh1);
  # Validation -----------------------------------------
```

```
    Ffval = fFeedforward(Xval, ActFun, a, b, Wh2, Wo,
                         Bh2val, Boval, WBh2, WBo,
                         Wh1, Bh1val, WBh1);
  # Test ---------------------------------------------
    Fftst = fFeedforward(Xtst, ActFun, a, b, Wh2, Wo,
                         Bh2tst, Botst, WBh2, WBo,
                         Wh1, Bh1tst, WBh1);
  #-------------------------------------------------------------

  # Error calculation - Sum Squared Error - SSE ----------------
  # Output layer error -----------------------------
    Eocal = Otcal - Ffcal$O;
    Eoval = Otval - Ffval$O;
    Eotst = Ottst - Fftst$O;
  # Sum Squared Error - SSE ------------------------
    SSEocal[epoch,1] = sum(Eocal^2.)/2.;
    SSEoval[epoch,1] = sum(Eoval^2.)/2.;
    SSEotst[epoch,1] = sum(Eotst^2.)/2.;
  #-------------------------------------------------------------

  # Checking generalisation hypothesis -------------------
  # Calculating the proportional SSEcheck change ---------
    if (epoch > 1) {
      SSEcheck = abs(SSEocal[epoch,1]-min(SSEBestAttempt[1,]))/
                 min(SSEBestAttempt[1,]);
      # Check new validation SSE - Generalisation hypothesis
      if ((SSEoval[epoch,1] > min(SSEBestAttempt[2,])) ||
          (SSEcheck < SSEcheckLimit)) {#If training is not improving
        if (epoch > SSEvalCheckDim) { #And this is recurrent, then
          if (sum(SSEvalCheck-1) == 0) { #Generalisation achieved
            OptimalSolution = TRUE;
            epoch = epochMax;
            break; # Optimal solution found, exit training loop
          } else {                       #Generalisation not achieved
            # SSEvalCheck update
            SSEvalCheck[SSEvalCheckCounter] = 1;
            SSEvalCheckCounter = SSEvalCheckCounter + 1;
          }
        }
      }
    }
  # Storing this solution if criteria are met ------------
    if ((epoch == 1) || (SSEoval[epoch,1]<min(SSEBestAttempt[2,]))) {
      # Restart the Validation SSE Stop array ----------------
      SSEvalCheckCounter = 1;
      SSEvalCheck        = array(0, dim=c(SSEvalCheckDim));
      # Storing best results ---------------------------
      # Epoch
      epochBestAttempt = epoch;
      # Outputs
```

```
    OcalBestAttempt = Ffcal$O;
    OvalBestAttempt = Ffval$O;
    OtstBestAttempt = Fftst$O;
    # Sum Squared Error
    SSEBestAttempt[1,1:epoch] = SSEocal[1:epoch,1]; #Calibration
    SSEBestAttempt[2,1:epoch] = SSEoval[1:epoch,1]; #Validation
    SSEBestAttempt[3,1:epoch] = SSEotst[1:epoch,1]; #Test
    # Weights
    Wh1BestAttempt  = Wh1;
    Wh2BestAttempt  = Wh2;
    WoBestAttempt   = Wo;
    WBh1BestAttempt = WBh1;
    WBh2BestAttempt = WBh2;
    WBoBestAttempt  = WBo;
    #-------------------------------------------------
  }
  #-----------------------------------------------------------

  # Calculate the Weight updates ---------------------------
  for (m in 1:5) { # u check loop
    # Calculate the Weight Corrections ------------------
    # Previous weight update
    deltaWp = deltaW;
    # Training function
    deltaW = fBackpropagation(trFun, u, Eocal,
                              Ffcal$So,  Ffcal$Yh2, Wo,
                              Ffcal$Sh2, Ffcal$Yh1, Wh2,
                              Ffcal$Sh1, Xcal,      Wh1,
                              Previous.Delta=deltaWp);
    # Update the weights
    WoTR  = Wo  + deltaW$deltaWo;
    Wh2TR = Wh2 + deltaW$deltaWh2;
    if (h1 != 0) { Wh1TR = Wh1 + deltaW$deltaWh1; }
    # WBoTR  = WBo  - t((1./u)*(-t(Bocal) %*% (Socal *Eocal)));
    # WBh2TR = WBh2 - t((1./u)*(-t(Bh2cal) %*% (Sh2cal*Eh2cal)));
    # WBh1TR = WBh1 - t((1./u)*(-t(Bh1cal) %*% (Sh1cal*Eh1cal)));
    # FEEDFORWARD ---------------------------------------
    # Close-Loop Data -----------------------
    if (Model.Type.Variant == "Close-Loop") {
      X = rbind(Xcal, Xval, Xtst);
      X = fCloseLoopData(id, X, splitFactor, Model.Type, d,
                         ActFun, a, b,
                         WoTR, WBoTR, Bo, Wh2TR, WBh2TR, Bh2,
                         Wh1TR, WBh1TR, Bh1);
      Xcal = as.matrix(X$Xcal);
      Xval = as.matrix(X$Xval);
      Xtst = as.matrix(X$Xtst);
    }
    # Calibration ---------------------------------------
    FfcalTR = fFeedforward(Xcal, ActFun, a, b, Wh2TR, WoTR,
```

```
                        Bh2cal, Bocal, WBh2TR, WBoTR,
                        Wh1TR, Bh1cal, WBh1TR);
    # Validation ---------------------------------------------
    FfvalTR = fFeedforward(Xval, ActFun, a, b, Wh2, Wo,
                        Bh2val, Boval, WBh2TR, WBoTR,
                        Wh1TR, Bh1val, WBh1TR);
    # Test ---------------------------------------------------
    FftstTR = fFeedforward(Xtst, ActFun, a, b, Wh2, Wo,
                        Bh2tst, Botst, WBh2TR, WBoTR,
                        Wh1TR, Bh1tst, WBh1TR);
    # Calculate the new SSE ----------------------------------
    # Output layer error
    EocalTR = Otcal - FfcalTR$O;
    EovalTR = Otval - FfvalTR$O;
    EotstTR = Ottst - FftstTR$O;
    # Sum Squared Error - SSE
    SSEoTR[1] = sum(EocalTR^2.)/2.;
    SSEoTR[2] = sum(EovalTR^2.)/2.;
    SSEoTR[3] = sum(EotstTR^2.)/2.;
    # -------------------------------------------------------
    message("u:␣",u,"␣|␣SSE:␣",SSEocal[epoch,1],"␣|␣SSE:␣",SSEoTR[1])
    # Check if calculations have produced errors -------------
    if (is.na(SSEoTR[1]) || is.na(SSEoTR[2]) || is.na(SSEoTR[3])) {
      # Return to previous weight configuration
      WoTR   = Wo;
      Wh2TR  = Wh2;
      Wh1TR  = Wh1;
      WBoTR  = WBo;
      WBh2TR = WBh2;
      WBh1TR = WBh1;
      deltaW = deltaWp;
      # Increase u and exit loop
      u = u*5.;
      if (trFun=="Steepest-Descent") { u=max(u, 1.); }
      break;
    } else { # Check if SSE increases or decreases ---------
      if (SSEoTR[1] > SSEocal[epoch,1]) {
        # Return to previous weight configuration
        WoTR   = Wo;
        Wh2TR  = Wh2;
        Wh1TR  = Wh1;
        WBoTR  = WBo;
        WBh2TR = WBh2;
        WBh1TR = WBh1;
        deltaW = deltaWp;
        u = u*2.; #Increase u
        if (trFun=="Steepest-Descent") { u=max(u, 1.); }
      } else {
        # Weight update
        Wo   = WoTR;
```

```
            Wh2  = Wh2TR;
            Wh1  = Wh1TR;
            WBo  = WBoTR;
            WBh2 = WBh2TR;
            WBh1 = WBh1TR;
            u = ifelse(trFun=="Steepest-Descent", u, u/2.)
            break; #Exit for loop
          }
        }
        #-------------------------------------------------------
      } # End of weight update process
      #---------------------------------------------------------
    } # End of epoch iteration
    #-----------------------------------------------------------
    #===========================================================

    # Check if optimal solution found is the best overall ------
    if ((nTrainingAttempts == 1) ||
        (SSEBestAttempt[1,epochBestAttempt] < SSEBest[1,epochBest])) {
      # Store the best result for this attempt -----------------
      epochBest = epochBestAttempt;
      # Index, Inputs and Outputs ------------------------------
      # Create the Index array
      idcal = cbind(idcal, 'Training');
      idval = cbind(idval, 'Validation');
      idtst = cbind(idtst, 'Test');
      # Store the best values
      idBest = rbind(idcal, idval, idtst);
      XBest  = rbind(Xcal, Xval, Xtst);
      OtBest = rbind(Otcal, Otval, Ottst);
      OBest  = rbind(OcalBestAttempt, OvalBestAttempt, OtstBestAttempt);
      # Store SSE and Weights ----------------------------------
      # Sum Squared Error - SSE
      SSEBest  = SSEBestAttempt;
      # Weights
      Wh1Best  = Wh1BestAttempt;
      Wh2Best  = Wh2BestAttempt;
      WoBest   = WoBestAttempt;
      WBh1Best = WBh1BestAttempt;
      WBh2Best = WBh2BestAttempt;
      WBoBest  = WBoBestAttempt;
    }
    #-----------------------------------------------------------
    gc(); # Release memory
  } # End of training attempt iteration
  #-------------------------------------------------------------
  #=============================================================

  # Post-processing the Input, Target and Output data ==========
  # Importing the best results -----------------------------
```

```
id = as.matrix(idBest);
X  = as.matrix(XBest);
Ot = as.matrix(OtBest);
O  = as.matrix(OBest);
# Normalisation Inverse, if necessary ----------------------
if (NormData == TRUE) {
  X  = fNormInv(X,  NormMethod, Xstat);
  Ot = fNormInv(Ot, NormMethod, Otstat);
  O  = fNormInv(O,  NormMethod, Otstat);
}
# Fixing the Cal, Val and Tst datasets ---------------------
X  = cbind(id, X);
Ot = cbind(id, Ot);
O  = cbind(id, O);
# Return the data to original ordering ---------------------
id = id[order(as.integer(id[,1]),decreasing=FALSE),];
X  = X[ order(as.integer(X[, 1]),decreasing=FALSE),];
Ot = Ot[order(as.integer(Ot[,1]),decreasing=FALSE),];
O  = O[ order(as.integer(O[, 1]),decreasing=FALSE),];
# Getting the Input, Target and Output datasets ------------
Xcal     = X[X[,2]   == "Training",]
Xval     = X[X[,2]   == "Validation",]
Xtst     = X[X[,2]   == "Test",]
Otcal    = Ot[Ot[,2] == "Training",]
Otval    = Ot[Ot[,2] == "Validation",]
Ottst    = Ot[Ot[,2] == "Test",]
OcalBest = O[O[,2]   == "Training",]
OvalBest = O[O[,2]   == "Validation",]
OtstBest = O[O[,2]   == "Test",]
# Dropping the ordering columns ----------------------------
X        = matrix(as.numeric(X[,       3:(i+2)]),ncol=i,byrow=FALSE);
Ot       = matrix(as.numeric(Ot[,      3:(j+2)]),ncol=j,byrow=FALSE);
O        = matrix(as.numeric(O[,       3:(j+2)]),ncol=j,byrow=FALSE);
Xcal     = matrix(as.numeric(Xcal[,    3:(i+2)]),ncol=i,byrow=FALSE);
Xval     = matrix(as.numeric(Xval[,    3:(i+2)]),ncol=i,byrow=FALSE);
Xtst     = matrix(as.numeric(Xtst[,    3:(i+2)]),ncol=i,byrow=FALSE);
Otcal    = matrix(as.numeric(Otcal[,   3:(j+2)]),ncol=j,byrow=FALSE);
Otval    = matrix(as.numeric(Otval[,   3:(j+2)]),ncol=j,byrow=FALSE);
Ottst    = matrix(as.numeric(Ottst[,   3:(j+2)]),ncol=j,byrow=FALSE);
OcalBest = matrix(as.numeric(OcalBest[,3:(j+2)]),ncol=j,byrow=FALSE);
OvalBest = matrix(as.numeric(OvalBest[,3:(j+2)]),ncol=j,byrow=FALSE);
OtstBest = matrix(as.numeric(OtstBest[,3:(j+2)]),ncol=j,byrow=FALSE);
# Calculating the efficiency criteria ----------------------
# Correlation - R
R[1,] = cor(Otcal, OcalBest); #Calibration
R[2,] = cor(Otval, OvalBest); #Validation
R[3,] = cor(Ottst, OtstBest); #Test
# Coefficient of Determination - R2
R2[1,] = fR2(Otcal, OcalBest); #Calibration
R2[2,] = fR2(Otval, OvalBest); #Validation
```

```
R2[3,] = fR2(Ottst, OtstBest); #Test
# Nash-Sutcliffe Efficiency Criteria - NSE
NSE[1,] = fNSE(Otcal, OcalBest); #Calibration
NSE[2,] = fNSE(Otval, OvalBest); #Validation
NSE[3,] = fNSE(Ottst, OtstBest); #Test
# Percent Bias - PBIAS
PBIAS[1,] = fPBIAS(Otcal, OcalBest); #Calibration
PBIAS[2,] = fPBIAS(Otval, OvalBest); #Validation
PBIAS[3,] = fPBIAS(Ottst, OtstBest); #Test
# Exporting the best results ----------------------------
idBest = id;
XBest  = X;
OtBest = Ot;
OBest  = O;
#=============================================================

# Clearing the auxiliary variables ==========================
rm(list=setdiff(ls(),
   c("id", "X", "O", "Ot", "Model.Structure", "Model.Type",
     "Model.Type.Variant", "d", "splitFactor", "ActFun", "a", "b",
     "Bias.Factor", "NormData", "NormMethod", "Xstat", "Otstat",
     "Wh1Best","Wh2Best","WoBest","WBh1Best","WBh2Best","WBoBest",
     "epochBest", "R", "R2", "NSE", "PBIAS", "SSEBest")));
#=============================================================

# Finishing the function ====================================
# Creating the list objects -----------------------------
ANnetDatabase = list(Indices=id, Input=X, Output=O, Target=Ot);
ModelSpecs    = list(Model.Structure=Model.Structure,
                     ModelType=Model.Type,
                     ModelTypeVariant=Model.Type.Variant,
                     TimeDelay=d, DatasetSplitFactor=splitFactor,
                     ActFunctionName=ActFun,
                     ActFunctionPrmA=a, ActFunctionPrmB=b,
                     BiasFactor=Bias.Factor);
DataNorm      = list(NormalisationCheck=NormData,
                     NormalisationMethod=NormMethod,
                     InputStatistics=Xstat,
                     TargetStatistics=Otstat);
Weights       = list(Wh1=Wh1Best,   Wh2=Wh2Best,   Wo=WoBest,
                     WBh1=WBh1Best, WBh2=WBh2Best, WBo=WBoBest);
TrainingRes   = list(epoch=epochBest, R=R, R2=R2, NSE=NSE,
                     PBIAS=PBIAS, SSE=SSEBest);
# Creating the ANnet object -----------------------------
ANnet = setClass("ANnet", slots = c(Database="list",
                                    ModelSpecifications="list",
                                    DataNormalisation="list",
                                    Weights="list",
                                    TrainingResults="list"));
gc(); # Release memory
```

```
  return(ANnet(Database=ANnetDatabase,
               ModelSpecifications=ModelSpecs,
               DataNormalisation=DataNorm,
               Weights=Weights,
               TrainingResults=TrainingRes))
  #============================================================
}
#==============================================================
```

ANnet Write Dataset

```
################################################################################
##################### ANnet - WRITE RESULTS TO CSV #############################
################################################################################
#
# This script contains some functions to write the datasets used by an
#   ANnet function.
#
# Specifications:
# fWriteDataset() --> Function: Write the desired dataset to a .csv file
# ANnet.Object    --> An ANnet object created by an ANnet function
# Dataset.Name    --> String to store the dataset name (Cal, Val, Test)
#
# Author: Arthur Hrast Essenfelder
# E-mail: arthur.essenfelder@gmail.com
#
# Version: 1.0
# Last update on: 18/11/2016
# Last modified by: Arthur Hrast Essenfelder
################################################################################
################################################################################

# Pre-Loading Libraries & Functions ------------------------------------
# Libraries
#-----------------------------------------------------------------------

# Write Dataset Function -----------------------------------------------
fWriteDataset = function(ANnet.List, Dataset.Name) {
  # Getting values ------------------------------------------
  net = ANnet.List;
  n   = length(net);
  if (missing(Dataset.Name)) { dsName = 'All'; }
  # Checking if input is correct ----------------------------
  if (!dsName %in% c('Training', 'Validation', 'Test')) {
    message("WARNING: The Dataset.Name in neither of the following:");
    message("         'Training' | 'Validation' | 'Test'");
    message("         Writing the full dataset instead");
```

```
    dsName = 'All';
  }
  #Select the file name to save ----------------------------------
  if (dsName == 'Training')   { dsFile = 'cal'; }
  if (dsName == 'Validation') { dsFile = 'val'; }
  if (dsName == 'Test')       { dsFile = 'tst'; }
  if (dsName == 'All')        { dsFile = 'all'; }
  # Writing the filtered dataset to file ---------------------
  for (i in 1:n) {
    # Getting values -----------------------------
    id = slot(net[[i]], "Database")$Indices;
    X  = slot(net[[i]], "Database")$Input;
    Ot = slot(net[[i]], "Database")$Target;
    # Filtering the dataset ----------------------
    X  = as.matrix(cbind(id, X));
    Ot = as.matrix(cbind(id, Ot));
    if (dsName!='All') {
      X  = as.matrix( X[which( X[,2]==dsName),]);
      Ot = as.matrix(Ot[which(Ot[,2]==dsName),]);
    }
    # Write the results to file ------------------
    write.csv(X,  file=paste('X',dsFile,'_',i,'.csv',sep=''));
    write.csv(Ot, file=paste('y',dsFile,'_',i,'.csv',sep=''));
  }
}
#-------------------------------------------------------------------------
```

Appendix 4 – PCA Results

This appendix chapter summarises the results of the PCA data processing by displaying the linear correlation values between the PCA components and variables for each of the sub-basins studied in Chapter 3. In order to facilitate the display of the data, the tables shown here are limited to the PCA component until which, cumulatively, describes at least 95% of the input data variance. The highlighted values correspond to values which the absolute linear correlation is higher than 0.50. Finally, the variables marked with a single star symbol (i.e. $*$) are the variables selected for both PCA Scenarios I and II, while the variables marked with a double star symbol (i.e. $**$) are the variables selected for the PCA Scenario II only.

PCA Results

Table A5.1: Linear correlation between PCA components and variables – Dese sub-basin.

Variables	Dim.1	Dim.2	Dim.3	Dim.4	Dim.5	Dim.6	Dim.7	Dim.8	Dim.9	Dim.10	Dim.11	Dim.12
FLOW*	0.43	0.45	-0.32	0.20	-0.11	0.39	-0.27	0.25	-0.25	0.06	-0.04	-0.07
EVAP*	**-0.94**	0.17	-0.09	0.14	-0.10	0.02	-0.01	0.00	0.03	0.11	-0.05	0.00
GWQ**	0.45	-0.15	-0.28	0.48	-0.27	0.27	-0.21	0.35	0.20	-0.09	0.17	-0.16
SW**	**0.68**	-0.16	-0.29	0.43	0.02	0.18	-0.09	0.05	0.11	0.00	-0.12	0.38
IRR**	-0.12	-0.01	0.01	-0.13	-0.13	**-0.57**	**-0.79**	0.05	0.00	0.00	0.00	0.03
HMD.80CF*	**0.71**	0.39	**0.50**	0.18	-0.07	-0.08	0.05	0.02	-0.01	0.01	0.02	-0.02
HMD.80MS	**0.61**	0.43	**0.52**	0.23	-0.06	-0.09	0.05	0.03	-0.01	0.08	0.02	-0.03
HMD.80OG	**0.67**	0.36	**0.51**	0.26	-0.08	-0.14	0.05	-0.04	0.01	0.07	-0.05	0.00
HMD.80TS	**0.67**	0.39	**0.54**	0.17	-0.09	-0.09	0.04	0.00	0.00	0.05	-0.01	0.03
HMD.80ZB	**0.67**	0.36	**0.52**	0.21	-0.10	-0.12	0.05	-0.05	0.01	0.08	-0.04	0.00
PCP.80CF*	0.30	**0.81**	-0.32	-0.14	-0.02	0.11	-0.07	-0.10	-0.21	0.01	0.00	0.01
PCP.80MS	0.28	**0.78**	-0.29	-0.14	-0.02	0.05	-0.04	-0.08	-0.26	-0.01	0.05	0.06
PCP.80OG	0.30	**0.75**	-0.31	-0.17	-0.02	0.05	-0.03	-0.17	0.30	0.01	-0.04	-0.05
PCP.80TS	0.30	**0.80**	-0.31	-0.17	-0.02	0.08	-0.06	-0.18	0.08	-0.02	0.00	-0.01
PCP.80ZB	0.31	**0.78**	-0.31	-0.16	-0.02	0.06	-0.04	-0.18	0.25	-0.02	-0.02	-0.02
SLR.80CF**	**-0.93**	0.00	-0.10	0.17	-0.11	0.08	-0.05	-0.11	0.03	0.22	-0.07	0.01
SLR.80OG	**-0.93**	0.02	-0.10	0.17	-0.10	0.07	-0.05	-0.10	0.01	0.21	-0.06	0.01
SLR.80ZB	**-0.93**	0.02	-0.10	0.17	-0.11	0.07	-0.05	-0.09	0.02	0.21	-0.06	0.00
TMP.80CF*	**-0.83**	0.47	0.23	0.09	0.02	0.00	0.01	0.11	0.01	-0.12	-0.07	0.00
TMP.80MS	**-0.83**	0.46	0.24	0.10	0.02	0.00	0.01	0.10	0.01	-0.12	-0.07	0.00
TMP.80OG	**-0.82**	0.48	0.24	0.08	0.02	0.00	0.01	0.12	0.00	-0.13	-0.01	0.00
TMP.80TS	**-0.82**	0.48	0.23	0.01	0.03	-0.01	0.02	0.11	0.01	-0.12	-0.07	0.00
TMP.80ZB	**-0.83**	0.47	0.23	0.09	0.02	0.00	0.01	0.11	0.00	-0.13	-0.06	-0.01
WND.80MS	0.11	0.32	**-0.67**	0.03	0.12	-0.34	0.24	0.38	0.01	-0.02	-0.03	0.15
WND.80TS**	0.10	0.28	**-0.69**	0.10	0.11	-0.39	0.24	0.28	0.01	0.20	-0.02	-0.16
Spring*	-0.27	0.06	-0.41	**0.67**	0.24	-0.20	0.00	-0.39	-0.07	-0.13	0.16	-0.03
Summer*	**-0.60**	0.32	0.30	-0.37	-0.35	0.06	0.08	0.22	0.05	0.12	0.30	0.15
Autumn*	0.38	0.00	0.31	-0.18	**0.75**	0.20	-0.20	0.20	0.06	0.11	-0.15	-0.05
Winter*	**0.51**	-0.38	-0.21	-0.13	**-0.64**	-0.05	0.12	-0.02	-0.04	-0.11	-0.31	-0.07

Table A5.2: Linear correlation between PCA components and variables – Zero sub-basin.

Variables	Dim.1	Dim.2	Dim.3	Dim.4	Dim.5	Dim.6	Dim.7	Dim.8	Dim.9	Dim.10	Dim.11	Dim.12
FLOW*	0.45	-0.39	0.33	-0.31	0.16	-0.41	0.21	-0.24	0.06	-0.07	0.06	0.37
EVAP*	**-0.94**	-0.16	0.10	-0.13	0.09	-0.02	0.00	0.00	-0.05	-0.09	0.05	-0.05
GWQ**	0.46	0.15	0.29	-0.49	0.30	-0.28	0.20	-0.32	-0.03	0.08	-0.17	-0.23
SW**	**0.69**	0.16	0.29	-0.44	-0.02	-0.18	0.01	-0.02	-0.03	0.04	0.08	-0.15
IRR**	-0.23	0.02	-0.01	0.28	0.19	0.37	**0.83**	-0.08	-0.01	0.00	0.02	-0.02
HMD.80CF*	**0.71**	-0.39	-0.49	-0.17	0.07	0.11	-0.02	-0.02	-0.02	-0.08	-0.01	-0.02
HMD.80MS	**0.61**	-0.43	**-0.51**	-0.22	0.06	0.12	-0.01	-0.03	-0.02	-0.09	0.00	-0.04
HMD.80OG	**0.67**	-0.37	**-0.50**	-0.24	0.08	0.17	-0.01	0.03	-0.06	-0.04	0.05	0.00
HMD.80TS	**0.67**	-0.39	**-0.54**	-0.16	0.09	0.12	-0.01	0.00	-0.03	-0.04	0.01	0.01
HMD.80ZB	**0.68**	-0.37	**-0.51**	-0.19	0.10	0.15	-0.02	0.05	-0.06	-0.05	0.04	0.02
PCP.80CF*	0.30	**-0.80**	0.32	0.16	0.02	-0.10	0.03	0.12	0.21	-0.12	0.02	-0.04
PCP.80MS	0.28	**-0.78**	0.29	0.16	0.01	-0.05	0.01	0.10	0.32	-0.16	0.00	-0.15
PCP.80OG	0.30	**-0.75**	0.31	0.18	0.01	-0.08	0.02	0.16	-0.28	0.14	0.00	-0.02
PCP.80TS	0.30	**-0.79**	0.31	0.18	0.02	-0.10	0.04	0.18	-0.04	0.04	-0.01	-0.03
PCP.80ZB	0.31	**-0.79**	0.32	0.16	0.02	-0.10	0.03	0.17	-0.21	0.12	-0.01	0.01
SLR.80CF**	**-0.92**	0.00	0.10	-0.18	0.11	-0.07	0.02	0.12	-0.12	-0.17	0.09	-0.03
SLR.80OG	**-0.93**	-0.02	0.10	-0.18	0.10	-0.06	0.02	0.12	-0.09	-0.18	0.09	-0.04
SLR.80ZB	**-0.93**	-0.02	0.10	-0.18	0.11	-0.06	0.03	0.11	-0.10	-0.18	0.09	-0.05
TMP.80CF*	**-0.83**	-0.47	-0.23	-0.11	-0.02	0.00	-0.01	-0.11	0.05	0.12	0.05	-0.01
TMP.80MS	**-0.83**	-0.46	-0.23	-0.11	-0.01	0.00	-0.01	-0.10	0.04	0.12	0.06	-0.01
TMP.80OG	**-0.82**	-0.48	-0.23	-0.09	-0.02	-0.01	-0.01	-0.12	0.06	0.12	0.05	-0.01
TMP.80TS	**-0.82**	-0.48	-0.23	-0.11	-0.02	0.00	-0.01	-0.11	0.05	0.12	0.05	-0.01
TMP.80ZB	**-0.83**	-0.47	-0.23	-0.10	-0.01	0.00	-0.01	-0.11	0.06	0.12	0.05	-0.01
WND.80MS	0.11	-0.32	**0.68**	-0.01	-0.12	0.35	-0.18	-0.41	0.01	0.04	0.01	-0.03
WND.80TS**	0.10	-0.28	**0.70**	-0.07	-0.12	0.42	-0.15	-0.31	-0.12	-0.16	0.05	0.04
Spring*	-0.27	-0.06	0.41	**-0.64**	-0.24	0.29	0.11	0.39	0.08	0.08	-0.16	0.08
Summer*	**-0.60**	-0.32	-0.30	0.34	0.35	-0.10	-0.14	-0.22	-0.07	-0.12	-0.30	0.01
Autumn*	0.38	0.00	-0.32	0.16	**-0.74**	-0.27	0.17	-0.20	-0.07	-0.08	0.16	-0.08
Winter*	**0.51**	0.38	0.20	0.14	**0.63**	0.08	-0.14	0.03	0.06	0.12	0.31	-0.02

Table A5.3: Linear correlation between PCA components and variables – Marzenego sub-basin.

Variables	Dim.1	Dim.2	Dim.3	Dim.4	Dim.5	Dim.6	Dim.7	Dim.8	Dim.9	Dim.10	Dim.11
FLOW*	0.45	**-0.56**	-0.36	0.06	-0.07	0.22	0.40	-0.05	-0.02	-0.07	0.10
EVAP*	**-0.95**	-0.15	-0.10	-0.09	-0.13	0.04	0.04	0.00	0.12	-0.02	0.03
GWQ**	**0.50**	0.17	-0.28	-0.21	-0.38	0.21	**0.51**	0.23	-0.10	0.16	0.14
SW**	**0.66**	0.19	-0.30	-0.36	-0.09	0.21	0.20	-0.04	0.11	-0.11	-0.43
IRR**	-0.13	0.01	0.03	0.24	-0.09	**-0.84**	0.45	-0.02	0.02	-0.02	-0.08
HMD.80CF	**0.69**	-0.40	0.48	-0.19	-0.16	-0.04	-0.03	0.05	0.06	0.03	0.03
HMD.80OG	**0.66**	-0.38	0.49	-0.27	-0.21	-0.09	-0.05	0.00	0.10	-0.01	0.04
HMD.80TS*	**0.66**	-0.40	**0.52**	-0.18	-0.18	-0.05	-0.04	0.00	0.05	0.01	0.01
HMD.80ZB	**0.67**	-0.38	**0.50**	-0.23	-0.21	-0.08	-0.06	-0.01	0.10	0.01	0.04
PCP.80CF	0.28	**-0.79**	-0.33	0.11	0.05	-0.02	-0.06	-0.07	-0.03	-0.02	0.03
PCP.80OG	0.30	**-0.77**	-0.35	0.13	0.05	-0.03	-0.07	-0.10	0.06	0.06	-0.06
PCP.80TS*	0.29	**-0.82**	-0.36	0.13	0.04	0.01	-0.01	-0.13	-0.03	-0.02	0.05
PCP.80ZB	0.30	**-0.80**	-0.36	0.12	0.05	-0.02	-0.05	-0.12	0.02	0.04	-0.04
SLR.80CF	**-0.93**	0.01	-0.12	-0.12	-0.13	0.04	0.06	-0.13	0.22	0.01	0.05
SLR.80OG	**-0.94**	-0.01	-0.12	-0.12	-0.12	0.03	0.06	-0.12	0.20	0.01	0.05
SLR.80ZB**	**-0.93**	-0.01	-0.12	-0.12	-0.13	0.03	0.06	-0.11	0.21	0.01	0.06
TMP.80CF	**-0.83**	-0.45	0.23	-0.09	-0.03	0.04	0.06	0.10	-0.10	-0.12	-0.03
TMP.80OG	**-0.82**	-0.46	0.23	-0.08	-0.02	0.04	0.06	0.10	-0.11	-0.12	-0.04
TMP.80TS*	**-0.82**	-0.46	0.23	-0.10	-0.03	0.04	0.06	0.10	-0.10	-0.12	-0.04
TMP.80ZB	**-0.83**	-0.45	0.23	-0.08	-0.03	0.04	0.06	0.10	-0.11	-0.12	-0.03
WND.80TS**	0.08	-0.23	**-0.64**	-0.12	0.08	-0.20	-0.22	**0.62**	0.17	-0.02	0.01
Spring*	-0.29	-0.03	-0.43	**-0.75**	0.06	-0.26	-0.13	-0.15	-0.19	0.11	0.02
Summer*	**-0.60**	-0.32	0.30	0.46	-0.25	0.15	-0.01	0.13	0.02	0.29	-0.17
Autumn*	0.39	-0.02	0.35	-0.01	**0.76**	0.11	0.29	0.05	0.16	-0.09	0.07
Winter*	**0.51**	0.38	-0.23	0.30	**-0.56**	0.00	-0.15	-0.03	0.01	-0.31	0.07

Table A5.4: Linear correlation between PCA components and variables – Montalbano sub-basin.

Variables	Dim.1	Dim.2	Dim.3	Dim.4	Dim.5	Dim.6	Dim.7	Dim.8	Dim.9	Dim.10	Dim.11
FLOW*	0.26	**-0.63**	-0.36	0.09	-0.07	0.02	-0.26	0.21	-0.49	0.04	-0.01
EVAP*	**-0.95**	-0.12	-0.04	0.11	-0.06	0.02	-0.04	-0.02	0.00	-0.10	0.03
GWQ**	0.48	0.16	-0.17	0.32	-0.29	0.08	**-0.64**	0.13	0.23	-0.03	-0.11
SW**	**0.59**	0.22	-0.32	0.49	0.13	0.03	-0.19	0.08	0.11	0.06	0.15
IRR**	-0.09	0.01	0.01	-0.06	-0.20	**-0.97**	-0.09	0.01	0.01	0.01	0.02
HMD.80DI	**0.69**	-0.36	**0.54**	0.19	-0.02	-0.01	0.01	-0.05	0.00	-0.09	0.02
HMD.80DV*	**0.69**	-0.35	**0.52**	0.21	-0.02	-0.02	0.01	-0.07	-0.02	-0.12	-0.03
HMD.80LE	**0.70**	-0.36	**0.51**	0.25	0.00	-0.01	0.04	-0.06	-0.03	-0.10	-0.01
HMD.80MM	**0.65**	-0.40	**0.55**	0.22	-0.01	-0.01	0.00	-0.03	0.00	-0.07	0.03
HMD.80VV	**0.66**	-0.39	**0.55**	0.25	0.00	-0.03	0.06	-0.05	-0.02	-0.08	0.03
PCP.80DI	0.25	**-0.78**	-0.39	-0.04	-0.02	-0.01	0.10	0.04	0.19	-0.02	-0.04
PCP.80DV*	0.25	**-0.80**	-0.41	-0.04	-0.03	-0.01	0.11	0.06	0.17	-0.02	-0.02
PCP.80LE	0.25	**-0.79**	-0.38	-0.01	-0.04	0.00	-0.01	0.06	-0.22	0.05	0.00
PCP.80MM	0.24	**-0.78**	-0.38	-0.02	-0.03	0.00	0.09	0.05	0.06	0.01	0.06
PCP.80VV	0.24	**-0.78**	-0.40	-0.04	-0.04	-0.01	0.13	0.07	0.20	-0.03	0.04
SLR.80DI	**-0.95**	0.01	-0.06	0.22	-0.02	-0.01	0.04	0.11	-0.01	-0.15	0.04
SLR.80DV**	**-0.95**	0.00	-0.06	0.22	0.03	0.00	0.04	0.11	-0.01	-0.15	0.04
SLR.80LE	**-0.95**	0.01	-0.05	0.20	-0.04	-0.01	0.04	0.11	-0.01	-0.17	0.02
SLR.80MM	**-0.95**	0.02	-0.07	0.21	-0.03	0.00	0.05	0.11	-0.01	-0.16	0.03
SLR.80VV	**-0.95**	0.01	-0.06	0.21	-0.03	-0.01	0.05	0.11	-0.01	-0.16	0.03
TMP.80DI	**-0.84**	-0.42	0.26	-0.02	0.03	0.02	-0.13	-0.09	0.03	0.11	0.08
TMP.80DV*	**-0.83**	-0.43	0.27	-0.02	0.03	0.02	-0.12	-0.09	0.03	0.12	0.08
TMP.80LE	**-0.84**	-0.42	0.28	-0.01	0.03	0.02	-0.12	-0.09	0.03	0.12	0.08
TMP.80MM	**-0.83**	-0.43	0.28	-0.01	0.03	0.02	-0.12	-0.09	0.03	0.12	0.08
TMP.80VV	**-0.83**	-0.43	0.27	-0.02	0.03	0.02	-0.12	-0.09	0.03	0.12	0.08
WND.80DV**	0.12	-0.09	**-0.61**	-0.18	0.17	0.00	-0.23	**-0.63**	-0.06	-0.29	0.06
Spring*	-0.30	-0.01	-0.30	**0.64**	**0.54**	-0.13	0.10	-0.16	-0.01	0.16	-0.19
Summer*	**-0.60**	-0.30	0.26	-0.30	**-0.50**	0.09	-0.05	-0.05	0.01	-0.07	-0.28
Autumn*	0.38	-0.04	0.26	**-0.51**	**0.57**	-0.03	-0.20	0.32	0.04	-0.16	0.15
Winter*	**0.53**	0.36	-0.22	0.17	**-0.61**	0.07	0.14	-0.10	-0.04	0.07	0.32

Università
Ca'Foscari
Venezia

DEPOSITO ELETTRONICO DELLA TESI DI DOTTORATO

DICHIARAZIONE SOSTITUTIVA DELL'ATTO DI NOTORIETA'
(Art. 47 D.P.R. 445 del 28/12/2000 e relative modifiche)

Io sottoscritto Arthur Hrast Essenfelder

nat o. a Curitiba - PR (Brasile) (prov. EE) il 13/03/1987

residente a Empoli (FI) in Via Bisarnella n. 13

Matricola (se posseduta) 956145 Autore della tesi di dottorato dal titolo:

Climate change and watershed planning: Understanding the Related Impacts and Risks

Dottorato di ricerca in Scienza e Gestione dei Cambiamenti Climatici

(in cotutela con .....)

Ciclo 29

Anno di conseguimento del titolo 2017

DICHIARO

di essere a conoscenza:
1) del fatto che in caso di dichiarazioni mendaci, oltre alle sanzioni previste dal codice penale e dalle Leggi speciali per l'ipotesi di falsità in atti ed uso di atti falsi, decado fin dall'inizio e senza necessità di nessuna formalità dai benefici conseguenti al provvedimento emanato sulla base di tali dichiarazioni;
2) dell'obbligo per l'Università di provvedere, per via telematica, al deposito di legge delle tesi di dottorato presso le Biblioteche Nazionali Centrali di Roma e di Firenze al fine di assicurarne la conservazione e la consultabilità da parte di terzi;
3) che l'Università si riserva i diritti di riproduzione per scopi didattici, con citazione della fonte;
4) del fatto che il testo integrale della tesi di dottorato di cui alla presente dichiarazione viene archiviato e reso consultabile via internet attraverso l'Archivio Istituzionale ad Accesso Aperto dell'Università Ca' Foscari, oltre che attraverso i cataloghi delle Biblioteche Nazionali Centrali di Roma e Firenze;
5) del fatto che, ai sensi e per gli effetti di cui al D.Lgs. n. 196/2003, i dati personali raccolti saranno trattati, anche con strumenti informatici, esclusivamente nell'ambito del procedimento per il quale la presentazione viene resa;
6) del fatto che la copia della tesi in formato elettronico depositato nell'Archivio Istituzionale ad Accesso Aperto è del tutto corrispondente alla tesi in formato cartaceo, controfirmata dal tutor, consegnata presso la segreteria didattica del dipartimento di riferimento del corso di dottorato ai fini del deposito presso l'Archivio di Ateneo, e che di conseguenza va esclusa qualsiasi responsabilità dell'Ateneo stesso per quanto riguarda eventuali errori, imprecisioni o omissioni nei contenuti della tesi;
7) del fatto che la copia consegnata in formato cartaceo, controfirmata dal tutor, depositata nell'Archivio di Ateneo, è l'unica alla quale farà riferimento l'Università per rilasciare, a richiesta, la dichiarazione di conformità di eventuali copie.

Data 31/05/2017 **Firma** _____

AUTORIZZO

- l'Università a riprodurre ai fini dell'immissione in rete e a comunicare al pubblico tramite servizio on line entro l'Archivio Istituzionale ad Accesso Aperto il testo integrale della tesi depositata;
- l'Università a consentire:
  - la riproduzione a fini personali e di ricerca, escludendo ogni utilizzo di carattere commerciale;
  - la citazione purché completa di tutti i dati bibliografici (nome e cognome dell'autore, titolo della tesi, relatore e correlatore, l'università, l'anno accademico e il numero delle pagine citate).

DICHIARO

1) che il contenuto e l'organizzazione della tesi è opera originale da me realizzata e non infrange in alcun modo il diritto d'autore né gli obblighi connessi alla salvaguardia di diritti morali od economici di altri autori o di altri aventi diritto, sia per testi, immagini, foto, tabelle, o altre parti di cui la tesi è composta, né compromette in alcun modo i diritti di terzi relativi alla sicurezza dei dati personali;
2) che la tesi di dottorato non è il risultato di attività rientranti nella normativa sulla proprietà industriale, non è stata prodotta nell'ambito di progetti finanziati da soggetti pubblici o privati con vincoli alla divulgazione dei risultati, non è oggetto di eventuali registrazione di tipo brevettuale o di tutela;
3) che pertanto l'Università è in ogni caso esente da responsabilità di qualsivoglia natura civile, amministrativa o penale e sarà tenuta indenne a qualsiasi richiesta o rivendicazione da parte di terzi.

A tal fine:
- dichiaro di aver autoarchiviato la copia integrale della tesi in formato elettronico nell'Archivio Istituzionale ad Accesso Aperto dell'Università Ca' Foscari;
- consegno la copia integrale della tesi in formato cartaceo presso la segreteria didattica del dipartimento di riferimento del corso di dottorato ai fini del deposito presso l'Archivio di Ateneo.

Data 31/05/2017 **Firma** 

La presente dichiarazione è sottoscritta dall'interessato in presenza del dipendente addetto, ovvero sottoscritta e inviata, unitamente a copia fotostatica non autenticata di un documento di identità del dichiarante, all'ufficio competente via fax, ovvero tramite un incaricato, oppure a mezzo posta

Firma del dipendente addetto ……

Ai sensi dell'art. 13 del D.Lgs. n. 196/03 si informa che il titolare del trattamento dei dati forniti è l'Università Ca' Foscari - Venezia.
I dati sono acquisiti e trattati esclusivamente per l'espletamento delle finalità istituzionali d'Ateneo; l'eventuale rifiuto di fornire i propri dati personali potrebbe comportare il mancato espletamento degli adempimenti necessari e delle procedure amministrative di gestione delle carriere studenti. Sono comunque riconosciuti i diritti di cui all'art. 7 D. Lgs. n. 196/03.

Estratto per riassunto della tesi di dottorato

Studente: Arthur Hrast Essenfelder **Matricola**: 956145

Dottorato: Scienza e Gestione dei Cambiamenti Climatici

Ciclo: 29°

Titolo della tesi:

Climate Change and Watershed Planning: Understanding the Related Impacts and Risks

Abstract:

The hydrologic cycle is the result of dynamics between human and water systems. The management of water resources, then, must take into account the linkages between these two systems. Currently, exists a lack of quantification regarding human adaptation actions and related feedbacks in human-water systems. This dissertation explores the possibility of using a Artificial Neural Networks (ANN) coupled with the physically-based hydrological model Soil and Water Assessment Tool (SWAT) as a method for improving the description of human-water systems when stressed by hydro-meteorological factors and under long-term time periods. Two case studies are considered: the Venice Lagoon Watershed (VLW) in Italy, and the Itajaí River Watershed (IRW) in Brazil. Results suggest that modifications in the SWAT source code may improve some of its limitations (e.g. dynamic atmospheric CO_2 concentration) when utilised in a context of long-term analysis, while the coupling with ANN models enables the consideration of dynamic adaptive management actions in watersheds.

Estratto:

Il ciclo idrologico è il risultato delle dinamiche tra I sistemi umani e idrici. La gestione delle risorse idriche, quindi, deve tener conto delle connessione tra questi due sistemi. Attualmente, esiste una mancanza capacità di quantificare azioni di adattamento umano e le sue relative risposte nei sistemi accoppiati umani-acque. Questa dissertazione esplora la possibilità di utilizzare reti neurali artificiali (ANN) accoppiate con il modello idrologico *Soil and Water Assessment Tool* (SWAT) come metodo per raffinare la descrizione dei sistemi accoppiati umani-acque quando stressati da fattori idrometeorologici e sotto lungo periodi. Sono considerati due casi di studio: il Bacino Scolante in Laguna di Venezia (VLW) in Italia e il Bacino Scolante del Fiume Itajaí (IRW) in Brasile. I risultati suggeriscono che modifiche nel codice sorgente SWAT possono migliorare alcune delle sue limitazioni (e.g. concentrazione dinamica di CO_2 in atmosfera) se utilizzata in un contesto di analisi a lungo termine, mentre l'accoppiamento con modelli ANN consente di considerare azioni dinamiche di adattamento in bacini scolanti.

Firma dello studente